January 2009

Mammalian Postcranial Evolution and Primate Extinction in the Middle Eocene of North America

Rachel Dunn
Washington University in St. Louis

WASHINGTON UNIVERSITY

Department of Anthropology

Dissertation Examination Committee:
D. Tab Rasmussen, Chair
Glenn C. Conroy
Allan Larson
Herman Pontzer
Jennifer R. Smith
Erik Trinkaus

MAMMALIAN POSTCRANIAL EVOLUTION AND PRIMATE EXTINCTION IN THE MIDDLE EOCENE OF NORTH AMERICA

by

Rachel Heather Dunn

A dissertation presented to the
Graduate School of Arts and Sciences
of Washington University in
partial fulfillment of the
requirements for the degree
of Doctor of Philosophy

August 2009

Saint Louis, Missouri

ACKNOWLEDGEMENTS

I would first like to thank Sigma Xi and Washington University for financial support, without which this dissertation would not have been possible. Numerous people deserve recognition for allowing me access to fossil and modern mammal collections at several institutions. I would like to thank Richard Stucky (Denver Museum of Natural History), Eileen Westwig and Judy Galkin (American Museum of Natural History), Daniel Brinkman, Kristof Zyskowski and especially Walter Joyce (Yale Peabody Museum), Linda Gordon, Jann Thompson, Robert Purdy, and Michael Brett-Surman (National Museum of Natural History, Smithsonian Institution), Bill Stanley, Bruce Patterson and William Simpson (Field Museum of Natural History), Pam Owen, Ernie Lundelius, Tim Rowe and Chris Kirk (Texas Memorial Museum), Amy Henrici, Alan Tabrum and Chris Beard (Carnegie Museum of Natural History). In addition to collections access, Amy Henrici has been an essential part of the continuing struggle to get the fossil collection housed at Washington University under control.

Although there are times when I actually prefer the company of dead animals to people, many friends around the country made my extensive travelling infinitely more pleasant and less exhausting. Thanks to Michelle Spaulding for giving me a place to stay in New York, working in the collections late so that I could too and providing lunch and dinner company. Stuart Fox deserves thanks for a similar list of things, but also for his encouragement and friendship and for showing me aspects of New York I would never have seen otherwise. Thanks to Doug Boyer for keeping me company both in Stony Brook and in the city, and for talking shop. Thanks to Christyna Solhan and the rest of the GWU crew for giving me a much-needed night out in D. C. Stephen Chester never

failed to provide me with a surface on which to sleep, food, conversation and entertainment in New Haven regardless of how inconvenient it may have been for him at the time. Thanks to Kristine Easton and Deb Wagner for providing shelter in Chicago, for pulling strings to get me into fun exhibits, showing me awesome fossils and taking me to the good bars. A special thank you to Anjan Bullar for spending hours perusing the TMM collections, for countless nights discussing phylogeny, your unfailing enthusiasm for all things evolutionary, and your unfaltering kindness, support and encouragement.

I am grateful to my dissertation committee: Herman Pontzer, Erik Trinkaus, Glenn Conroy, Allan Larson and Jen Smith for wading through my typos and giving me essential feedback. I am particularly indebted to my advisor and committee chair Tab Rasmussen. I don't quite know where to begin. Thank you, Tab, for believing in me from the beginning, for trusting me in the prep lab, for encouraging me to think increasingly outside the primate box and for making me a paleontologist. You gave me my first fossil to study and you put me in the field, things that have become increasingly essential parts of my life and sources of joy. In a very real and tangible sense, I could not have gotten this point without you. Thank you for being my mentor and my friend.

I need to thank the people who have allowed me to maximize the time I have spent in the field. Beth Townsend and Dana Cope generously allowed me to collect as part of their crew in the Uinta Basin for two seasons and have embraced me as a colleague. I consider it an honor to have been part of the Fayum field crew headed by Elwyn Simons, Prithijit Chatrath and Erik Seiffert in 2005. Chris Kirk deserves far more thanks than I can express. He not only invited me to be a part of his field crew in the Devil's Graveyard formation in west Texas (which has always been a dream of mine),

but has encouraged and supported me as both a friend and a colleague since I met him in my last year of college. Thanks to Jon Bloch for inviting me to spend time with his Bighorn Basin crew and for indulging my fossil-identification questions. I have spent four amazing field seasons with Ken Rose and his crew. You have been an incredible mentor, I have learned so much from you (and not just through osmosis!) Thank you for my first field experience. Thank you for inviting me back again and again. Thank you for making me feel at home. Thank you for imparting to me generations of paleontological tradition and for making me a part of it. Thanks also to Amy Chew and Gina McKusick Voegele, my field partners in crime. I look forward to many years of Amy-Gina field seasons!

I am indebted to so many people at Washington University for getting me through my six years here in a professional and personal capacity. Thanks to Elaine Beffa, Kathleen Cook and Carrie O'Guin for dealing with money, paperwork and the numerous building failures. Thanks to Heather Lawson for writing me R code (and for Punk-Rock Sunday). Katie Goodenberger has been a very good sport about performing the monotonous and frustrating lab tasks that I have given her these last few months. Thanks to Kathleen Muldoon and Beth Townsend for lending a sympathetic ear. Thanks to Libby Cowgill and Catrina Adams for weight lifting and for picking me up again and again. Thanks to Jessica Joganic for taking me defense clothes shopping, numerous dinners, and many colorful dissection opportunities (to say the least). I will never forget that day and I will never forget the squirrel that does not exist. Mercedes Gutierrez deserves many, many thanks for years of friendship and support through the highs and the lows, and for being strong when I wasn't. Joseph Orkin has fed me countless times, every one

memorable and delectable. Thank you, Joe, for your puns (Bed, Bath and Beyond Thunderdome), your jokes, your loyalty, and above all your kindness and friendship. Thanks to all of my cohort for encouraging me (=giving me hell) and being an ever-reliable source of support (=distraction). I especially want to thank Chris Schaffer for being Chris Schaffer, Lisa Kelley and Anna Warrener (not in my cohort, but I'll let that slide) for being awesome office-mates, and Blaine Maley. Blaine: you were always there when it counted, you were always straight with me, and you could always make me laugh (either with joy or disgust). You are a wonderful friend. Thanks.

There is a handful of people that deserve special mention. Thank you Liza Shapiro for teaching me functional morphology. You started it. To Erika Hagler: Thank you for your seemingly unending love and enthusiastic support. Sometimes I think you're more excited about my accomplishments than I am. To Ben Sparks: until I met you I was sure no one like you existed. Thank you for your patience and your appreciation of my idiosyncrasies. I have loved sharing your time and your space this past six months. To Sierra Jarzem: words cannot suffice. You are my sister and my best friend. I would be nowhere without you. I love you.

Finally, my family has been an enduring source of support. To my mother, Rosanna Dunn: thanks for loving me and for being proud. To my grandfather, George Jackson Dunn: you are always in my heart. I am sorry you are not here to see me finish. To my grandmother, Rachel Pauline Dunn: thank you for your love of all things old, your stories and your amazing life. To my (step-) mother, Lissette Lopez: there was never any doubt in my mind that you wanted to be a part of my life. Thank you for allowing me to be a part of yours. To Lancelot and Nimue: snuggles, kisses, and treats. Thanks for

keeping me sane and loving me as long as you were fed first. To my father, Gregory Dunn: you, more than any other single person are responsible for building me. You raised me. You instilled in me a love of life, inquiry and creativity. You always trusted me to do the right thing and forgave me when I didn't. You gave me my sense of independence and responsibility, and you always put me first. I couldn't possibly recount all you have done for me, but I know I couldn't have accomplished this without you. I am proud to be your daughter. Thank you.

TABLE OF CONTENTS

LIST OF TABLES

LIST OF FIGURES

INSTITUTIONAL ABBREVIATIONS

AMNH	American Museum of Natural History, New York, NY
CM	Carnegie Museum of Natural History, Pittsburgh, PA
DMNH	Denver Museum of Natural History, Denver, CO
USNM	United States National Museum of Natural History, Smithsonian Institution, Washington, DC
WU	Washington University, Saint Louis, MO
YPM	Yale Peabody Museum, New Haven, CT
YPM-PU	Yale Peabody Museum, Princeton University Collection, New Haven, CT

ABSTRACT OF THE DISSERTATION

Mammalian Postcranial Evolution and Primate Extinction in the Middle Eocene of North America

by

Rachel Heather Dunn

Doctor of Philosophy in Anthropology

Washington University in St. Louis, 2009

Professor D. Tab Rasmussen, Chairperson

Primates constituted a dominant part of the mammalian faunas of North America during the early and middle parts of the Eocene (55-46 ma). Beginning in the Uintan North American Land Mammal Age (46-42 ma) primates declined in diversity and abundance in the Rocky Mountain region. This decline has been linked to the recession of tropical rain forests out of northern latitudes at that time. Climatic change of this magnitude would presumably have an impact on the contemporary mammalian faunas, with reduction or extinction of forest groups like primates, but perhaps radiation of mammals that preferred more open habitats such as artiodactyls. In this dissertation I describe and analyze the postcranial morphology of Uintan mammals from the Uinta Formation in Utah to address which lineages evolved to take advantage of arid habitats and which did not.

The primary goal of this dissertation is to examine the relationship between mammalian postcranial functional adaptations and habitat change in the Uintan and its implications for primate decline. To this end I: (1) describe and analyze new fossil

skeletal material from primates, rodents, insectivores and primitive eutherian mammals to reconstruct the paleobiology of these groups, (2) identify measurements of the astragalus and distal humerus that consistently discriminate open-country from closed-country taxa in a diverse sample of modern mammals, and (3) apply the astragalar measurements to a sample of artiodactyl astragali from the Uinta Formation to evaluate morphological responses to habitat change stratigraphically.

My results suggest that groups of mammals that show features related to increasing terrestriality or cursoriality in the late Uintan compared to their early Uintan or Bridgerian ancestors continue to radiate after the Uintan, whereas those that retain forest or aquatic adaptations become increasingly scarce after the Uintan. Further, I suggest that artiodactyls acquire astragalar features related to locomotion in an open-habitat gradually throughout the Uintan possibly tracking gradual habitat changes, rather than abruptly as would be expected if they were responding to a sudden drying event. These results strengthen evidence for a link between primate extinction and loss of forests in the middle Eocene.

"Lake Uinta and the surrounding countryside did not always present a picture of smiling beauty, with forests and green meadows. Instead during the later half of its existence death and starvation laid heavy hands upon the community…[T]he rains came less frequently: the very life-giving source of moisture began gradually but surely to dry up. Under the pitiless summer sun the more lush plants withered and finally gave up, weary of waiting for the rain. Animals wandered away in search of water…Indeed, after thousands of years of slow dwindling Lake Uinta finally became, at its lowest ebb, a truly horrid thing—a great festering abscess breathing its stench into the shimmering summer heat…This lowest stage in the history of Lake Uinta indicates that the climate had changed from fairly humid to arid…[T]he water became more and more shallow, and stream-laid deposits pushed ever farther and farther out into the basin until there remained only a vast alluvial plain dotted with swamps and small ponds. The streams that had so long paid tribute to Lake Uinta finally overwhelmed it and brought its rule to an end."

—Wilmot H. Bradley (1937: 286–288)

CHAPTER ONE

Introduction

1.1 Introduction

Primates of modern aspect first appear in the earliest Eocene (ca. 55 ma) and constitute a dominant and diverse part of North American early and middle Eocene faunas (Bown and Rose, 1987; Gunnell, 1997; Rose, 2006). Towards the end of the middle Eocene primate populations in the Rocky Mountain region of the continent begin to decline in diversity and abundance. By the end of the Eocene they are locally extinct in the western interior of North America (Gazin, 1958; Gunnell and Rose, 2002; Lillegraven, 1980; Rasmussen et al., 1999; Robinson, 1968; Townsend, 2004). The diversification and subsequent decline of primates is thought to be related to the proliferation of rainforests toward the poles during the early Eocene and their subsequent retreat. The initial loss of rainforests that begins in the middle Eocene occurs during a time period known as the Uintan North American Land Mammal "Age" (NALMA; 46-42 ma). This time period is the focus of this dissertation. By the Oligocene (34 ma) rainforests had retreated to a distribution similar to their modern configuration (Dunn et al., 2006; Janis, 1993; Prothero, 1996; Rasmussen et al., 1999; Townsend, 2004; Wing, 1987; Wolfe, 1992).

North American Land Mammal "Ages" have been used to divide the Eocene into intervals based on characteristics of the mammal faunas. The Uintan is the longest NALMA of the Eocene and was named for the distinctive fossil faunas found in the Uinta Formation in northeastern Utah (Berggren et al., 1992; Hintze, 1988; Prothero, 1996).

Over one third of modern mammal families worldwide appear during this time period, giving Uintan faunas a more modern taxonomic composition than earlier ones (Black and Dawson, 1966; Janis et al., 1998b; Rasmussen et al., 1999). The Uinta Formation contains terrestrial fossiliferous sediments that span this period of primate decline and habitat degradation (Prothero, 1996; Townsend, 2004; Townsend et al., 2006; Walsh, 1996). An analysis of the community structure of early and late Uintan faunas from the Uinta Formation indicates that the faunal communities found within the formation show a change in taxonomic and ecological configuration consistent with loss of a tropical environment. This shift is coincident with the decline in primate taxa that is occurring during this time both within the formation and throughout the western interior of North America (Townsend, 2004).

The purpose of this dissertation is to extend this work to look specifically at functional adaptations of individual mammal taxa, including primates, during this critical time period. In this chapter, I briefly discuss previous studies of Eocene climate change, introduce the Uinta Formation and discuss the history of study in this area, introduce relevant fossil mammal groups of the Uinta Formation, and discuss ecomorphological approaches to habitat reconstruction. I then present the research questions addressed in this dissertation.

1.2 Eocene Faunal Transitions

The co-occurrence of faunal turnover and environmental change is well documented in the fossil record. In particular, three Eocene faunal transitions have been well studied with respect to climatic and environmental change. The first occurs at the Paleocene-Eocene boundary (55 ma). This boundary is associated with increasing global

temperatures, the spread of tropical rain forests north and south of the equator to encompass most of the globe, and the appearance of the first true primates (Fairon-Demaret and Smith, 2002; Maas et al., 1995; Rose, 2006; Rose and O'Leary, 1995; Wilf, 2000). The second major transition is the Wasatchian-Bridgerian boundary (52 ma) representing the transition from early to middle Eocene faunas. This boundary is curious in that there is extensive faunal turnover at this time, but there is little evidence for significant differences between the environment of the late Wasatchian and early Bridgerian (Gunnell, 1997; Stucky, 1992). The Bridgerian-Uintan boundary is poorly studied, but is important in the context of the climatic deterioration that began in the middle Eocene. The third well-documented boundary is the Eocene-Oligocene boundary at the end of the Eocene (34 ma). It is at this time that all but a few primates become extinct in the northern continents, associated with increasing seasonality and aridity, and the spread of more open habitats especially in the western interior of North America and Europe (Hooker, 1992; Prothero, 1992; Stucky, 1992; Legendre and Hartenberger, 1992; Blondel, 1998).

1.2.1 Paleocene-Eocene Boundary

The Paleocene-Eocene transition in the Northern Hemisphere shows an increase in mammal diversity, the appearance of the modern mammalian orders Perissodactyla, Artiodactyla and Euprimates (or “primates of modern aspect”), and the extinction of archaic mammal groups such as the majority of the plesiadapiforms and multituberculates (Bloch et al., 2007; Bowen et al., 2002; Gingerich, 1976; Maas et al., 1988; Robinson et al., 2004; Rose, 1981, 2006; Rose and O'Leary, 1995; Rose and Walker, 1985; Theodor, 1996). The dramatic increase in mammal diversity in the Wasatchian of North America is

due in large part to dispersal of mammals from Europe and Asia, all of which were connected during the late Paleocene until the middle Eocene (Janis, 1993). Mammals that dispersed into North America at this time include perissodactyls, artiodactyls, primates and the extinct creodont family Hyaenodontidae (Beard and Dawson, 1999; Bowen et al., 2002; Maas et al., 1995; Smith, 2006; Stucky, 1992). Wasatchian mammal communities experienced a warmer climate than the Paleocene fauna although closed tropical forests characterized both time periods (Clyde, 1998; Wilf, 2000; Wing et al., 1995; Wing and Harrington, 2001). Analysis of carbon isotopes across the Paleocene-Eocene boundary indicates that this warming was caused by an expulsion of sedimentary methane into the atmosphere that caused rapid global increase in mean annual temperature and contributed to the thermal event called the Paleocene-Eocene Thermal Maximum (PETM; Currano et al., 2008; Magioncalda et al., 2004; Smith, 2006).

1.2.2 Wasatchian-Bridgerian Boundary

The Wasatchian-Bridgerian boundary in the Rocky Mountain region of western North America occurs during a time period of warm climate and high mammal and reptile diversity (Clyde, 1998, 2001; Hutchison, 1992). The Holarctic continents remained connected, as during the early Eocene (Janis, 1993). This transition is well defined biostratigraphically and is characterized by several taxonomic first and last occurrences, an increase in the diversity of perissodactyls, rodents and artiodactyls, and a decrease in the diversity of condylarths (Clyde, 1998, 2001; Krishtalka and Stucky, 1984; Robinson et al., 2004). The diversity of primates remains high although relative abundances within groups of primates change somewhat (Gunnell, 1997). The climate and environment of the late Wasatchian and early Bridgerian do not appear to be

fundamentally different based on analyses of mammal and reptile diversity and community structure (Gunnell, 1997; Hutchison, 1992; Stucky, 1992), although an analysis of paleosols indicates that the Bridgerian was characterized by more flooding (Gunnell, 1997).

1.2.3 Eocene-Oligocene Boundary

The Eocene-Oligocene transition from moist tropical to arid and seasonal conditions in Europe is marked by a major faunal turnover event called the "Grande Coupure" (Blondel 1998, 2001; Hooker 1992; Hooker et al., 1995, 2004; Legendre and Hartenberger 1992). During this time and beginning in the late middle Eocene, North America became separated from Europe to the east, but remained in contact with Asia via the Beringean land bridge (Janis, 1993). In contrast, the Oligocene climatic crash in North America was preceded by more gradual environmental deterioration beginning in the middle Eocene (Bradley, 1937; Gazin, 1958; Hutchison, 1992; Prothero, 1985, 1996; Prothero and Swisher, 1992; Terry, 2001). Evidence from several sites in the continental interior of North America suggests that the climatic deterioration occurred from west to east (Evanoff et al., 1992; Terry, 2001). Deposits in Oregon, San Diego, and the eastern Gulf Coast indicate that forests persisted into the late Eocene in coastal regions of North America (Retallack, 2007; Retallack et al., 2004), suggesting that increasing aridity began in the continental interior and spread outward towards the coast (Stucky, 1992). Despite differences in the rate of transition between the two continents, evidence indicates that the change in climate was a global phenomenon associated with increasing seasonality and decreasing winter temperatures (Hutchison, 1992; Ivany et al., 2000; Miller, 1992; Terry, 2001). This global climate crash is associated with the radiation of

rodents and artiodactyls, the dramatic decline in the archaic groups Condylarthra, Apatotheria, and Pantolesta, and near extinction of primates in the Northern Hemisphere (Blondel, 1998, 2001; Gunnell and Bartels, 1999; Hooker, 1992; Köhler and Moyà-Solà, 1999; Legendre and Hartenberger, 1992; Stucky, 1992).

1.2.4 Bridgerian-Uintan Boundary

The Bridgerian-Uintan boundary is poorly studied in part because there are very few fossil-bearing localities containing latest Bridgerian and earliest Uintan sediments (Prothero, 1996). The early Uintan is characterized in part by the abundance of selenodont artiodactyls, which were absent during the Bridgerian. Paleobotanical data suggest that the late Eocene climatic deterioration began in the late Bridgerian (Stucky, 1992; Wing, 1987); however, analysis of mammal communities from the late Bridgerian and early Uintan suggests that the habitat was still characterized by closed forests (Townsend, 2004). Late Uintan sediments and fauna, specifically from the Uinta Formation in northeastern Utah, suggest that the climate was drier than during the early Uintan in the continental interior. Thus the upper Uinta Formation may represent the first evidence of increasing aridity during the gradual climatic deterioration of the later Eocene (Townsend, 2004). This will be discussed in greater detail in the sections that follow.

1.3 History of Study in the Uinta Formation

Mammals from the Uinta Formation were first collected by O. C. Marsh of the Yale Peabody Museum in 1870 (Marsh 1875a, b; Rasmussen et al., 1999) and again in the 1880s by Francis Speir of Princeton University (Rasmussen et al., 1999; Scott and Osborn, 1887; Scott and Osborn, 1890). Although Marsh (1875b) made a preliminary

report on fossils found during the Yale expeditions, Scott and Osborn (1887, 1890) were the first to attempt a thorough description of the mammal fossils from the Uinta Formation. They noted that the Uinta Formation was distinct from the Bridgerian in the more modern taxonomic configuration of the fossil faunas and regarded it as latest Eocene in age (Scott and Osborn, 1890). In 1893 and 1894, O. A. Peterson led American Museum of Natural History expeditions to the Uinta Formation (Osborn, 1895). In the early 1900s the Field Museum sent an expedition (Black and Dawson, 1966; Riggs, 1912) and the Carnegie Museum began regular expeditions to the Uinta Formation that continued for the first half of the century (Black and Dawson, 1966; Peterson, 1919; Rasmussen et al., 1999). In 1993, Washington University began leading regular expeditions to the Uinta Formation specifically to recover small mammals, which had been overlooked by many earlier expeditions (Rasmussen et al., 1999). In this section, I review what is currently known about the stratigraphy and paleoecology of the Uinta Basin within a historical framework, with emphasis on the Uinta Formation in particular.

1.3.1 Lithostratigraphy of the Uinta Formation

The Uinta Formation has a complicated stratigraphic history. This is due to two major issues: (1) multiple redefinitions of lithological boundaries, and (2) the conflation of lithological with biochronological units. Lithological units are defined on the basis of physical properties of the rocks and reflect the processes that were occurring at the time of deposition of the specific lithological unit (Walsh, 1998a). Two depositional environments that occur synchronously, such as lacustrine and alluvial environments, produce two different contemporaneous lithological facies, so there is usually not a tight correspondence between differences in lithology and differences in time. The first person

to divide the Uinta Formation into lithological units was O. A. Peterson (in Osborn, 1895), who designated 3 members: the Uinta A, B, and C. The Uinta A member was defined as "hard brown sandstones immediately overlying the Green River Shales" and the Uinta B as the "[s]oft coarse sandstones and clays" immediately overlying Uinta A (in Osborn, 1895). The Uinta C, also called the "true Uinta" by Peterson, was noted to be the most fossiliferous section of the formation and was distinguished from the Uinta B by the dominance of red beds in contrast to the predominantly gray to greenish color of the older rocks (Figure 1.1; Osborn, 1895).

In the same paper, Osborn (1895) attempted a preliminary biostratigraphy of the Uinta Formation based mainly on the presence of different brontothere taxa within each of Peterson's lithological members. Osborn (1895) called the Uinta C the "*Diplacodon elatus* beds" and distinguished them from the other members by the presence of certain taxa considered by him to be indicative of the "true Uintan" (*Protoreodon*, *Leptotragulus* and *Diplacodon*). He called the Uinta B the "*Telmatotherium cornutum* beds" and considered this member transitional in faunal composition between the early Uintan Uinta A and the true Uintan. Finally, he named the Uinta A "*Telmatotherium megarhinum* beds" and distinguished this stratum from the overlying members as well as the earlier Bridgerian by the presence of *Amynodon*, *Triplopus*, and *Uintatherium* (Osborn, 1895). In so doing, Osborn (1895) made the assumption that the lithological members of the Uinta Formation corresponded with distinct chunks of time, each with its own distinct fauna that lived during that time rather than treating faunal succession as independent of lithology.

Osborn (1929) made the first modification to the stratigraphic placement of

Peterson's original member boundaries. He shifted the contact between the Uinta A and B members stratigraphically lower, designating Uinta A as only the non-fossiliferous zone at the base of Peterson's original Uinta A, and naming the upper part of the original Uinta A "Uinta B1" (Prothero, 1996; Townsend et al., 2006). Although there seems to have been historical agreement on the relocation of the Uinta A/B boundary, or at least to the subdivision of the Uinta A into "upper" and "lower" (Douglass, 1914), there has been less agreement on the location of the Uinta B-C boundary (Walsh, 1996). Douglass (1914) stated that the matter of the Uinta B-C boundary had been discussed by himself, Peterson, Osborn and Riggs and that he and Peterson were in agreement (p. 420), which presumably means that Osborn and Riggs had differing opinions. Nevertheless, Osborn (1929; and Osborn and Matthew, 1909) relocated the Uinta B-C boundary to the "*Amynodon* sandstone" (of Riggs, 1912), well below Peterson's original designation. This change was made on the basis of perissodactyl taxonomy, again conflating the ideas of lithological units and biological units. At the time, Osborn considered the *Amynodon* sandstone to be laterally continuous across the Uinta Basin based on the work of Riggs (1912). However, further investigation into the stratigraphy of the basin revealed that the *Amynodon* sandstone was not one laterally continuous bed but one of a series of channel sandstones located at various stratigraphic positions throughout the basin (Cashion, 1986; Robinson et al., 2004; Townsend, 2004; Townsend et al., 2006).

Finally, Wood (1934) combined the Uinta A and Uinta B (of Osborn, 1929) together into the Wagonhound Member and named the Uinta C (of Osborn, 1929) the Myton Member, decreasing the number of members in the Uinta Formation from three to two, although Uinta A, B, and C were (and are) still widely used.

Townsend (2004; and Townsend et al., 2006) has advocated returning the Uinta B-C boundary to Peterson's original location due to the variability in stratigraphic position of the *Amynodon* sandstone and due to the fact that the floodplane strata just above the channel sandstones do not differ lithologically from those immediately below them, therefore not warranting distinction as a separate lithological unit.

1.3.2 Biostratigraphy of the Uinta Formation

As a result of these boundary changes, it is often difficult to determine from which member a fossil was collected (Prothero, 1996; Robinson et al., 2004; Walsh, 1996). Fossils that were collected before the publication of Osborn's 1929 revision, for example, may be recorded as being from simply the Uinta A but would now be regarded as coming from the Uinta B1 member. Similar issues exist with specimens collected early on from the Uinta B and Uinta C. This together with the poor stratigraphic resolution of early collections and lack of micromammals in historical Uinta Basin collections has made it difficult for researchers to compile a precise and reliable biostratigraphy of the Uinta Formation (Prothero, 1996; Robinson et al., 2004; Townsend, 2004; Townsend et al., 2006; Walsh, 1996).

Another hindrance to the compilation of a thorough biostratigraphy of the Uinta Formation is the fact that most researchers have explicitly defined the early/late Uintan faunal transition as coincident with the Uinta B-C lithological boundary despite the fact that the placement of the B-C boundary should have no effect on the placement of the early-late Uintan transition (Walsh, 1996). Often "early Uintan" and "Uinta A time" or "Uinta B time" were considered synonymous terms (also "late Uintan" and "Uinta C time"), which assumes that the Uintan members were all deposited at the same time and

span the same amount of time across the Uinta Basin. This is not the case, however, as the upper part of the Uinta B in the western part of the Uinta Basin was deposited at the same time as the lower Uinta C in the eastern Uinta Basin. The contact between the Uinta Formation and Duchesne River Formation is likewise time transgressive (Walsh, 1996).

Following the preliminary biostratigraphy from his earlier paper (Osborn, 1895), Osborn (1929) named each lithologic unit for the brontothere taxa within it but gave little detail in justification (Prothero, 1996). Later authors did not use Osborn's (1929) biostratigraphic names but instead continued to discuss the age of fossils in lithological terms (Wood et al., 1941). Gunnell (1989) designated Ui1 and Ui2 faunal zones based upon the appearance of *Epihippus* in Ui1 and upon the appearance of camelids and canids in Ui2, but noted that Ui1 encompassed all of Uinta A and B (the Wagonhound Member of Wood, 1934) and that Ui2 consisted of Uinta C (Wood's Myton Member). Although the names were new, it was assumed that the taxonomic units were roughly equivalent to the members, and no real effort was made to ascertain whether this was, in fact, true. Later Robinson et al. (2004) expanded the number of biochrons to three (Ui1, Ui2 and Ui3) and based their definition upon Uintan age fossils from Texas, Wyoming and southern California (Black and Dawson, 1966; Gunnell, 1989; Robinson et al., 2004) where there is more stratigraphic control. Fossils from the historic Uinta Formation collections for which the stratigraphy is uncertain were added onto this framework (Robinson et al., 2004).

The fact that recent attempts to divide the Uintan into biostratigraphic units incorporate fossils from several different formations is helpful in disengaging the names of the members of the Uinta Formation from biochronology, but many of the taxa used in

these attempts have not been studied in a precise stratigraphic context within the Uinta Basin. The faunal transition from the early to the late Uintan has recently been refined using the stratigraphically precise locality data of the Washington University Uinta Formation collection containing over 1000 identified specimens of approximately 50 mammalian genera and over 200 localities from the Uinta B2 and Uinta C (Townsend, 2004; Townsend et al., 2006). From these analyses it appears that the beginning of the faunal transition occurs 14-17 meters lower than the lithological Uinta B-C transition as originally defined by Peterson and approximately 59 meters above the *Amynodon* sandstone (Townsend, 2004; Townsend et al., 2006). Two of the genera used to designate this early Uintan-late Uintan boundary (Townsend, 2004; Townsend et al., 2006), *Mesomeryx* and *Protoptychus*, were also used by Robinson et al. (2004), which is a positive step towards integration of new micromammals from the Uinta Basin collections into the continental Uintan biostratigraphy.

1.3.3 Paleoenvironment of the Uinta Basin

The Eocene Epoch was a time in which tropical to sub-tropical environments dominated the Northern Hemisphere (Clyde, 1998; Janis, 1993; Novacek, 1999; Retallack et al., 2004; Rose, 2006; Wilf, 2000; Wing et al., 1995; Wing and Harrington, 2001; Wolfe, 1992). In Europe, these conditions changed abruptly at the end of the Eocene in an event called the "Grande Coupure" to the more seasonal arid conditions that persisted during the Oligocene. Approximately 60 percent of European mammals including most primates became extinct at this event (Blondel, 2001; Hooker, 1992; Hooker et al., 2004; Hooker et al., 1995; Legendre and Hartenberger, 1992). In contrast, North America experienced a more gradual environmental deterioration beginning in the

middle Eocene of the continental interior, preceding the transition from tropical to seasonal climates (Hutchison, 1992; Prothero, 1985; Prothero, 1994; Retallack et al., 2004; Stucky, 1992). Several lines of evidence suggest that the Bridgerian was still mainly tropical (Gunnell et al., 1995; Townsend, 2004). The earliest signs of continental aridification appear in the Uinta Formation. Sediments from the Uinta B indicate wet conditions during the time of deposition, whereas Uinta C sediments indicate more arid conditions (Bradley, 1937; Gazin, 1955; Gazin, 1958; Rasmussen et al., 1999; Townsend, 2004; Townsend et al., 2006). Additional faunal evidence suggests that the climate of the late Uintan was drier than the early Uintan in the continental interior (Hutchison, 1992; Stucky, 1992).

Based on the transition from lake deposits in the underlying Green River Formation to alluvial deposits in the Uinta Formation, Bradley (1937) was the first to suggest that the Uinta Formation underwent a drying event that affected the faunal community. Gazin (1955, 1958) reiterated Bradley's assertion and used it to explain the increase in artiodactyl diversity and decrease in primate diversity throughout the Uinta Formation. The most recent analysis of Uinta Formation paleoclimates is that of Townsend (2004). She used ecomorphological analysis of faunal communities from several faunal assemblage zones from the late Bridgerian to early Uintan of the Bridger Basin, Wyoming, and the early to late Uintan of the Uinta Basin, Utah, to assess the timing and degree of environmental change in the Rocky Mountain region of North America. Her analysis revealed a shift in community structure within the Uinta Formation that roughly coincides with both the lithological transition from the Uinta B member to the Uinta C member and the faunal transition from the early Uintan to the late

Uintan (Townsend et al., 2006).

Townsend (2004) used diet and locomotor variables of 20 extant Neotropical mammal communities to distinguish between four macrohabitats that were defined on the basis of percent tree cover, annual rainfall, and general climate. She divided the Uinta Formation fauna into three faunal assemblage zones (FAZ) to represent three communities characteristic of the Uinta Formation at different points in time (Townsend, 2004; Walsh, 2000). The fauna from the first Uinta Formation FAZ (UFAZ1) falls closest to woodland habitats in community structure. UFAZ2 was classified as being more open than UFAZ1 but with some tree cover. Both of these zones fall within Uinta B rocks. The large component of primates and other small mammals that inhabit primarily closed environments suggests that the environment of the early Uintan included at least a moderate amount of tree cover, and the presence of larger bodied cursorial, folivorous forms such as perissodactyls and artiodactyls suggests that there were at least some open savannah-like patches. The proportion of large-bodied terrestrial taxa relative to small-bodied arboreal taxa increases in UFAZ2.

Faunal Assemblage Zone 3 most closely resembled the modern Neotropical open habitats examined in her study (Townsend, 2004). The UFAZ3 fauna is characterized by few small arboreal and frugivorous taxa and a lack of insectivorous taxa. It is dominated by terrestrial taxa, especially the larger, more cursorial folivorous mammals such as artiodactyls and perissodactyls. Only one species of primate, *Mytonius hopsoni*, is found in Uinta C rocks, and it is rare. These findings suggest that a significant amount of aridization had occurred by the late Uintan and might have begun slightly earlier.

The rough co-occurrence of these three transitions (lithological, taxonomic and

community) in the Uinta Formation suggests that a change in climate or habitat occurred at this time (Townsend, 2004).

1.4 The Uintan Fossil Fauna

An understanding of the biological role of all Uintan mammals is important to the study of habitat change and primate decline within the Uinta Formation. It allows us to evaluate potential niche overlap of non-primates with primates and also allows us to evaluate which niches were being filled by members of the faunal community, which in turn informs us about the habitat in which the animals lived (Bock and Wahlert, 1965). This can be demonstrated with several hypothetical scenarios: If primates were to decline at the same time as other arboreal specialists continued to thrive, this would imply that primate decline was not due to loss of arboreal habitats, whereas if all taxa that exploited arboreal resources were to become rare, loss of habitat would appear to be the cause of the decline. In another scenario, if it were found that most taxa were not capable of exploiting arboreal substrates, it would suggest that the arboreal habitats available to primates were limited and again imply that the lack of primates was due to loss of arboreal habitats. These examples demonstrate how other members of the faunal community can be used to inform our view about the habitat in which they lived and about the taxa with which they coexisted. Primates themselves can also contribute to understanding their decline: if one discovered that primates showed anatomical evidence of becoming becoming more terrestrial, this would suggest that primates were adapting to a more terrestrial way of life, in which case, their decline could not be tied to loss of arboreal habitats.

Ideally, to evaluate the hypothesis of habitat change, one would like to sample the

entire fauna before and after an event to compare the adaptations of the whole faunal community and those within individual lineages. Unfortunately, not all members of the faunal community make it into the fossil record, and even fewer of them are known from adequate postcranial remains to allow a functional assessment. Fortunately, the Uinta Formation is unique in its abundance of postcranial relative to dental remains (Rasmussen et al., 1999; Townsend et al., 2006). Several taxa are represented either by single fairly complete associated specimens or many fragmentary remains that can be evaluated together as a composite. The taxa addressed in this dissertation are introduced below.

1.4.1 Primates

Four genera and species of primate are currently known from the Uinta B member of the Uinta Formation: three relatively large bodied omomyids, *Ourayia uintensis, Chipetaia lamporea* and *Macrotarsius jepseni* (Dunn et al., 2006; Rasmussen, 1996; Rasmussen et al., 1999; Robinson, 1968) and a new species of the anaptomorphine *Trogolemur* (Rasmussen, 1996; Rasmussen et al., 1999). *Chipetaia lamporea* is known only from a single locality in the Uinta Formation (Rasmussen et al., 1999). Robinson (1968) named *Hemiacodon jepseni* from a single specimen (YPM-PU 1631) originally identified as *Ourayia uintensis* (Simons, 1961) from the Princeton Museum collections, citing slight differences in the morphology of the P_4 and $M_{1\text{-}2}$. It was subsequently returned to *Ourayia uintensis* by Szalay (1976) and revalidated as *Macrotarsius jepseni* by Krishtalka (1978). Most authors since have followed Krishtalka (Beard et al., 1992; Gunnell, 1995; Gunnell and Rose, 2002) in retaining the specimen as distinct from *O. uintensis*, although no other specimens have been found. Continuing collection in the Uinta Formation has yielded a much larger sample of *O. uintensis* (Robinson had only 6

specimens for comparison in 1968) including relatively un-worn specimens. Based upon this expanded sample, it is likely that *M. jepseni* represents a young specimen of *O. uintensis* (Rasmussen, pers. comm.). *Ourayia* is known also from the Uintan of Wyoming, southern California and Texas.

Robinson (1968) erected a new subfamily, Mytoniinae, and a new genus and species, *Mytonius hopsoni*, for two large omomyine specimens from Uinta C beds. The validity of this genus was considered questionable by Szalay (1976), who synonymized the genus with *Ourayia uintensis*. Krishtalka (1978) revalidated the genus and species, and Gunnell (1995) transferred *M. hopsoni* to the genus *Ourayia* but kept the species-level distinction. Most recently, Kirk (2007) has revived the genus *Mytonius* based on features of the upper dentitions recently recovered from Texas. *Mytonius hopsoni* is the only primate known from dental remains from the Uinta C member of the Uinta Formation and is also known from the Uintan of Wyoming, California and Texas.

Until recently, these Uintan omomyids were not known from postcrania. The omomyid genera best represented postcranially were the Bridgerian omomyines *Omomys* (Anemone and Covert, 2000) and *Hemiacodon* (Simpson, 1940), and the Wasatchian anaptomorphines *Arapahovius* (Covert and Hamrick, 1993; Savage and Waters, 1978) and *Absarokius* (Covert and Hamrick, 1993). These taxa are younger than the Uintan omomyids and all are below 500 g in body mass (Dunn et al., 2006). In contrast, *Chipetaia* has been estimated to have a body mass between 500 and 700 g and *Ourayia uintensis* a body mass of approximately 1500 – 2000 g (Dunn et al., 2006). Recent recovery of hindlimb elements belonging to *O. uintensis* and *C. lamporea* indicates that these mammals were specialized for arboreal leaping and thus dependent on trees (Dunn

et al., 2006). Since the publication of these elements, more primate postcrania have been recovered from Uinta Formation collections (Dunn, 2007), including a damaged distal tibia, complete astragalus and partial calcaneus of *C. lamporea*, and a distal tibia, distal femur, astragalar head and cuboid of *O. uintensis*. A complete calcaneus of *Ourayia* has been collected from southern California. The first postcranial remains of *M. hopsoni* and of a new smaller species of primate from the Uinta C have also been found in the Carnegie Museum collection housed at Washington University. These new elements allow a more complete analysis of the postcranial adaptations of the Uintan omomyids.

1.4.2 Rodentia

Uintan rodents are represented by forms as small as *Microparamys* with individual molars measuring less than a millimeter in length, up to animals as large as *Pseudotomus eugenei*, which was comparable in size to contemporary horses and medium sized artiodactyls (Dunn and Rasmussen, 2007; Rasmussen et al., 1999; Townsend, 2004). Especially diverse during the Uintan were the large bodied manitshine rodents in the subfamily Paramyinae (Korth, 1994; Wood, 1962), for which fragmentary postcrania are known but poorly studied. The Uinta C member has recently yielded the virtually complete skeleton of *Pseudotomus eugenei*, which allows a thorough behavioral assessment of these large rodents (Dunn and Rasmussen, 2007). Another common paramyine rodent, especially in the Uinta B, is *Uintaparamys leptodus*. This species was previously assigned to the genus *Leptotomus* by Wood (1962). However, this genus was found to be preoccupied by a beetle by McKenna and Bell (1997; Anderson, 2008); the correct name is *Uintaparamys* Kretzoi 1968. A complete associated skeleton for this taxon is not known, but enough partial material is known to allow a more thorough

analysis than has been attempted previously (Wood, 1962).

The earliest manitshines are Bridgerian in age and belong to the genus *Pseudotomus* (Korth, 1994; Matthew, 1910; Simpson, 1941; Wood, 1962). During the Bridgerian, manitshines were not particularly diverse, being represented by only two well-defined species, *P. horribilis* and *P. robustus*, from the Bridger Basin, Wyoming (Korth, 1985; Wood, 1962). Manitshines reach their peak species diversity during the Uintan (Korth, 1994). During that time they were also geographically widespread, with records from California, Utah and Texas (Korth, 1985; Korth, 1994; Wood, 1962). After the late Uintan, manitshine fossils are conspicuously absent with the sole exception of *Manitsha tanka* from the Orellan of South Dakota, which is known only from the type specimen (Korth, 1994; Simpson, 1941). Although many of the Bridgerian and early Uintan manitshines are represented by both dental and skeletal elements, the later Uintan and Oligocene manitshines are poorly known (Wood, 1962).

The locomotor behavior of manitshines has remained unresolved since the definition of the tribe by Simpson in 1941. In his 1962 monograph, Wood agreed with Matthew (1910) and Simpson (1941) that the older members of the Paramyinae belonging to the genus *Paramys* were most likely arboreal but noted that the morphology of the manitshines is ambiguous.

The new skeleton of *Pseudotomus eugenei*, a very large bodied late Uintan paramyine known only from the Uinta Formation, represents the most complete manitshine specimen known, and allows direct comparison to all other manitshine skeletons. The skull is crushed and distorted, but most of the axial and appendicular skeleton is in remarkably good shape with only minor damage and affords the unique

opportunity to evaluate behavioral adaptations and diversity of the Manitshini.

Uintaparamys occurs in the Bridgerian and early Uintan. The only previous analysis of locomotor behavior for this genus concluded that all members of this genus were accomplished diggers that probably fed on soft tubers and bulbs (Wood, 1962). In contrast, the postcranial specimens at Washington University suggest that *U. leptodus* was arboreal.

1.4.3 Insectivora

During the Tertiary (65 to 1.8 Ma) there were at least five families of erinaceomorphs and numerous genera of uncertain familial affiliation found throughout North America, Europe and Asia (McKenna and Bell, 1997; Rose, 2006). Matthew (1909) suggested that extant members of Insectivora were specialized remnants of the more diverse and abundant early Tertiary group, the members of which played a more central role in their ecosystems. It might be expected that early Tertiary insectivorans manifest a wider range of morphologies and adaptations than those surviving today. This idea seems to be well supported for Erinaceomorpha, and for Insectivora as a whole, based on paleontological work that has led to the discovery of many extinct insectivoran groups (Bown and Shankler, 1982; Krishtalka, 1976; Lillegraven et al., 1981; Novacek, 1976, 1985; Novacek et al., 1985; Van Valen, 1967; Walsh, 1998b).

Whereas insectivores are known from the Uinta Formation, they are rare and fragmentary in comparison to other similarly sized taxa such as rodents (Rasmussen et al., 1999). One new genus and two new species of erinaceomorph insectivores have been recovered from the Uinta B member of the Uinta Formation. The new insectivores are notable for two reasons, the first being their large size. The new taxa are larger than any

North American erinaceomorphs from the earlier Wasatchian and Bridgerian land mammal ages, and are matched or exceeded in size only by other Uintan and Duchesnean erinaciomorphs known from southern California (Walsh, 1996, 1998b).

The new erinaceomorphs are also notable because both are known from associated postcrania, unlike most Eocene insectivores, which are represented only on the basis of published teeth, jaws and cranial fragments. The postcranial elements recovered from Utah provide the basis for analyzing the locomotor behavior and adaptations of the new erinaceomorphs and allow inference as to the type of habitat in which they lived within the Uinta Formation.

1.4.4 Pantolestidae

Several groups of "insectivore-grade" mammals are included in the unnatural group Cimolesta (McKenna and Bell, 1997). There is no indication that this group is monophyletic and many of these taxa are placed into their own orders as their phylogenetic affinities remain uncertain (Boyer and Georgi, 2007; Rose, 2006). Three groups of cimolestans are found in the Uinta Formation: Pantolestidae (often put into the order Pantolesta), Apatamyidae (often referred to the order Apatotheria) and *Simidectes* (sometimes suggested to belong to the Pantolesta). Of these groups, pantolestids and apatemyids are known from good skeletal remains from the early Eocene Green River Formation in Wyoming and from the middle Eocene Messel locality in Germany (Koenigswald et al., 2005; Matthew, 1909; Rose and Koenigswald, 2005), but nothing has been reported from as late as the Uintan. No associated postcranial remains of *Simidectes* have been reported from the Uinta Formation to date.

Pantolestidae is a group of primitive mammals of poorly understood phylogenetic

affinities known from the Paleocene through the early Oligocene in North America, Europe, Asia and possibly Africa (Boyer and Georgi, 2007; Rose and Koenigswald, 2005). Their teeth suggest an omnivorous diet, and fossilized stomach remains of the middle Eocene European genus *Buxolestes* from Messel, Germany reveal a diet including fish and other vertebrates (Rose and Koenigswald, 2005). Ecologically they appear to have been similar to river otters and beavers in being semi-aquatic and good burrowers (Rose and Koenigswald, 2005). Postcrania are well known for the North American Bridgerian pantolestids *Palaeosinopa* and *Pantolestes natans*, and for the middle Eocene *Buxolestes* from Germany (Matthew, 1909; Rose and Koenigswald, 2005). Isolated postcranial remains for other North American Bridgerian pantolestids have also been reported (Matthew, 1909; Rose and Koenigswald, 2005).

Although pantolestids occur in the Uintan of North America, they have received little or no attention. Three species of *Pantolestes* have been reported from the early Uintan Washakie B member of the Washakie Basin, Wyoming (McCarrol et al., 1996), and *Pantolestes natans* has been reported from the early Uintan of the Sand Wash Basin, Colorado (Stucky et al., 1996), but these are reported only in faunal lists and no new species of pantolestids have been described that are Uintan in age. No pantolestids have been reported from the Uinta Formation. However, there are at least four species of pantolestid in the Washington University collection, at least one of which is new. An unidentified pantolestid specimen in the Peabody collection at Yale University consisting of a complete mandibular postcanine dentition and partial postcranium is referable to the Uinta B2. This specimen is the most complete Uintan pantolestid known and has rested peacefully in a drawer at Yale University since 1936 identified only as “Insectivore?”

More fragmentary postcranial material belonging to a range of different pantolestids has been found in the CM collections housed at Washington University.

An important question to ask in the analysis of the postcranial adaptations of this Uintan pantolestid specimen is how dependent on an aquatic environment was it? It is well established that Bridgerian pantolestids had aquatic adaptations and probably spent their lives in and around bodies of water (Matthew, 1909; Rose and Koenigswald, 2005). In the increasingly arid Uintan of the Uinta Formation pantolestids could potentially show fewer aquatic characteristics than their older relatives. Alternatively, they may retain aquatic skeletal specializations and be restricted only to certain areas of the basin where slowly shrinking pools of water preserved a more typically Eocene environment.

1.4.5 Artiodactyla

Among modern large herbivores there are two dominant orders, the Perissodactyla, or odd-toed ungulates, and the Artiodactyla, the even-toed ungulates. In geologically recent times, and continuing to the present, artiodactyls have been the most diverse of these two groups, but this has not always been true. In the early and early middle Eocene the perissodactyls were both more abundant and more diverse than the artiodactyls. In the Middle Eocene, and especially in the Uintan, the artiodactyls begin to surpass the perissodactyls in diversity and establish their position as the dominant large-bodied herbivores that persist today (Black and Dawson, 1966; Rasmussen et al., 1999). An important component of this middle Eocene radiation of artiodactyls is the evolution and diversification of selenodont artiodactyls, which contrast with the more primitive bunodont artiodactyls in having sharp crescent-shaped cusps and crests on their teeth that are adapted for processing tough fibrous plant material. The presence and spread of

selenodonty might indicate the beginning of a grazing lifestyle, as opposed to the less specialized, omnivorous diets of earlier artiodactyls.

The main artiodactyl groups in the Uinta Formation are the Dichobunidae, Homacodontidae, Agriochoeridae, Oromerycidae, and the Protoceratidae. The dichobunids are generalized primitive forms with bunodont dentitions and are relatively rare in the Uinta Formation. The homacodonts are a group of buno-selenodont small-bodied artiodactyls. In general their dentitions are generalized and their molar crowns are squarer, but they demonstrate the development of some selenodont features. The smallest homacodont, *Mesomeryx*, is known postcranially from several unassociated ankle bones. These indicate that the homacodonts retained the full complement of five digits on the hind foot and that the lateral digits were becoming reduced in size. The tarsals of *Mesomeryx* had also undergone minimal fusion (Townsend and Rasmussen, 1995). This evidence suggests that the homacodonts were not specialized cursors but more generalized in their locomotor adaptations and similar to earlier Wasatchian and Bridgerian artiodactyls (Rasmussen et al., 1999; Rose, 1985).

The remaining families are all characterized by the development of true selenodont molars. The agriochoerid *Protoreodon* is the most common artiodactyl in the Uinta Formation. The teeth of *Protoreodon* have a selenodont morphology but tend to be wider and retain more accessory cusps than do those of the other selenodont artiodactyl families. *Protoreodon* is fairly well known postcranially, and demonstrates a generalized postcranium with the retention of all five metatarsals and without the elongation of the limbs seen in more cursorial forms (Theodor, 1999). The oromerycids are more specialized than the agriochoerids in both dentition and in postcranial morphology. They

have more slender, high-crowned teeth that are more suited for cutting fibrous foods, and elongate and gracile limbs with greatly reduced lateral digits characteristic of cursorial taxa. The oromerycids are a rare component of the Uintan fauna (Theodor, 1996). The Protoceratidae is represented primarily by *Leptotragulus*, the second most common artiodactyl of the Uinta Formation. Dentally they are more specialized than the agriochoerids but not as specialized as oromerycids. Postcranially they are poorly known (Rasmussen et al., 1999; Townsend, 2004). It has long been noted that there is an inverse relationship between primate and artiodactyl diversity during the Uintan of North America (Gazin, 1955, 1958; Gunnell and Bartels, 1999; Stucky, 1992; Williams and Kirk, 2008); both have been linked to loss of trees. This makes artiodactyls a particularly interesting group when addressing habitat change and primate decline.

1.5 Ecomorphology

In order to assess whether individual lineages of mammals are adapting to changing environments during the time encompassed by the Uinta Formation, it is necessary to have a good sample of these taxa from various stratigraphic levels within the formation. Whole skeletons hold the most information about adaptations, but they are not abundant enough to be useful in a statistical sense. One way to increase the sample size is to use single elements that are abundant and ecologically informative, such as astragali and distal humeri, and examine them in stratigraphic sequence using ecomorphological techniques.

Ecomorphology is the study of the link between the structure of an organism, be it cranial, dental or postcranial, and the environment in which it occurs. The underlying assumption of ecomorphology is that morphology reflects the interaction between an

organism and its environment (Bock and Wahlert, 1965; Losos and Miles, 1994; Van Valkenburgh, 1994; Wainright and Reilly, 1994). Theoretically, postcranial morphology will covary with habitat structure because postcrania must allow the organism to function effectively in its local habitat, and so depends on the structure of that habitat (Bock, 1990; Bock and Wahlert, 1965; DeGusta and Vrba, 2003). Postcranial morphology also reflects aspects of behavior not directly related to locomotion such as manipulation of food items, use during prey capture, and posture (Andersson, 2004; Carrano, 1997; Rose, 1988; Van Valkenburgh, 1987).

Ecomorphological analysis of postcranial elements is commonly used by paleontologists to reconstruct the paleohabitat of fossil localities. There are a variety of ways to apply ecomorphological techniques toward this goal. The most common method used in reconstructing Paleogene environments is ecological diversity analysis (EDA) in which the ecological profile of the community as a whole is used to infer habitat type (Gagnon, 1997; Gunnell, 1995; Reed, 1998; Townsend, 2004). It is also common to use EDA to trace the evolution of community structure through time (Van Valkenburgh, 1994, 1995; Tang and Pantel, 2005).

A common method in the reconstruction of Neogene habitats concerns the analysis of single elements that are numerous at a certain locality such as astragali, phalanges, femora, or humeri, (Bishop, 1994; DeGusta and Vrba, 2003; Elton, 2001; Kappelman, 1988; Kappelman et al., 1997). In contrast to EDA, this element-specific method focuses on identifying ecologically meaningful morphological features that can be used to distinguish habitat exploitation in ecologically diverse groups. Once these features are identified in extant animals, they can be applied to isolated fossil elements

and used to estimate the habitat in which those animals most probably lived (DeGusta and Vrba, 2003; Kappelman, 1988; Kappelman et al., 1997; Van Valkenburgh, 1994).

Another ecomorphological technique that combines elements of EDA and the element-specific methods discussed above is often used to trace the evolution of "guilds" through time. In this method, ecological indicators are measured in living and extinct mammals in order to place them in ecological categories or guilds. These consist of animals that do a similar ecological job and differ from other animals for this particular ecological variable. For example, all carnivores might be placed in one guild, while folivores or insectivores are placed in another (Kay et al., 1999; Van Valkenburgh, 1999; Wesley-Hunt, 2005). This method allows analysis of how different mammal lineages might evolve into new ecological roles, how the taxonomic contents of some guilds might change through time, and how these groups reflect changes in environment (Jernvall et al., 1996, 2000; Jacobs et al., 1999; Kay et al., 1999; Van Valkenburgh, 1999; Wesley-Hunt, 2005).

Previous ecomorphological studies using the element-specific method have mainly involved Neogene taxa, most of which are closely related to modern taxa (DeGusta and Vrba, 2003; Kappelman, 1988; Kappelman et al., 1997; Reed, 1998). This is problematic for Eocene artiodactyls, most of which are not closely related to modern groups (Janis et al., 1998; Lander, 1998; Martinez and Sudre, 1995; Prothero, 1998a, b; Stucky, 1998). Eocene artiodactyls, as a whole, retain many primitive characteristics compared to modern ones and so, in a phenetic analysis, will tend to group with more "primitive"-looking modern taxa rather than with taxa that share a habitat preference. The so-called "taxon free" methods that look at features in taxonomically diverse guilds can

do so because the features they use to analyze ecological trends have been found to reflect ecology in a wide range of taxa (Evans et al., 2007; Jernvall, 1996, 2000). To identify habitat preference in Eocene taxa one must identify features that correlate with habitat preference across a broad range of modern taxa. If such features can be found, one can assume that these features responded similarly in the past and can be used to study ecomorphology in fossils.

1.6 Research Questions and Hypotheses

The primary objective of this research is to evaluate how functional adaptations of several mammalian groups evolved as a response to habitat change that was occurring during the Uintan as represented by the Uinta Formation and to discuss the implications of these results for the dwindling primate populations there. To this end, I will (1) undertake the description and functional morphological analysis of newly recovered skeletal material from primates as well as several other taxa (discussed in section 1.3) from the Uinta Formation in order to assess the ecological role of these taxa within the Uintan faunal community; (2) apply measurements that discriminate mammals from open and closed environments (Andersson, 2004; Carrano, 1997; DeGusta and Vrba, 2003; Kappelman, 1988; Kappelman et al., 1997; Van Valkenburgh, 1987) in a broad sample of extant mammals to identify morphological responses to habitat change that hold across mammals and are more applicable to fossils with uncertain phylogenetic affiliation; and (3) use these measurements to identify ecomorphological evolution that coincides with local habitat change in a sample of artiodactyl astragali located stratigraphically throughout the Uinta Formation. The following questions will be addressed:

1. **Do mammals from the upper and lower parts of the Uinta Formation differ in locomotor adaptations?** I predict that mammal skeletons from the upper part of the Uinta Formation will consistently show more terrestrial and cursorial adaptations with reference to their relatives from the lower part of the Uinta Formation.

2. **Does the shape of the astragalus in open-country taxa differ consistently from that of closed-country taxa in a wide range of extant mammal groups?** Based on analyses of astragalar morphology (Carrano, 1997; DeGusta and Vrba, 2003), I predict that the astragalus of taxa from more open habitats will be distinguishable from that of taxa from more closed habitats, including the following: (**a**) deeper trochlear furrow; (**b**) proximodistally shorter astragali relative to intermediate dorsoventral thickness; (**c**) dorsoventrally deeper head.

3. **Does the shape of the distal humerus in open-country taxa differ consistently from that of closed-country taxa in a wide range of extant mammal groups?** Based on analyses of elbow-joint morphology (Andersson, 2004; Rose, 1988, 1993), I predict that the distal humerus of taxa from more open habitats will be distinguishable from that of taxa from more closed habitats including the following: (**a**) a more proximo-distally expanded and mediolaterally compressed "boxy" shape; (**b**) a narrower trochlea.

4. **Does the shape of the astragalus of fossil artiodactyls from the Uinta Formation change over time?** I predict that: (**a**) the shape of the astragalus of artiodactyls from

UFAZ 1 and UFAZ 2 will be similar in shape to those of extant mammals from closed habitats; (**b**) the shape of the astragalus of artiodactyls and perissodactyls from UFAZ 3 will be similar to those of extant mammals from open habitats.

If the fossil elements from the Uinta Formation show morphological differences consistent with a shift towards more open habitats higher in the section relative to those lower in the section, the implication is that the artiodactyls of the Uinta Formation were undergoing adaptive change in response to the aridification and opening of habitats. It is also possible that some taxa with existing cursorial morphologies were relegated to small open patches in the early Uintan and simply spread as the environment became more arid. In this case, the predominant morphology in the upper portions of the section will also be present but rare in the lower portions. On the other hand, morphological change may reflect immigration of already cursorial taxa from elsewhere rather than in situ evolution.

All of the above scenarios would explain the radiation of artiodactyls and the decline of primates during the Middle Eocene and support the current hypothesis that primates did not adapt to the changing habitat. It is possible that the fossil taxa will not show any changes throughout the section, suggesting that Uintan artiodactyls did not respond to environmental changes morphologically and, by extension, behaviorally. This outcome would weaken the argument that primate decline was due to a lack of adaptation to changing habitats and suggest that other factors must have been responsible.

1.7 Organization of Dissertation

In this dissertation I first describe new postcranial remains from several mammal groups from the Uinta Formation and attempt to reconstruct their habitat preferences.

Secondly I identify several metrics of the astragalus and distal humerus that are indicators of habitat preference across a variety of modern mammals, and lastly I apply the astragalar metrics to a sample of artiodactyl astragali from the Uinta Formation to trace the evolution of their morphology and habitat preference. More specifically, the chapters are organized as follows:

Chapter Two: Skeletal Remains of Primates from the Uinta Formation contains a description of new hindlimb elements from Uinta Formation primates and a functional analysis of those remains compared to other fossil and extant primates.

In **Chapter Three: Skeletal Morphology and Locomotor Behavior of *Pseudotomus eugenei* (Rodentia, Paramyinae) from the Uinta Formation, Utah**, I describe a new virtually complete skeleton of the late Uintan species *Pseudotomus eugenei* in comparison to more fragmentary remains from the common early Uintan species *Uintaparamys leptodus*. I argue that the differences in their skeletal morphology highlight the differences between early and late Uintan habitats in which rodents are living.

Chapter Four: The Skeleton of *Zionodon* is a description of postcranial elements of a new insectivore genus from the Uinta Formation. This genus is often found at the same localities as primates and is thus argued to inhabit environments similar to those primates preferred.

In **Chapter Five: The Skeleton of Uintan *Pantolestes***, I describe isolated postcranial remains from pantolestids from the early and late Uintan of the Uinta Formation as well as the early Uintan of the Washakie Formation in Colorado. I discuss the implications for primate evolution of the presence of pantolestids in the late Uintan of

the Uinta Formation.

Chapter Six: Ecomorphological Trends in Extant Mammals describes a pairwise technique to identify metrics in a wide range of mammalian taxa. I discuss my method of selecting taxa, standardizing measurements for body size, and accounting for phylogeny. I present the results and identify metrics that successfully separate open from closed country taxa in extant mammals.

In **Chapter Seven: A Quantitative Assessment of Ecomorphological Change Across the Uinta B-C Border**, I apply metrics from Chapter Six to a sample of artiodactyl astragali from the Uinta Formation and evaluate how they change from the early Uintan to the late Uintan. I discuss the implications of the results for habitat preference of early vs. late Uintan artiodactyls and for Uintan primates.

Chapter Eight: Conclusions is a summary of the results presented in the other chapters. I discuss the significance of this study for primate extinction toward the end of the Eocene and present future directions of this research.

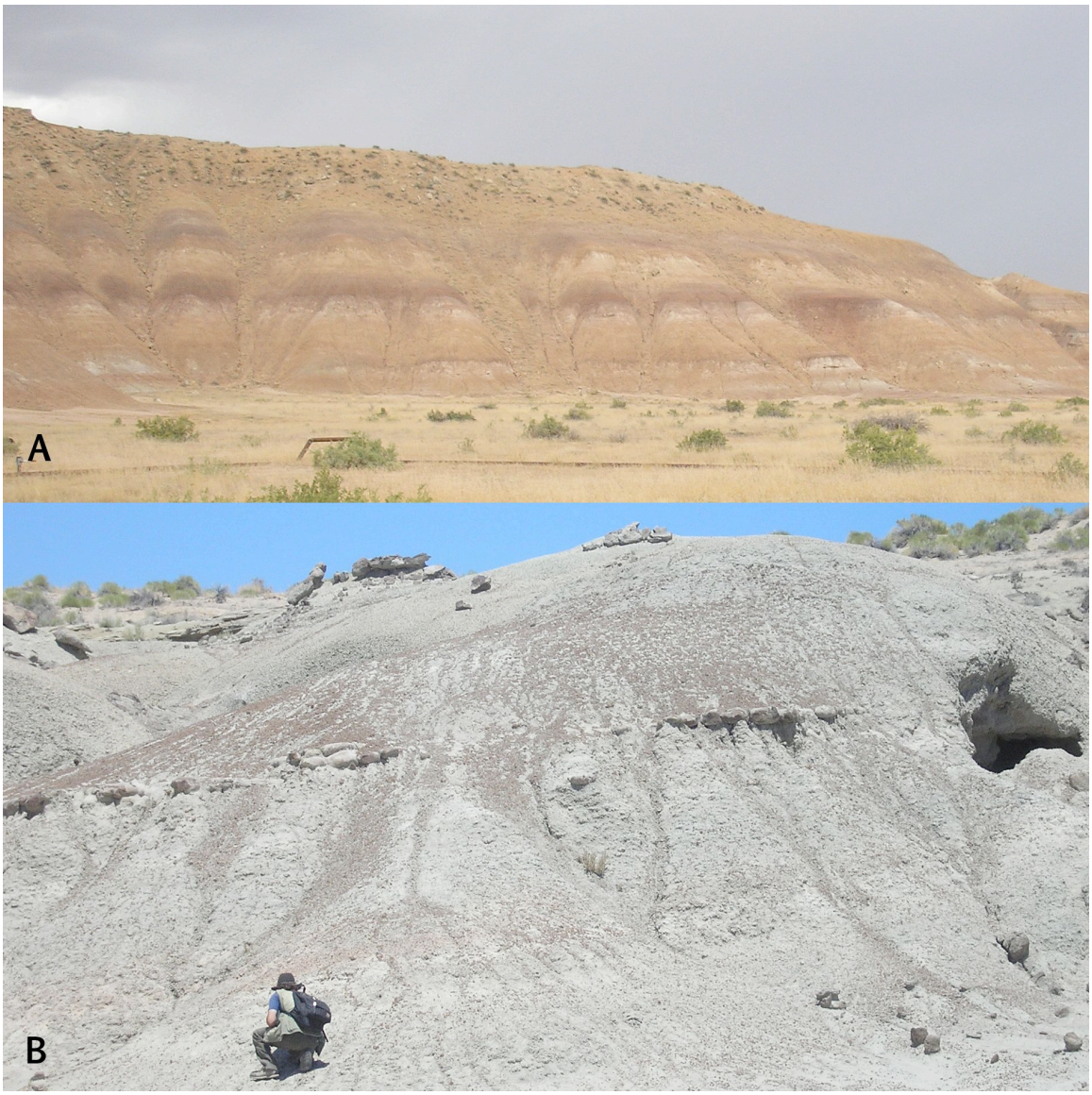

Figure 1.1. Exposures of the Uinta C member (**A**) and Uinta B member (**B**) in the Uinta Formation, Utah. Note the more heterogeneous clast size and drab gray-green of the Uinta B deposits in **B** as opposed to the more homogeneous bright red-purple sediments of the Uinta C in **A**.

CHAPTER TWO

Primate skeletal remains from the Uinta Formation

2.1 Introduction

During the Early Eocene primates were diverse, abundant and widespread in North America. The decline of primates in the late middle Eocene is thought to be related to the retreat of rainforests towards the equator from more northern latitudes, which begins in the Rocky Mountain region of North America during the Uintan North American Land Mammal "Age" or NALMA (Janis, 1993; Rasmussen et al., 1999; Townsend, 2004; Townsend et al., 2006; Wing, 1987; Wolfe, 1992). This is reflected in low generic richness of primates in the western interior of North America such as the Uinta Formation (UF) in northeastern Utah, compared to their higher diversity in places that remain more tropical such as Texas and California (Stucky et al., 1996; Walsh, 1996; Williams and Kirk, 2008). There are at most five genera and species of primates currently known from the Uinta Formation: four relatively large-bodied omomyines, *Ourayia uintensis, Chipetaia lamporea*, *Mytonius hopsoni*, and *Macrotarsius jepseni* (Dunn et al., 2006; Rasmussen, 1996; Rasmussen et al., 1999; Robinson, 1968; Williams and Kirk, 2008), and a new species of the small-bodied anaptomorphine *Trogolemur* (Rasmussen et al., 1999). Of these, *Ourayia*, *Chipetaia*, *Macrotarsius*, and *Trogolemur* are known from the Uinta B member, which is early Uintan in age and probably represents a forested paleoenvironment (Townsend, 2004; Townsend et al., 2006). The two most common primates in the UF are *O. uintensis* and *C. lamporea*. *O. uintensis* is known from several localities throughout the Uinta B member, but *C. lamporea* is known only from a single

locality in the UF (Rasmussen et al., 1999). *Mytonius hopsoni* is the only primate known from the late Uintan Uinta C member of the UF, which probably represents a more arid, open environment than the Uinta B (Rasmussen et al., 1999; Townsend, 2004; Townsend et al., 2006). *O. uintensis* and *M. hopsoni* are also known from the Uintan of Wyoming, southern California and Texas (Walsh, 1996; Williams and Kirk, 2008).

Based on dental and postcranial material, *C. lamporea* and *O. uintensis* rank among the largest omomyid primates (over 500 g in body mass). Both have been reconstructed as having been primarily frugivorous, and *Chipetaia* may have incorporated seeds or fruit with tough rinds into its diet (Conroy, 1987; Dunn et al., 2006; Rasmussen, 1996; Rasmussen et al., 1999). This is in contrast to most earlier omomyids, which were smaller than 500 g and probably relied on insects as a source of protein (Rose, 2006; Szalay, 1976). A recent description of hindlimb elements belonging to *O. uintensis* and *C. lamporea* indicates that, like earlier-occurring small bodied omomyids, these primates were specialized for arboreal leaping, and thus were dependent on forest environments (Dunn et al., 2006).

The purpose of this chapter is to describe new primate hindlimb elements from the UF and California that have been identified since the publication of the study by Dunn et al. (2006). The new primate remains include additional material of *O. uintensis* and *C. lamporea*, the first material from *M. hopsoni* and a possible new primate from the Uinta C. Here I provide a functional analysis of the new remains to supplement the previous study of postcranial adaptations of the Uintan omomyids and endeavor to identify potential changes in locomotor behavior between the primates from the Uinta B and Uinta C members.

2.2 Description and Comparisons

2.2.1 Allocation of Specimens

None of the primate remains in the Uinta Formation have been found in direct association with dentitions. However, the remains can be confidently allocated to genera—and in most cases species—based upon the stratigraphic position of and presence of dental remains from the localities in which the postcrania were found. The diagnostic characteristics that allow each element to be identified as primates are discussed as the elements are described. The following sub-sections relate to the stratigraphic and locality information that allowed the postcrania, once identified as primates, to be assigned to a specific taxon. The new specimens are listed in tables 2.1 and 2.2.

2.2.1.1 *Chipetaia lamporea*

Chipetaia lamporea is the only species in its genus and the only primate of its size found in the Uinta Formation. It is known only from one locality, WU-18 (Rasmussen, 1996). All postcranial specimens attributed to *Chipetaia lamporea* were found at locality WU-18. So far, WU-18 has yielded dental remains of only one primate, *C. lamporea*, and all primate postcrania from WU-18 agree well in size with that dental material (Dunn et al., 2006). The primate postcrania from this locality can be confidently attributed to *Chipetaia lamporea*.

2.2.1.2 *Ourayia*

The calcaneus from southern California (SDNM 4020) can be attributed to *Ourayia* due to its large size. *Ourayia* is the largest primate found in southern California, with the next largest omomyid being *Hemiacodon* (Walsh, 1996). The new calcaneus is

much larger in size than that of *Hemiacodon* and can be confidently assigned to the genus *Ourayia*. The dental specimens of *Ourayia* from southern California belong to a new species and are currently undergoing description (Walsh, 1996).

Ourayia is the largest and most common omomyid genus known from the Uinta Formation, and only one species, *O. uintensis*, is found in the UF. The primate postcrania attributed to *O. uintensis* were found at localities that also yielded dental remains of that species. The only exceptions are WU-115, which has yielded only an edentulous jaw attributed to *O. uintensis*, and WU-65, which has not yielded any primate dental remains. These localities are from a similar stratigraphic level as those that also yield dental and postcranial remains, and the elements found at these localities agree in size morphology with those found at other localities. *Macrotarsius jepseni* has also historically been found from the Uinta Formation and is approximately the same size as *Ourayia uintensis*. However, only one specimen is attributed to *M. jepseni* and there is some debate about the validity of this taxon as distinct from *O. uintensis* (Gunnell and Rose, 2002; Krishtalka, 1978; Robinson, 1968; Szalay, 1976). Although it is possible that some of the postcrania may be attributable to *M. jepseni* rather than *O. uintensis*, their overall size and morphological similarity makes this unlikely. The calcaneal fragments from the Uinta Formation collections at the AMNH (AMNH 2019) can also be assigned to *Ourayia uintensis* based on their similarity in size to the other specimens of *O. uintensis* despite the fact that precise locality information has not been retained.

2.2.1.3 *Mytonius hopsoni*

Chipetaia lamporea and *Ourayia uintensis* have been found only in localities stratigraphically located within the Uinta B member (Rasmussen, 1996; Rasmussen et al.,

1999; Townsend 2004; Townsend et al. 2006). Within the Uinta Formation, *Mytonius hopsoni* is found only in the Uinta C member and is the only species of the genus (Townsend, 2004). Based on dental remains, *M. hopsoni* is slightly smaller than *O. uintensis* and much larger than *C. lamporea*. The postcranial elements attributed to *M. hopsoni* are also slightly smaller than the corresponding elements known for *O. uintensis*. Primate dental remains have not been found at the localities yielding postcrania of *M. hopsoni*; however, they are known from localities within the Uinta C member as are those yielding dental remains. Based on size and stratigraphic position, it is most probable that the elements belong to *M. hopsoni*, although it is possible (but less probable) that they belong to an unknown omomyid of similar size.

2.2.2 Femur

One new femoral head of *Ourayia uintensis* has been found (CM 71161). It is cylindrical in shape with the head expanded posteriorly onto the neck as is seen in extant galagos and tarsiers and the fossil taxa *Omomys*, *Hemiacodon*, and *Shoshonius* (Anemone and Covert, 2000; Dagosto et al., 1999). The femoral head of *O. uintensis* is virtually identical to that of *Chipetaia lamporea* in shape (Dunn et al., 2006) and differs only in its larger size.

Four distal femora of *O. uintensis* have been recovered (Figure 2.1). Three specimens consist only of the lateral condyle and part of the patellar groove, but one specimen (CM 71130) is a complete distal femur that is minimally distorted, although it does exhibit minor mediolateral crushing. The femur is deeper anteroposteriorly than it is mediolaterally wide, with a deep patellar groove that is raised anteriorly off of the shaft, and a lateral patellar rim that is rounded and extends farther anteriorly than the medial

rim. These features are typical of leaping prosimians, fossil omomyids, and notharctines (Figure 2.2; Anemone and Covert, 2000; Dagosto, 1993; Dagosto et al., 1999; Gregory, 1920; Rose and Walker, 1985). There is a notch or indentation where the medial condyle meets the medial patellar rim, resembling the condition seen in fossil omomyids and leaping prosimians. This notch is more pronounced in tarsiers than in galagos and omomyids (Dagosto, 1993). *Ourayia* resembles other omomyids in this feature. The distal femur of *O. uintensis* does not show the anterior bulging of the medial epicondyle typical of vertical clingers and leapers (Dagosto, 1993; Dagosto et al., 1999); rather, the anterior portion of the femur is narrow, most resembling fossil omomyids such as *Hemiacodon* and *Shoshonius*. In overall shape, the distal femur of *Ourayia* most closely resembles the fossil omomyines *Shoshonius*, *Omomys* and *Hemiacodon* (Anemone and Covert, 2000; Dagosto, 1993; Dagosto et al., 1999; Simpson, 1940).

2.2.3 Tibia

Three new distal tibias of *Ourayia uintensis* and one of *Chipetaia lamporea* have been found (Figure 2.3). The proximal tibia has been described in detail (Dunn et al., 2006). The distal tibial specimens of *C. lamporea* are fragmentary. The most complete specimen (CM 80276) is attributed to *O. uintensis* and consists of a distal portion of the shaft with the astragalar articular facet and medial malleolus. The medial malleolus of the other specimens is broken where it contacts the main tibial shaft. The distal tibiae can be assigned to the order Primates based upon the shape of the astragalar articular facet, which is anteroposteriorly deeper than mediolaterally broad, and the pyramidal, anteriorly-rotated medial malleolus (Anemone and Covert, 2000; Dagosto, 1985). The distal tibia can be further identified as belonging to an omomyid due to the parallel

orientation of the anterior and posterior edges of the astragalar facet and in the low amount of medial malleolar rotation. This is in contrast to the condition seen in adapoids and strepsirhines in which the anterior and posterior edges of the tibia diverge laterally and the malleolus exhibits a greater degree of rotation (Dagosto, 1985). On the anterior rim of the distal tibia is a small concave facet for articulation with the neck of the astragalus when the ankle is dorsiflexed (often called a "squatting facet"); such facets are common in omomyids (Dagosto, 1985; Godinot and Dagosto, 1983; Savage and Waters, 1978; Szalay, 1976).

The lateral surface of the distal tibial shaft in *O. uintensis* and *C. lamporea* does not display an articular surface indicative of a synovial joint between the distal tibia and fibula. This is characteristic of omomyid tibias but is variable among primates (Anemone and Covert, 2000; Barnett and Napier, 1953; Dagosto, 1985). The distal tibias of strepsirhines and platyrrhines typically display a large synovial articulation with the fibula, although the facets differ in shape between the two groups (Ford, 1988). This is also true of the Oligocene primate *Apidium phiomense* (Dagosto and Gebo, 1994; Fleagle and Simons, 1983, 1995). Catarrhines are variable in this feature, ranging from a tiny articular surface to absence of a synovial joint in cercopithecoids, with hominoids being even more variable (Ford, 1988). Two distinct bony ridges extend proximally towards each other from the anterior and posterior corners of the distolateral tibia, indicating the presence of a syndesmosis between the tibia and fibula similar to the condition seen in extant small galagos (Figure 2.3 A,C and E). Proximal to these ridges, a distinct roughened protuberance is present, probably denoting a second contact point for the fibula (Anemone and Covert, 2000; Dagosto, 1985).

Many fossil and extant primates show varying degrees of tightening the contact between the tibia and fibula associated with limiting rotation between these two bones at the upper ankle joint (Anemone and Covert, 2000; Barnett and Napier, 1953; Covert and Hamrick, 1993; Dagosto, 1985; Dagosto and Gebo, 1994; Fleagle and Simons, 1983, 1995; Ford, 1988). All known fossil omomyids show signs of reinforcing this joint. In most cases, this is done by strengthening and proximally expanding the ligamentous attachment of the fibula to the tibia, as is seen in *Omomys*, *Hemiacodon*, *Shoshonius* and *Absarokius* (Anemone and Covert, 2000; Covert and Hamrick, 1993; Dagosto, 1985; Dagosto et al., 1999). In *Necrolemur* and *Afrotarsius*, however, the tibia and fibula are extensively synostosed, resembling the condition in extant *Tarsius* (Dagosto, 1985; Rasmussen et al., 1998). Compared to fossil omomyids, the syndesmosis between the tibia and fibula in *Ourayia* is similar to but less extensive than that in *Omomys*, *Hemiacodon*, *Absarokius* and *Shoshonius*, although *Hemiacodon* does not display the tubercle for secondary fibular contact that is seen in the other taxa. This is most likely due to the larger body size of *Ourayia*, as it has been noted that the extent of tibio-fibular articulation is greater in small-bodied leapers such as *Galago senegalensis* and *Microcebus* than in larger-bodied ones such as *Galago crassicaudatus* (Anemone and Covert, 2000; Covert and Hamrick, 1993; Dagosto, 1985; Dagosto et al., 1999).

2.2.4 Astragalus

The astragalar bodies of *Chipetaia lamporea* and *Ourayia uintensis* have been described in detail by Dunn et al. (2006) and will not be described again here. Two new astragalar bodies attributed to *Mytonius hopsoni*, a complete astragalus of *C. lamporea*, and an astragalar head of *O. uintensis* have been found since the publication of that paper

(Figure 2.4). The body of the astragalus of *C. lamporea* is damaged, but the head and neck are in fairly good condition. The morphology of the astragalar heads of both taxa are virtually identical except for size. When compared to the known partial astragali of *C. lamporea*, the new astragalus agrees in morphology and is slightly smaller. The astragalar neck is long and straight, resembling the astragali of other omomyines such as *Omomys*, *Hemiacodon* and *Shoshonius* in general proportions. The dorsal trochlear surface extends onto the dorsal and lateral surfaces of the neck of the astragalus, terminating in a distinct crest as is seen in other omomyines such as *Hemiacodon* (Dagosto, 1993; Simpson, 1940). The astragalar head is spherical and the navicular facet extends onto the dorsal surface and well onto the medial surface of the head. The navicular and sustentacular facets are continuous and extend onto the medial surface of the neck. There is a facet on the lateral aspect of the neck bounded medially by a bony ridge where the neck meets the body for articulation with the distal tibia when the ankle is dorsiflexed. This "squatting facet" corresponds to that on the distal tibia described above and is common in omomyids (Dagosto, 1985; Godinot and Dagosto, 1983; Savage and Waters, 1978; Szalay, 1976).

The straight astragalar neck is characteristic of omomyids and extant leaping prosimians (Figure 2.4 E). This contrasts with the condition seen in adapoids and slow-clambering prosimians such as *Nycticebus*, in which the neck is curved plantarly and slightly medially. The shape of the astragalar head is slightly wider than it is tall, resembling that of other omomyids and those of extant primates that are generalized leaping quadrupeds and specialized leapers. Among omomyids, the astragalar head index most closely resembles that of *Hemiacodon* and *Omomys* (Dagosto et al., 1999).

Two astragalar bodies from the Uinta C member of the UF probably represent the rare species *Mytonius hopsoni*. The astragali can be identified as belonging to a primate by their relatively deep bodies, medial and lateral trochlear crests of equal height, moderately grooved astragalar trochleas and strongly concave ectal facets (Dagosto, 1988). In general, these astragali resemble omomyids in having a straight fibular facet that flares laterally at the plantar border. The medial trochlear crest is rounded and angles gradually towards the lateral crest posteriorly. The lateral crest is sharp and straight. The articular surface is wide anteriorly and narrows posteriorly where it terminates just above the posterior trochlear shelf. The shelf is broken medially but appears to have been poorly developed.

The astragalus of *M. hopsoni* is slightly smaller than that of *O. uintensis* (as are known dental elements) and differs morphologically from the other previously described Uintan primates in several ways. One of the most striking differences is in the morphology of the tibial articular surface. In *O. uintensis* and *C. lamporea* the medial trochlear crest curves sharply laterally and the articular surface terminates well before contact with the posterior shelf, whereas in *M. hopsoni* the surface tapers more gradually and extends farther posteriorly. In this way, the astragalus of *M. hopsoni* more closely resembles other omomyines such as *Omomys*. The posterior shelf of *M. hopsoni* is broken, but it was undoubtedly significantly smaller than the large, well-developed shelf of *O. uintensis* and of *C. lamporea*. The shape of the ectal facet also suggests that the posterior shelf was smaller in *Mytonius*. In *Ourayia*, the ectal facet is expanded medially and laterally onto the plantar surface of the posterior shelf, making the facet appear pinched just anterior to this point. In *Mytonius*, the medial edge of the facet is straight

and the lateral edge only slightly expanded, which suggests that the posterior shelf was not robust medially as in the earlier Uintan species.

2.2.5 Calcaneus

The calcaneus of *Ourayia* is now known from two fragmentary specimens from the Uinta Formation, probably belonging to *O. uintensis* in the collections at the American Museum of Natural History, New York (AMNH), and a single complete specimen belonging to a new species of *Ourayia* from the Uintan of San Diego. One fragmentary calcaneus comes from stratigraphically high in the Uinta Formation, and most likely represents *Mytonius hopsoni*. The calcaneus of *Chipetaia lamporea* is known from fragmentary material, the most complete of which (CM 71168, Figure 2.5 C) preserves the calcaneal heel, ectal and sustentacular facets. The calcanei of *O. uintensis* and *M. hopsoni* are substantially larger than all other omomyines, and that of *C. lamporea* is slightly larger than the calcaneus of *Hemiacodon* (Figures 2.6, 2.7).

Features of the calcaneus that are shared by omomyids include: posterior calcaneal (= ectal) facet short and strongly convex, slight medial curvature of the calcaneal heel, elongation of the distal calcaneus, distinct groove plantar to sustentaculum tali, posterior calcaneal facet raised above calcaneal heel, straight plantar surface of the calcaneus, proximally placed lateral tubercle, and a semilunar cuboid facet (Gebo, 1988). Where these features are preserved in the new specimens, they agree in morphology with omomyids. Many of these characters are also present in extant galagines and *Tarsius* as well as other leaping primates and are interpreted as adaptations for leaping (Gebo, 1988). The following description refers mainly to the calcaneus of *Ourayia*, as those of *M. hopsoni* and *C. lamporea* are fragmentary and are virtually identical in features that

can be compared except for differences in size. Where the calcanei differ in morphology, this is noted.

The length of the distal calcaneus of *C. lamporea* and *M. hopsoni* cannot be calculated. Enough of the distal end is preserved in the specimens of *M. hopsoni* to determine that it was elongated as in other omomyids. This feature cannot be evaluated for calcanei of *C. lamporea*. The degree of elongation seen in the distal calcaneus in *Ourayia* most resembles that of extinct North American omomyines such as *Hemiacodon* and *Omomys* and extant cheirogaleids such as *Cheirogaleus* rather than galagines and tarsiers. The distal calcaneus is slightly less elongate than in *Omomys* (Anemone and Covert, 2000) and *Hemiacodon*, (Gebo, 1988) and closer to the degree of elongation seen in *Cheirogaleus medius*.

In all specimens, there is a small, roughened lateral tubercle just plantar to the ectal facet ("peroneal tubercle" of Gebo [1988]; see discussion below). In one of the partial calcanei of *C. lamporea* (CM 71168) as well as the specimen of *O. uintensis* from the AMNH (AMNH 2019), this tubercle is marked by two pits, possibly for the insertion of astragalocalcaneal and calcaneofibular ligaments (Decker and Szalay, 1974; Figure 2.6 C). This structure is relatively larger in the calcaneus of *C. lamporea* than in that of *Ourayia*. On the calcaneus of AMNH 2019 there is a pronounced sulcus lateral to the distal elongation of the sustentaculum. This sulcus is not present in the other specimens examined. On the medial calcaneus, the sustentacular facet extends distally and stops just short of the cuboid facet. The distal-most portion of this facet is raised above the calcaneal body and projects medially, creating a small flange, the plantar surface of which is grooved for the tendon of the flexor hallucis longus muscle. The calcaneus lacks

a facet for articulation with the navicular. The distal body of the calcaneus flares abruptly just before it terminates at the cuboid facet, creating a distal lip.

The shape and orientation of the cuboid facet closely resembles that of extant cheirogaleids. The long axis of the facet is oblique to the dorsal plane of the calcaneus and the dorso-lateral border of the facet is rounded. In galagines the dorsal border of the cuboid facet is more square due to the distally located lateral process onto which the cuboid facet has migrated. This process is smaller in cheirogaleids and does not affect the shape of the cuboid facet. There is a conical depression on the medio-plantar aspect of the cuboid facet for the conical pivot of the proximal cuboid (Figure 2.5 B). This depression is deeper in the specimen of *C. lamporea* than in those of *Ourayia*. The depression of both fossil species is deeper than what is seen in cheirogaleids, but shallower than in galagines.

Sources conflict as to the presence of an articular facet for the navicular on the distal calcaneus of omomyids. Szalay (1976) noted that there is no such facet present on omomyid calcanei, while Gebo (1988) stated that this facet is typical of omomyids. It appears that the raised portion of the sustentaculum is what is being identified as a navicular facet. It is my opinion that this is merely an extended facet for articulation with the sustentacular facet of the astragalus rather than the site of a synovial articulation with the navicular, as there is not a corresponding facet on the navicular for the calcaneus.

There is also disagreement as to the presence of a peroneal tubercle in omomyids. Decker and Szalay (Szalay, 1976, 1973) stated that the small tubercle distal to the ectal facet in omomyids may represent the insertion point for the astragalocalcalcaneal and calcaneofibular ligaments rather than a peroneal tubercle, while Gebo (1988) listed a

reduced and proximally located peroneal tubercle to be characteristic of omomyids. A distinct peroneal tubercle is present just distal to the ectal facet in some adapoids, as are one or more smaller tubercles located more proximally for the insertion of ligaments. However, in omomyids there is only a small tubercle, placed relatively proximally, making reliable identification of this tubercle problematic (Decker and Szalay, 1974; Szalay, 1976). On the calcanei of *Ourayia*, *C. lamporea*, and *M. hopsoni* as in all other omomyids, this tubercle is roughened, much like a site for ligamentous or muscular attachment, and there is no groove present for the tendon of the peroneus longus muscle, as is sometimes found in other taxa with a distinct peroneal tubercle. The presence of distinct pits on the tubercle in some specimens also supports the suggestion that this was a site of ligamentous attachment rather than a peroneal tubercle. Due to the uncertainty of the homology of the lateral tubercle of omomyids with the peroneal tubercles of other taxa, the use of "lateral tubercle" to describe this structure (*sensu* Decker and Szalay [1974]) is preferable to "peroneal tubercle."

In addition to the new material of *Ourayia* and *Chipetaia*, there is a small calcaneal fragment from WU-123, very high in the Uinta C member of the Uinta Formation. Together with an astragalar specimen of *Mytonius*, this represents the youngest primate material from the Uinta Formation. The fragment consists of a calcaneal heel and ectal facet, and it is smaller than any known omomyid from this member of the Uinta Formation. Based on the length of the ectal facet, this calcaneus is similar in size to those of *Shoshonius* and small cheirogaleids (Figure 2.7). The smallest omomyid primate from the Uinta Formation is a new species of *Trogolemur* and this is found only low in the Uinta B member of the UF. The calcaneus resembles omomyids in

having an ectal facet that is short, strongly convex and raised above the calcaneal heel, and in the distinctive, proximally placed lateral tubercle (Gebo, 1988). As there are no small primate teeth known from this high stratigraphic position, the identification of this element is tentative. However, the presence of this small calcaneus demonstrates that small mammals can be preserved at high stratigraphic levels in the UF and highlights the importance of screen washing at these levels.

2.2.6 Cuboid

In overall form, the cuboid resembles that of other omomyines. A distinctive feature of omomyine cuboids is that they are mediolaterally narrower at the distal end than the proximal end (Anemone and Covert, 2000; Savage and Waters, 1978; Szalay, 1976), rather than remaining the same width throughout the entire length, as is seen in extant primates (Figure 2.8). In galagines, the cuboid is elongate and narrow, and in lemurids it is shorter and mediolaterally broader (Figure 2.9).

On the lateral surface of the cuboid of *O. uintensis* there is a lateral tubercle with a large raised surface, possibly for the tendon of the peroneus longus, resembling the condition seen in *Hemiacodon*, *Tetonius*, and *Omomys*. In *Hemiacodon*, there is a deep groove for the tendon of the peroneus longus on this surface, in contrast to the condition in *O. uintensis* in which the surface is relatively flat. The cuboid of the diminutive omomyid, *Arapahovius*, is more gracile with less of a disparity between the width of the proximal and distal ends. Distal to the lateral tubercle of the cuboid of *O. uintensis*, the groove for the peroneus longus tendon is deep and spirals distally and plantarly to terminate directly plantar to the distal metatarsal facet as in other primates with elongated cuboids. The distal facet for articulation of metatarsal IV is concave and continuous with

a much smaller convex lateral lip for articulation with metatarsal V. The calcaneal facet is moderately elongated like that of other omomyines. The conical pivot on the medio-plantar margin of this surface fits tightly into the corresponding indentation on the calcaneus.

The medial surface of the cuboid exhibits one large, proximally-located facet for the navicular and ectocuneiform, and a small distal articular facet, also for the ectocuneiform, that abuts the edge of the articular surface for metatarsals IV and V. In galagines and other omomyines there are also two facets for articulation with the ectocuneiform, one situated just distal to the navicular facet and one distal to that at the disto-dorsal corner of the medial side of the cuboid. In galagines, the proximal ectocuneiform facet angles outward distally, and the distal facet is flat. In *Cheirogaleus*, there is one continuous facet for the navicular and ectocuneiform, the majority of which is located proximally with a small finger-like extension onto the distal portion of the cuboid. The ectocuneiform facets of *Ourayia* are somewhat intermediate between galagines and cheirogaleids in that the proximal ectocuneiform facet is a finger-like extension of the navicular facet and flat, like that of *Cheirogaleus*, but the facets are separated as in galagines. Overall, the cuboid of *O. uintensis* resembles that of *Hemiacodon*.

2.2.7 First Metatarsal

Six first metatarsals have been recovered for *Chipetaia*, only one of which (CM 71166) preserves the morphology of the peroneal tubercle and the articular surface for the entocuneiform (although the plantar border of the peroneal tubercle is abraded; Figure 2.10). The morphology of the first metatarsal of *Chipetaia* resembles that of *Ourayia* and

other omomyids in the following ways: the peroneal tubercle is dorsoplantarly deep and mediolaterally narrow and the joint surface is less open. This contrasts with the dorsoplantarly shallow and mediolaterally broad peroneal tubercle and the more open joint surface that is seen in adapoids (Dagosto et al., 1999; Dunn et al., 2006; Gebo et al., 1999; Szalay and Dagosto, 1988). As in all prosimian primates, the proximal facet for the entocuneiform is saddle shaped, being convex mediolaterally and concave proximodistally (Gebo et al., 1999; Szalay and Dagosto, 1988).

2.3 Functional Interpretations

2.3.1 *Ourayia uintensis* and *Chipetaia lamporea*

Overall, the new postcranial elements lend supporting evidence to the idea that *Ourayia uintensis* and *Chipetaia lamporea* retained the leaping behavior of their smaller ancestors despite increases in body mass. The semi-cylindrical femoral head and deep distal femur of *O. uintensis* suggest the use of leaping behaviors. The distal femur is lacking features that are typical of extant vertical clinging and leaping primates such as a more pronounced notch of the medial condyle and anterior bulging of the medial epicondyle. The distal tibia of both *O. uintensis* and *C. lamporea* indicates that the fibula was tightly bound to the distal tibia as in other omomyids, but not synostosed as in tarsiers and *Necrolemur*, also suggesting leaping behavior. The presence of a squatting facet on the neck of the astragalus of *Ourayia* and *Chipetaia* suggests that the tibia and astragalus came into contact during dorsiflexion such as is seen in vertical clinging. In humans this facet exists in high frequencies in populations that habitually adopt a squatting posture for resting, and is largely absent in populations that do not squat. This suggests that the presence of this facet is a direct result of repeated contact between the

two bones and, at least in humans, may be indicative of habitual hyper-dorsiflexion (Thomson, 1889; Trinkaus, 1975). On the other hand, this facet has been found to be nearly ubiquitous in many groups of primates, including those that do not engage in vertical clinging behavior, and has been suggested to be primitive for omomyids (Baba, 1975; Dagosto, 1985; Decker and Szalay, 1974). It is possible that all omomyids were vertical clingers, and thus all exhibit this feature as an indication of shared behavior. It is also possible that this feature is related to plantigrade locomotion with a habitually bent knee, which requires a high degree of dorsiflexion. Whereas the presence of this facet is fairly unambiguous in humans, it is less diagnostic for other, non-human primates. The astragali of *O. uintensis* and *C. lamporea* have the long, straight necks and spherical heads characteristic of omomyids as a whole and indicative of leaping behavior.

The calcanei of *O. uintensis* and *C. lamporea* are both distally elongated, but only two specimens of *O. uintensis*, one from southern California and one from the UF, preserve a complete distal end. The two specimens differ in their degree of elongation, with that from southern California being slightly shorter, close to dimensions of the extant primates *Cebus* and *Lepilemur*, whereas the specimen from the UF is significantly longer and well within the range of values for *Hemiacodon* (Figure 2.6; Table 2.3). The distal calcaneus of both specimens of *O. uintensis* is significantly more elongated than that of the North American adapoid *Notharctus*, which is interpreted to have been a leaper, and is lemur-like in body proportions (Gregory, 1920). The degree of elongation seen in the calcaneus of *O. uintensis* does not approach that of extant tarsiers and galagos, but it is higher than that seen in extant cheirogaleids, resembling extinct, small bodied omomyids. In relation to the length of the ectal facet the distal calcaneus of *O. uintensis*

from the UF has the highest residual of any non-tarsiid or non-galagine. The specimen from southern California also has a high residual similar to those for *Hemiacodon*. Both the large Bridgerian omomyid *Hemiacodon* and *O. uintensis* have more elongated distal calcanei than does the small Wasatchian omomyid *Shoshonius*, which is considered to be a quadrupedal leaper (Dagosto et al., 1999).

The navicular of *O. uintensis* and *C. lamporea* are also elongated, as is seen in extant leaping primates. Much like the calcaneal index, the navicular index of the two Uintan taxa is similar to those of *Hemiacodon* and extant cheirogaleids, larger than what is seen in most extant lemuriforms, lorisines and platyrrhines, but not as large as in galagines and tarsiers. The North American notharctines are similar to extant lemuriforms in degree of navicular elongation. When navicular length is plotted as a function of navicular width, *O. uintensis* and *C. lamporea* fall farther above the regression line than any primate in the sample with the exception of galagines and tarsiers (Figure 2.11), indicating that they have a longer navicular than most primates in the sample for their body size. *Cantius*, *Notharctus*, and *Hemiacodon* group comfortably within the upper range of extant lemuriforms.

The cuboid of leaping primates does not show the extreme elongation that occurs in calcanei and naviculars, and so cuboids have not been used as indicators of locomotor behavior very often. One exception is the cuboid of *Omomys*, which is drastically elongated in relation to those of other primates (Anemone and Covert, 2000). However, as a general rule, cuboids of leaping primates tend to be longer than those of non-leapers (Anemone and Covert, 2000). Among extant strepsirhines, the cuboids of galagines are the longest and those of lorisines the shortest. Anthropoids have short cuboids regardless

of leaping ability and overlap with lorisines in degree of elongation. Tarsiers have short cuboids despite their extreme adaptation to arboreal leaping, together with an odd cuboid morphology that sets them apart from all other primates (Gebo, 1987). Compared to extant strepsirhines, the cuboid of *O. uintensis* is longer than cheirogaleids and lemurids, and similar in length to that of galagines (Figure 2.9).

2.3.2 *Mytonius hopsoni*

The fragmentary nature of the material of *Mytonius hopsoni* precludes metric comparison with other taxa. However, several features of the astragalus in relation to that of *Ourayia uintensis* may have functional implications. The shallower astragalar trochlea in *M. hopsoni* may suggest an ankle joint less restricted to movement in a parasagittal plane, and less of an emphasis on leaping. Two other features of the astragalus offer some support for this interpretation. The first is a tibial articular surface that extends farther posteriorly in *M. hopsoni* compared to one that terminates before contacting the posterior shelf in *O. uintensis* (and *Chipetaia*). It was suggested by Dunn et al. (2006) that the anteriorly restricted articular surface of *Ourayia* and *Chipetaia* may be associated with habitually dorsiflexed postures. If so, the posteriorly extensive articular facet may indicate that the ankle was utilized through a broader range of flexion and extension in *Mytonius* than in the earlier Uintan omomyids, suggesting a wider range of foot postures associated with less leaping and more quadrupedal gaits.

The second feature is the reduction in size of the posterior shelf in *Mytonius* as compared to *Ourayia* and *Chipetaia*. The function of the posterior shelf is not well understood. This structure is absent in plesiadapiforms and is first seen in euprimates (Decker and Szalay 1974). Among modern primates, it is best developed in indriids and

reduced to varying degrees in other strepsirhines, anthropoids and tarsiers. It is well developed in notharctines compared to adapines (Decker and Szalay, 1974; Gebo, 1988), and is best developed in *Necrolemur* among omomyids, though there is a significant amount of variation in this group (Anemone and Covert, 2000; Dunn et al., 2006; Gebo, 1988; Szalay, 1976; Tornow, 2005). Decker and Szalay (1974) suggested that the shelf serves as a bony stop for the tibia during extreme plantar flexion, such as that seen at the beginning of a leap (Dagosto, 1983). The reduction in size of the shelf in *Mytonius* as compared to the earlier Uintan primates suggests that leaping did not play as large a role in its locomotor repertoire.

2.4 Discussion

There has been considerable debate about the genus and species to which *Mytonius hopsoni* should be allocated (Gunnell, 1995; Kirk, 2007; Krishtalka, 1978; Szalay, 1976). Most recently, Kirk (2007) revalidated the genus *Mytonius* based upon newly recovered maxillary fragments from Texas. The degree of morphological difference between the astragali of *Ourayia* and *Mytonius* supports the retention of *Mytonius hopsoni* in its own genus.

The new hindlimb elements of *Ourayia* and *Chipetaia* confirm and refine previous ideas about the locomotor behavior of the two genera. There is now further evidence that they were frequent leapers that lacked extreme morphological specializations found in extant vertical clingers and leapers. Although their morphology is not as specialized as that of galagos and may be considered closer in many ways to that of cheirogaleids, this does not necessarily mean that their behavior was cheirogaleid-like as has been suggested by some authors (Anemone and Covert, 2000; Dunn et al., 2006;

Gebo, 1988). There are no exact extant analogs for these two early Uintan primates. Extant cheirogaleids are among the most generalized primates in terms of locomotor patterns and engage in almost equal amounts of leaping, quadrupedal walking and climbing (Gebo, 1987). This is in contrast to most galagos, which spend the majority of the time leaping and significantly less time using quadrupedal or climbing locomotion. The only galago that has been studied that spends less than half of its locomotor repertoire leaping is the largest galago (*Galago crassicaudatus*), which still leaps more frequently than most cheirogaleids (Gebo, 1987; Off and Gebo, 2005). Although *G. crassicaudatus* leaps significantly less frequently, there are not corresponding modifications of the hindlimb anatomy from other galagos, suggesting that that this is a fairly young lineage (Dunn et al., 2006). Where the large omomyids depart from the morphology of their smaller ancestors and from cheirogaleids, it is in the direction of being more specialized for leaping. This is true of the length of the calcaneus, cuboid and navicular (Figures 2.6, 2.9, 2.11; Table 2.3). This suggests that the early Uintan primates probably engaged in leaping more frequently than extant cheirogaleids, less-frequently than the smaller galagos, and were perhaps similar in locomotor repertoire to the larger galago, *G. crassicaudatus*, and smaller indriids such as *Lepilemur* or *Propithecus* (Dunn et al., 2006; Gebo, 1987). Although little information can be gleaned from the small calcaneal fragment from high in the Uinta C member of the Uinta Formation, past the preliminary assignment to the Omomyidae, its presence raises the possibility that more primates survived into the late Uintan of the Uinta Formation than previously thought (Rasmussen et al., 1999; Dunn et al., 2006).

The partial astragali of *Mytonius hopsoni* suggest that this species was not specialized for leaping, perhaps being more of an arboreal quadruped. More complete material is needed to refine this assessment. The lack of leaping specializations in *Mytonius* does not necessarily suggest less reliance on tree cover. It is possible that *Mytonius* occurred primarily in dense remnant gallery forests along rivers where the canopy was continuous, making leaping less necessary. These remnant forests were more characteristic of the late Uintan of Uinta C than earlier Uintan habitats. In contrast, *Ourayia* and *Chipetaia* could have exploited more open woodland habitats that were more common in the early Uintan (Townsend, 2004), using leaping to bridge gaps in the less continuous canopy.

The postcranial remains of *Mytonius* are too fragmentary to conduct a detailed analysis of locomotor behavior. However, considering its general resemblance to other omomyids, all of which are interpreted to be arboreal, the conclusion that it was also arboreal is a conservative assessment. The presence of *Mytonius* in other more tropical Uintan localities such as Texas and southern California also supports this conclusion. A recent study of extant galagos of similar body size and with similar postcranial morphology, one of which lived in tropical forests and the other of which lived in thorn scrubland, found that their locomotor repertoire was remarkably similar despite the differences in habitat (Off and Gebo, 2005). This suggests that morphology may play as significant a role in determining locomotor behavior as habitat, at least in galagos. It is not unreasonable to assume, then, that *Mytonius* retained the arboreal leaping behavior of its ancestors. The probable arboreal adaptations of *Mytonius* suggest that it was still reliant on life in trees and was not using more terrestrial substrates despite the increasing

scarcity of arboreal environments. This supports the hypothesis that the decline of trees and the decline of primates during the Uintan in the continental interior of North America were linked.

2.5 Summary

The primary goal of this chapter was to describe new hindlimb elements of *Ourayia uintensis*, *Chipetaia lamporea*, and *Mytonius hopsoni* from the UF and California and to analyze their locomotor adaptations. A new calcaneus of a small omomyid primate from high in the Uinta C was also described. The new primate material suggests that the primates were arboreal leapers most similar in locomotor patterns to *Galago crassicaudatus* and *Lepilemur*. The postcranial remains of *Mytonius hopsoni* from the Uinta C member suggest that this genus was arboreal. This in turn indicates that primates remained dependent on trees as they were becoming less plentiful in the late Uintan.

Table 2.1. Hindlimb elements of *Chipetaia lamporea* from the Uinta Formation.

Element	CM no.	Locality	Description
Chipetaia			
Femur	70903	WU-018	Left, proximal end
	70916	WU-018	Left, head & neck
	80206*	WU-018	Right, head & neck
	80238*	WU-018	Left, head
	80246*	WU-018	Left head
Tibia	71168*	WU-018	Left, distal end
Astragalus	70914	WU-018	Right, body only
	71167*	WU-018	Right, head & neck
	71178*	WU-018	Left, entire, damaged
	80208*	WU-018	Left, body only
	80231*	WU-018	Right, body only
	80235*	WU-018	Left, body only & unassociated head
	80253*	WU-018	Left, body only
Calcaneus	80235*	WU-018	Right, distal end
	80253*	WU-018	Left, fragment
	80590*	WU-018	Right, fragment
Navicular	70904	WU-018	Right, entire
	70912	WU-018	Right, proximal end
	70913	WU-018	Left, proximal end
	71176*	WU-018	Left, distal end
	71178*	WU-018	Left, proximal end
Entocuneiform	70910	WU-018	Right, entire
	70911	WU-018	Left, entire
	70915	WU-018	Left, entire
Metatarsal I	71166*	WU-018	Right, proximal end
	71168*	WU-018	Right, proximal joint surface
	71170*	WU-018	Right, proximal joint surface
	80221*	WU-018	Left, proximal joint surface
	80235*	WU-018	Left, proximal joint surface
	80253*	WU-018	Left, proximal joint surface

* denotes elements identified since the publication of Dunn et al. 2006.

Table 2.2. Hindlimb elements of *Ourayia uintensis*, *Mytonius hopsoni* and indeterminate omomyid from the Uinta Formation.

Ourayia			
Femur	71039*	WU-117	Right, distal end
	71130*	WU-110	Left distal condyles and shaft (2)
	71161*	WU-002	Left, head & neck
	80248*	WU-116	Right, distal end
	80260*	WU-110	Right, distal end
Tibia	70906	WU-117	Right, proximal end
	80259*	WU-110	Right, distal end
	80276*	WU-116	Right, distal end
Astragalus	70902	WU-116	Left, body only
	70905	WU-110	Right, body only
	71091*	WU-110	Right, body only
	80247*	WU-065	Left, body only
	80262*	WU-115	Left, body only
	80272*	WU-110	Right, body only
	80274*	WU-116	Left, body only
	80587*	WU-110	Right, head & neck
Calcaneus	80783*	WU-110	Right, fragment
Navicular	70917	WU-117	Right, entire
	70920	WU-115	Right, entire
	80207*	WU-002	Right, proximal end
Cuboid	70918*	WU-116	Right, entire
	80266*	WU-116	Left, proximal end
	80587*	WU-110	Left, entire
Entocuneiform	70907	WU-115	Right, entire
	70908	WU-110	Right, entire
	70909	WU-115	Right, entire
	70921	WU-116	Left, entire
	71186*	WU-002	Left, entire
	80279*	WU-110	Right, entire
Metatarsal I	70900	WU-115	Left, proximal end
	70901	WU-117	Left, proximal end
	70919	WU-110	Left, proximal joint surface
	80623*	WU-180	Left, proximal joint surface
Mytonius			
Astragalus	80267*	WU-123	Right, body only
	80586*	WU-174	Right, body only
Calcaneus	71174*	WU-210	Left, fragment
Omomyide indet.			
Calcaneus	71158*	WU-123	Left, fragment

* denotes elements identified since the publication of Dunn et al. 2006.

Table 2.3. Hindlimb indices illustrated in graphs in a selection of extant and fossil primates. In general, primates that leap more frequently have higher indices than non-leapers. Ourayia and Chipetaia have higher indices more similar to leaping primates and other Eocene omomyids. The raw measurements and specimen numbers from which these indices were calculated are listed in Appendix 2.

Taxon	Condylar Index	Calcaneal index 1	Calcaneal index 2	Navicular index	Cuboid index
Cheirogaleus major	95.79	48.32	189.81	165.91	176.61
Microcebus murinus rufus	98.92	60.65	301.79	294.66	216.67
Daubentonia madagascariensis	88.09	42.66	132.23	72.38	141.52
Varecia variegata	94.80	38.40	110.74	81.73	155.49
Eulemur mongoz	95.60	48.20	182.84	152.59	152.77
Eulemur fulvus	93.69	47.21	155.62	137.56	143.45
Lemur catta	96.80	42.74	155.27	135.60	148.50
Hapalemur griseus griseus	102.13	49.65	174.71	149.47	163.34
Propithecus diadema diadema	102.41	40.83	124.18	65.86	156.45
Avahi laniger	111.25	42.11	108.71	90.73	146.50
Lepilemur mustelinus	107.40	46.86	219.26	162.24	164.40
Perodicticus potto	68.23	36.30	115.38	52.84	112.66
Loris tardigradus tardigradus	71.59	–	–	–	–
Nycticebus coucang	82.64	46.06	187.25	43.04	212.97
Arctocebus calabarensis calabarensis	82.02	42.25	163.18	57.67	116.89
Galago alleni	106.28	70.84	647.14	382.86	301.20
Galago crassicaudatus	100.83	66.11	454.22	287.99	220.29
Galago senegalensis	116.52	73.55	698.32	527.53	256.32
Tarsius bancanus	123.52	78.13	704.40	613.11	138.35
Tarsius spectrum	120.57	77.08	666.12	625.68	158.52
Tarsius syrichta carbonarius	124.96	76.36	731.64	434.38	147.64
Aotus trivirgatus	81.08	45.99	152.71	90.80	108.68
Chiropotes satanus	73.78	40.67	126.22	94.72	111.30

Table 2.3 continued

Cebus apella	73.23	48.06	201.87	83.81	123.12
Saimiri oerstedii	81.98	45.84	155.26	87.50	115.21
Callimico goeldii	82.43	44.51	155.16	60.77	113.94
Leontopithecus rosalia	79.56	44.05	157.46	65.15	103.40
Callithrix jacchus	84.06	47.07	179.93	66.60	107.07
Saguinas oedipus	80.86	44.11	141.49	69.43	94.70
Cebuella pygmaea	79.19	45.57	173.37	70.48	140.73
Cantius	104.54	–	–	128.93	159.18
Notharctus	101.54	42.25	288.92	–	–
Shoshonius cooperi	111.49	52.09	226.67	–	–
Hemiacodon gracilis	102.32	52.11	414.61	182.83	173.06
Ourayia uintensis	–	–	389.10	185.41	189.45
Ourayia sp.	–	49.78	354.14	–	–
Chipetaia lamporea	–	–	–	225.66	–

Condylar index = depth of femoral condyles / breadth across condyles * 100
Calcaneal index 1 = length of distal calcaneus / total length * 100
Calcaneal index 2 = length of distal calcaneus / ectal facet length * 100
Navicular index = length of navicular / width of proximal navicular * 100
Cuboid index = length of cuboid / calcaneal facet width * 100

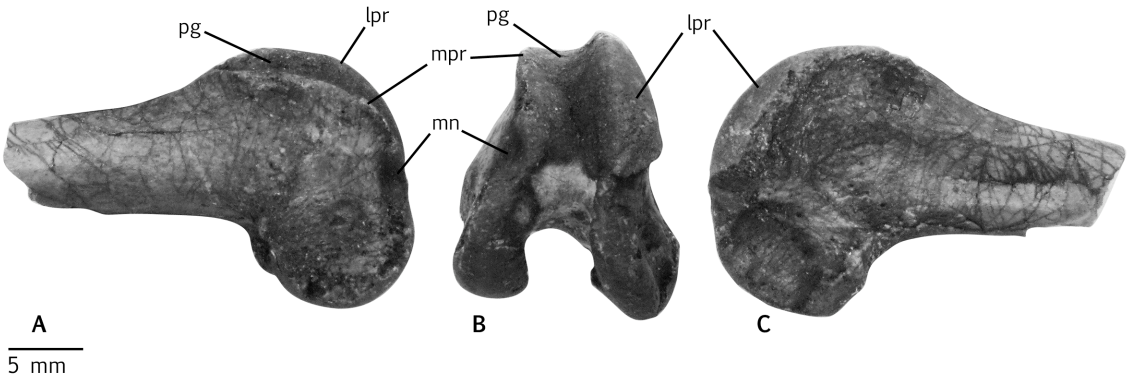

Figure 2.1. Distal femur of *Ourayia uintensis* (CM 71130). **A**, medial view; **B**, distal view; **C**, lateral view. Note the overall narrow appearance of the distal femur; narrow, raised patellar groove; high, rounded lateral patellar rim; and medial condylar notch. **lpr**, lateral patellar rim; **mn**, medial notch; **mpr**, medial patellar rim; **pg**, patellar groove.

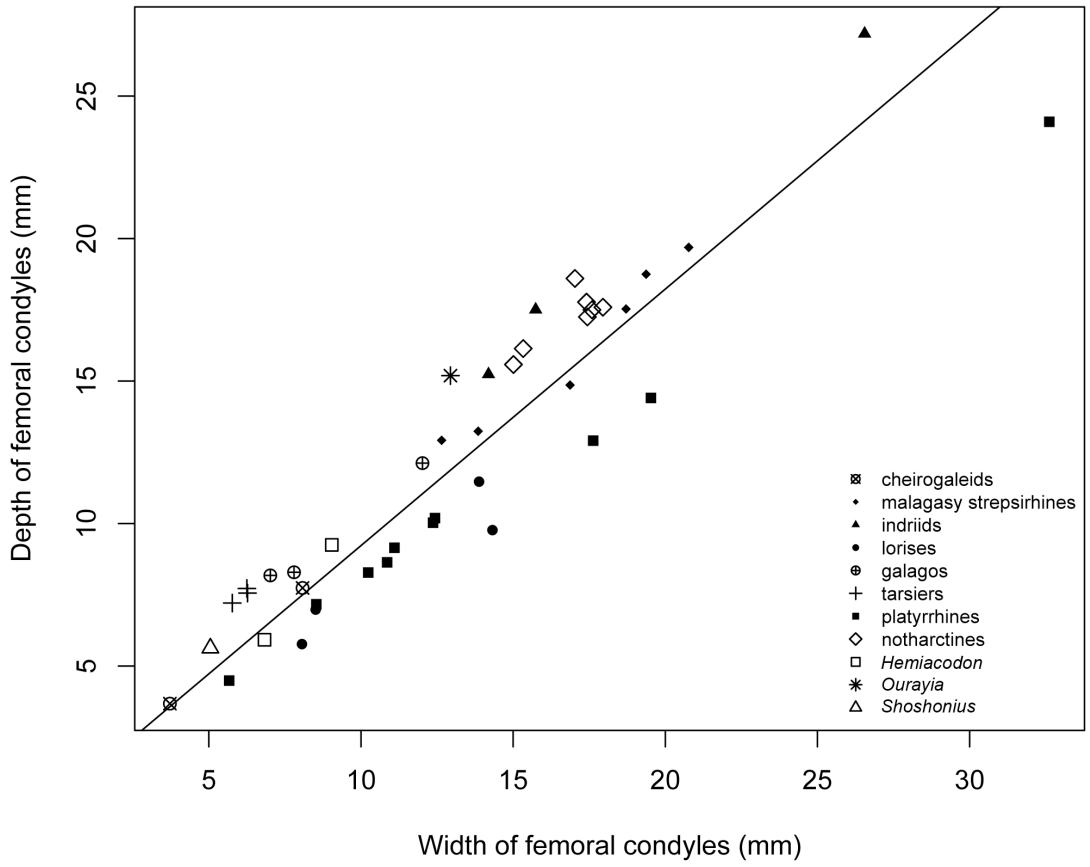

Figure 2.2. Bivariate plot of the depth of the femoral condyles relative to width across the femoral condyles in a selection of extant and fossil primates. The line is a least squares regression of femoral condylar depth on width across the femoral condyles in extant primates. Most leaping primates have positive residuals whereas non-leaping ones have negative residuals. Platyrrhines all fall below the regression line. The Wasatchian omomyid *Shoshonius* has a relatively deeper distal femur than cheirogaleids, and the Bridgerian genus *Hemiacodon* similar in proportion to cheirogaleids. *Ourayia* (CM 71130) has a distal femur similar in proportion to notharctines and indriids, although the depth may be slightly exaggerated by crushing.

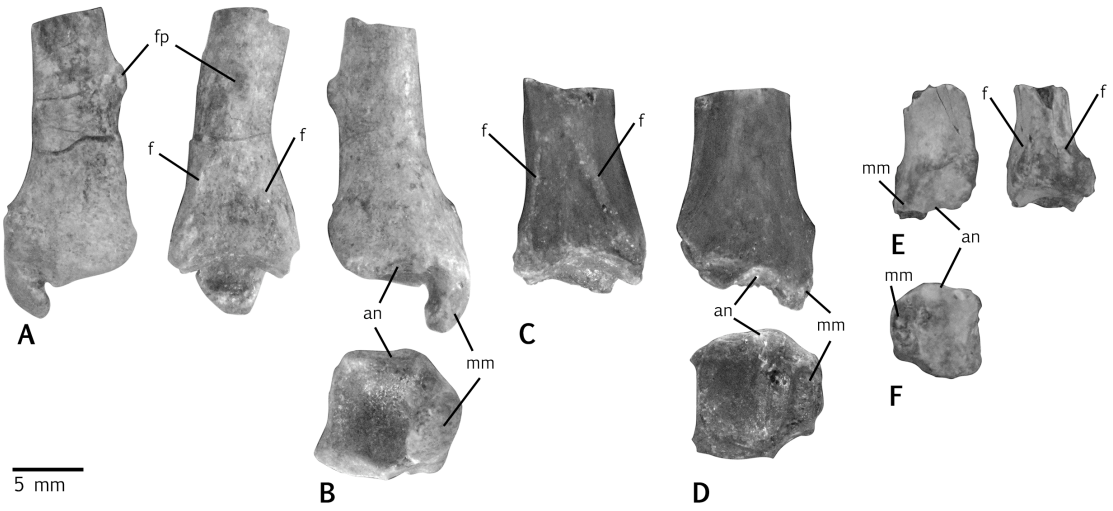

Figure 2.3. Distal tibia of *Ourayia uintensis* (**A**, **B** CM 80276; **C**, **D** CM 80259) and *Chipetaia lamporea* (**E**, **F** CM 71168). Note the rotated medial malleolus in **A**, and the parallel anterior and posterior borders of the distal articular surface. **an**, facet for the astragalar neck; **f**, site of syndesmosis with the fibula; **fp**, protuberance for articulation with the fibula; **mm**, medial malleolus.

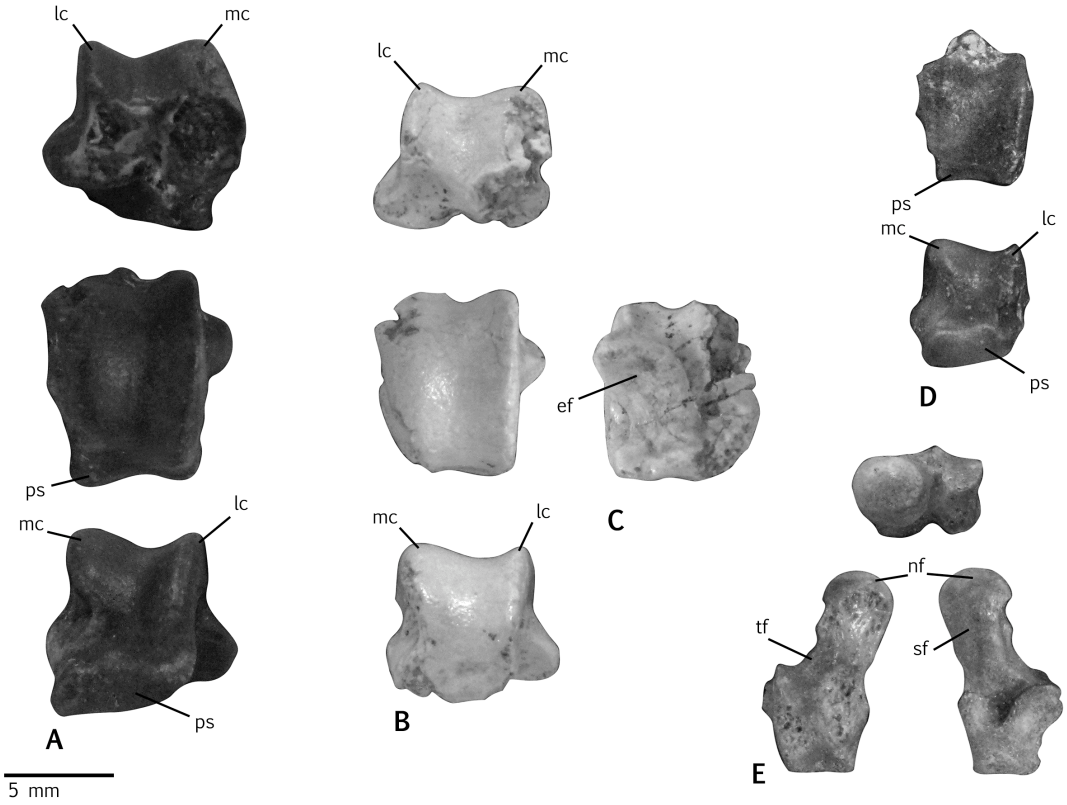

Figure 2.4. Astragalus of *Ourayia uintensis* (**A**, CM 70905), *Mytonius hopsoni* (**B**, **C**, CM 80586), and *Chipetaia lamporea* (**D**, CM 70914, **E**, CM 71178). Note the posterior continuation of the tibial articular surface in **B**, as opposed to **A** and **D**, in which the articular surface terminates before contacting the posterior shelf. Also note the sharply angled medial condyle in **A** and **D** as opposed to the more parallel medial and lateral condyles in **B**. **ef**, ectal facet; **lc**, lateral condyle; **mc**, medial condyle; **nf**, navicular facet; **ps**, posterior shelf; **sf**, sustentacular facet; **tf**, tibial facet.

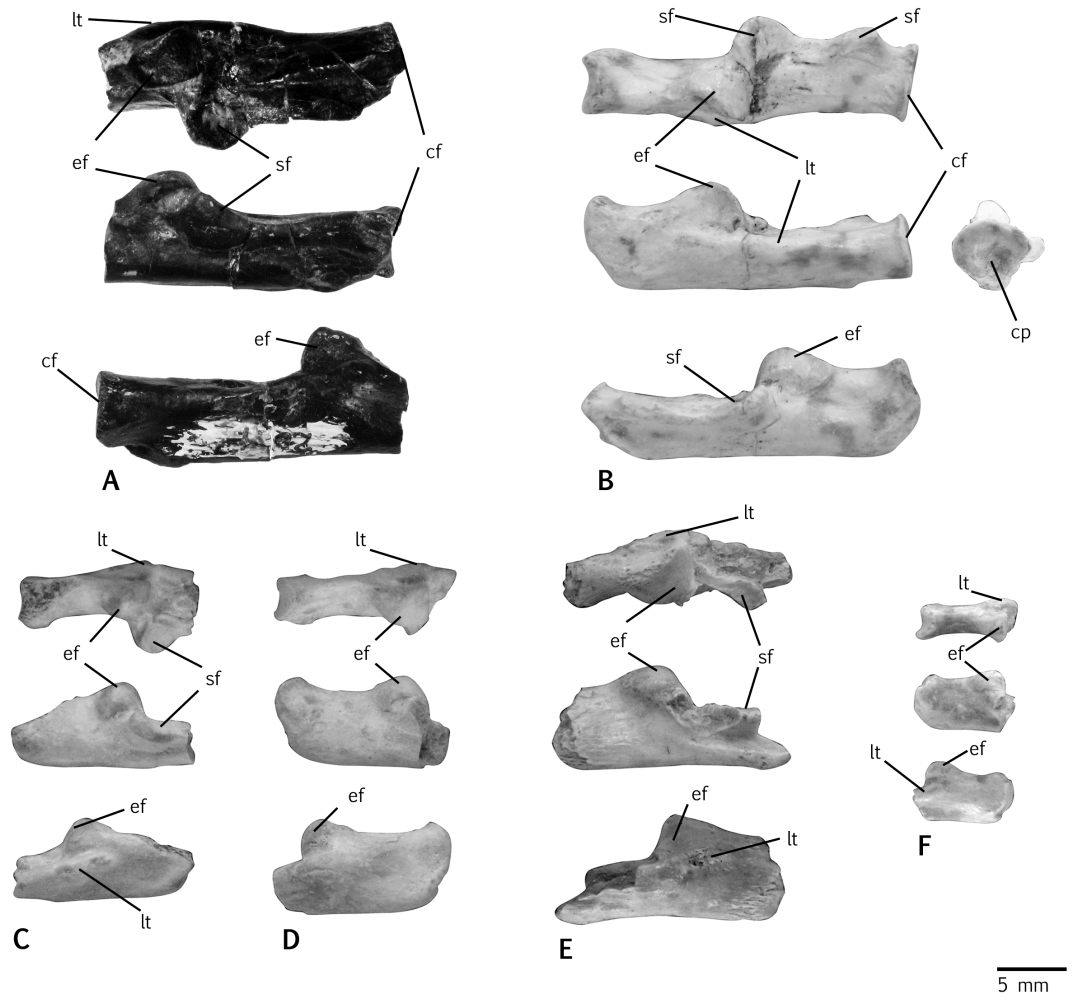

Figure 2.5. Calcaneus of *Ourayia uintensis* from the Uinta Formation (**A**, AMNH 2019), *Ourayia* sp. from southern California (**B**, SDNM 4020), *Chipetaia lamporea* (**C**, CM 71168, **D**, CM 80253), *Mytonius hopsoni* (**E**, CM 71174), and small primate from WU-123 (**F**, CM 71158). Note the tightly curved ectal facet, short calcaneal heel and proximally placed lateral tubercle present in all specimens. Also note the distal elongation of the calcaneus in **A** and **B**. **cf**, cuboid facet; **cp**, depression for cuboid pivot, **ef**, ectal facet; **lt**, lateral tubercle; **sf**, sustentacular facet.

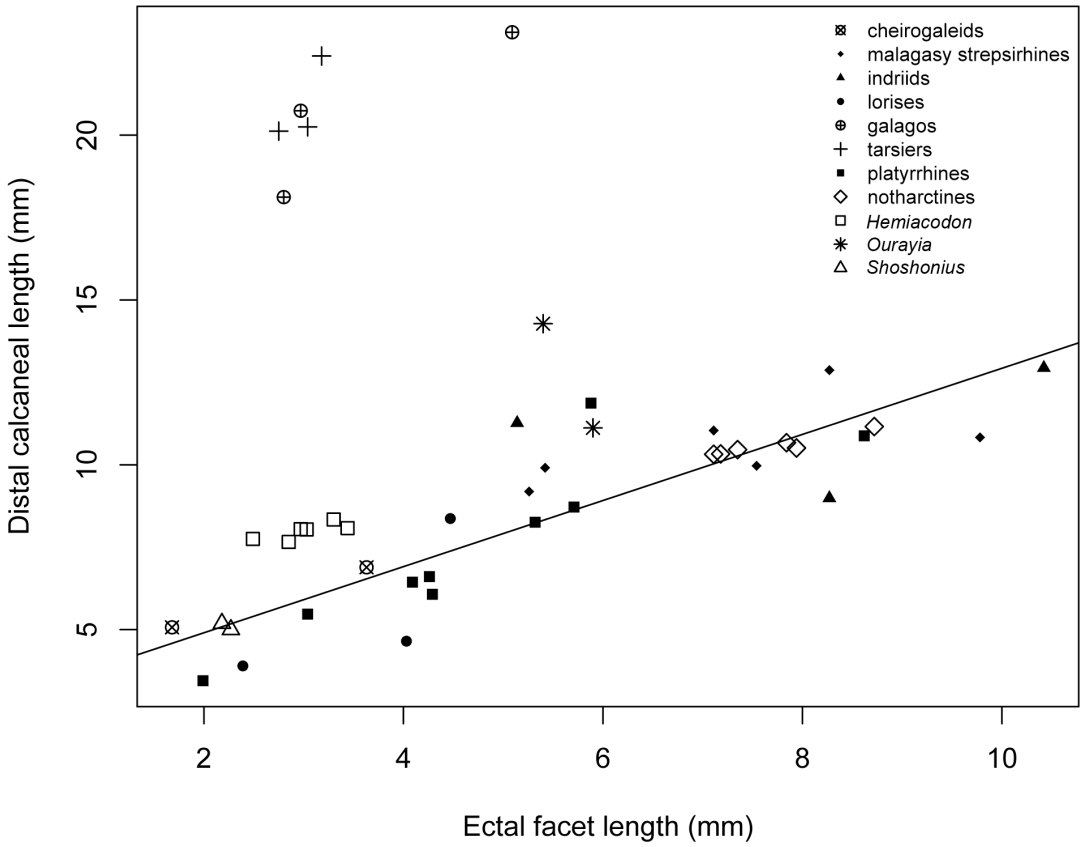

Figure 2.6. Bivariate plot of the length of the distal calcaneus relative to the length of the ectal facet in a selection of extant and fossil primates. The line is a least squares regression of distal calcaneus length on ectal facet length in extant non-leaping primates (i.e. excluding tarsiers and galagos). The Wasatchian omomyid *Shoshonius* is similar in proportions to cheirogaleids, and the Bridgerian genus *Hemiacodon* has proportionately longer distal calcanei than extant cheirogaleids. The specimen of *Ourayia* from San Diego (SDNM 4020) is similar proportionately to those of *Hemiacodon*, but absolutely larger, whereas the specimen of *Ourayia* from the AMNH (AMNH 2019) is much longer proportionately than cheirogaleids and the other omomyids in the sample.

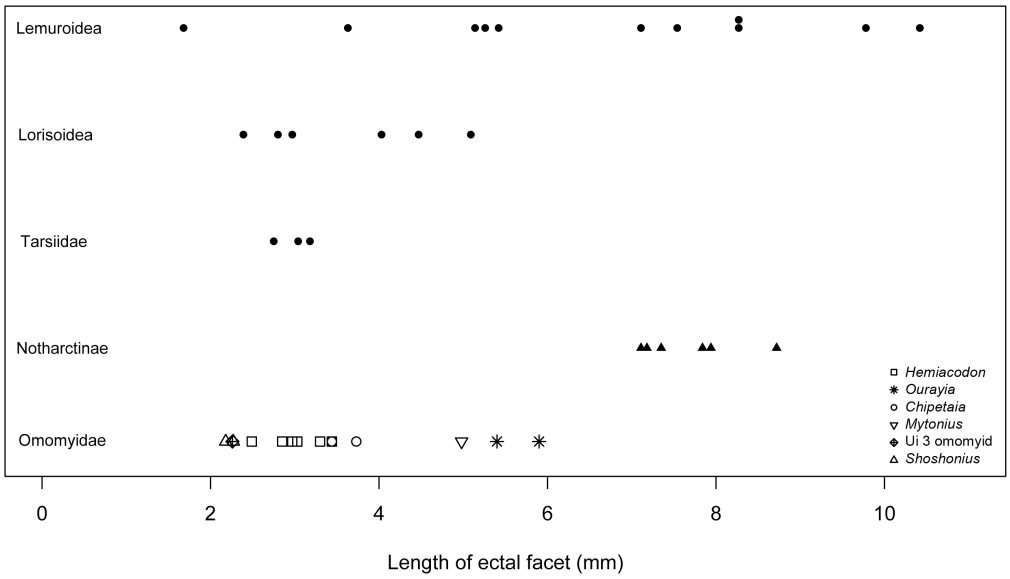

Figure 2.7. Univariate plot of the length of the ectal facet in extant and fossil primates. Note the large size of *Ouryaia* and *Mytonius* compared to other omomyids and the overlap in size between *Chipetaia* and large specimens of *Hemiacodon*. The new possible omomyid from the Uinta C member is significantly smaller than the other Uintan primates and overlaps in size with *Shoshonius*.

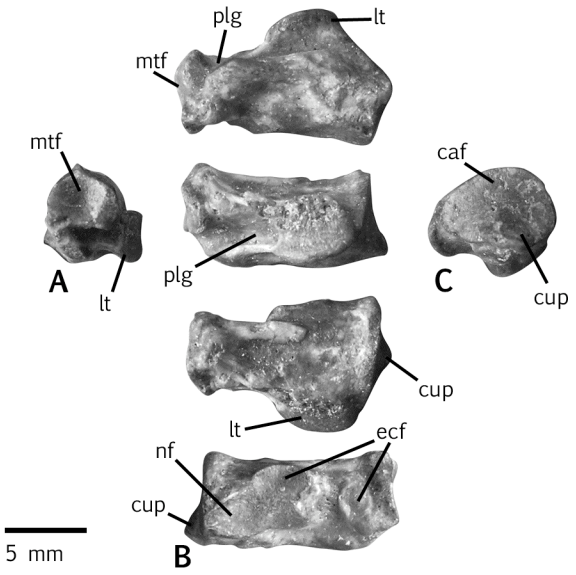

Figure 2.8. Cuboid of *Ourayia uintensis* (CM 80587). **A**, distal view; **B**, top to bottom: plantar, lateral, dorsal and medial views; **C**, proximal view. Note the narrow distal end as compared to the wider proximal end. **caf**, facet for calcaneus; **cup**, cuboid pivot; **ecf**, facet for the ectocuneiform; **lt**, lateral tubercle; **mtf**, facet for metatarsals IV and V; **nf**, navicular facet; **plg**, groove for peroneus longus.

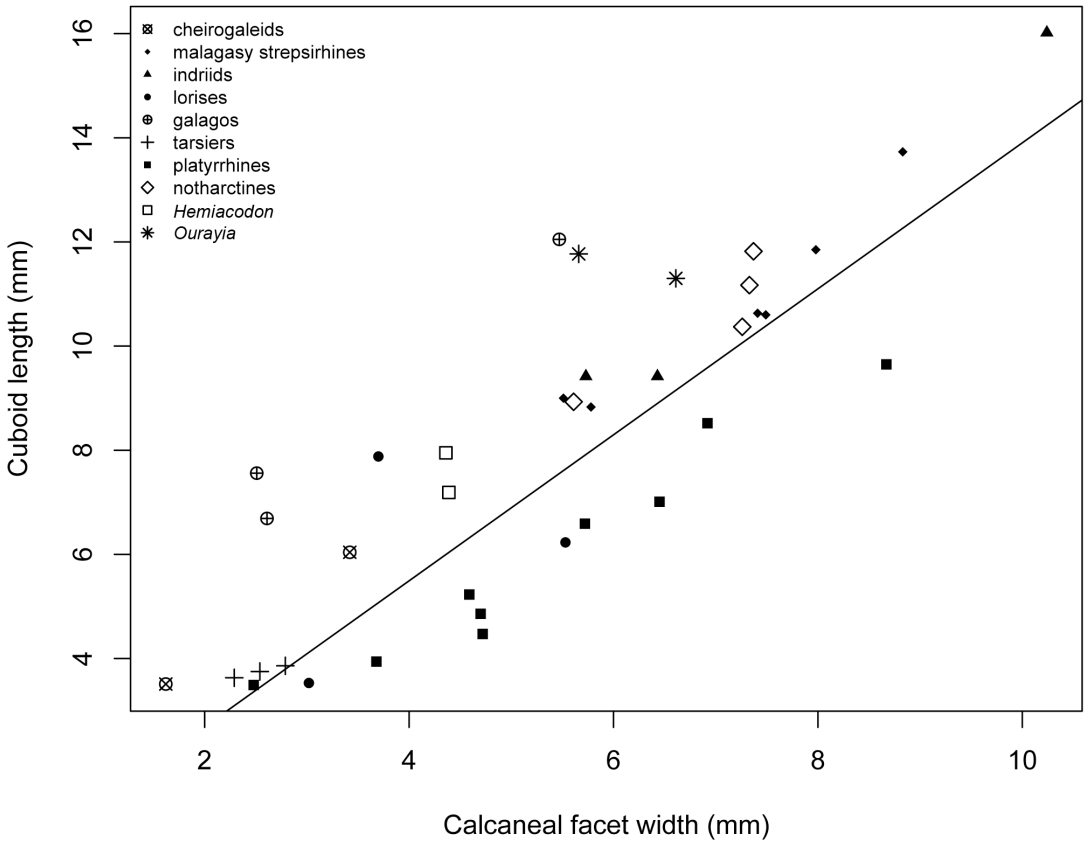

Figure 2.9. Relative length of the cuboid in a selection of extant and fossil primates. The line is a least squares regression of cuboid length on calcaneal facet width in extant non-leaping primates (i.e. excluding tarsiers and galagos). Note that one specimen of *Ourayia* falls close to the extant galago *Galago crassicaudatus* in cuboid proportions, and all omomyids fall above the line with leaping prosimians.

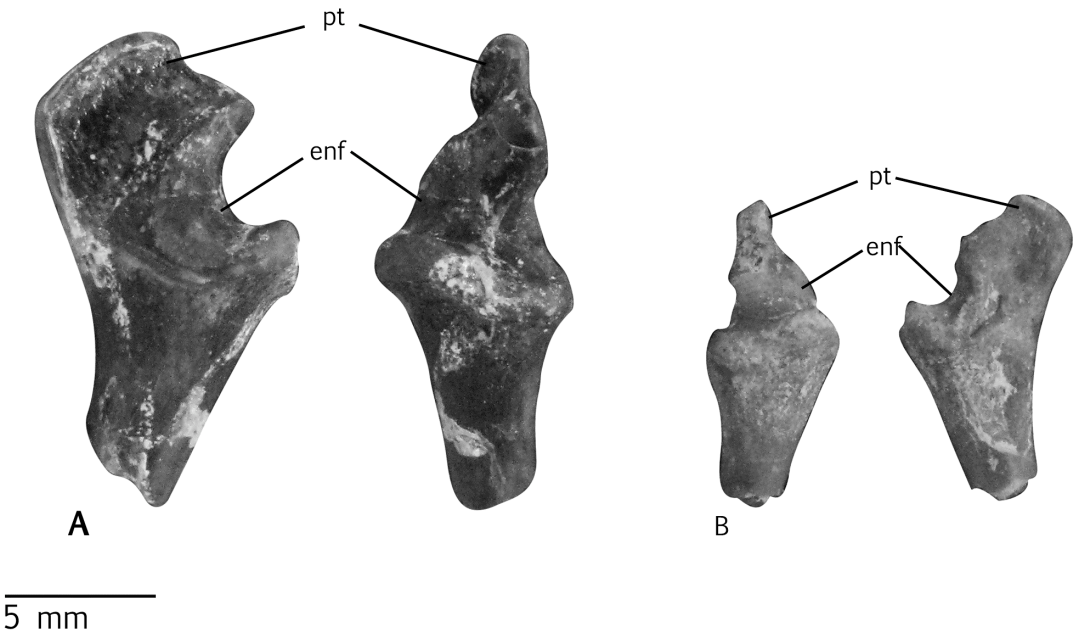

Figure 2.10. Proximal first metatarsal of *Ourayia uintensis* (**A**, CM 70900) and *Chipetaia lamporea* (**B**, CM 71166). **A**, medial view (left) and plantar view (right). **B**, plantar view (left) and medial view (right). **enf**, facet for entocuneiform; **pt**, peroneal tubercle

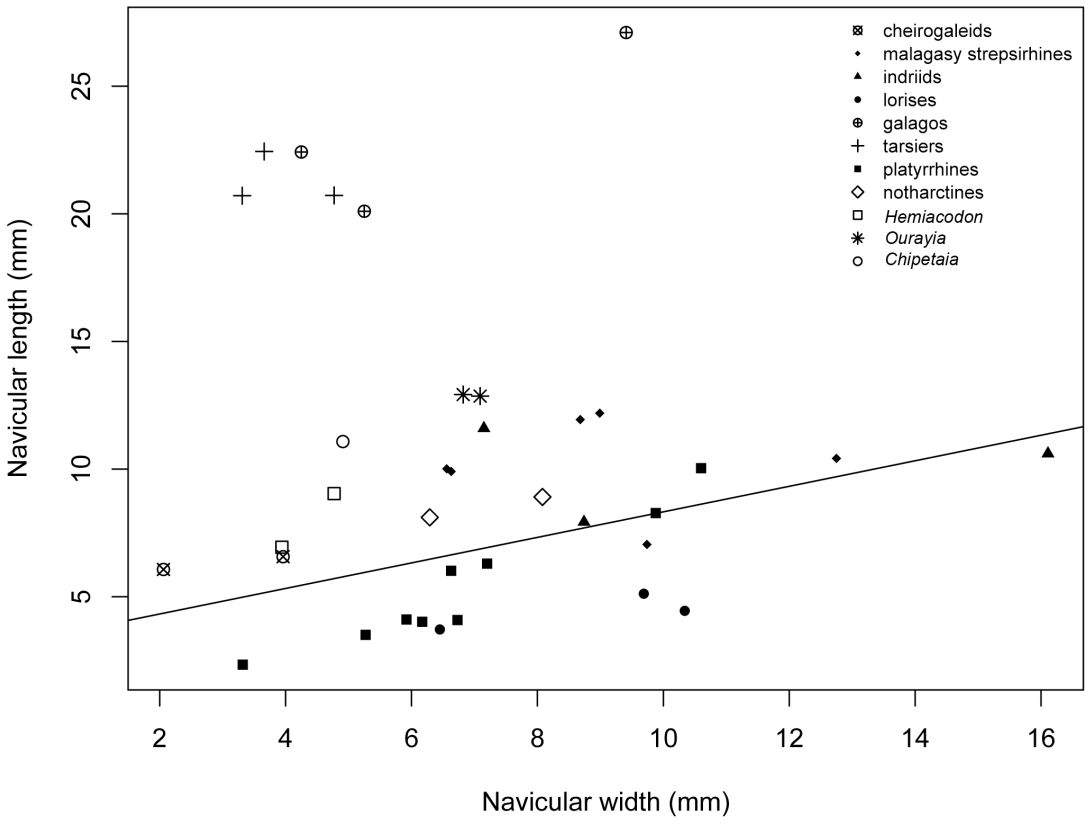

Figure 2.11. Relative length of the navicular in a selection of extant and fossil primates. The line is a least squares regression of distal calcaneus length on ectal facet length in extant non-leaping primates (i.e. excluding tarsiers and galagos). Note that the naviculars of *Ourayia* and *Chipetaia* are longer relative to their width than those of extant and fossil primates of similar size, but neither has a navicular as elongated as that of extant galagos and tarsiers.

CHAPTER THREE

Skeletal Morphology of *Pseudotomus eugenei* and *Uintaparamys leptodus* (Rodentia, Paramyinae) from the Uinta Formation, Utah

(Excerpted from: Dunn and Rasmussen, 2007 J Vert Paleo 27:987-1006)

3.1 Introduction

Paramyines are the most abundant rodents in the Eocene of North America. They are first found in the Clarkforkian (Rose and Chinnery, 2004; Wood, 1962) and make their final appearance in the Orellan of South Dakota (Simpson, 1941). The latest surviving paramyines belong to the tribe Manitshini, and are characterized by their large size and simple, robust dentitions (Korth, 1985; Simpson, 1941; Wood, 1962). The earliest manitshines are Bridgerian in age and belong to the genus *Pseudotomus* (Korth, 1994; Matthew, 1910; Simpson, 1941; Wood, 1962). During the Bridgerian, manitshines were not particularly diverse, being represented by only two well defined species, *P. horribilis* and *P. robustus*, from the Bridger Basin, Wyoming (Korth, 1985; Wood, 1962). Manitshines reach their peak species diversity during the Uintan (Korth, 1994). During that time they were also geographically widespread, with records from California (*P. californicus* and *P. littoralis*), Utah (*P. petersoni* and *P. eugenei*) and Texas (*P. johanniculi*, Korth, 1985, 1994; Wood, 1974). After the late Uintan, manitshine fossils are conspicuously absent with the sole exception of *Manitsha tanka* from the Orellan of South Dakota, which is known only from the type specimen (Korth, 1984, 1994; Simpson, 1941). Though many of the Bridgerian and early Uintan manitshines are

represented by both dental and skeletal elements, the late Uintan and Oligocene manitshines are poorly known (Wood, 1962).

Also common in the Eocene are rodents belonging to the tribe Paramyini. These include *Paramys*, the most primitive of the paramyines, and other genera that are characterized by more gracile dentitions than the manitshines (Anderson, 2008; Wood, 1962). One genus, *Uintaparamys* is extremely common in the Uinta B member of the Uinta Formation and occurs from the late Wasatchian through the Duchesnean, although the species from the late Wasatchian (*U. parvus*) may be referable to the genus *Paramys* (Korth, 1984). The type species, *U. leptodus*, is commonly found in Uintan-aged localities in Texas, Wyoming and Utah, and is the most common rodent found in the Uinta B member from the Uinta formation (Anderson, 2008; Wood, 1962; Rasmussen, 1999). The postcrania of *Uintaparamys* are poorly represented in the published literature but isolated elements are common in the collections from the UF.

The locomotor behavior of paramyine rodents has never been well understood. In his 1962 monograph, Wood agreed with Matthew (1910) and Simpson (1941) that *Paramys* was most likely arboreal. They suggested that *Pseudotomus* had characteristics of both arboreal and fossorial rodents and that *Uintaparamys* was primarily fossorial. Simpson noted that the forelimb morphology of *Manitsha*, the largest and most derived manitshine, would have been equally well suited for digging or climbing, and suggested that it was even possible that *Manitsha* was semi-aquatic, though there was no unambiguous evidence to support any of these conclusions. The most compelling evidence that the paramyines *Manitsha*, *Pseudotomus* and *Uintaparamys* were terrestrial is their large size (Matthew, 1910; Simpson, 1941; Wood, 1962).

One factor making reconstruction of postcranial behavior in these rodents difficult is that their large size makes the choice of living analogs problematic. Postcranially, paramyines are usually compared to extant sciurids because sciurids are considered to be primitive among extant rodents and because members of this family present a diverse array of behaviors from fossorial forms to arboreal specialists. However, many sciurids are far too small to compare with rodents of such a large size as the manitshines. The smallest manitshines and *U. leptodus* are larger than the largest sciurid, *Marmota*. Most of the large rodents alive today belong to postcranially specialized groups such as the South American caviomorphs and the African hystricomorphs (Elissamburu and Vizcaíno, 2004; Simpson ,1941), which thus presents problems in making comparisons. Some murid rodents have reached moderately large size, but none reach manitshine proportions.

Another complicating factor in reconstructing manitshine behavior is the nature of their fossil record. Few taxa that have been described preserve elements in common with each other. The only specimen of *Manitsha tanka* preserves much of the skull and portions of the forelimb including a partial humerus, radius, proximal ulna, both clavicles and partial manus (Simpson, 1941). *Pseudotomus robustus*, *P. horribilis*, and *P. petersoni* are also known from postcrania, but there is no element in *Manitsha* that is also present in all of these species. The remains of the Bridgerian species (*P. robustus* and *P. horribilis*) both include the radius, ulna and scapula, and *P. robustus* is also represented by the humerus. The forelimb of the smaller Uintan species, *P. petersoni*, is known from metacarpals and manual phalanges including a single ungual phalanx (Wood, 1962). Consequently, functional comparisons between *Manitsha* and earlier manitshines have

consisted of general descriptive comparison of manual proportions and ungual phalanx morphology (Simpson, 1941; Wood, 1962). The postcrania known for *U. leptodus* is even more fragmentary, consisting of a crushed femur, partial scapula, fragmentary manus and a broken calcaneus (Wood, 1962).

Simpson noted (as did Matthew, 1910) that the Bridgerian species *Pseudotomus robustus* closely resembles the primitive paramyine *Paramys delicatus* in postcranial morphology and shows no specializations that would indicate a change in adaptive pattern except for its larger size. The unguals of *P. robustus* are short, deep and laterally compressed, resembling more those of arboreal sciurid rodents than terrestrial ones (Matthew, 1910; Simpson, 1941; Wood, 1962). *P. petersoni*, on the other hand, has long, shallow, uncompressed unguals, suggesting that this species was more fossorial. The ungual phalanges of *Manitsha* are described as long and deep, not closely resembling those of either *Pseudotomus petersoni* or *P. robustus* (Simpson, 1941). The only reconstruction of behavior for *Uintaparamys* is that of Wood (1962) in which he suggests that this genus was fossorial feeding on "succulent bulbs or roots (p. 72)."

In the Uinta Formation, the most common rodent in the Uinta B is *U. leptodus*, which all but disappears in the Uinta C, when rodents of the genus *Pseudotomus* become more common and the species *P. eugenei* appears for the first time. Previous researchers have commented that the teeth of rodents become increasingly hypsodont in the Uintan, as the climate becomes more open and there are fewer fruits and soft foods and they must process more resistant foods such as grasses or tough foliage (Black and Dawson, 1966; Korth, 1994; Rasmussen et al., 1999). The question of whether parallel trends occur in the postcrania of rodents has been difficult to address based on previously known

postcrania. The differences in postcranial morphology between the most common rodent in the early Uintan, *U. leptodus*, and *P. eugenei*, which is only found in the late Uintan and known only from the UF is of particular interest. A new skeleton of *Pseudotomus eugenei* (CM 71105) has been recovered by a WU field crew in 2001 from locality WU-210, which is stratigraphically high in the Uinta C member and near the region in which the holotype of *P. eugenei* (CM 11983) was found (Burke, 1935). This represents the most complete manitshine specimen known. Ongoing collection in the UF by WU since 1994 has recovered additional isolated remains of *U. leptodus*. Although a complete skeleton has yet to be found, the new fossils add to what was previously known of *U. leptodus* and allow a better functional interpretation.

The purpose of this chapter is to describe the skeletal morphology of *Pseudotomus eugenei* in relation to that of other manitshines and to *Uintaparamys leptodus*. I will assess the locomotor behavior and potential habitat preference of manitshines and *U. leptodus* and how it relates to habitat change within the Uinta Formation during the Uintan and the implications for primate evolution. Much of this chapter has been published previously as a coauthored paper (Dunn and Rasmussen, 2007). I have omitted the portions on systematic paleontology and cranial functional morphology, as these were written primarily by my coauthor. I made all postcranial comparisons and took the measurements of extant and fossil rodents, wrote the description of the postcranial skeleton, provided the functional interpretation, performed the statistical tests and prepared the figures which make up the majority of this chapter. I added the sections on *Uintaparamys* after the paper was published for the purpose of this dissertation.

3.2 Description and Comparisons

3.2.1 Methods

I undertook a variety of comparisons including qualitative and quantitative methods. My primary comparisons were to close relatives among manitshines that are also known from limb elements. These taxa include *Manitsha tanka*, *Pseudotomus robustus* and *P. petersoni*; the fossil skeletal remains of these taxa are curated at the AMNH. My comparisons involved original observations at the AMNH as well as reference to published studies on extant and other fossil taxa, as cited in the text when relevant.

To assess the relationship between skeletal form and behavior I compiled a sample of bone measurements from 24 extant species representing two broadly defined behavioral categories: arboreal and terrestrial (The terrestrial category can be subdivided into cursorial, fossorial, generalized and semi-aquatic). The extant comparative sample consists of relatively large-bodied rodents from several families and geographic regions (Table 3.1), which I compared to relevant fossil taxa (Table 3.2). Standard indices such as the brachial index were calculated and subjected to two kinds of analysis. Raw index values were evaluated for statistical differences among behavioral categories. Because the indices do not control for possible allometric affects of size, I also regressed index values as a function of size (size was measured as the summed lengths of the humerus, radius, femur and tibia) and evaluated the residuals in relation to locomotor categories.

3.2.2 Axial Skeleton

3.2.2.1 Vertebrae

Most of the fossil vertebrae consist only of a body with the neural arch broken away. Portions of the neural arch are preserved in some of the cervical vertebrae and anterior thoracics. The vertebral count consists of seven cervicals, at least 12 thoracics, at least five lumbars, one true sacral vertebra and one possible pseudo-sacral vertebra (but the immature nature of the skeleton makes this difficult to interpret). The shape of the atlas and axis are typical of large rodents, being similar to those of *Castor* (Figure 3.1 A and 3B). All cervical vertebrae possess a complete transverse foramen. The seventh cervical can be allocated with confidence to the cervical column because it was found in articulation with the rest of the cervicals, and it has a more robust base of the neural spine (most of the spine is broken off). The transverse process is also more robust than that of the first thoracic, and the vertebra does not have rib facets. The thoracic vertebrae can be recognized by distinct rib facets on the vertebral bodies (Figure 3.1 C). The first thoracic is the only vertebra preserving the tip of a transverse process and it does display a clear rib facet. The vertebral bodies increase in length craniocaudally throughout the thoracic column. The lumbar vertebrae can be recognized by their larger size, the lack of rib facets, and their strong ventral keel (Figure 3.1 D). One caudal half of a vertebral body is assigned to the lumbar series on the basis of its strong keel, though it could have had rib facets on the cranial portion, representing the last thoracic vertebra. In *Castor*, the caudal thoracics and cranial lumbar vertebrae have a similar keel, but the keel is strongest in the cranial lumbar vertebrae. The sacral vertebra has a body that is wider than it is long with robust allae (Figure 3.1 E). The possible pseudo-sacral vertebra is fragmentary and

consists of a cranioventral fragment of the body and base of a transverse process; its transverse process is more robust than that of any other vertebra and is positioned more ventrally on the body, such that it is consistent with a pseudo-sacral vertebra.

The tail represents the most damaged and incomplete part of the column, but it was long and tapered, as is indicated by a partial sequence of caudal vertebrae culminating in very small units. (Figure 3.1 F). There are at least six proximal caudal vertebrae articulating through synovial joints with fully developed neural arches and transverse processes. Two more specimens are ambiguous, with possible synovial articulation. One proximal caudal vertebra for which a transverse process is preserved indicates that the process was long and robust. Two other proximal caudals indicate that the neural arch was long and mediolaterally compressed. There is no evidence for a stronger than average flexor system of the tail like that found in prehensile-tailed animals (Ankel, 1972; Shapiro, 1993).

3.2.3 Forelimb

3.2.3.1 Scapula

Portions of the right and left scapulae are represented. The left scapula is the best preserved and consists of the glenoid fossa, a portion of the acromion process, and the base of the coracoid process (Figure 3.2 A). The morphology of the glenoid fossa resembles that of other paramyines and sciurids in being concave and pyriform. The coracoid process is incomplete, but from the preserved portion, it appears that it was robust and simple in morphology. This does not resemble the bony projection that is glued to this spot in the AMNH specimen of *Manitsha*, which has a dorsal and ventral projection; I suspect that this may be a misplaced part. Just caudal to the glenoid fossa is

a deep pit for the attachment of the long head of the triceps, with a less distinct pit placed more laterally and cranially for the teres minor muscle.

3.2.3.2 Humerus

The left humerus is complete with minimal damage, while the right is more fragmentary. The proximal humeral epiphysis was not yet fused to the shaft, and distally the epiphyseal line is still evident on the medial epicondyle. The humerus is relatively robust with strong muscle markings (Figure 3.2 B). The humerus of *P. eugenei* resembles that of *Manitsha* in general proportions and appearance except when noted. The humeral head of *P. eugenei* is hemispherical. Both the greater and lesser tubercles are low and do not project above the head (Figure 3.2 B), in contrast to the situation in *Manitsha* and Miocene mylagaulids in which the greater tubercle is clearly raised above the level of the humeral head (Fagan, 1960; Gidley, 1907). The greater tubercle is somewhat distorted, but it appears to have been larger than those of arboreal sciurids, more closely resembling those of terrestrial species. There is a large pit for the insertion of the infraspinatus on the lateral surface of the greater tubercle. The pit resembles those of terrestrial sciurids and *Castor* in being surrounded by a raised rim, rather than being continuous with the articular surface as in arboreal squirrels. The lesser tubercle projects medially more than what is seen in Wasatchian paramyines from the Big Horn Basin, but less so than in many sciurids.

Most of the deltopectoral crest is damaged, but the remaining portion indicates a robust, laterally directed crest that extends well over halfway down the shaft (Figure 3.2 B). The deltopectoral crest of *Manitsha* is also large and laterally directed, but only extends approximately halfway down the shaft. *Marmota* and *Castor* resemble *Manitsha*

in having the deltopectoral crest extend to the midshaft of the humerus and not farther. In Miocene mylagaulids the deltopectoral crest extends over halfway down the shaft as in *P. eugenei*, but differs in its overall morphology (Fagan, 1960; Gidley, 1907). Lateral deviation of the deltoid ridge is seen in terrestrial sciurids, but not in arboreal species (Rose and Chinnery, 2004). Distal to the lesser tubercle and just proximal to midshaft is an elongated ridge marking the insertion of the latissimus dorsi and teres major. This ridge is longer than those of Wasatchian paramyines, and is only slightly raised. In *Manitsha*, this ridge is also elongated, but is markedly raised. The extent to which this crest is raised varies in larger bodied rodents, being particularly well marked in *Ratufa*, *Erethizon* and *Castor*, and less so in *Marmota* and *Myocastor*.

The posterior face of the humeral shaft is flat and preserves a faint line originating at the lesser tubercle and traveling laterally to join with the lateral supracondylar ridge (Figure 3.2 B). This marks the origin of the lateral head of triceps brachii. The lateral supracondylar ridge is damaged, but enough remains to determine its origin just distal to midshaft. This condition contrasts with *Marmota* in which the supracondylar ridge originates just proximal to midshaft, but more closely resembles the shape in *Castor*. In *Erethizon* and *Ratufa*, this ridge originates more distally and is much smaller. The supracondylar ridge curves smoothly throughout, rather than having a more irregular and angular border, most closely resembling *Marmota*. The anterior surface of the ridge is shallowly concave, and the posterior is gently convex. The lateral epicondyle is continuous with the supracondylar ridge as in *Castor*, *Aplodontia*, and ground squirrels.

The entepicondyle is large and robust with distinct pits and ridges for attachment of flexor muscles of the wrist and digits (Figure 3.2 B). It is more robust and longer

proximodistally than those of extant sciurids, Wasatchian paramyines and *Manitsha*. The entepicondyle is oriented straight medially rather than mediodistally as in the other taxa; this is due to the proximal expansion of the epicondyle. In the shape and position of the epicondyle, *P. eugenei* most closely resembles *Aplodontia*. An entepicondylar foramen is present. As in Wasatchian rodents, there is a large pit on the posterior surface between the trochlea and medial epicondyle for the humero-ulnar ligament. In *P. eugenei*, this pit is large and deep, more closely resembling the condition seen in *Castor* and *Aplodontia* than in sciurids, in which no pit is present.

The capitulum is cylindrical with a slight central swelling. The radial fossa is deep, there is no coronoid fossa and the supratrochlear foramen is absent. The medial lip of the trochlea is steeply angled. Posteriorly the trochlea projects out from the rest of the humerus. The lateral trochlear ridge is robust posteriorly and extends to the most distal part of the humerus where it blends with the capitulum. Much of the olecranon fossa is damaged, but the lateral aspect indicates that it was a deep, proximodistally narrow trough, resembling the condition seen in *Marmota*, *Castor* and *Myocastor*. Among extant rodents, the distal humerus most closely resembles that of *Marmota*.

The greatest difference between the humeri of *P. eugenei* and *Manitsha* is in the shape of the distal end. The absolute width of the distal humerus across the epicondyles is approximately the same in both taxa despite the significantly longer humerus of *Manitsha*. The entepicondyle of *Manitsha* is more robust at the base than that of *P. eugenei* and tapers to a point rather than flaring out at the tip. It is posteriorly directed in *Manitsha* rather than medially directed, as in *P. eugenei*, and is stouter overall. The medial and lateral keels of the trochlea are high and well defined in *Manitsha*, more so

than in *P. eugenei* or *P. robustus*. The trochlear groove is aligned parasagittally in *Manitsha* rather than obliquely as in *P. eugenei* and *P. robustus*. The supracondylar ridge is most developed in *P. eugenei*, least developed in *P. robustus*, and intermediate in *Manitsha* The shape of the capitulum among these taxa is similar, though *Manitsha* has a relatively narrower capitulum than either *P. eugenei* or *P. robustus*.

Comparisons with U. leptodus—Several proximal humeri from the UF most likely belong to *U. leptodus*. They all preserve low greater and lesser tubercles that do not rise to the level of the head, more characteristic of arboreal rodents than terrestrial ones. The tubercles are lower and smaller in size than those of *P. eugenei*. The lesser tuberosity of *U. leptodus* flares medially as is seen in arboreal sciurids and unlike that of *P. eugenei* and terrestrial sciurids. The distal humerus is also known from several specimens, but only the morphology of the distal articular surface and epicondyles is well represented. The capitulum of *U. leptodus* is rounder than that of *P. eugenei* and of terrestrial sciurids, closely resembling that of *Sciurus*. The medial keel of the trochlea does not project as far distally as that of *P. eugenei*, extending approximately to the distal edge of the capitulum. The medial epicondyle is prominent, but is not expanded proximo-distally as in *P. eugenei* and mostly projecting medially. The lateral epicondyle is small and does not project laterally. Although the lateral supracondylar ridge is not fully preserved in any specimen it, appears that it did not flare drastically, in contrast to the condition in *P. eugenei*.

3.2.3.3 Ulna

Both ulnae are present. The distal epiphysis was not yet fused. The proximal epiphysis is fused, but the epiphyseal line is visible. The right ulna best preserves the

shape of the shaft, but the proximal radial and humeral articulations are damaged. The proximal articular surface is undamaged on the left ulna.

The ulnar shaft is nearly straight throughout with a slight dorsal inflection at the distal end, resembling the case in *Manitsha* (Figure 3.2 D). Large extant rodents (e.g. *Myocastor*, *Castor* and *Marmota*) often have a more pronounced bowing of the distal shaft, with *Castor* being the most extreme in this feature. The olecranon process of *P. eugenei* does not curve cranially as is seen in Wasatchian paramyines, *Manitsha*, and arboreal extant rodents. Rather, the posterior edge of the olecranon process is straight, while the anterior edge is slightly cranially inflected. When compared to extant rodents, the olecranon of *P. eugenei* most closely resembles the condition seen in *Marmota*. The olecranon process of *P. eugenei* is medially inflected to a lesser degree than in *Marmota* and *Manitsha* but to a greater degree than in arboreal rodents. The point of insertion for the triceps tendon is strongly marked and the olecranon process is long. The semilunar notch of *P. eugenei* and *Manitsha* is relatively closed in lateral view, rather than open as in arboreal rodents and Wasatchian paramyines. The medial margin of the semilunar notch extends proximally, resembling that of Wasatchian rodents and *Marmota*. The radial notch is offset from the semilunar notch at a higher angle than those of most arboreal sciurids and early Eocene paramyines, resembling instead terrestrial sciurids (Rose and Chinnery, 2004). The radial notch is flat and broad, resembling terrestrial sciurids and *Manitsha* in this respect more than arboreal sciurids and Wasatchian paramyines.

The lateral fossa of the ulnar shaft in *P. eugenei* is relatively deeper than in *Mylagulus* (Fagan ,1960), *Manitsha* or *Marmota*, and is similar to the deep grooves seen

in *Aplodontia*, *Myocastor*, *Castor* and early Eocene paramyines. The lateral fossa of *P. eugenei* persists for almost the entire length of the shaft (Figure 3.2 D). In contrast, the lateral fossa is poorly defined in arboreal sciurids and *Erethizon*. In *Castor* and *Myocastor*, the lateral fossa is deep proximally and disappears in the distal third of the shaft, while in *Aplodontia* it persists to the last quarter. In sum, the ulna is deeply furrowed on both sides in *P. eugenei* when compared to most other rodents, thereby being shaped like an I-beam, to resist fore and aft movements that would be exerted during flexion and extension.

The pit for the insertion of the brachialis just distal to the coronoid process is deep and well defined. In *Manitsha* the pit is present, but shallower. The pit is better defined in terrestrial species than in arboreal species. The anterior margin of the ulna in *P. eugenei* forms a sharp interosseus crest that extends to the distal end of the diaphysis. In *Manitsha* and *Marmota* this crest is more rounded. The crest for the pronator quadratus is present, but not as well defined as it is in *Manitsha* and *Marmota*.

Comparisons with U. leptodus—A complete ulna is not preserved in *U. leptodus*, but several proximal ulnae are known. The olecranon process of *U. leptodus* is short, robust and straight, contrasting starkly with that of *P. eugenei*, which is long and medially inflected. The radial facet is not offset as sharply from the semilunar notch in *U. leptodus* and is broader than the condition in *P. eugenei* but like the condition in this genus, the radial notch of *U. leptodus* is flat to concave, rather than convex as is seen in arboreal sciurids.

3.2.3.4 Radius

Both right and left radii are well preserved.. The proximal epiphysis was in the process of fusing at the time of death; on the left side it is partially detached while on the right side it is in place and not distorted. The distal epiphysis of the radius was not fused to the shaft.

The radial shaft of *P. eugenei* is dorsally bowed and expands in depth and breadth distally (Figure 3.2 C). This expansion is less well developed than in mylagulids (Fagan, 1960; Gidley, 1907) and best resembles the condition seen in *Marmota*. The radius of *Manitsha* is also bowed, but to a lesser degree. The radial head of *P. eugenei* is ovoid with a distinct capitular eminence, which resembles that of *Marmota* in general shape. The radial head of *Manitsha* is more elliptical than that of *P. eugenei*. The flexor surface of the radial shaft is flat in *P. eugenei*, not concave as is seen in *Marmota*. *P. eugenei* has a ridge demarcating the origin of the flexor digitorum profundus and pronator teres muscles. Unlike primitive Wasatchian paramyines, the ridge is not sharp but extends onto the dorsal surface of the radial shaft where it forms a shallow pit just distal to the midshaft. This is similar to the condition seen in *Marmota* and *Castor*. The interosseus crest is sharper and more flaring than its equivalent in *Manitsha* and *Marmota*. The extensor surface of the distal radius is expanded and flat, but not to the extent seen in terrestrial sciruids such as *Marmota,* or in *Manitsha*. The styloid process on the distal epiphysis is not strongly projecting, resembling the process of Wasatchian rodents. The distal articular surface is broad, gently concave and roughly ovoid in outline; this is unlike the condition in *Marmota*, where the articular surface is restricted in area.

Comparisons with U. leptodus—Only the proximal radius of *U. leptodus* is represented in the CM collection at WU. The radial head is similar to that of *P. eugenei*, but it is slightly rounder in outline.

3.2.3.5 Carpus

All carpals were recovered except for the centrale and trapezoid; the lunate and pisiform are incomplete. The scaphoid and lunate are separate elements as in other manitshines and *Douglassciurus* (Emry and Korth, 2001; Emry and Thorington, 1982; Wood, 1962; Figure 3.3). In the paramyines *Leptotomus* and *Reithroparamys* and among extant rodents, the scaphoid and lunate are fused into a single element (Thorington and Darrow, 2000; Wood, 1962). The carpus of *Pseudotomus* is organized into two distinct integrated halves: the radial half with scaphoid, lunate, magnum, centrale, trapezoid, trapezium, and falciform; and the ulnar half with pisiform, triquetrum and unciform.

The lateral palmar border of the scaphoid is damaged, but another specimen allocated to *P. eugenei* (CM 71049) preserves the whole element. It articulates ulnarly with the lunate and distally with the magnum and trapezoid. Two tubercles are present on the plantar surface of the scaphoid, rather than the single one that occurs on the scaphoid of *P. robustus*. Some extant rodents show a slight swelling medial to the scaphoid tubercle, but not a fully developed tubercle. The scaphoid tubercle is more prominent in *P. eugenei* than in *P. robustus*, and it has a more hooked medial border. This serves as the primary radial insertion for the flexor retinaculum. The groove created by the sharp medial border and the tubercle medial to it probably housed the tendon of the flexor carpi radialis, which dives under the flexor retinaculum and inserts onto the base of metacarpal II in extant rodents (Thorington et al., 1998). There is a radial sesamoid (falciform)

present in *P. eugenei*, as in *P. petersoni*. This bone is similar to that seen in extant rodents and closely resembles that of *Marmota*. In extant squirrels, with the exception of flying squirrels, the falciform bone forms part of the flexor retinaculum (Thorington and Darrow, 2000). No other paramyine specimens have been associated with a radial sesamoid, but this is most likely due to the absence of well preserved paramyine hands, as this bone is ubiquitous in extant rodents. Only the palmar half of the lunate is preserved in CM 71105. It articulates with the scaphoid radially, the triquetrum ulnarly and the unciform and magnum distally.

The triquetrum is similar in shape to that of *P. robustus* and *P. petersoni*, being elongate, broad dorsally and tapering palmarly. Proximally, the triquetrum articulates with the pisiform and the styloid process of the ulna. The ulnar styloid sits in a cup formed by a proximal groove on the triquetrum and a shallow fossa on the head of the pisiform. Distally, the triquetrum primarily articulates with the unciform and also has a small facet for metacarpal V. The head of the pisiform is radio-ulnarly elongate with a slight radial hook. The distal portion of the pisiform is broken, but the part that is preserved is rod-like rather than flaring as in *P. robustus* and *P. petersoni*. The unciform is a stout, quadrate bone similar to that of *P. robustus* except that it is radio-ulnarly narrower. It articulates with the triquetrum proximally, the lunate, magnum and metacarpal III radially, and metacarpals IV and V distally.

The magnum is crescent shaped in lateral view with small dorsal and palmar non-articular surfaces. It articulates with the lunate and perhaps the scaphoid proximally, though in *P. robustus* and *P. petersoni* the magnum is reconstructed as contacting only the lunate proximally. On its ulnar aspect it contacts the unciform, and radially the

trapezoid and presumably the centrale. Matthew (1910) and Wood (1962) disagreed on where the centrale was located within the carpus of *P. petersoni*. Matthew (1910) reconstructed the centrale as articulating with the lunate, trapezoid and scaphoid, whereas Wood (1962) argued that it also articulated with the magnum. As the centrale is absent in this specimen, it is difficult to address this issue with certainty, but it appears that the centrale would have contacted the magnum. Proximally, the magnum articulates with metacarpals II and III.

3.2.3.6 Manus

The left manus is fairly complete including four metacarpals and several phalanges. Metacarpals II and III are damaged and somewhat distorted. On the right side, metacarpals III, IV, and the head of metacarpal II are also preserved and are less distorted. The first metacarpal was not recovered.

The second metacarpal is waisted, being broad proximally and even broader distally with a narrower central shaft (Figure 3.3). The head of the left metacarpal is damaged, but the head attributed to right metacarpal II is well preserved. All the metacarpals possess a strong keel on the palmar surface of the metacarpal head. The head is cylindrical and asymmetrical. There is a "W" shaped articular surface at the metacarpal base for articulation with the magnum laterally, the trapezium medially, and the trapezoid proximally. On the lateral surface of the base is a concave surface for articulation with the third metacarpal.

Metacarpal III is the longest metacarpal. The proximal end has a concave articular surface for the magnum and a convex articular surface pointing proximolaterally for the unciform. Medially, the articular surface for metacarpal II is convex and crescentic. The

articular surface for the fourth metacarpal is located on the dorso-lateral surface of the base and is shallowly concave. There may have been a second articular surface palmarly for metatarsal IV, but both third metacarpals are damaged in this area, making this inconclusive. On the dorso-medial aspect of the proximal shaft is a scar for the extensor carpi radialis brevis. The head of the third metacarpal is cylindrical and symmetrical.

Metacarpal IV is shorter than the third metacarpal, but longer than metacarpal II. Like metacarpal III, the base is narrow and the head broad. Medially, the base of the metacarpal articulates with the third metacarpal, and laterally with metacarpal V. Proximally, the base articulates with the unciform. The head is also symmetrical and cylindrical like that of metacarpal III. On the dorso-lateral surface of the proximal shaft, there is a scar, similar to that on metacarpal III.

The fifth metacarpal is the shortest, so in sequence, the metacarpals are ranked from longest to shortest as III, IV, II, V. The shaft of metacarpal V differs from the other metacarpals in being strongly curved dorso-palmarly rather than straight. The head also differs in shape from the other metacarpals in being more spherical rather than cylindrical. Proximally, the largest articular surface is for the unciform, and there is a smaller one for articulation with the triquetrum. The medial surface of the base articulates with the fourth metacarpal.

The proximal phalanges of the manus are heavily built bones. The flexor sheath ridges on the palmar aspect are evident, but not strongly developed. The proximal articular surface is grooved at its palmar edge for accommodation of the keel on the head of the metacarpals. The middle phalanges are also strongly built. Their proximal articular surface is concave with a dorsal lip. The distal articular surface is shallowly grooved and

extends well onto the dorsal aspect of the bone. The ungual phalanges are long; those that are nearly complete in length are similar to or surpass the length of the proximal phalanges (Figure 3.3). They are not strongly keeled or strongly curved and are similar in shape to those of fossorial animals (MacLeod and Rose, 1993). The plantar tubercle of the flexor digitorum profundus is well developed and the dorsal extensor tubercle is discernable, but not especially well developed.

The manus of *Pseudotomus robustus* and *Manitsha tanka* are generally similar to that of *P. eugenei*, but differ in some interesting ways. The metacarpals of *P. robustus* are similar in absolute length to those of *P. eugenei*, but are more gracile. The manus of *Manitsha* is both relatively larger and more robust than that of *P. eugenei*. The metacarpal heads of *P. eugenei* and *P. robustus* resemble each other; the current mounted position of the specimen of *Manitsha* obscures the metacarpal heads but Simpson (1941) noted their resemblance to those of *P. robustus*. The proximal phalanges of *P. robustus* and *Manitsha* possess distinct flexor tubercles on the palmar aspect that are visible in dorsal view. These are largest in *Manitsha* and smallest in *P. robustus*. The flexor ridges in *P. eugenei* are smaller than those of *Manitsha*, but they are more similar to *Manitsha* than to *P. robustus*. In *Manitsha* the third proximal phalanx is approximately 2/3 as long as MC III. This differs from the situation in *P. eugenei* in which the longest proximal phalanx is only half as long as MC III. The middle phalanges of *Manitsha* and *P. eugenei* are significantly shorter than the proximal phalanges, whereas in *P. robustus*, they are only slightly shorter. Miocene mylagaulids also show greater reduction of the length of the phalanges than is seen in *P. eugenei* (Fagan, 1960; Gidley, 1907). In *P. robustus*, the ungual phalanges are laterally compressed, dorsoventrally deep, and shorter than hind

unguals (Matthew, 1910; Simpson, 1941). The ungual phalanges of *Manitsha* are not compressed and are at least as long as the middle phalanges, more closely resembling those of *P. petersoni* and *P. eugenei* than those of *P. robustus*. Simpson (1941) described the unguals of *Manitsha* and *P. robustus* as being deeper than those of *P. petersoni*, but now the depth is difficult to assess because of the way the specimens are mounted. The ungual phalanges of *Manitsha* appear to be similar in both relative length and depth to those of *P. eugenei*.

3.2.4 Hindlimb

3.2.4.1 Innominate

Portions of the right and left innominates are preserved. The left innominate is the most complete and preserves the acetabulum, almost complete ischium, and a large portion of the ilium. The left femoral head is preserved still inside the acetabulum.

The innominate is comparable in size to that of *Castor*, though the acetabulum is relatively larger in the fossil and is more robust. The left acetabulum, though complete, is obscured by the left femoral head that is in articular position, and the morphology of the acetabular surface cannot be assessed. The right side shows that the anterior acetabular surface is expanded relative to the posterior surface.

The anterior inferior iliac spine is well developed and is connected to the anterior acetabular rim by a thick, rough ridge (Figure 3.4 A). The spine is relatively larger and more projecting than in the other rodents examined. The lateral surface of the ilium is divided into three planes: dorsal, lateral and ventral. These three planes are separated by prominent rounded ridges. In other rodents including other paramyines (Rose and Chinnery, 2004; Wood, 1962) and *Mylagaulus* (Fagan, 1960), the ilium is divided into

only two planes, a dorsal gluteal plane and a ventral iliac plane. In *Cuniculus* and *Dasyprocta* there is some development of a third, but it is not as extensive as in *P. eugenei*. It is unclear which planes are homologous to the gluteal and iliac planes in other rodents, but it appears likely that the dorsal plane is the gluteal and the lateral is the iliac. In this case, the ventral plane is most likely not an area for muscle attachment, but an extra strip of bone running ventral to the sacrum (alternatively, the ventral plane may represent the iliac plane and the lateral plane may represent a bare area between the gluteal and iliacus muscles).

The ischial spine is a prominent and blunt tubercle placed well caudal to the acetabulum (as is seen in sciuromorphs, and also in the hystricomorphs *Myocastor* and *Hydrochoerus*) rather than the hook-like, sharply defined spur seen in the other caviomorphs examined. In *Erethizon* and *Coendou*, the ischial spine is larger than it is in the other taxa. The ischial tuberosity of *P. eugenei* is well developed dorsally. The ischium and ilium angle dorsally as they diverge from the acetabulum. In *Castor* and the caviomorph rodents examined, the ilium and ischium are more or less in line with each other, making a more obtuse angle than in *P. eugenei*, though the condition in the fossil could be a result of post-depositional deformation.

3.2.4.2 Femur

Most of the left and right femora are preserved. The left femur is the most complete of the two, preserving the entire length of the shaft as well as the distal end and greater trochanter. The left femoral head is inside the acetabulum of the left innominate, and the femoral neck is not preserved. The epiphyses were not yet fused to the diaphysis, including that of the greater trochanter. The left patella is present.

The proximal ends of both femora are damaged, so it is difficult to determine the relative height of the greater trochanter, but based on what is preserved of the left femur it most likely extended to about the level of the femoral head. The greater trochanter encloses a trochanteric fossa that is relatively deeper and longer than in either *Marmota* or *Castor* (Figure 3.4 B). All caviomorphs examined had a deep trochanteric fossa, but they were not as proximodistally elongated. The lesser trochanter is more robust than in *Marmota* but less so than in *Castor*, and points posteromedially as in these genera and Wasatchian paramyines. In caviomorphs, the lesser trochanter is reduced. In *Pseudotomus robustus*, the lesser trochanter resembles that of *P. eugenei* in shape but projects more posteriorly. The greater and lesser trochanters are not connected by an intertrochanteric crest. This contrasts to the condition seen in arboreal sciurids, South American caviomorphs, *P. robustus* and Wasatchian rodents, in which the crest is present, but varies in prominence.

The third trochanter of *P. eugenei* differs significantly from that of *P. robustus*, Wasatchian paramyines (Rose and Chinnery, 2004), Miocene mylagaulids (Fagan, 1960), and ground squirrels in being positioned much farther distally. The third trochanter is broken off of both the right and left shafts, but its position and length can be determined. The middle of the broken base of the third trochanter falls approximately at midshaft (Figure 3.4 B), in contrast to a position well proximal to midshaft in other taxa. In this feature, *P. eugenei* most closely resembles *Castor*. *P. eugenei* has a distinct, rough linea aspera between the lesser and third trochanters. The distal femur of *P. eugenei* is approximately equally broad as it is deep. The patellar groove is deep and raised above the condyles resembling the condition in *P. petersoni* rather than *P. robustus*. The

condyles of *P. eugenei* and *P. petersoni* are relatively deeper than those of *P. robustus*. The medial condyle extends further distocaudally than the lateral condyle, but this condition is not as extreme as that of *Castor*. Fabellae are present as judged from the facet for them on the condyles.

3.2.4.3 Tibia and Fibula

Both the right and left tibias are well preserved with minimal damage. Neither the proximal nor the distal epiphyses are fused to the shaft, but both were recovered for both tibias. The fibula shafts are missing, but the bone is represented by unfused proximal and distal epiphyses on the left side and the proximal epiphysis on the right.

In general, the tibial plateau resembles those of extant sciurids (Figure 3.4 C). The tibial cotylae are deeper and the tibial tuberosity is more strongly projecting in *Pseudotomus eugenei* and *P. petersoni* than in *P. robustus*, in which the tibial plateau has an overall broader, flatter appearance. The medial condyle is substantially lower than the lateral condyle of *P. eugenei*, resembling Wasatchian rodents and *P. petersoni* rather than *P. robustus*, in which they are more even in height. In *P. robustus* the medial condyle is rounder in shape than in *P. eugenei* and the intercondylar region is broad and flat. In *P. petersoni* and *P. eugenei* the intercondylar region is narrow and raised above the condyles. *P. robustus* resembles Wasatchian paramyines in this feature. The proximal fibular facet is large and sigmoidal as is also found in *Sciurus* and Wasatchian paramyines.

The tibial crest in *P. eugenei* is sharper and more distinct than that of *P. robustus* and extends approximately to midshaft (Figure 3.4 C), resembling the tibial crest of *Castor*. In *P. robustus*, the crest only extends down the proximal third of the shaft, as is

also seen in *Marmota*. The popliteal fossa is deeper than the tibialis anterior fossa, though neither fossa is very deep.

The posterior process of the distal tibia is large, as in other paramyines (Figure 3.4 C). The groove for the flexor fibularis on the posterior aspect of the process is deep and the medial lip more elevated than the lateral lip, similar to the condition in *P. robustus*, caviomorphs, and Wasatchian paramyines, but different from the condition in *Marmota*, in which the medial and lateral lips are equally pronounced. The medial malleolus is large, projecting nearly as far distally as the posterior process, the primitive condition for paramyines. There is a shallow, indistinct groove for the flexor tibialis tendon on the posterior surface of the medial malleolus, but the groove is not as well developed as in extant sciurids or early Eocene paramyines.

The distal articular surface of *P. eugenei* is wider mediolaterally than anteroposteriorly (Figure 3.4 C), unlike the condition seen in Wasatchian paramyines and *P. robustus*, in which the distal articular surface of the tibia is as wide mediolaterally as anteroposteriorly. The articular surface for the medial astragalar crest is deep and the lateral articular surface slopes more gradually, as is characteristic of rodents in general. The articular surface of the lateral astragalar facet extends slightly onto the anterior surface of the distal tibia, providing a stop for the astragalus during dorsiflexion, as in primitive paramyines. The posterolateral margin of the distal facet is notched for the attachment of the posterior tibiofibular ligament, as in some Wasatchian paramyines and *P. robustus*. The distal articular surface does not exhibit any of the medial torsion characteristic of Miocene mylagaulids (Fagan, 1960; Gidley, 1907). The distal fibular facet is just anterior to this notch; it is small and semi-lunar in shape, similar to the

condition in *Erethizon*. There is no obvious raised interosseus crest or roughening on the distal tibial shaft that would indicate a strong syndesmosis between the distal fibula and tibia.

The proximal and distal fibular epiphyses are robust and resemble those of *P. robustus* in general appearance, suggesting that the fibula was not reduced (Figure 3.4 D and 3.4 E). No paramyines for which fibular morphology is preserved show reduction of the fibula. The lateral malleolus of the fibula presents a large convex facet on its medial surface for articulation with the lateral body of the astragalus (Figure 3.4 E). Just posterior to this facet is a strong pit for the attachment of the posterior astragalo-fibular ligament.

Comparisons with U. leptodus—Only the distal tibia is known from the UF. The posterior process of the tibia is well-developed as in *P. eugenei* and other paramyines, but the distal articular surface is not as wide as in *P. eugenei*, giving it a more triangular outline in distal view. The groove for the flexor fibularis is not well-defined, consisting of a shallow sulcus with a raised medial lip in contrast to the condition in *P. eugenei* in which the groove and lateral lip are well defined. The medial malleolus is large and projecting as in all paramyines, and the groove for the tibialis posterior is deep and is limited medially by a sharp ridge. This resembles the condition in extant sciruids and early Eocene paramyines more than that in *P. eugenei*. The facet for the fibula is large, flat and semilunar in shape resembling early Eocene paramyines and being larger in size than that of *P. eugenei*.

3.2.4.4 Tarsals

The entire left ankle of *P. eugenei* is well preserved with minimal damage. In addition, portions of the right astragalus and calcaneus, and the entire right ento- and ectocuneiforms are present. The proximal calcaneal epiphysis had recently fused and the epiphyseal line is well defined.

3.2.4.4.1 Astragalus

The astragalus differs from those of Wasatchian paramyines in that the medial trochlear crest is about 75% the length of the lateral crest (Figure 3.5 B). In most Wasatchian rodents the trochlear crests are more equal in length. The medial and lateral trochlear crests are approximately equal in height, with the medial crest being sharper, and the lateral crest sloping more gradually. The trochlea is deeply grooved. The medial and lateral articular surfaces for the malleoli of the tibia and fibula are vertical. The astragalar neck is similar in degree of medial deviation to those of other paramyines but it may be proportionally shorter than those of *Paramys*, judging from illustrations in Rose and Chinnery (2004). The navicular facet of the astragalus is a dorso-ventrally compressed ellipsoid which extends substantially medially (Figure 3.5 B and 3.5 F).

On the plantar aspect of the astragalus, the ectal facet is pyriform, narrower distally but more squared off proximally. This facet is strongly concave, resembling the condition in *Castor* and *Myocastor* rather than *Erethizon* in which the facet is flatter. The sustentacular facet is also roughly pyriform in shape with a distinct sustentacular hinge at its proximal end, which is typical of other paramyines and *Erethizon.* Distally, however, the sustentacular facet is continuous with the navicular facet via a narrow bridge of subchondral bone and a proximal expansion of the plantar surface of the navicular facet.

Continuity of these two facets has not been reported in other paramyines, and as only one astragalus is known, it is unclear whether this is typical of *P. eugenei* or simply due to individual variation. This condition does not resemble extant rodents in which there is a broad contact between the two facets. The sustentacular facet does not contact the trochlear articular but is separated from it by a raised, nonarticular area. In other paramyines, the trochlear surface wraps around to the plantar surface of the astragalus.

Comparison to U. leptodus—The astragalus of *U. leptodus* differs from that of *P. eugenei* in the greater degree of medial inflection of the neck and in the more symmetrical condyles. The medial condyle is approximately 82% of the length of the lateral condyle, more comparable in length to that of Wasatchian paramyines (Rose and Chinnery, 2004). A sustentacular hinge is also present in *U. leptodus* and in contrast to *P. eugenei*, the sustentaculum does not contact the navicular facet. In most other aspects, the astragalus of *U. leptodus* resembles that of *P. eugenei* and other paramyines.

3.2.4.4.2 Calcaneus

The calcaneus of *P. eugenei* is similar to those of other paramyines in general form (Figure 3.5 A); among rodents, it is most similar to that of *Myocastor* in relative dimensions and in morphology, but is substantially larger. The calcaneal tuber is relatively longer than in extant sciurids, making up approximately 40% of the length of the calcaneus rather than one third of its length, as is seen in sciurids. The tuber is slightly expanded proximally, but not to the degree seen in extant arboreal sciurids, more resembling Wasatchian paramyines and other large Eocene paramyine rodents. There is a slight groove for the insertion of the Achilles tendon. The dorsal border is less constricted than in arboreal squirrels, more resembling the condition found in ground squirrels and

Wasatchian paramyines. The ectal facet is strongly arched and of uniform width throughout, and oriented obliquely to the long axis of the calcaneus. It is helical in shape, facing medially at the proximal end and distally at the distal end, thereby resembling other paramyines. The sustentaculum tali is prominent and the sustentacular facet is ovoid and slightly concave. The shape of the sustentacular facet is similar to that of large paramyines and contrasts with the smaller Wasatchian paramyines and extant sciurids in being flattened and expanded distally with a rounded proximal border rather than being circular in shape. The sustentacular and ectal facets are separated by a deep sulcus, resembling *Spermophilus* and *Douglassciurus* (Emry and Thorington, 1982). The ectal and sustentacular facets overlap considerably at the mid-calcaneal level, resembling terrestrial sciurids and other paramyines more than arboreal sciurids. Distal to the ectal facet, the calcaneus is short, as in other paramyines. The cuboid facet is damaged laterally, but it appears to have been similar to that of other paramyines in being ovoid in shape (Figure 3.5 F). The dorsomedial corner of this facet is slightly offset proximally as a small facet for articulation with the navicular. There is a prominent plantar tubercle extending proximally just beneath the sustentaculum that is relatively smaller than the tubercle in *P. petersoni* and in Wasatchian rodents. This tubercle is strongly grooved medially for the tendon of the flexor fibularis, resembling the condition seen in *Myocastor*.

Comparison to U. leptodus—The calcaneal heel is relatively longer than in *P. eugenei*, being 43% of the length of the calcaneus and longer than that of early Eocene paramyines (Rose and Chinnery, 2004). The dorsal border of the calcaneal heel is constricted and forms a narrow ridge running from the proximal end of the ectal facet to

the calcaneal tubercle as is seen in arboreal sciurids, whereas in *P. eugenei* this resembles the condition seen in terrestrial squirrels. The sustentaculum is rounder than in *P. eugenei*, more resembling the condition in Wasatchian paramyines, but resembles *P. eugenei* in the high degree of overlap between the ectal and sustentacular facets. The distal end of the calcaneus is also short in *U. leptodus*, and the cuboid facet is round rather than ovoid. The plantar tubercle is smaller in *U. leptodus* than in *P. eugenei* and is situated near the planto-medial edge of the cuboid facet rather than directly plantar to it as in other rodents. The peroneal tubercle of *U. leptodus* is robust and proximo-distally extensive, beginning below the ectal facet and extending just opposite the distal border of the sustentaculum. This process is broken in *P. eugenei*, but it was positioned farther distally than in *U. leptodus*. The condition in *U. leptodus* is similar to that in Wasatchian paramyines.

3.2.4.4.3 Navicular

The navicular is similar to other paramyine naviculars in general outline but differs significantly in some important features (Figure 3.5 D). Proximally, the facet for the astragalar head is strongly concave dorsoventrally, and less so mediolaterally. The navicular does not wrap around the astragalar head medially as has been described for other species of *Pseudotomus* (Wood, 1962). In addition, there is a facet for articulation with the calcaneus on the planto-lateral edge of the navicular. This facet has not been noted for any other paramyines; it is clearly absent from the navicular of *P. robustus*, while the relevant portions are damaged and it is absent in *P. petersoni*. The navicular of caviomorph rodents sometimes has a small articular facet for the calcaneus, but this feature is variable. This calcaneal facet is located on the proximal surface of the cuboid

facet, which is itself expanded in *P. petersoni* and *P. eugenei* relative to *P. robustus* (as described by Wood, 1962) and is oriented proximally and slightly dorsally. The calcaneal facet of caviomorphs is located proximal to the cuboid facet and points laterally rather than proximally. The cuboid facet in *P. eugenei* is triangular and gently concave, with the apex pointing proximally and plantarly, and the entire facet points distoplantarly. The surface of the ectocuneiform facet is damaged, so the nature of the demarcation between the mesocuneiform and ectocuneiform facet cannot be assessed. There would have been a sharp angle demarcating the ectocuneiform facet from the cuboid facet. There is a distinct angle between the plane of the mesocuneiform and the entocuneiform facets, the mesocuneiform facet pointing distally and the entocuneiform facet being oriented more distolaterally as it wraps medially around the navicular.

Comparison to U. leptodus—The navicular is not large enough to have been in contact with the entire astragalar head as in other paramyines. There is no evidence of a medial sesamoid, but one might have been present. The facet for the cuboid is large and strongly concave, more concave than that of *P. eugenei*. The ectocuneiform facet is strongly offset from the mesocuneiform facet and faces disto-laterally. The mesocuneiform facet points more distally and is convex at the distal edge and flatter for most of its surface. The entocuneiform facet is angled obliquely to a parasagittal plane, dorso-plantarly narrow and convex mediolaterally. This contrasts to the flatter facet of *P. eugenei*.

3.2.4.4.4 Cuboid

The cuboids of *Pseudotomus* vary in their degree of robustness relative to length. The smallest species, *P. petersoni,* has a cuboid that is short and broad, while that of

larger *P. robustus* is of comparable breadth but greater length. The much larger species *P. eugenei* has a cuboid the length of *P. robustus* but broader. This suggests that no simple allometric relationship is governing proportions of this bone. The proximal calcaneal articular surface of the cuboid is sub-rectangular in shape and gently convex from the dorsomedial corner to the plantolateral corner. The calcaneal facets of *P. robustus* and *P. petersoni* are more elongate mediolaterally than is that of *P. eugenei*. On the medial surface of the cuboid of *P. eugenei* there is a large, gently convex facet for the navicular. This facet meets the calcaneal facet proximally and the facet for the ectocuneiform distally (Figure 3.5 C). The ectocuneiform facet is located approximately midway along the medial surface of the cuboid. The distal facets for metatarsals IV and V are roughly triangular, tapering plantarly. The facet for metatarsal IV is concave and large, occupying the entire distal articular surface except for the extreme lateral edge. The facet for metatarasal V is crescentic and offset at an angle to the articular surface for metatarsal IV. The lateral tubercle is large and distally located with a deep groove for the peroneus longus muscle.

3.2.4.4.5 Cuneiforms

The ectocuneiform shows a proximal articular facet for the navicular that is slightly convex and triangular. On the proximolateral surface is a long, narrow facet for the cuboid that meets the navicular facet at approximately right angles. The distal facet for the third metatarsal is a concave, ventrally tapering triangle. On the distomedial surface are two circular facets for articulation with metatarsal II. The mesocuneiform is the smallest tarsal bone (Figure 3.5 E), as in other paramyines. In *P. robustus* the size difference between the meso- and ectocuneiforms is not as great as in *P. eugenei*. The

distal articulation between the mesocuneiform and metatarsal II is saddle shaped, being concave mediolaterally and convex dorsoventrally. The medial facet for the entocuneiform is crescentic and lies at a right angle to the navicular facet.

The entocuneiform is trapezoidal with a long plantar edge and a short dorsal edge. Wood (1962:197) described the lateral surface of the entocuneiform as receiving "the head of metatarsal II" in *Ischyrotomus*, but there is no indication that these two bones met. The distal articular surface for metarsal I is elongated and concave dorsoventrally. The lateral surface is expanded outward and is somewhat convex, making the joint approximate a saddle-shaped configuration. The entocuneiform of *P. robustus* has a medial ridge not present in *P. eugenei*.

Comparison to U. leptodus—The entocuneiform of *U. leptodus* is similar in shape to that of *P. eugenei* in being trapezoidal with a long plantar and short dorsal border. The proximal articular surface is more concave than that of *P. eugenei* and fits tightly with the corresponding facet on the navicular. The biggest disparity in morphology between the entocueiforms *Pseudotomus* and *U. leptodus* lies in the distal articulation for MT I. This facet in *P. eugenei* and *P. robustus* points straight distally so that the hallux is in adducted and inline with the rest of the metatarsals. In *U. leptodus* this facet is dorsoplantarly concave and mediolaterally convex (as in species of *Pseudotomus*) but the joint surface points distolaterally so that the hallux is somewhat divergent from the rest of the pes, though not to the degree seen in primates.

3.2.4.5 Pes

All left metatarsals are present as are several pedal phalanges. Portions of the right foot were also recovered, including metatarsal and phalangeal fragments. The head

of metatarsal III had not yet fused to the shaft, and the heads of metatarsals II, IV and V were either recently fused or were held in place by matrix. The base of metatarsal I was recently fused and the epiphyseal line is still evident.

The metatarsals of *P. eugenei* are more robust than those of other large paramyines, especially distally. They are similar in length to those of *P. robustus* but are much heavier bones. The robust metatarsals of *P. eugenei* are similar in relative length to those of other large paramyines such as *P. robustus* as described by Wood (1962), except that MT I and MT V are shorter relative to MT III. The primary difference between *P. eugenei* and other large paramyines is in the proportions of the metatarsus to the tarsus. In other taxa, the length of the longest metatarsal (usually metatarsal III) exceeds the length of the tarsus, whereas in *P. eugenei*, the metatarsals are shorter than tarsus length. In *P. eugenei*, the sequence of metatarsal lengths from shortest to longest is MT I, V, II, IV, III, with the two lateral ones (MT I, V) being unusually reduced when compared to other paramyines. In sum, *P. eugenei* has proportionally short metatarsals with relatively greater reduction of lateral elements than what is seen in primitive paramyines.

In *P. eugenei*, the first metatarsal is the shortest, but is quite robust (Figure 3.5 E). The peroneal tubercle on the lateral aspect of the plantar surface of the metatarsal is distinct, but not large. The head of metatarsal I is asymmetrical with a cylindrical articular surface for the proximal phalanx located laterally. There is a prominent medial keel on the plantar surface, as in all of the metatarsals.

The second metatarsal is almost twice as long as the first. The shaft is narrow proximally and flares at its distal end. This is also true of the shafts of MT III and IV. In *P. robustus*, the shaft of each metatarsal is narrower throughout its length and does not

flare distally. The proximal articular surface between MT II and the mesocuneiform is vaguely saddle-shaped and the two bones articulate tightly. Two facets on the lateral surface of the MT II base articulate with the respective facets on the ectocuneiform. Metatarsal III is the longest metatarsal. The proximal articulation for the ectocuneiform is damaged, but appears to have been flat to slightly concave (Figure 3.5 E). The dorsolateral edge of the MT III base flares laterally to create an overhang that articulates with a convexity at the base of the fourth metatarsal. The head of MT III is cylindrical and symmetrical, with the long axis oriented mediolaterally. The fourth metatarsal is slightly shorter than the third, but longer than the second. The proximal articular surface for the cuboid is convex and triangular, tapering ventrally. The medial articulation for metatarsal III is partially broken, but was clearly a significant convex projecting surface. Laterally, the base of MT IV flares out to accommodate the medial portion of the base of MT V. The head is asymmetrical, similar to the condition of the second metatarsal.

Metatarsal V is longer than the first metatarsal, but shorter than the second. The shaft of MT V is rounder and less robust than the other metatarsals, and it is distinctly bowed dorsoventrally. The shaft of the fifth metatarsal of *P. robustus* is also bowed, but to a lesser degree. Proximally, MT V articulates with both the cuboid and metatarsal IV, with the articular surface for metatarsal IV being the larger of the two surfaces. Both articular surfaces are concave and separated by a ridge. On the lateral aspect of the base is a prominent tubercle for attachment of peroneus brevis. The metatarsal head is asymmetrical and it is more spherical than cylindrical.

The proximal and middle phalanges of *P. eugenei* are relatively shorter than those of *P. robustus*. The proximal phalanges are heavily built and resemble those of

other large paramyines. The proximal articular surface for the metatarsals is angled somewhat dorsally, rather than straight proximally, suggesting habitually or commonly used extended positions. The plantar ridges for attachment of the flexor sheaths are extremely well developed and can be seen as a flaring of the midshaft in dorsal view. This is characteristic of other large paramyines as well.

The middle phalanges are also strongly built. The proximal articular surfaces are concave and directed dorsally, similar to the situation observed in the proximal phalanges. There is a strong dorsal process overhanging the proximal articular surface. The ungual phalanges are all broken distally, so that their length cannot be exactly determined. The proximal surface is strongly convex with a faint ridge for articulation with the middle phalanges. The flexor tubercle is very well developed, while the extensor tubercle is small. The unguals are laterally compressed and strongly keeled dorsally as in *P. robustus*. Although the length cannot be determined exactly, they were probably not as long as the manual unguals. Wood (1962) suggested that this was the case in *P. petersoni*, though only manual unguals are known from this taxon. In *P. robustus*, the pedal unguals are longer than the manual unguals. *P. eugenei* is unique among known paramyines in that the manual and pedal unguals are morphologically different. Those on the forelimb are shallow, uncompressed, and curve gradually, whereas the pedal unguals are more similar to earlier paramyines and *P. robustus* in morphology, in being deeper, compressed and straighter (Wood, 1962). This disparity in morphology and in length between the manual and pedal unguals is seen in extant fossorial rodents, such as *Marmota* and *Aplodontia*.

Comparison to U. leptodus—There is only a proximal MT I of *U. leptodus* preserved. The surface for articulation with the entocuneiform extends farther laterally than medially, contributing to the abduction of the hallux. The peroneal process is not especially well-developed and is similar in size to that of *P. eugenei* and other paramyines. There is a complete MT III and several other fragmentary distal metatarsals. The shafts are narrow and extremely gracile when compared to that of *P. eugenei*. The distal articular surfaces for the proximal phalanges are spherical rather than cylindrical as is the condition in *P. eugenei*.

3.3 Functional Interpretations

3.3.1 Glenohumeral Joint

In general, arboreal mammals have lightly developed muscle markings in the shoulder region compared to terrestrial and fossorial ones (Koenigswald et al., 2005; Rose and Chinnery, 2004; Rose and Lucas, 2000). *Pseudotomus eugenei* has very prominent greater and lesser tubercles and distinct muscle scars for the latissimus dorsi, teres major, and deltoid muscles, among others. In this respect, *P. eugenei* differs notably from the arboreal rodents I have examined. The proximal humerus of *Manitsha tanka* differs from that of *P. eugenei* in its higher greater tubercle, better developed attachments for teres major, pectoralis major, and latissimus dorsi, and the more proximal termination of the deltopectoral crest. The proximal humerus of *Uintaparamys leptodus* has lower tubercles, suggesting that it may have been more arboreal. The higher greater tubercle and the more proximal deltopectoral crest are reminiscent of the cursorial modifications seen in caviomorph rodents and cursorial mammals (Argot, 2001; Rose, 1985; Rose, 1990; Rose, 1999). In *Manitsha*, the head of the humerus is anteroposteriorly elongated

and offset posteriorly from the axis of the shaft; both of these features are well developed in cursorial mammals (Argot, 2001; Fleagle and Simons, 1982). These attributes suggest that the forelimbs of *Manitsha* were involved more in weight bearing during terrestrial locomotion than were the forelimbs of *P. eugenei* and *U. leptodus*. *P. eugenei* and *U. leptodus* have rounder humeral heads than *Manitsha*, that are aligned with the shaft axis, suggesting greater flexibility at the joint (Koenigswald et al., 2005), but the relatively massive development of tubercles and deltoid crest muscles in *P. eugenei* compared to *U. leptodus* suggests that *P. eugenei* was more terrestrial than *U. leptodus*.

3.3.2 Elbow Joint

A broad, robust distal humerus is characteristic of fossorial rodents (Elissamburu and Vizcaíno, 2004; Rose and Chinnery, 2004) and other fossorial mammals (Koenigswald et al., 2005; Rose and Lucas, 2000). *P. eugenei* has a relatively broader distal humerus than *Manitsha*, suggesting a greater capacity for digging behavior in the former than the latter. The relative breadth of the distal humerus can be expressed as a proportion of humerus length (Elissamburu and Vizcaíno, 2004). This index in *P. eugenei* is within the range of semi-fossorial taxa and outside the range of variation for both the arboreal and terrestrial taxa measured (Table 3.4). The index in *Manitsha* falls just outside the range of variation seen in semi-fossorial taxa and well within the ranges of arboreal and terrestrial species. *P. eugenei* has a slightly more flaring supracondylar ridge and more rugose and proximodistally expanded entepicondyle. Although a complete humerus is not available for *U. leptodus*, the distal humerus appears more gracile, and the medial epicondyle is less expanded proximodistally, though it projects medially. This suggests that compared to *Manitsha* and *P. eugenei*, *U. leptodus* was more arboreal.

Previous authors have used the term "semi-fossorial" to refer to mammals that are capable of digging, and show some slight skeletal adaptations for digging, but which are not extremely specialized morphologically in this direction. Examples of specialized fossorial mammals are talpids, dasypodids, and extinct palaeanodots (Rose, 1990; Rose and Lucas, 2000). Among large rodents, specialized diggers would include *Castor*, *Myocastor* and the Miocene mylagaulids (Fagan, 1960; Gidley, 1907). Some rodents, however, dig intensively but retain more generalized skeletons. For example, the sciurid *Cynomys* (the prairie dog) constructs extensive burrows and spends a considerable amount of time below ground (Hoogland, 1996), but it does not show the degree of postcranial specialization for digging seen in other fossorial taxa (Rose, 1999; Rose and Chinnery, 2004). I use the term "semi-fossorial" when certain skeletal features suggest digging abilities, even though much of the skeleton remains primitively generalized.

The posteriorly directed entepicondyle in *Manitsha* supports the conclusion that its forelimb was used in weight-bearing locomotion more than that of *P. eugenei* (Argot, 2001; Fleagle and Simons, 1982; Jenkins, 1973). The cylindrical capitulum of *Manitsha* and *P. eugenei* together with the steep angle of the medial trochlear crest suggest terrestrial locomotion, whereas the round capitulum and shallow angle of the medial trochlear crest in *U. leptodus* suggest arboreal habits (Andersson, 2004; Heinrich and Rose, 1997; Rose, 1994; Rose, 1988). The shallow olecranon fossa and cranially inflected anterior border of the olecranon process of *P. eugenei* suggests that the forelimb was habitually flexed (Argot, 2001; Fleagle and Simons, 1982; Heinrich and Rose, 1997). The straight posterior border of the olecranon process, strong groove for the triceps, and

relatively closed semilunar notch also suggest terrestrial rather than arboreal habits (Argot, 2001; Rose and Chinnery, 2004).

The proximal ulna of *Manitsha* is more difficult to interpret as the entire olecranon process is cranially inflected, as is seen in arboreal rodents, but the semilunar notch is closed as in *P. eugenei*, which resembles terrestrial rodents. The olecranon index (olecranon process length/ulnar shaft length) of *P. eugenei* is slightly higher than that of *Manitsha* (Table 3.4, Figure 3.6A). Both fall well within the range for terrestrial and semi-fossorial taxa, and are outside the range of arboreal species. The flat radial facet that is offset from the semilunar notch at a high angle also suggests terrestrial rather than arboreal habits for *P. eugenei* and *Manitsha* (Rose and Chinnery, 2004). The main difference between the olecranon process of these two manitshines and *U. leptodus* is in the shorter length and lack of medial inflection in the latter species. This also suggests arboreal rather than terrestrial locomotion in *U. leptodus*.

The distal expansion and distinct bowing of the radial shaft in *P. eugenei* and *Manitsha* also suggest a terrestrial way of life; arboreal taxa such as *Ratufa* have radii that are straighter and less flared (Rose and Chinnery, 2004; Rose and Lucas, 2000). Both *Pseudotomus* and *Manitsha* show a large capitular eminence, the functional significance of which is unclear. It has been suggested that the capitular eminence may stabilize the radius when the elbow is flexed (Heinrich and Rose, 1997), or serve as a bony stop limiting rotation of the radius (Davis, 1964). However, Gebo and Rose (1993) noted that the capitular eminence does not seem to limit supination in climbing carnivores.

Despite the prominent capitular eminence, the shape of the radial head in *P. eugenei* more closely resembles those of arboreal rodents than terrestrial or semi-fossorial

species, in that it is rounded rather than squared off (Table 3.4, Figure 3.6 A). The radial index (maximum diameter/minimum diameter) of *P. eugenei* and *U. leptodus* fall well within the range for extant arboreal taxa and completely outside the range for terrestrial and semi-fossorial species, with the exception of *Pedetes*. The radial index of *Manitsha* falls towards the low end of the terrestrial and semi-fossorial ranges, but is also within the range of arboreal taxa. This suggests that the two manitshines retained the ability to supinate the forearm despite the terrestrial and semi-fossorial features seen elsewhere in the forelimb. A rounder radial head in *U. leptodus* is not surprising given the arboreal features throughout the rest of the forelimb. A rounded radial head in *P. eugenei* may reflect pronation and supination abilities in contexts other than arboreality. For example, the African specialized rodent *Pedetes* is a bipedal semi-fossorial saltator, which has a radial head rounder than any rodent in the sample, including arboreal taxa. This is due to the use of its forelimbs exclusively for manipulation of food items and for burrowing (Kingdon, 1974). *P. eugenei* has a much higher intermembral index than does *Pedetes*, suggesting that *P. eugenei* was not a bipedal saltator (Table 3.3). Overall, the elbow joint of *P. eugenei* is suggestive of terrestrial habits with a tendency towards scratch-digging and manipulative behaviors. The elbow of *Manitsha* is more indicative of terrestrial weight bearing with more restricted supinatory ability.

3.3.3 Wrist

The functional morphology of rodent carpals is poorly understood. In general the carpus of *P. eugenei* resembles that of sciurids and murids, which have a more mobile carpus, in having a single convex facet on the proximal surface of the scaphoid. Terrestrial and cursorial caviomorph rodents, in contrast, have a scapho-lunate with a

radial concavity and an ulnar convexity, similar to the condition seen in ungulates, which allows flexion and extension at the proximal carpal joint but prevents medio-lateral movements (Koenigswald et al., 2005; Rose and O'Leary, 1995; Yalden, 1971).

3.3.4 Hip

The position of the third trochanter has been suggested to reflect locomotor adaptations. The third trochanter is proximally placed in arboreal taxa, but it is generally more distally placed in semi-fossorial taxa (Hildebrand, 1985). Cursors and saltators resemble arboreal taxa in having the third trochanter more proximally placed in order to produce faster extension at the joint. The position of the third trochanter in *P. eugenei* is very distal, indicating powerful hip extension.

3.3.5 Knee

The deep patellar groove with raised rims together with the anteroposterior depth of the femoral condyles suggest that the knee of *P. eugenei* had restricted mediolateral movements and was used primarily in flexion and extension (Heinrich and Rose, 1997; Rose, 1985; Rose, 1999; Rose and Koenigswald, 2005). The orientation of the patellar groove and condyles suggests that the knee was habitually flexed (Argot, 2002). The slightly posteriorly directed tibial plateau and large tibial tuberosity also support the interpretation of a flexed position of the knee (Dunn et al., 2006)

The concave popliteal fossa on the posterior proximal tibia indicate that the muscles of knee flexion were well developed (Rose and Koenigswald, 2005). The extent of flexion of the hind limb is generally greater among arboreal taxa compared to terrestrial taxa although both utilize flexed knee postures. The limitation of the knee joint to flexion and extension would suggest more terrestrial habits, as arboreal taxa generally

have more mobile knees (Argot, 2002; Heinrich and Rose, 1997; Rose and Koenigswald, 2005). In all characters that can be compared, the knee joint of *P. petersoni* is similar to that of *P. eugenei* and suggests similar use of the hind limb. The shallower and broader patellar groove, antero-posteriorly shallower femoral condyles and tibial plateau, and more proximal position of the tibial crest in *P. robustus*, all suggest that it had a more laterally mobile knee, similar to arboreal taxa such as the extant *Ratufa* and *Sciurus* (Rose and Chinnery, 2004).

3.3.6 Ankle and Pes

The ankle joint of *P. eugenei* offers little of distinction in terms of inferring behavior. It is a generalized, primitive rodent ankle that lacks any obvious specializations for novel lifestyle. The astragalar trochleas of both *P. eugenei* and *U. leptodus* are low but have moderately high trochlear crests, unlike the flatter trochleas of mammals with a significant amount of lateral mobility at the ankle joint, although rodent astragali in general including those of arboreal rodents retain this restricted configuration (Heinrich and Rose, 1997). The trochleas of both *P. eugenei* and *U. leptodus* do not extend backwards around the posterior border of the astragalus, indicating that the range of flexion and extension was reduced compared to that of early paramyines (Heinrich and Rose, 1997; Rose and Chinnery, 2004).

The midtarsal joint of *P. eugenei* is also adapted for stability. The astragalar head is markedly convex, while the cuboid facet of the calcaneus is slightly concave, prohibiting lateral movements or rotation at the midtarsal joint. There is interlocking between diagonal elements at the midtarsal joint, as the navicular contacts the calcaneus at a small facet. The midtarsal joint of *U. leptodus* shows less interlocking than does that

of *P. eugenei*, in lacking an articulation between the navicular and the calcaneus and in having a flatter cuboid facet. This together with the more proximally placed peroneal tubercle suggests a more arboreal lifestyle in *U. leptodus* than *P. eugenei* (Heinrich and Rose, 1997).

The divergent hallux of *U. leptodus* can also be interpreted as indicative of a more arboreal lifestyle as opposed to the adducted hallux of *P. eugenei*. An abducted hallux is often seen in arboreal mammals more than terrestrial ones (Argot, 2001; Bloch and Boyer, 2002; Sargis, 2002; Szalay, 1985). Likewise, the round metatarsal heads of *U. leptodus* may indicate a more mobile metatarso-phalangeal joint rather than the hinge-like one in *P. eugenei* also suggesting arboreal versus terrestrial habits.

3.3.7 Limb proportions

The statistical analysis of extant rodents in relation to their locomotor adaptations yielded one consistent result: arboreal and terrestrial rodents can be consistently separated from each other by measurements of the forelimb, hand and foot (Table 3.5). This can be seen with statistical testing and graphically where polygons of arboreal taxa overlap minimally or not at all with polygons of non-arboreal taxa (Figures 3.7, 3.8, 3.9, 3.10, 3.11,3.12). For example, arboreal taxa have relatively shorter olecranon processes (Figure 3.7, 3.11) and relatively short metacarpals and metatarsals in relation to phalanx and limb lengths (Figure 3.8). In our analyses, *P. eugenei* and the other manitshines fall outside the range of arboreal rodents but within or near the assemblage of terrestrial rodents.

Terrestrial rodents have shorter MT I and V relative to MT III length on average. In other words, they show reduction of peripheral digits around a central axis, as in

ungulates (Figure 3.10). The ranges of arboreal and terrestrial taxa in the sample overlap in this feature, with cursorial taxa such as *Dasyprocta* showing complete loss of lateral metatarsals and more generalized, rock-climbing terrestrial taxa such as *Marmota* showing less reduction. Nevertheless, the peripheral metatarsals of *P. eugenei* are shorter than those for many of the extant terrestrial rodents in our sample, suggesting a more cursorial terrestrial lifestyle. *P. robustus* has relatively longer peripheral metatarsals than *P. eugenei*, but they are relatively shorter than the arboreal rodents in the extant sample, suggesting that *P. robustus* was less committed to a terrestrial way of life. I have considered the possibility that *P. eugenei* was digitigrade rather than plantigrade, but in the end, I could not find any traits within our sample of rodents that consistently indicate one or the other posture. The dorsal orientation of the proximal phalangeal facets is suggestive but not definitive in this respect.

Quantitative data seem very effective at identifying arboreal adaptations (Table 3.6). These data are less effective at distinguishing among different types of terrestrial rodents. Specifically, terrestrial rodents that also swim or that are relatively specialized burrowers could not be distinguished from generalized terrestrial rodents. One reason for this is that in many cases rodents that are large and terrestrial also swim and burrow, as is seen in *Castor*. I simply do not have a sample of rodents that are exclusively burrowers or swimmers. Similarly, very cursorial rodents such as *Pedetes* and *Dolichotis* also burrow. Among large rodents, burrowing and terrestriality are correlated. I can look at how manitshines compare to these large extant rodents, and in most cases they fall within or near a variety of extant forms. For example, *P. eugenei* falls directly within the terrestrial rodent sample in relative length of the manual and pedal phalanges (Figure 3.9

and 3.10), and above terrestrial rodents, being more similar to fossorial ones, in relative width of the distal humerus (Figure 3.12). In other cases, one or more of the manitshines fall outside the range of variation of the extant forms, and sometimes they vary widely among each other, for example in the length of the phalanges relative to metacarpal length (Figure 3.10). Our interpretation of these results is that manitshines are fairly generalized terrestrial rodents in most ways, but with some evolutionary novelty in hand proportions that I cannot interpret at this time.

Relative hand and finger proportions have been the subject of previous study among mammals. For example, it has been suggested that aquatic mammals have significantly longer fingers than terrestrial ones (Gingerich, 2003). Among the manitshines, *Manitsha* seems to have very long phalanges, while those of *P. eugenei* seem to be relatively short, with *P. robustus* lying in between. While one might try to interpret these results as reflecting relative degrees of swimming behavior, it is important to note that *Castor*, an expert swimmer, does not differ significantly from generalized terrestrial rodents in degree of phalangeal elongation. This opens the question as to whether the general mammal pattern of elongated fingers in swimmers holds true for rodents, and it also complicates any interpretation of the long phalanges in *Manitsha*.

In proportions of their limbs, hands and feet, the manitshines are not remarkably different in their functional characteristics from extant rodents, particularly large ones. A reasonable interpretation is that the manitshines were generalized in their proportions and capable of a variety of behaviors possibly including digging, running and swimming. They may have been able to climb trees if necessary, like *Marmota*, but they were not specialized to do this by any means.

3.4 Discussion

Pseudotomus eugenei is characterized by a generalized skeleton in terms of individual joint function as well as overall proportions. For example, the tail of *P. eugenei* was long and unreduced relative to its older relatives and the sacrum also consists of a single element, with no indication of the additional fusion seen in many fossorial animals. Overall, the forelimb is generalized in morphology, but heavily muscled. The hind limb of *P. eugenei* is also generalized, but departs from earlier manitshines in its deeper patellar groove and deep femoral condyles, and in the reduction of the peripheral metatarsals, suggesting a stronger commitment to terrestrial life. The most distinctive features of *P. eugenei* occur in the forelimb and include the extremely broad distal humerus, relatively rounded radial head, long olecranon process, and elongated, uncompressed manual unguals. These features suggest that when *P. eugenei* diverges from other manitshines, it is in a semi-fossorial direction. It does not display a highly specialized degree of fossorial specialization seen in some other rodents such as the Miocene mylagaulids (Fagan, 1960; Gidley, 1907). Based on an analysis of the skeleton, I reconstruct its behavior as a generalized terrestrial rodent that would have been able to dig and run. It does not have features that would indicate an arboreal lifestyle, and whether or not it had aquatic tendencies is difficult to assess. It must be considered that generalized terrestrial running and digging in this large Eocene rodent have very different ecological implications than similar adaptations in an extant rodent would have, because *P. eugenei* was as large as or larger than most contemporary artiodactyls, creodonts, carnivores, and many perissodactyls. Large size in and of itself would have provided *P. eugenei* with ecological benefits and opportunities not available

to similarly sized rodents in extant mammal communities, and it may have favored dietary and locomotor generalization.

With regard to the adaptations of *P. robustus* and *Manitsha*, there is little to add to the previous analyses of Matthew (1910), Simpson (1941) and Wood (1962). *P. robustus* is more generalized than *P. eugenei* and, although it is larger than the arboreal rodents in the extant sample, it sometimes more closely resembles arboreal taxa in morphology. The locomotor behavior of *Manitsha* remains ambiguous. This analysis indicates that it was probably terrestrial and that the evidence against an arboreal lifestyle was stronger than Simpson (1941) thought. The extremely long proximal phalanges of *Manitsha* are intriguing from a functional point of view and difficult to explain; the possibility that *Manitsha* was aquatic is still open to debate. *Manitsha* does not show development of the more fossorial features seen in *P. eugenei*.

The new remains of *U. leptodus*, while fragmentary, suggest an arboreal rather than fossorial as suggested by Wood (1962). This is reflected in the morphology of the lower humeral tuberosities in the shoulder; the rounder capitulum, less angled medial trochlear crest, rounder radial head and shorter olecranon process in the elbow; and in the proximally-placed peroneal tubercle, round metatarsal heads and divergent hallux in the foot.

3.4.1 Implications for Primate Evolution

The contrast in locomotor behavior of *U. leptodus* and *P. eugenei* is extremely interesting in relation to the question of primate evolution and diversity in the Uinta Formation. *U. leptodus* is found in many of the same localities as the primate *Ourayia uintensis*, suggesting that these two animals at least sometimes shared the same habitat.

U. leptodus also declines dramatically at the end of the early Uintan in the Uinta Formation and is rarely found in Uinta C rocks. This combined with an arboreal lifestyle may suggest that the primates and *U. leptodus* were both adversely affected by the receding rainforests at the end of the early Uintan. The fact that *U. leptodus* is found in the late Uintan of Texas where tropical conditions are retained supports this (Anderson, 2008).

Pseudotomus eugenei is not present before the late Uintan and occurs only in the late Uintan of the Uinta Formation. A reconstruction of this taxon as terrestrial suggests that new terrestrial ecosystems were becoming available for new animals to exploit. This lends support to the hypothesis that the Uinta Formation was becoming more open at this time.

3.5 Summary

In this chapter I have described and analyzed a nearly complete skeleton of the formerly enigmatic species *Pseudotomus eugenei*, the largest rodent known from the Eocene, which clarifies its adaptations. It confirms that *P. eugenei* was terrestrial with some fossorial behavior. I have also described new postcranial remains of *U. leptodus*, which support an arboreal lifestyle for this rodent rather than a fossorial one. The implications for primate evolution and diversity in the Uinta Formation were discussed.

Table 3.1. The comparative sample of extant rodents used in statistical analysis listed by locomotor behavior.[a]

Behavior (N)	Species	Specimen No.	Size (mm)[b]
Arboreal (8)	*Aeromys thomasi*	FMNH 90437	418.43
	Anomalurus pelii	FMNH 62223	404.58
	Coendu mexicanus	FMNH 15611	280.08
	Erethizon dorsatum	FMNH 47173	441.40
	Petaurista magnifica	FMNH 114365	389.66
	Phloeomys sp.	FMNH 101751	249.23
	Ratufa bicolor	FMNH 46649	302.68
	Sciurus carolinensis	FMNH 156885	215.62
Fossorial (5)	*Aplodontia rufa*	FMNH 41388	210.32
	Castor canadensis	FMNH 44871	425.50
	Cynomys ludovicianus	FMNH 60483	192.68
	Myocastor coypus	FMNH 49892	365.51
	Ondatra zibethicus	FMNH 34897	193.91
Terrestrial (11)	*Atherurus africanus*	FMNH 148912	259.10
	Capromys piloroides	FMNH 47770	320.58
	Cavia porcellus	FMNH 122239	168.60
	Cricetomys gambianus	FMNH 177861	224.82
	Cuniculus paca	FMNH 152058	355.59
	Dasyprocta leporina	FMNH 46207	399.77
	Dinomys branickii	FMNH 166523	492.1
	Hydrochoeris hydrochoeris	FMNH 60735	708.51
	Hystrix africaeaustralis	FMNH 47389	423.33
	Marmota monax	FMNH 41087	317.44
	Thryonomys gregorianus	FMNH 108212	278.86
	Trichys fasciculate	FMNH 68750	221.03

[a] locomotor behavior taken from: Carraway and Verts (1993); Eisenberg (1989); Emmons (1997); Hoogland (1996); Jenkins and Busher (1979); Kingdon (1974); Koprowski (1994); Kwiecinski (1998); Mones and Ojasti (1986); Nowak (1991); Pérez (1992); White and Alberico (1992); Willner et al. (1980); Woods (1973); Woods et al (1992)
[b] size calculated as length of humerus + radius + femur + tibia

Table 3.2. The comparative sample of fossil rodents.

Species	Spec. No.	Description
Pseudotomus petersoni	AMNH 2018[a]	Skull, dentaries and assoc. postcrania
Pseudotomus petersoni	AMNH 1990	Left dentary with P_4-M_2
Pseudotomus petersoni	AMNH 2017	Left and right dentaries with M_1-M_3, P_4-M_1
Pseudotomus robustus	YPM 13346[ab]	Isolated RM_2 and LM_3
Pseudotomus robustus	AMNH 13091	L dentary and assoc. skeleton
Pseudotomus eugenei	CM 11983[ab]	Both dentaries and partial LM^3
Pseudotomus eugenei	CM 11793[b]	L dentary
Manitsha tanka	AMNH 3908	Skull and partial forelimb
Uintamys leptodus	CM 71146	Dental frags and postcrania
Uintamys sp.	CM 80537	Associated postcrania
Uintamys sp.	CM 80593	Associated postcrania
Uintamys sp.	CM 80554	Associated postcrania
Uintamys sp.	CM 80785	L distal humerus
Uintamys sp.	CM 80786	Unassociated distal tibias

[a] indicates holotype

[b]original specimens unavailable, observations made from casts

Table 3.3. Limb lengths and Intermembral Index (IMI)[a] of *Pseudotomus eugenei* and selected fossil paramyines and extant rodents[b]. Measurements are in mm.

Species	Specimen no.	Humerus	Radius	Ulna	Femur	Tibia	IMI
Pseudotomus eugenei	CM 71105	95.7	82.8	106.9	134.7	137.0	65.70
Paramys delicatus[c]		–	–	–	–	–	68.40
Pseudotomus robustus[c]		–	–	–	–	–	61.30
Manitsha tanka	AMNH 3908	120.4	98.6	126.3	–	–	–
Pedetes capensis[d]	FMNH 154054	49.4	44.7	57.0	98.0	133.7	40.62
Sciurus carolinensis	FMNH 156885	45.5	43.8	53.1	59.2	67.2	70.68
Cuniculus paca	FMNH 152058	83.1	66.2	88.3	107.3	99.1	72.37
Castor canadensis	FMNH 44871	86.3	92.7	122.1	112.1	134.4	72.63
Ratufa bicolor	FMNH 46649	72.3	58.7	70.0	86.1	85.6	76.30
Hydrochoeris hydrochoeris	FMNH 60735	180.5	127.0	167.5	204.5	196.5	76.69
Myocastor coyups	FMNH 49892	76.4	85.0	107.1	92.5	111.7	79.03
Hystrix africaeaustralis	FMNH 47389	103.8	86.2	116.0	122.5	110.9	81.38
Aplodontia rufa	FMNH 41388	49.0	45.6	59.9	57.6	58.2	81.72
Cynomys ludovicianus	FMNH 60483	44.5	42.3	52.6	52.7	53.2	81.94
Dinomys branickii	FMNH 166523	117.5	105.9	136.4	137.4	131.3	83.14
Marmota monax	FMNH 41087	78.0	67.2	86.1	87.6	84.5	84.36
Erethizon dorsatum	FMNH 47173	103.7	106.9	131.0	116.6	114.3	91.21

[a] IMI (Intermembral Index) = (humeral length + radius length) / (Femur length + tibia length) * 100

[b] extant rodents listed in order of ascending IMI. IMI was not found to be a good predictor of locomotor behavior in rodents, see text for further discussion of limb proportions.

[c] IMI taken from Wood (1962)

[d] *Pedetes capensis* is a bipedal saltator, behavior of all other rodents is listed in table 3.1

Table 3.4. Limb index values for fossil taxa and range of index values for extant taxa by locomotor behavior.

Index[a]	*P. eugenei*	*Manitsha*	*P. robustus*	*U. leptodus*	Arboreal	Terrestrial	Fossorial
RI	135.2	142.2	—	129.3	115.4–138.2	141.2–192.0	141.4–176.8
OPI	27.0	24.9	—	—	6.9–21.0	18.2–35.5	22.7–30.5
MCIII/HL	26.5	31.5	—	—	14.7–30.2	19.5–35.0	24.1–30.0
PL/MCIII	43.5	66.1	61.0	—	57.7–102.3	30.9–57.1	50.1–68.0
PL/MTIII	41.2	—	44.4	—	65.6–75.2	33.4–50.5	42.9–61.1
MTI/MTIII	50.6	—	56.5	—	65.6–75.2	25.9–65.6	52.0–66.6
MTV/MTIII	66.5	—	71.1	—	76.2–108.6	46.8–87.6	62.3–92.0
DHW/HL	35.1	27.7	—	—	14.3–30.2	16.6–30.3	28.8–40.0
BI	86.5	81.9	—	—	81.1–103.1	70.4–96.5	93.0–111.3
CI	101.7	—	108.2	—	94.1–105.6	89.9–118.7	102.2–132.9

[a] indices calculated as follows: RI (Radial Index) is the maximum diameter of radial head/minimum diameter; OPI (Olecranon Process Index) is the length of the olecranon process/ulnar shaft length; MCIII/HL is the length of third metacarpal/length of humerus; PL/MCIII is the length of the third proximal manual phalanx/length of third metacarpal; PL/MTIII is the length of third proximal pedal phalanx/length of third metatarsal; MTI/MTIII is the length of first metatarsal/length of third metatarsal; MTV/MTIII is the length of fifth metatarsal/length of third metatarsal; DHW/HL is the mediolateral width of the distal humerus across epicondyles/length of the humerus; BI (Brachial Index) is the length of the radius/length of the humerus; CI (Crural Index) is the length of the tibia/length of the femur

Table 3.5. Limb indices that discriminate arboreal (A) from terrestrial (T) rodents.

Index[a]	Relationship	P[b]	Description
RI	A < T	<0.01	Arboreal rodents have rounder radial heads
OPI	A < T	<0.01	Arboreal rodents have shorter olecranon processes
MCIII/HL	A < T	<0.05	Arboreal rodents have shorter metacarpals relative to humerus length
PL/MCIII	A > T	<0.01	Arboreal rodents have longer manual phalanges relative to the length of the third metacarpal
PL/MTIII	A > T	<0.05	Arboreal rodents have longer pedal phalanges relative to the length of the third metatarsal
MTI/MTIII	A > T	<0.05	Arboreal rodents have longer first metatarsals relative to the length of the third metatarsal
MTV/MTIII	A > T	<0.01	Arboreal rodents have longer fifth metatarsals relative to the length of the third metatarsal

[a] indices as for table 3.3
[b] p-value from Mann-Whitney U test

Table 3.6. Limb indices that discriminate fossorial (F) rodents from all others (O).[a]

Index[b]	Relationship	P[c]	Description
DHW/HL	F > O	<0.01	Rodents that dig have a mediolaterally broader distal humerus relative to humeral length
BI	F > O	<0.01	Rodents that dig have a longer radius relative to humeral length
CI	F > O	<0.05	Rodents that dig have a longer tibia relative to femur length

[a] relatively long distal limb segments in fossorial rodents, indicated by the higher brachial and crural indices, may actually be indicative of swimming as many rodents in our extant sample are also swimmers

[b] indices as for table 3.3

[c] p-value from Mann-Whitney U test

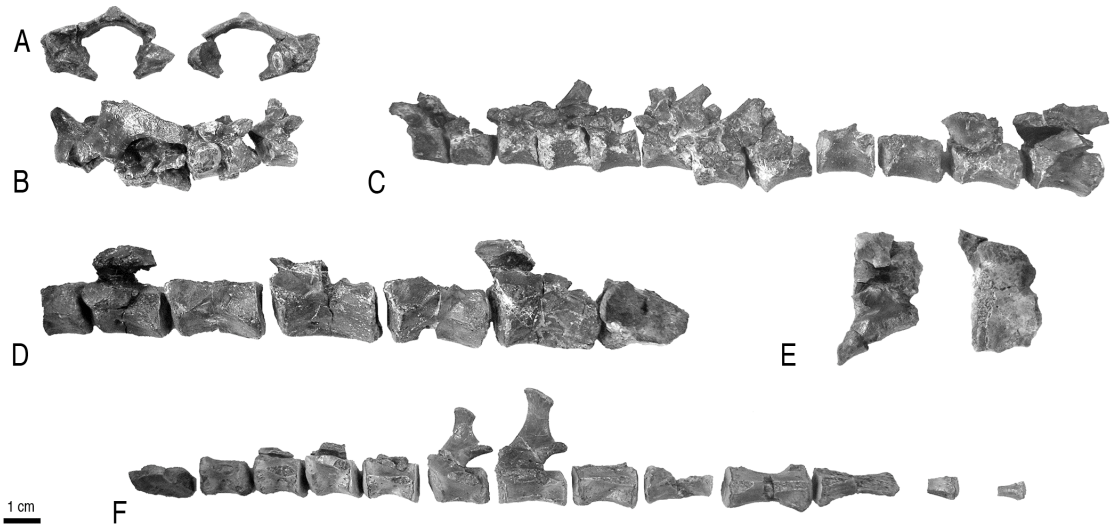

Figure 3.1. Vertebrae of *Pseudotomus eugenei* (CM 71105). **A**, atlas in cranial (left) and caudal (right) views. **B**, the cervical series in left lateral view, C2-C7 (left to right). **C**, thoracic vertebrae in side view seriated in size and morphology from cranial (left) to caudal (right). **D**, lumbar vertebrae in side view seriated in size and morphology from cranial (left) to caudal (right). **E**, sacrum in dorsal (left) and ventral (right) views (Cranial end to left). **F**, caudal vertebrae in side view seriated in size and morphology from cranial to caudal.


cp
sgt
ac
tb
A
is
tb
eef
me
hul
le
B
lt
gt
dpc
sr
tm &
ld
tb
rn
br
ioc
pq
rf
sp
C
ce
puf
ioc
bt
fdp &
pt
sp
duf
1 cm
D
lt
gt
E
F
rn
G

Figure 3.2. Forelimb of *Pseudotomus eugenei* (**A**–**D**; CM 71105) and *Uintaparamys* (**E**–**G**). **A**, scapular fragment of showing glenoid region in articular (left) and dorsal (right) views. **B**, humerus in (left to right): dorsal, lateral, ventral and proximal, and medial views. **C**, radius in: dorsal and proximal view (Far left), medial, ventral, lateral views (left to right). **D**, ulna in (left to right) medial, ventral and lateral views. **E**, (CM 71146) proximal humerus in (left to right): dorsal, lateral, ventral and proximal, and medial views. **F**, (CM 80785) distal humerus in (left to right): ventral and dorsal veiws. **G**, (CM 71146) ulna in (left to right): medial, ventral and lateral views. **Abbreviations**: **ac**, acromion process; **br**, brachialis; **bt**, bicipital tuberosity; **ce**, capitular eminence; **cp**, coracoid process; **dpc**, deltopectoral crest; **duf**, distal ulnar facet; **eef**, entepicondylar foramen; **fdp**, flexor digitorum profundus; **gt**, greater tubercle; **hul**, humero-ulnar ligament; **ioc**, interosseus crest; **is**, infraspinatus; **le**, lateral epicondyle; **ld**, latissimus dorsi; **lt**, lesser tubercle; **me**, medial epicondyle; **pq**, pronator quadratus; **pt**, pronator teres; **puf**, proximal ulnar facet; **rf**, radial facet; **rn**, radial notch; **sgt**, supraglenoid tubercle; **sp**, styloid process; **tb**, triceps brachii; **tm**, teres major.

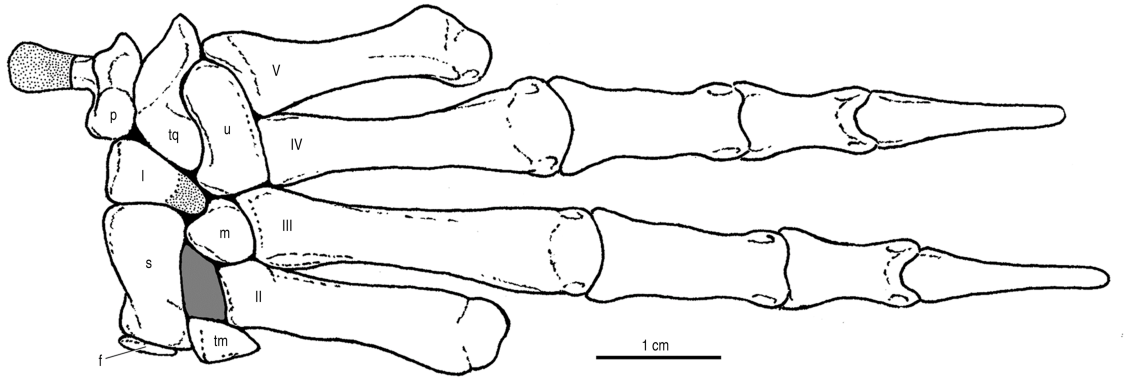

Figure 3.3. Schematic illustration of the left manus of *Pseudotomus eugenei* based on elements preserved in CM 71105. Stippled areas represent missing portions of carpal elements; gray shading identifies the space for the missing trapezoid and centrale. **Abbreviations**: **f**, falciform; **l**, lunate; **m**, magnum; **p**, pisiform; **s**, scaphoid; **tm**, trapezium; **tq**, triquetrum; **u**, unciform; **II**, **III**, **IV**, **V**, represent the second through fifth metacarpals.

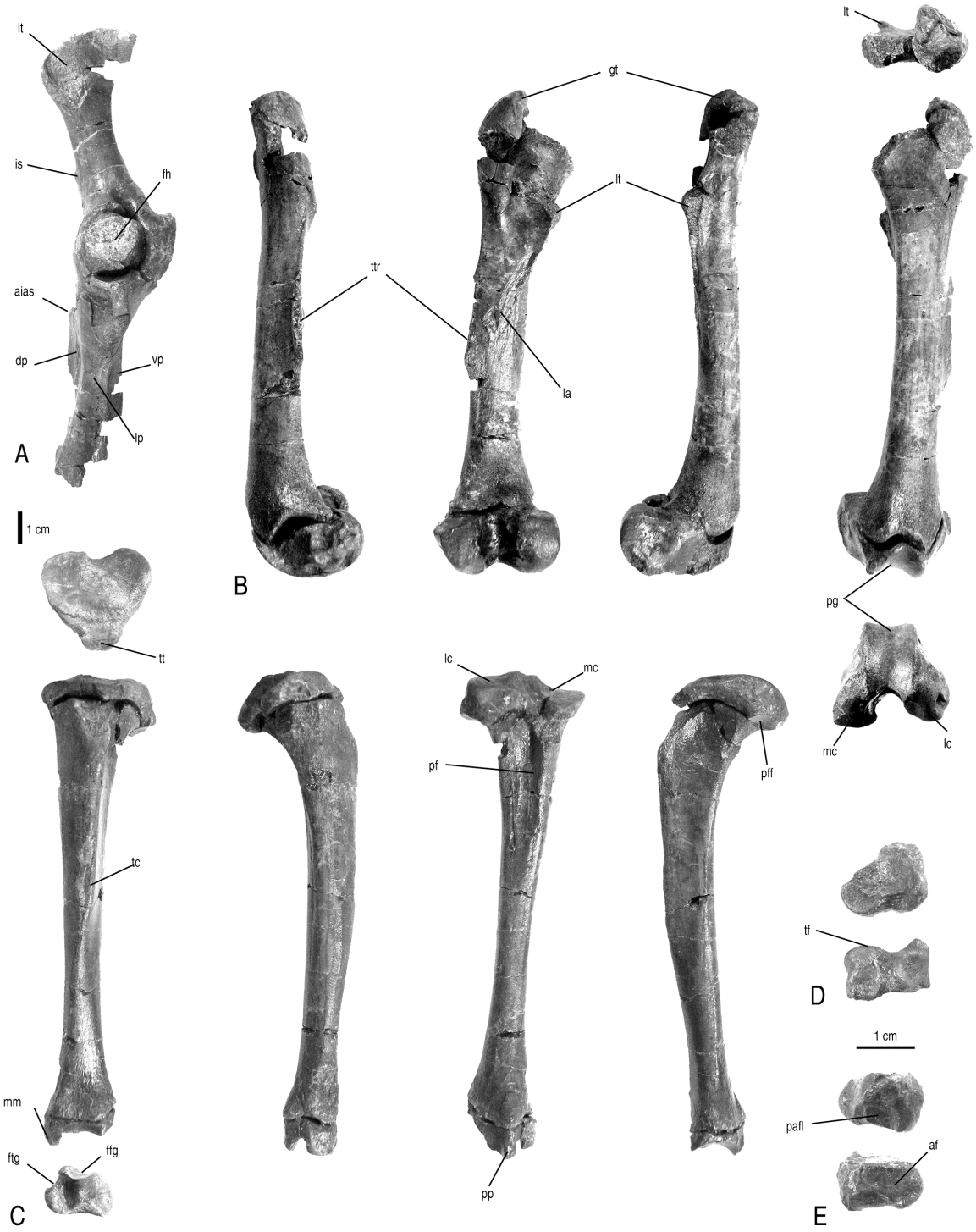
it
is
fh
aias
dp
vp
lp
A
1 cm
tt
tc
mm
ftg
ffg
C
gt
lt
ttr
la
B
lc
mc
pf
pp
pff
lt
pg
mc
lc
tf
D
1 cm
pafl
af
E

Figure 3.4. Left hind limb of *Pseudotomus eugenei* (CM 71105). **A**, innominate in lateral view (Caudal end towards top). **B**, femur in (left to right): lateral, ventral, medial views; and (Far right) proximal, dorsal, and distal views. **C**, tibia in: (Far left) proximal, dorsal, and distal views; and (left to right) medial, ventral, and lateral views. **D**, proximal fibular epiphysis in proximal (Top) and lateral (bottom) views. **E**, distal fibular epiphysis in medial (Top) and lateral (bottom) views. **Abbreviations**: **af**, astragalar facet; **aias**, anterior inferior iliac spine; **dp**, dorsal plane; **ffg**, flexor fibuaris groove; **fh**, femoral head; **ftg**, flexor tibialis groove; **gt**, greater trochanter; **is**, ischial spine; **it**, ischial tuberosity; **la**, linea aspera; **lc**, lateral condyle; **lp**, lateral plane; **lt**, lesser trochanter; **mc**, medial condyle; **mm**, medial malleolus; **pafl**, posterior astragalo-fibular ligament; **pf**, popliteal fossa; **pff**, proximal fibular facet; **pg**, patellar groove; **pp**, posterior process; **tc**, tibial crest; **tf**, tibial facet; **tt**, tibial tuberosity; **ttr**, third trochanter; **vp**, ventral plane.

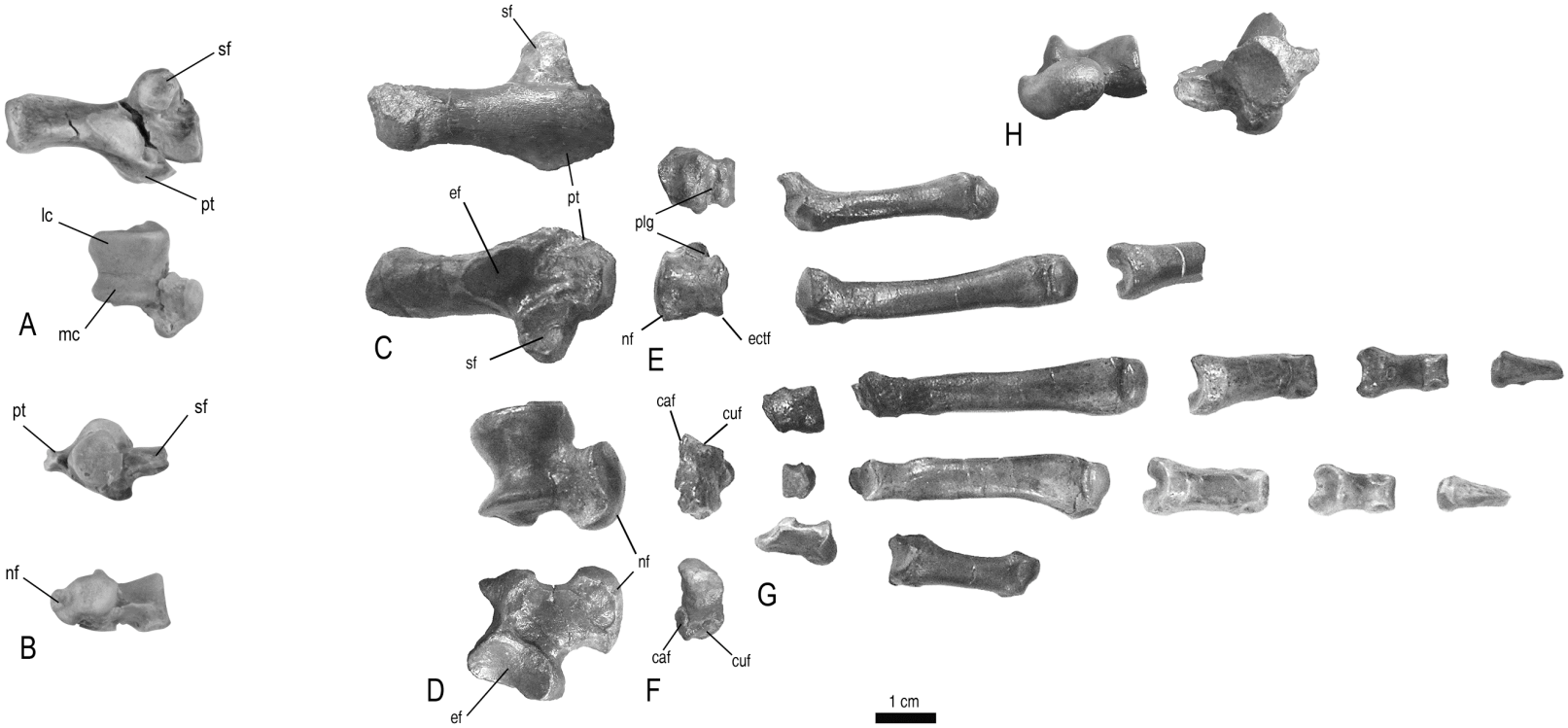

Figure 3.5. Pedal elements of *Uintaparamys* (**A** and **B;** CM 71146) and *Pseudotomus eugenei* (**C**–**H**; CM 71105). **A**, right calcaneus (top) and left astragalus (bottom) in dorsal view. **B**, right calcaneus (top) and left astragalus (bottom) in distal view. **C**, calcaneus in plantar (Top) and dorsal (bottom) views. **D**, astragalus in plantar (bottom) and dorsal (Top) views. **E**, cuboid in plantar (Top) and dorsal (bottom) views. **F**, navicular in plantar (bottom) and dorsal (Top) views. **G**, cuneiforms, metatarsals and phalanges in dorsal view. **H**, astragalus (left) and calcneus (right) in distal view. Abbreviations: **caf**, calcaneal facet; **cuf**, cuboid facet; **ectf**, facet for ectocuneiform; **ef**, ectal facet; **nf**, navicular facet; **plg**, peroneus longus groove; **pt**, peroneal tubercle; **sf**, sustentacular facet.

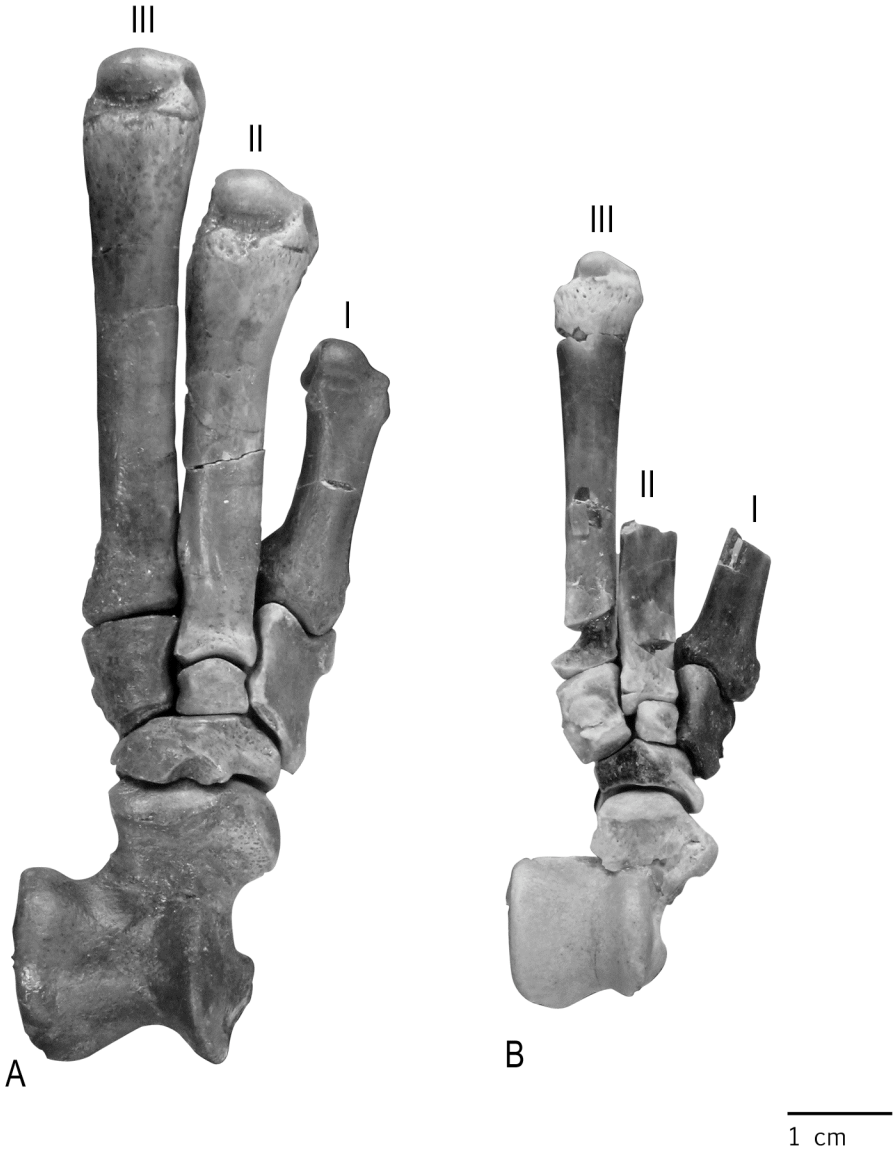

Figure 3.6. Partial left pedes of *Pseudotomus eugenei* (**A**; CM 71159) and *Uintaparamys* (**B**; CM 71146). Note that the astragalar neck of *P. eugenei* is wider and less medially deviated, and the astragalar trochlea is deeper. The metacarpals of *P. eugenei* are more robust with larger, more cylindrical heads compared to the small spherical head in *Uintaparamys*. The first metacarpal of *Uintaparamys* is slightly divergent when compared to that of *P. eugenei*.

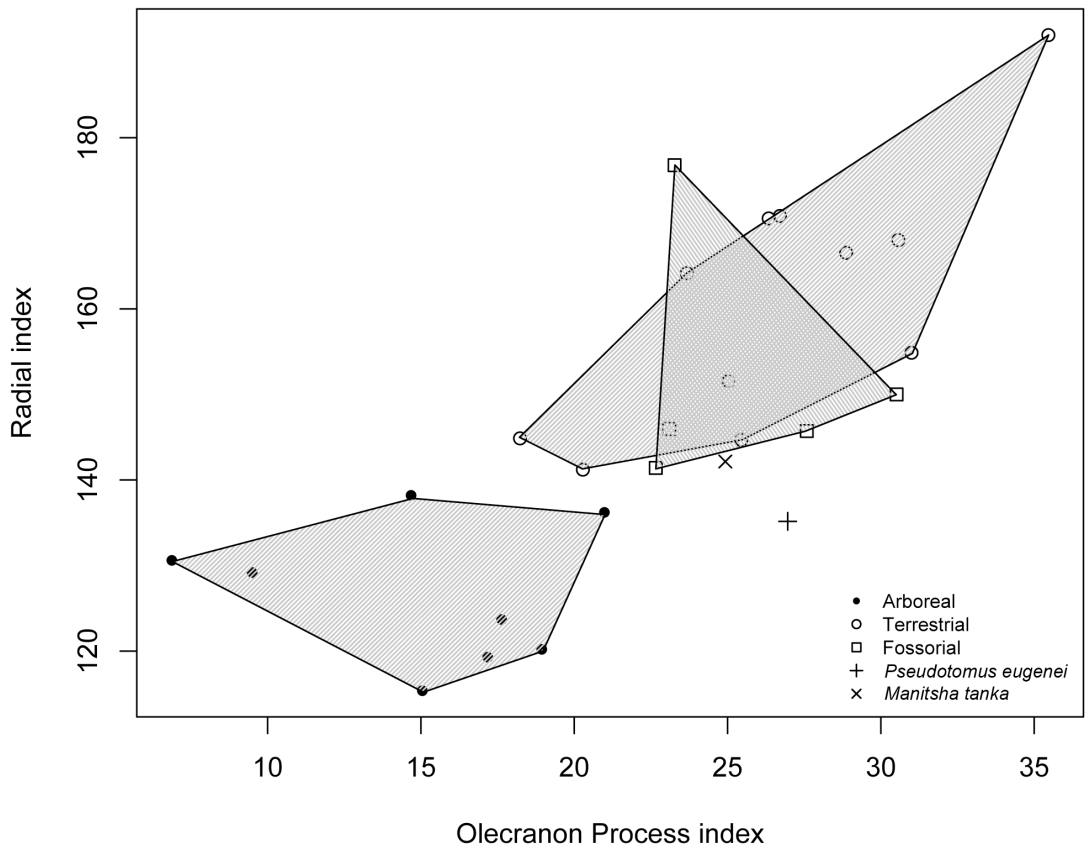

Figure 3.7. Bivariate plot showing the relationship between the shape of the radial head (radial index) and relative length of the olecranon process (olecranon process index) in extant and fossil rodents. Arboreal rodents do not overlap with terrestrial or fossorial rodents in head shape, having consistently rounder radial heads. Terrestrial and fossorial rodents have longer olecranon processes than arboreal taxa with minimal overlap between the two ranges. The fossil rodents fall well within the terrestrial range and outside of the arboreal range in olecranon process index. *P. eugenei* falls within the arboreal range of radial index values, whereas *M. tanka* is closer to terrestrial and fossorial taxa.

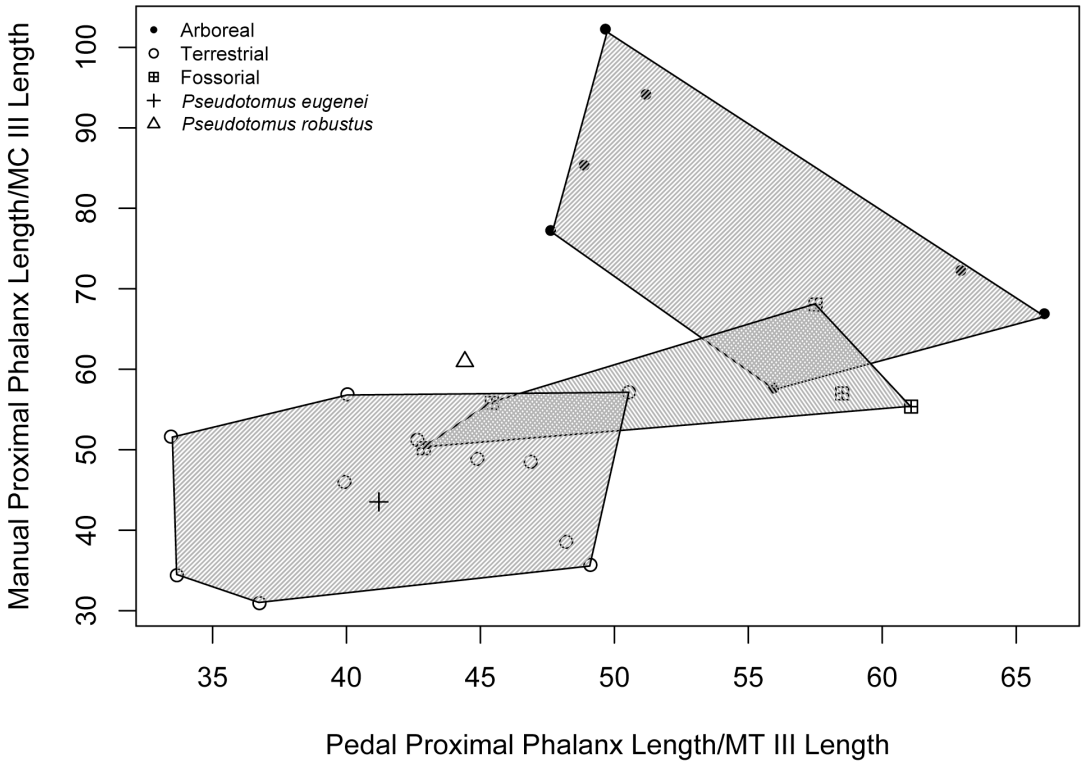

Figure 3.8. Bivariate plot showing manual phalanx length relative to metacarpal III length (y-axis) and pedal phalanx length relative to metatarsal III length (x-axis). Arboreal rodents tend to have longer phalanges relative to metapodials and terrestrial rodents have shorter ones. Fossorial rodents span between the two groups. This may be due to the fact that some of these fossorial rodents are also semi-aquatic, as aquatic mammals tend to have longer phalanges (Gingerich 2003). *P. eugenei* falls outside the range of arboreal and fossorial rodents and in the middle of the polygon for terrestrial rodents. *P. robustus* has longer manual phalanges than extant terrestrial rodents, and overlaps the ranges of both fossorial and arboreal ones. *P. robustus* has shorter pedal phalanges than extant arboreal rodents and is within the range of both terrestrial and fossorial rodents.

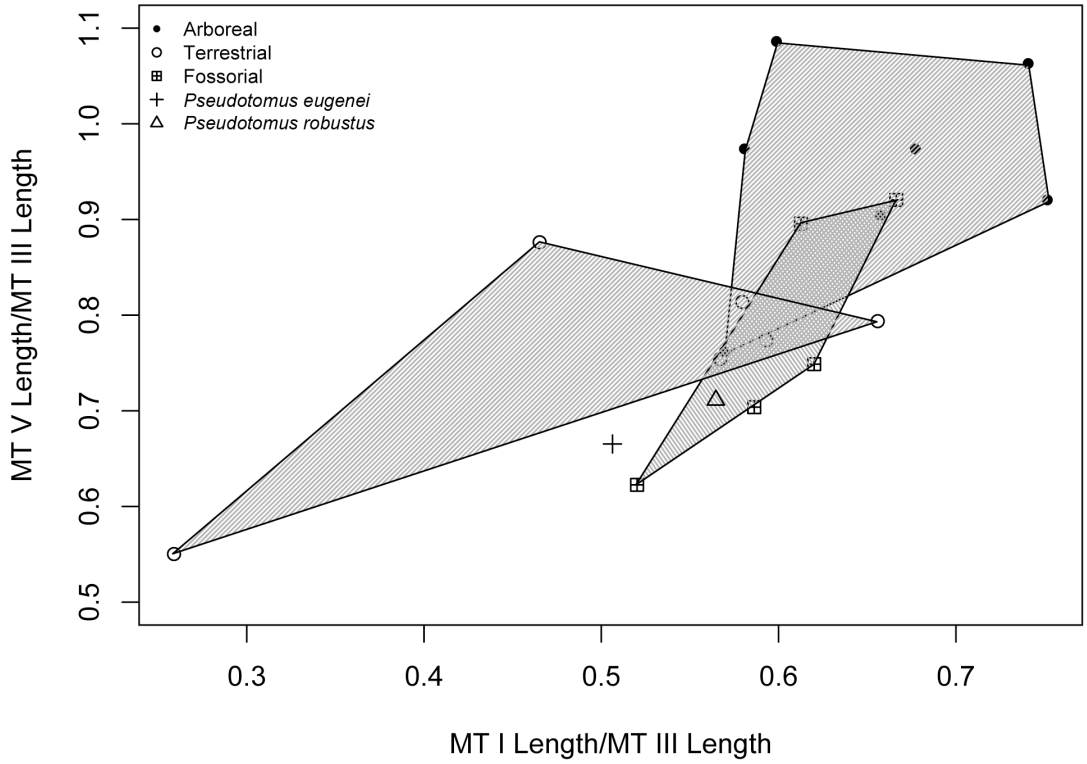

Figure 3.9. Bivariate plot of the length of metatarsal V relative to metatarsal III (y-axis) and the length of metatarsal I relative to metatarsal III. Arboreal rodents have longer lateral metatarsals than terrestrial ones, but there is some overlap. Again, fossorial rodents overlap both groups. *P. eugenei* has lateral metatarsal proportions similar to extant terrestrial and fossorial rodents. *P. robustus* falls within the range of fossorial rodents and close to the range of terrestrial ones in both measurements. *P. robustus* has relatively longer lateral metatarsals than *P. eugenei*.

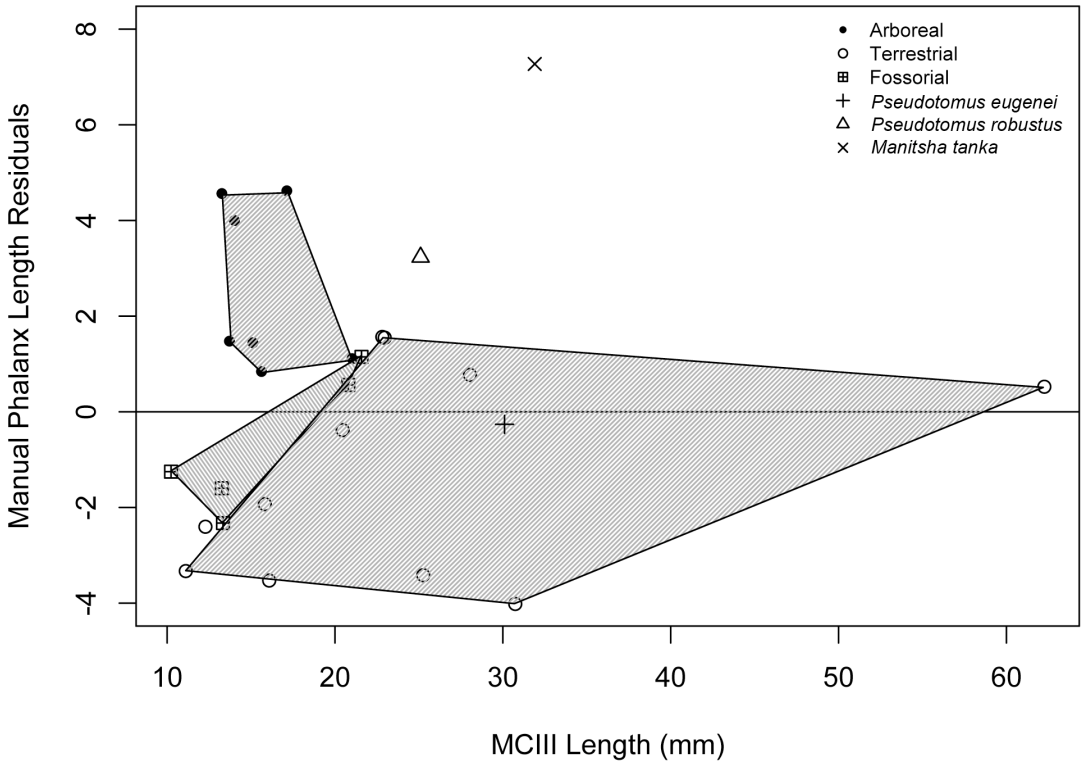

Figure 3.10. Bivariate plot showing residuals for the length of the third manual phalanx when regressed on metacarpal III length (y-axis), and the length of metacarpal III (x-axis). Larger residuals indicate longer proximal phalanges relative to metacarpals. Arboreal taxa have the longest phalanges of the extant taxa, but those of *Manitsha* are far longer than any taxon in the sample. *P. robustus* falls closest to the arboreal taxa in phalanx dimensions, but is absolutely larger than the arboreal taxa in the sample, and *P. eugenei* falls within the range of the terrestrial taxa.

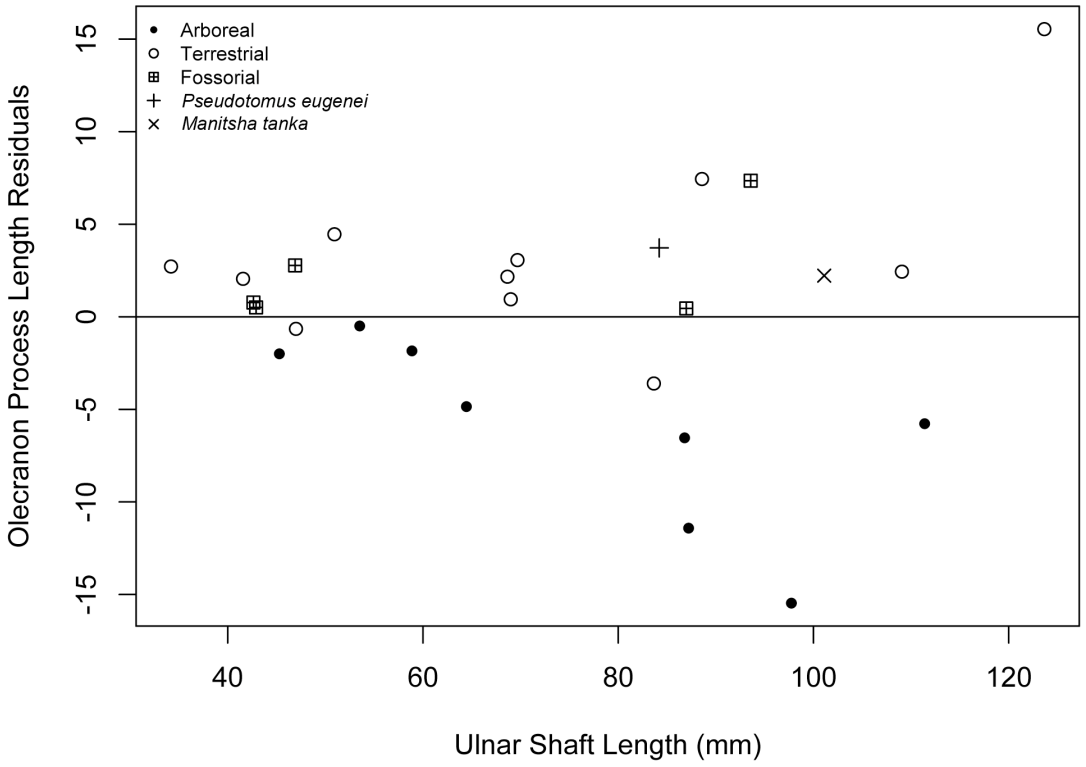

Figure 3.11. Bivarite plot showing residuals for the length of the olecranon process when regressed on ulnar shaft length (y-axis) and ulnar shaft length (x-axis). Larger residuals indicate longer olecranon processes relative to ulnar shafts (the length of the ulna – the length of the olecranon process). Terrestrial and fosorial rodents (with two exceptions) have longer olecranon processes than arboreal ones. *P. eugenei* and *M. tanka* both have longer olecranon processes than do extant arboreal rodents.

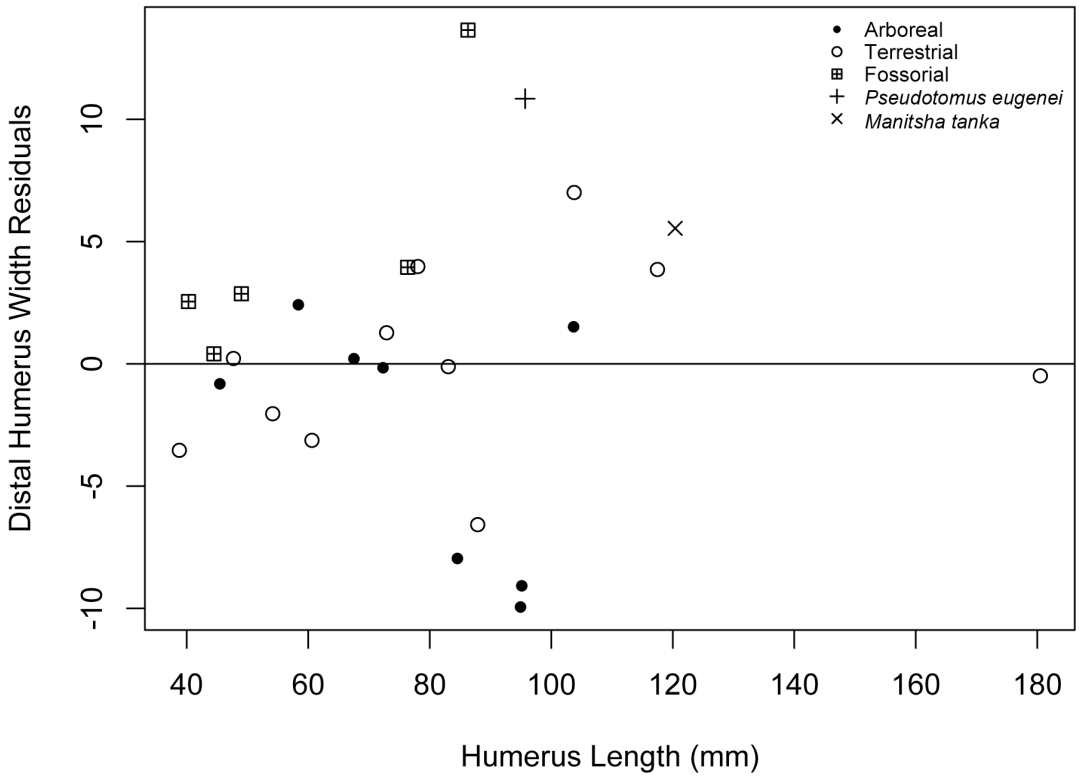

Figure 3.12. Bivariate plot showing residuals for the width of the distal humerus when regressed on humerus length (y-axis) and humerus length (x-axis). Larger residuals indicate wider distal humeri relative to humeral length. Extant fossorial rodents have wider distal humeri than extant terrestrial and arboreal rodents combined with humeri of similar length. *P. eugenei* and *M. tanka* both have relatively wide distal humeri for their humeral length.

CHAPTER FOUR

Skeletal Morphology of *Zionodon* (Mammalia, Erinaceomorpha)

(Excerpted from: Dunn and Rasmussen, 2009 J Mammalogy 90)

4.1 Introduction

Extant erinaceomorphs are restricted taxonomically to the family Erinaceidae and geographically to the Old World (Nowak, 1991; Rose, 2006). There are 2 living subfamilies, the Erinaceinae (hedgehogs) and the Galericinae (or Hylomyinae; the gymnures or moon rats). They range in body size from approximately 15 g to 1,400 g. All erinaceines and most galericines are nocturnal and typically use a generalized terrestrial locomotion, but can run, climb, and swim well (Gould, 1978; Reeve, 1994). Most are plantigrade, walking on the soles of the feet, and all exhibit fusion of the tibia and fibula (Barnett and Napier, 1953; Eisenberg and Gould, 1970; Gould, 1978; Nowak, 1991; Reeve, 1994; Vaughan et al., 2000). The low diversity among extant forms is not a good model, however, for the much greater taxonomic and adaptive diversity of past erinaceomorph radiations.

During the Tertiary (65 to 1.8 MYA) there were at least 5 families of erinaceomorphs and numerous genera of uncertain familial affiliation found throughout North America, Europe and Asia (McKenna and Bell, 1997; Rose, 2006). Matthew (1909) suggested that extant members of Insectivora (= Lipotyphla) are specialized remnants of the more diverse and abundant Early Tertiary group that played a more central role in their ecosystems. It might be expected that Early Tertiary insectivorans manifest a wider range of morphologies and adaptations than those surviving today. This

idea seems to be well supported for Erinaceomorpha based on paleontological work that has led to the discovery of many extinct groups (Bown and Shankler, 1982; Krishtalka, 1976; Lillegraven et al., 1981; Novacek, 1976, 1985; Novacek et al., 1985; Van Valen, 1967; Walsh, 1998).

The postcranial skeleton and locomotor adaptations of fossil erinaceomorphs (and fossil insectivores in general) are poorly known with the notable exceptions of *Macrocranion* and *Pholidocercus* from Eocene deposits in Messel, Germany (Schaal and Ziegler, 1992; Storch, 1993, 1996; Storch and Richter, 1994). The genus *Macrocranion* is also known from cranial and dental material in North America (Krishtalka, 1976). In the Messel deposits, the genus *Macrocranion* consists of two species: *M. tupaiodon* was a cursorial terrestrial quadruped with the ability to saltate bipedally, whereas *M. tenerum* was smaller, more gracile, and an obligate biped that may have progressed by ricochetal saltation (Smith et al., 2002) much like extant macroscelidians or dipodomyines. Bipedal saltation and terrestrial cursoriality are locomotor specializations not seen in extant lipotyphlans (Nowak, 1991; Vaughan et al., 2000). The other Messel genus, *Pholidocercus*, is postcranially generalized, but is notable for the armor-like scales that covered the crown of the skull and the tail (Schaal and Ziegler, 1992). These fossils indicate that the ecological diversity of insectivores during the Eocene was very different from that seen among extant lipotyphlans.

The Uinta Formation preserves approximately 5 million years of Uintan-aged continental sediments (Prothero, 1996). Although insectivores are known from the Uinta Formation, they are rare and fragmentary in comparison to other similarly sized taxa such as rodents (Rasmussen et al., 1999). *Zionodon* is notable for its large size. *Z. satanus*, the

smaller of the two new species has molars approximately 1.5 times larger in linear dimensions than those of *Scenopagus edenensis*, a large erinaceomorph known from older, Bridgerian deposits in the Uinta Basin, and over twice the size in linear dimensions of *Talpavus duplus*, the only previously described erinaceomorph from the Uinta Formation (Krishtalka, 1976; Rasmussen et al., 1999). The new taxa are larger than any North American erinaceomorphs from the earlier Wasatchian and Bridgerian land mammal ages, and are matched or exceeded in size only by other Uintan and Duchesnean erinaceomorphs known from southern California (Walsh, 1996; Walsh, 1998).

Both species of *Zionodon* are also notable because both are known from associated postcrania, unlike most Eocene insectivores, which are represented only on the basis of published teeth, jaws and cranial fragments. The postcranial elements recovered from Utah provide the basis for analyzing the locomotor behavior and adaptations of the new erinaceomorphs.

The purpose of this chapter is to provide a functional assessment of the postcrania of *Zionodon* as well as an assessment of the habitat in which it is likely to have lived. *Zionodon* is found in localities also yielding primate remains, so knowledge about the habitats in which *Zionodon* lived provide independent information about the habitat of the Uinta Formation primates. Much of this paper has been published previously as part of a coauthored paper (Dunn and Rasmussen, 2009). My coauthor's main contribution to that manuscript was the systematic description of the new taxa, which I have omitted here. The comparisons, measurements, description, functional interpretation and figures were all my contributions. The comparisons with *Creotarsus* in this chapter were added subsequent to the acceptance of the aforementioned manuscript, and so are unique to this

dissertation.

4.2 Description

4.2.1 Materials and Methods

The fossils were recovered from the Uinta Formation during field seasons in 1993-1995. The localities that yielded the fossils are all located stratigraphically low within the Uinta B2 member (table 4.1), which is Early Uintan (Ui2) in age. The comparative samples of extant taxa examined for this chapter are housed at the YPM and at the FM; I examined four genera of the Erinaceidae belonging to both subfamilies (Nowak, 1991; Vaughan et al., 2000) along with representatives of the Tenrecidae, Soricidae, Talpidae, Dasypodidae, Tubulidentata, Pholidota, Mustellidae, Ailuridae, Procyonidae, Dermoptera, Ochotonidae, Leporidae, Macroscelidea, Dasyuridae, Didelphidae, and Phalangeroidea. Additional comparisons were made via relevant publications. As the skeletal remains of *Zionodon* are too fragmentary to provide extensive measurements for statistical analysis, traditional comparative methods were used in the functional analysis (Bock and Wahlert, 1965).

The postcranial remains of *Zionodon satanus* include several vertebral fragments probably belonging to the lumbar and caudal regions; right glenoid fossa; right and left proximal humeri; portions of the humeral shafts and left medial epicondyle; portions of the left proximal ulna; fragments of the right and left distal radii; right bases of MCII and MCIII; portions of the right and left acetabulae; femoral head; greater trochanter; portions of the right and left femoral shafts; distal right femur and partial left lateral femoral condyle; left tibial plateau; right and left distal tibia; right left distal fibula; left astragalus and MTIII base; right calcaneus and cuboid. Postcranial remains of the 2nd new species

include right distal femur, right proximal tibia, right partial astragalus and right distal calcaneus, complete left astraglus and left distal calcaneus. The fossils are catalogued in the collections at the CM and are currently housed at WU.

4.2.2 Axial skeleton

4.2.2.1 Vertebrae

The vertebrae of *Zionodon satanus* are fragmentary, consisting only of centra; most appear to belong to the caudal and lumbar regions. None of the centra bear demi-facets for articulation with ribs, implying that they are not thoracic vertebrae. Many of the vertebrae are compressed dorsoventrally as in leptictids (Rose, 1999), possibly accentuated by post-depositional distortion. Some possess a slight ventral keel and others a median sulcus. Other centrum fragments are more cylindrical and robust. One complete centrum suggests that the proximal caudal vertebrae were somewhat elongated and robust, whereas other fragments indicate long, thin caudal vertebrae. This suggests that the tail was long and robust.

4.2.3 Forelimb

4.2.2.1 Scapula and Humerus

The forelimb is fragmentary and crushed, but some features are worthy of mention. The right scapula preserves a distinct pit for the insertion of the triceps brachii m. caudal to the rim of the glenoid fossa.

On the proximal humerus (preserved on both the right and left side), the pit for the infraspinatus m. on the greater tuberosity and the pectoralis crest on the proximal shaft are distinct. The bicipital groove is broad. Two fragments of shaft are preserved. The deltoid and lateral supracondylar crests were both pronounced, but it is not possible to

determine the relative proximodistal extent of either crest. On one fragment of the distal end, the medial epicondyle is robust and proximodistally expanded. Preserved portions of the proximal ulna indicate that the olecranon process is robust at the base, but the length cannot be determined.

4.2.2.2 Radius and Ulna

Only the distal epiphysis of the right radius and a few millimeters of the shaft and distal articular surface of the left radius are preserved (Figure 4.1 C). The distal radius is wider mediolaterally than it is anteroposteriorly and exhibits a single concave facet for the scaphoid over most of its surface. The styloid process is small. The flexor surface of the radius is convex and the extensor surface is flat to concave. The most distinctive feature of the distal radius is a large dorsolaterally projecting tubercle on the extensor surface and corresponding lateral groove. A similar, but more prominent crest is present in extinct Palaeanodonta and extant dasypodids and serves to separate the tendons of the extensor indicis m. laterally from the abductor pollicis m. medially and as an insertion for pronator and supinator muscles (Rose et al., 1992; Rose and Lucas, 2000). This structure is also prominent on the distal radius of the extinct arctocyonid *Chriacus* (see O'Leary and Rose, 1995 Figure 10).

4.2.3.3 Metacarpals

Distinct tubercles for insertion of the extensor carpi radialis m. are present on the bases of metacarpals II and III (Figure 4.1 D). Such tubercles are present in the fossil mammal groups Leptictida and Paleanodonta, and in extant dasypodids (Rose, 1999, 2007; Rose et al., 1992). When articulated, the two proximal surfaces for articulation with the carpals do not form a continuous articular surface, but are offset from each other.

4.2.4 Hindlimb

4.2.4.1 Innominate and Femur

We have several small fragments of innominate bones that do not fit together. The acetabulae are incomplete and crushed. The iliopubic eminence of the innominate bone is well defined and mediolaterally compressed and the ischial spine is pronounced. The femoral head of both species is hemispherical with a sharp lip delimiting head from neck. The greater trochanter preserves a deep trochanteric fossa, though its height relative to the femoral head cannot be determined. The third trochanter of *Z. satanus* is well developed, thin and bladelike and was probably relatively proximally placed. The distal femur of *Z. satanus* is crushed, but that of *Z. walshi* is preserved; it is anteroposteriorly deeper than it is medio-laterally wide (Figure 4.2 A). The patellar groove is deep and proximodistally long, resembling that of Eocene leptictids (Rose, 1999).

4.2.4.2 Tibia and Fibula

The proximal tibia of *Z. walshi* is damaged but better preserved than that of *Z. satanus* and preserves some features worth noting. The medial condyle is concave and distinctly lower than the lateral condyle, which is convex. The articular surface of the medial condyle extends onto the posterior aspect of the proximal tibia into the region of the popliteal fossa, a resemblance to the proximal tibia of Early Eocene leptictids (Rose, 1999). Although the lateral condyle is broken posteriorly, a portion of the proximal fibular facet is preserved and suggests that the articulation was large, flat, and oriented horizontally. The tibial tuberosity is proximally placed and projecting, rather than being situated more distally and low. In the morphology of the tibial tuberosity, *Zionodon* resembles Eocene leptictids , terrestrial marsupials, and tupaiids; it contrasts with

ptilocercids and arboreal marsupials in which the tibial tuberosity is lower and more distally placed (Argot, 2002; Sargis, 2002).

The distal tibia of *Z. satanus* is well preserved. The medial malleolus is robust and slightly hooked, in contrast to Eocene leptictids in which the malleolus is reduced in size and simple in morphology (Rose, 1999, 2007) and to extant erinaceids in which the malleolus is reduced or absent. There is a large posteriorly directed flange on the posterior aspect of the medial malleolus demarcating the medial margin of a groove for the tendon of the tibialis posterior m. (Heinrich and Rose, 1997). The anterolateral margin of the distal tibia exhibits a short interosseus crest just above a small semilunar fibular facet, indicating that the fibula was only loosely tied to the tibia distally. This is in contrast to extant erinaceids and *Macrocranion* in which the tibia and fibula are fused distally (Barnett and Napier, 1953; Storch, 1993), to extinct leptictids in which there is extensive fusion (Rose, 1999, 2007), and to extinct palaeanodonts in which the bones are sometimes fused but are usually separate with extensive ligamentous attachments (Rose and Lucas, 2000). The nature of the tibio-fibular articulation of *Z. satanus* most closely approximates the condition indicated by Barnett and Napier (1953) to be primitive for Eutheria.

The distal tibial facet for articulation with the astragalus tapers laterally with the articular surface for the medial astragalar condyle being anteroposteriorly longer than that for the lateral astragalar condyle (Figure 4.3 A). The medial part of the facet is nearly perpendicular to the long axis of the tibial shaft, whereas the lateral part is angled more sharply. A distinct, smooth ridge represents the intercondylar furrow of the astragalus. There is a small facet for the neck of the astragalus on the anterior surface of the distal

tibia (squatting facet). A similar facet is found in many primates as well as hedgehogs, tenrecs, lagomorphs, macroscelideans, and *Macrocranion vandebroeki*.

The distal fibula of *Zionodon satanus* is robust (Figure 4.3 B). The astragalar facet is sagittally oriented and flat. A short interosseus scar, more tubercle-like than crest-like, is present above the astragalar facet. A horizontally oriented calcaneal facet is present on the plantar surface of the lateral malleolus. There is a prominent ridge on the posterior surface of the lateral malleolus forming the medial border of the peroneal groove.

4.2.4.3 Tarsals and Pes

The astragalar trochlea of both species of *Zionodon* is grooved, with the medial condyle being flatter and the lateral condyle angling steeply (Figures 4.2 C and 4.3 D). The condyles are unequal in size with the medial condyle having a smaller radius of curvature than the lateral one. A shallow cotylar fossa is present on the medial astragalar body for the tibial malleolus. In both species a superior astragalar foramen is present, but this foramen is much larger in the specimen of *Zionodon satanus* than in the specimen of *Z. walshi*. Both species exhibit a groove on the posterior astragalus plantar to the trochlea for the tendon of the flexor fibularis m.; this groove appears to be better defined in *Zionodon satanus*. The posterior calcaneal (ectal) facets of both species are concave and face laterally and the sustentacular facets are slightly convex and do not contact the navicular facet. Just posterior to the sustentacular facet of *Z. walshi* is a concave depression that receives the posterior lip of the calcaneal sustentaculum, sometimes called a sustentacular hinge. This portion of the astragalus of *Z. satanus* is broken, so the presence of this depression cannot be evaluated.

The astragalar neck is relatively longer in *Zionodon satanus* than in *Z. walshi*, but is not especially long in either species. The lateral surface of the neck contacts the anterior rim of the distal tibia in dorsiflexion where the neck meets the astragalar body. The astragalar head is mediolaterally broader than dorso-plantarly high and obliquely oriented to a coronal plane through the trochlea, so that it wraps from plantomedial to dorsolateral. The head is farther expanded medially than laterally and the articular surface extends substantially onto the dorsal aspect of the neck.

The astragalus of *Zionodon* closely resembles that of the enigmatic Wasatchian proteutherian *Creotarsus* (Matthew, 1918). *Creotarsus* is known from two specimens, both from the Wasatchian NALMA. The type specimen originally included a dentary with $P_4 – M_2$ (Figure 4.4) and associated tarsal bones. Although resemblance of the tarsals to members of the archaic carnivore group Creodonta gave the genus its name, Matthew noted dental and postcranial similarities between *Creotarsus* and several different groups including Insectivora, Leptictida, Artiodactyla and the archaic ungulate groups Condylarthra and Mesonychia (Gunnell et al., 2008; Matthew, 1918). Simpson placed this genus within the Creodonta, but later authors suggested that *Creotarsus* was closely related to the Erinaceomorpha (McKenna and Bell, 1997; Simpson, 1945; Van Valen, 1967). Most recently, *Creotarsus* has been placed within the Proteutheria pending further study. Unfortunately, the tarsal elements that were included in the holotype have been lost, but they are illustrated in Matthew (1918). The astragalus of *Zionodon* resembles that of *Creotarsus* more closely than any other taxon I examined. From what can be assessed from the illustration (Figure 4.5), both have deeply grooved astragalar trochleas, an articular surface for the navicular that extends onto the dorsal aspect of the

neck, a sustentacular facet that is ovoid and does not contact the navicular facet, a superior astragalar foramen, and a well-defined flexor fibularis groove. The presence of cotylar fossa, asymmetry of the condyles and a facet for the tibia on the neck cannot be assessed from the illustration.

In general, the astragalus of *Zionodon* resembles that of leptictids and *Macrocranion vandebroeki* in some ways (Godinot et al., 1996; Rose, 1999). However it differs from leptictid astragali in having a dorso-ventrally deeper body, presence of a superior astragalar foramen (absent in leptictids), presence of a squatting facet (also absent in leptictids), less medial expansion of the navicular facet, greater development of the navicular facet onto the dorsal aspect of the neck, and in having a head that is oriented obliquely to the coronal plane of the trochlea rather than parallel to it (Rose, 1999). The astragalus of *Zionodon* differs from that of *M. vandebroeki* in having a more rounded (less sharp) medial condyle, presence of a superior astragalar foramen (absent in *M. vandebroeki*), and having separate sustentacular and navicular facets (confluent in *M. vandebroeki*) (Godinot et al., 1996). The astragalus of *Zionodon* also bears some resemblance to that of the extinct Nyctitheriidae (Hooker, 2001). The shape of the body in these taxa is similar in the asymmetry of the condyles and the presence of a squatting facet, but nyctithere astragali lack a superior astragalar foramen, have contact between the sustentacular and navicular facets, a more medially expanded navicular facet, and a head that is parallel to rather than oblique to the coronal plane of the trochlea.

The calcaneal heel of *Zionodon satanus* is short, less than one-half the length of the entire calcaneus, and is distinctly medially inflected and slightly bowed plantarly (Figure 4.3 C). Among extant erinaceids, the calcaneal heel is often short, but

dorsoventrally deep, whereas in *Zionodon* the heel is almost round in cross section, being only slightly deeper dorsoventrally than wide mediolaterally. The calcaneal heel of *Z. walshi* is not preserved. The ectal facet of *Z. walshi* is medially oriented and well demarcated by a crisp ridge from the dorsally facing fibular facet (Figure 4.2 D). The ectal and fibular facets are continuous anteriorly but posteriorly the fibular facet terminates whereas the ectal facet continues farther posteriorly. Just posterior to the termination of the fibular facet is a pit where the fibula comes into contact with the calcaneus, resembling the condition in the Wasatchian carnivoran *Didymictis* (Heinrich and Rose, 1997). The sustentacular facet is small and nearly flat, and the plantar aspect of the sustentaculum is grooved for the tendon of the flexor fibularis. The ectal and sustentacular facets overlap considerably in proximodistal extent, rather than the sustentaculum being placed distinctly distal to the ectal facet. Distally, the calcaneus of both species of *Zionodon* is short, unlike fossil leptictids that have an elongated distal calcaneus (Rose, 1999, 2007). The cuboid facet is nearly flat and oriented at an acute angle to the long axis of the calcaneus. The plantar tubercle is poorly developed and does not extend to the distal margin of the calcaneus. Likewise, the peroneal tubercle was almost certainly poorly developed, though the lateral border of the distal calcaneus is damaged in all specimens.

The calcaneus of *Zionodon* again resembles that of *Creotarsus* more than any other fossil or extant taxon. Both taxa share a short calcaneal heel, short distal calcaneus, the retention of a fibular facet, substantial overlap of ectal and sustentacular facets, and an acute orientation of the cuboid facet to the long axis of the calcaneus. The calcaneal heel of *Creotarsus* appears to have lacked any plantar or medial inflection. The calcaneal

heel of *Macrocranion vandebroeki* is straighter and more robust, and the distal calcaneus is more elongate than that of *Zionodon*. The calcaneus of *M. vandebroeki* also lacks a fibular facet. The shape and angle of the cuboid facet, size of the peroneal tubercle and degree of overlap of the sustentacular and ectal facets in *Zionodon* resemble the condition of *M. vandebroeki*. The relative length of the calcaneal heel in *Zionodon* is comparable to that of leptictids as is the amount of overlap between the sustentacular and ectal facets, but those are the only similarities. Leptictid traits that differ from *Zionodon* are: a straight, robust calcaneal heel, lack of a fibular facet, more transversely oriented ectal facet, long distal segment, well developed peroneal tubercle and plantar process, and a more transverse orientation of the cuboid facet in leptictids (Rose, 1999). The calcaneus of nyctitheres resembles that of *Zionodon* in retaining a fibular facet, but differs in the proximodistal separation of the sustentacular and ectal facets, in having a robust peroneal tubercle and a more distally placed plantar process (Hooker, 2001).

The cuboid of both species of *Zionodon* is short. That of *Z. satanus* is broken both medially and laterally. The cuboid of *Z. walshi* is wider proximally than distally (Figure 4.2 E). The surface of the calcaneal facet is somewhat cylindrical being convex dorsoventrally and straight mediolaterally. There is a concave facet on the proximomedial surface for the astragalar head and an irregularly shaped facet on the medial surface for the navicular and the ectocuneiform; these facets are at nearly right angles to one another. The peroneal tubercle on the plantar aspect of the cuboid is prominent and the peroneal groove is deep. The cuboid presumably articulated distally with both metatarsals IV and V. There is a single continuous articular facet on the distal cuboid which could indicate either that metatarsal V was not abducted from metatarsal IV or that it was absent or

significantly reduced such that it did not articulate with the cuboid. The cuboid of *Creotarsus* also exhibits a distinct concave astragalar facet on the proximal articular surface.

4.3 Functional Interpretations

4.3.1 Forelimb

The fragmentary and crushed condition of the forelimb skeleton precludes functional analysis of both joint morphology and limb proportions. All that can be said about the forelimb is that the proximal humerus probably retained a good deal of mobility at the shoulder joint judging by the low greater and lesser tubercles (Rose and Chinnery, 2004). The development of the deltoid and supinator crests suggest a heavily muscled shoulder, and the expanded entepicondyle is suggestive of strong wrist and digital flexors. The large extensor tubercle on the radius also suggests well-developed forearm musculature. Similar structures are found in diggers such as dasypodids and palaeanodonts (Rose et al., 1992; Rose and Lucas, 2000) and in mammals reconstructed as climbers such as *Chriacus* (Rose, 1987). The presence of well-developed tubercles on MC II and III for insertion of extensor carpi radialis suggest that *Zionodon* engaged in at least some digging. Of the other taxa that typically display similar tubercles, palaeanodonts and dasypodids are specialized fossorial mammals, whereas leptictids were saltatorial forms that probably engaged in some digging (Rose, 1999, 2007; Rose et al., 1992). The large extensor tubercle on the distal radius is consistent with digging behavior as it is also found in palaeanodonts and dasypodids (Rose et al., 1992; Rose and Lucas, 2000).

4.3.2 Hip and knee

The morphology of the hip and knee suggests that *Zionodon* was terrestrial rather than arboreal. The articular surface of the femoral head does not extend onto the neck as is often seen in mammals with an abducted and mobile hip, and suggests that the range of abduction was limited (Heinrich and Rose, 1997; Jenkins and Camazine, 1977). This is somewhat contradicted by the presence of a small but well-developed ischial spine, which is associated with well-developed gamelli muscles, which abduct and laterally rotate the femur. Heinrich and Rose (1997) stated that this feature is well developed in arboreal carnivores compared to terrestrial ones, but *Sylvilagus* (cottontail), a terrestrial leaper, also has a well-developed ischial spine, indicating that this trait is not necessarily indicative of arboreality or of mobile hips.

The depth of the femoral condyles and distinctly grooved patellar surface indicate an emphasis on limiting the movement of the knee to flexion and extension as is seen in terrestrial mammals (Heinrich and Rose, 1997; Rose 1990, 1999; Sargis, 2002) and is often indicative of fast terrestrial running (Sargis, 2002). Although a deep knee and well-defined patellar groove is most pronounced in terrestrial mammals (Argot, 2002; Sargis, 2002), these features do not necessarily indicate a terrestrial way of life (Argot, 2002). Both of these features are also found in arboreal leaping mammals, such as galagos, which utilize powerful extension at the knee to leap between arboreal substrates (Anemone, 1993; Sargis, 2002).

The concave medial and convex lateral tibial condyles are other features indicative of a stable knee, which prevents mediolateral movement between the distal femur and proximal tibia, while allowing rotation around a pivot point, the medial

condyle (Argot, 2002). As is the case with the morphology of the distal femur, this feature of the tibial plateau is often associated with terrestriality, but is also seen in leaping arboreal mammals (Argot, 2002; Dunn et al., 2006; Sargis, 2002).

4.3.3 Ankle

The ankle of *Zionodon* exhibits a combination of traits typical of both cursorial terrestrial mammals and more flexible climbing mammals. The presence of a cotylar fossa on the astragalus and corresponding process on the tibial malleolus are found in terrestrial cursorial carnivores and not in arboreal ones (Heinrich and Rose, 1997). The well-grooved astragalar trochlea and dorsal migration of the articular surface for the navicular onto the astragalar neck are also indicative of terrestrial locomotion in many mammalian taxa (Carrano, 1997; Rose, 1990; Van Valkenburgh, 1987). The presence of a sustentacular hinge in *Z. walshi* would appear to limit the movement of the astragalus on the calcaneus, and would seem to be consistent with a terrestrial way of life, but its presence in both arboreal and terrestrial sciurids as well as in a diverse assortment of Eocene mammals makes its significance unclear (Rose and Chinnery, 2004).

The presence of an astragalar foramen is often associated with limited plantarflexion and plantigrady (Heinrich and Rose, 1997; Wang, 1993), but it is not clear to what extent the structures passing through this foramen actually limit plantarflexion as the astragalar trochlea extends beyond this foramen in many fossil mammals (Heinrich and Rose, 1997; Szalay, 1977). The unequal sizes of the medial and lateral astragalar condyles are often seen in arboreal mammals that utilize inverted and everted ankle postures (Dunn et al., 2006; Heinrich and Rose, 1997), whereas the condyles of terrestrial mammals tend to be more symmetrical (Carrano, 1997; Heinrich and Rose, 1997).

The presence of a squatting facet on the anterior distal tibia and corresponding facet on the astragalar neck of *Zionodon* is functionally ambiguous. Virtually all that has been said about the presence of such facets in mammals is that they provide a bony stop for the tibia as it rotates around the astragalar condyles (Decker and Szalay, 1974). However, any bony structure in the vicinity of the astragalar neck will stop the tibia from rotating, and does not necessitate an articular facet to do so. The presence of an articular facet implies that these bones were in contact often and for prolonged periods. It then follows that the presence of such a facet indicates that the animal spent some amount of time resting on dorsiflexed ankles. This is seen in some vertical clinging primates, such as galagos (Gebo, 1988). Other mammals that show such facets include hedgehogs and tenrecs that utilize crouched limb postures, many of which are plantigrade (Eisenberg and Gould, 1970; Gould, 1978; Reeve, 1994). Leporid distal tibiae have a similar facet, which may be attributed to the fact that rabbits often rest in a crouched plantigrade position and travel with a digitigrade posture (Best, 1996). However, the interpretation of this trait is not that simple as macroscelideans also show such a facet, and they are extremely specialized bipedal saltators. Although it may be tempting to attribute the presence of a squatting facet in *Zionodon* as indicative of habitual dorsiflexion, the significance of this trait is far from clear.

The calcaneal morphology of *Zionodon* is somewhat perplexing in that its distinctive suite of characters is not seen in any living or extinct insectivores or in any other mammals examined. A short calcaneal heel paired with a short distal and long middle calcaneus is not common among terrestrial mammals and more closely resembles the calcaneal proportions of slow arboreal climbers such as lorises (Gebo, 1988). A

plantar curvature to the calcaneal heel is associated with plantigrady in some taxa (Rose, 1990; Sarmiento, 1983), but it is morphologically different from the dorsoplantar orientation of the entire heel that is seen in *Zionodon*, which more closely resembles that of the deliberate climbing and suspensory lorises (Gebo, 1988, 1993), and the fossil primates *Adapis* (Decker and Szalay, 1974) and *Paleopropithecus* (Wunderlich et al., 1996). In these taxa, the plantar orientation of the calcaneal heel is considered indicative of powerful digital grasping, which is necessitated by a slow arboreal locomotion (Gebo, 1988; Rose, 1990; Sarmiento, 1983). The medial inflection of the calcaneal heel is also reminiscent of primates and other animals in which inverted foot postures are used habitually (Gebo, 1988; Wunderlich et al., 1996). However, the considerable overlap of ectal and sustentacular facets proximodistally and the flat and acutely oriented cuboid facet are usually interpreted as terrestrial traits (Heinrich and Rose, 1997; Rose and Chinnery, 2004).

4.4 Discussion

All extant erinaceids share specialized features of the postcranial skeleton, many of which are present in the majority of extant insectivore groups. These include a distally fused tibiofibula and loss of a fibular facet on the calcaneus, features that are also found in *Macrocranion* (Schaal and Ziegler, 1992; Storch, 1993), a reduction or loss of the medial malleolus of the tibia, and a distinctive astragalar morphology (which consists of a shallow body, a distinctly grooved trochlea with condyles of approximately equal height or with a higher medial than lateral condyle, and a short, straight neck with a small, spherical head; Hooker, 2001). These features are evident in isolated fossil astragali from the Bridgerian of Wyoming, indicating that erinaceids had begun to acquire their

specialized morphology by approximately 50 million years ago (Matthew, 1909). *Zionodon* represents the most primitive erinaceomorph postcranium yet known (at least in ankle morphology), as the fibula is robust and shows no evidence of tibio-fibular fusion, the medial malleolus is large and unreduced, a large fibular facet is present on the calcaneus, and none of the specialized features characteristic of erinaceid astragali is present. The strong resemblance of *Zionodon* to *Creotarsus* is very interesting in that there is such a large chunk of time separating the two taxa. Both are of uncertain phylogenetic affiliation and both have been linked with erinaceomorphs (Dunn and Rasmussen, 2009; McKenna and Bell, 1997; Van Valen, 1967). Many of the features that are shared between *Creotarsus* and *Zionodon* may be primitive for Eutheria, such as the superior astragalar foramen and fibular facet on the calcaneus, but others are probably not, most strikingly the well-developed astragalar facet on the cuboid. The phylogenetic significance of these traits will not become clear until comparable elements of other Eocene erinaceomorphs are found.

The postcranial morphology of *Zionodon* does not fit cleanly with any commonly utilized behavioral category making interpretation difficult. The fragmentary forelimb suggests at least some digging behavior. A systematic look at the hindlimb suggests that the hip and knee were stable hinge-like joints suited for forward propulsion rather than mediolateral mobility. The morphology of the calcaneus, on the other hand, would seem to indicate that the foot was habitually used in inverted postures, which would suggest a more mobile ankle. The astragalus displays a mixture of features suggesting restriction of mediolateral translation and use of sagittal movement, combined with evidence of use of inverted and everted postures. We suggest that *Zionodon* was terrestrial, but habitually

used uneven substrates, such as a debris-strewn forest floor or rocky talus slopes, rather than more even ground. Paleoenvironmental and sedimentological evidence suggests the former is more likely (Townsend, 2004). This would require restriction of movement to a parasagittal plane in the proximal hindlimb for forward propulsion, while necessitating mobility at the ankle for maintaining contact with the complex substrate. Although we reconstruct *Zionodon* as terrestrial, it is important to realize that many of the traits commonly associated with terrestriality, especially those associated with knee morphology, are also found in agile arboreal leapers (Anemone, 1993; Argot, 2002; Dunn et al., 2006; Gebo, 1993; Sargis, 2002). It is likely that, like many other small and morphologically generalized mammals including extant erinaceids (Eisenberg and Gould, 1970; Gould, 1978; Reeve, 1994), *Zionodon* would have been able to utilize arboreal as well as terrestrial substrates.

4.4.1 Implications for Primate Evolution

The postcranial remains of *Zionodon* suggest a closed rather than an open habitat. As *Zionodon* is frequently found in localities that also frequently yield primates, this supports the idea that primates also inhabited closed habitats. *Zionodon* has only been found in Uinta B rocks that date to the early Uintan. Dental remains of *Zionodon* are rare, but postcranial remains of *Z. walshi* are common especially at WU-18. The lack of *Zionodon* in the late Uintan of the Uinta Formation suggests that the habitats in which it and primates lived are no longer common.

4.5 Summary

The goal of this chapter was to reconstruct the postcranial morphology of *Zionodon* and to assess the probable locomotion and habitat in which it lived. The

postcrania of *Zionodon* suggest that it was terrestrial but likely could dig and climb well and probably traveled over uneven substrates such as a forest floor rather than more open ground. *Zionodon* is extremely primitive in ankle morphology compared to most extant and fossil erinaceomorphs and most closely resembles the enigmatic *Creotarsus* in ankle morphology, suggesting that there may be a special relationship between the two taxa.

Table 4.1. Localities from which *Zionodon* is known

Locality	Species	Primate
WU-5, "Hedgehog Hill"	*Z. walshi*	
WU-18, "Gnat out of Hell"	*Z. walshi*	*Chipetaia lamporea*
WU-72	*Zionodon* sp.	
WU-75	*Z. walshi*	
WU-86	*Z. walshi*	
WU-180	*Z. walshi*	*Ourayia uintensis*

Table 4.2. Postcranial measurements of *Zionodon* (in mm).

		Zionodon satanus[a]	*Zionodon walshi*[b]
Femur	depth of condyles (a-p)[c]	–	10.7
	width of condyles (m-l)[d]	–	9.6
	condylar index[e]	–	111.5
Calcaneus	total length	14.0	–
	distal length	5.1	5.5
	heel length	6.1	–
Astragalus	total length	7.9	8.8
	head width	4.3	4.8
	trochlear width	4.1	4.7
Cuboid	total length	4.8	5.6

– denotes missing value

[a] CM 71139

[b] CM 71140 (femur and cuboid) and CM 71142 (astragalus and calcaneus)

[c] a-p: antero-posterior

[d] m-l: medio-lateral

[e] condylar index = a-p / m-l * 100

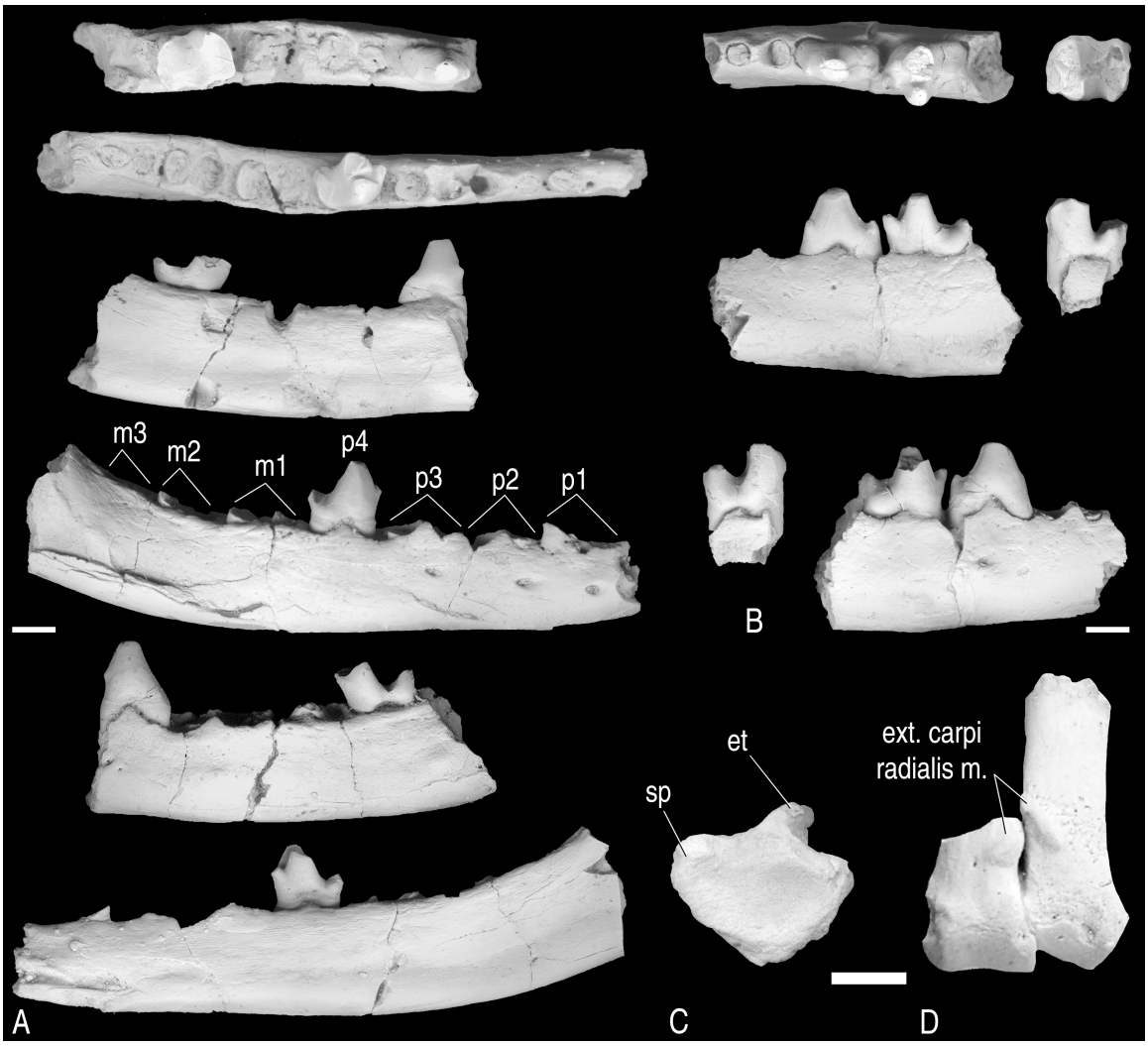

Figure 4.1. Dentition of *Zionodon*; radius and metacarpals of *Z. satanus*. **A**, CM 71139 left and right dentaries of *Zionodon satanus* in occlusal view (top pair), left lingual, right buccal view (middle pair), left buccal, right lingual view (bottom pair). **B**, CM 71141 right p3-4 and CM 71138 right m2 of *Zionodon walshi* in occlusal view (top), lingual view (middle) and buccal view (bottom). **C**. Left distal radius in distal view. **D**, Right bases of metacarpals II and III in dorsal view, indicating tubercles for insertion of the extensor carpi radialis muscle. **et**, extensor tubercle; **sp**, styloid process. Scale bar = 2 mm.

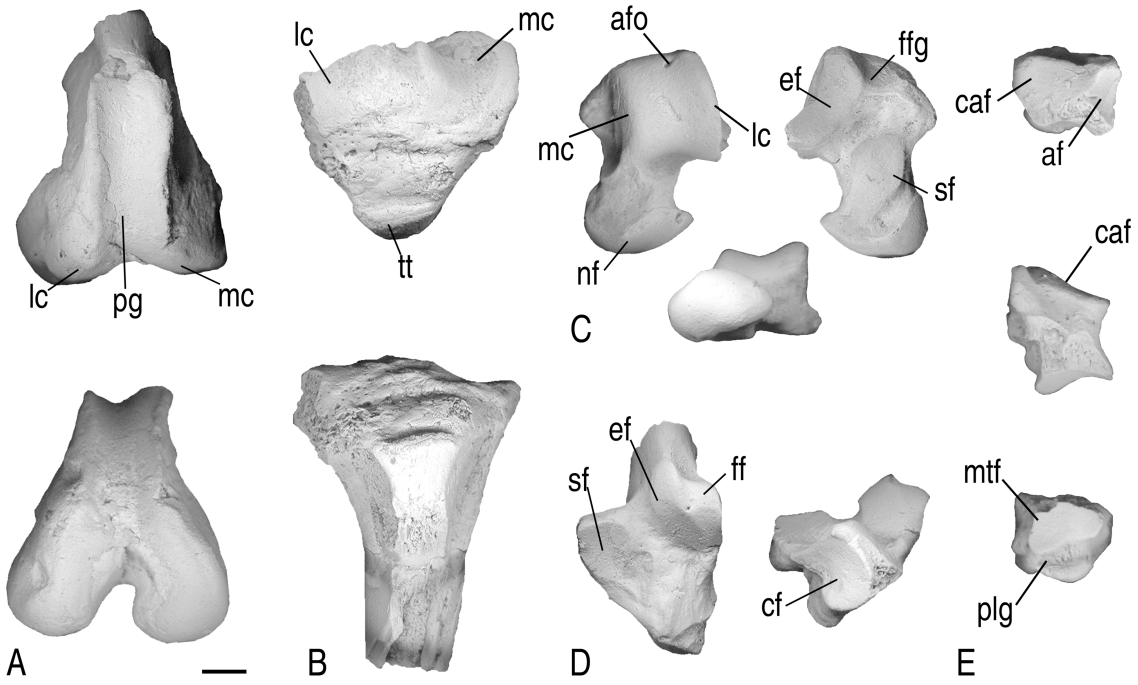

Figure 4.2. Hindlimb elements of *Zionodon walshi*. **A**, CM 71140 right distal femur in anterior (top) and distal (bottom) views. **B**, CM 71140 right proximal tibia in proximal (top) and anterior (bottom) views. **C**, CM 71142 left astragalus in dorsal view (left), plantar view (right), and distal view (middle). **D**, CM 71142 distal calcaneus in dorsal view (left) and distal view (right). **E**, CM 71140 left cuboid in proximal (top), dorsal (middle) and distal (bottom) views. **af**, astragalar facet; **afo**, superior astragalar foramen; **cf**, cuboid facet; **caf**, calcaneal facet; **ef**, ectal facet; **ff**, fibular facet; **ffg**, flexor fibularis groove; **lc**, lateral condyle; **mc**, medial condyle; **mtf**, facet for metatarsals IV and V; **pg**, patellar groove; **plg**; groove for the peroneus longus; **sf**, sustentacular facet; **tt**, tibial tuberosity. Scale bar = 2 mm.

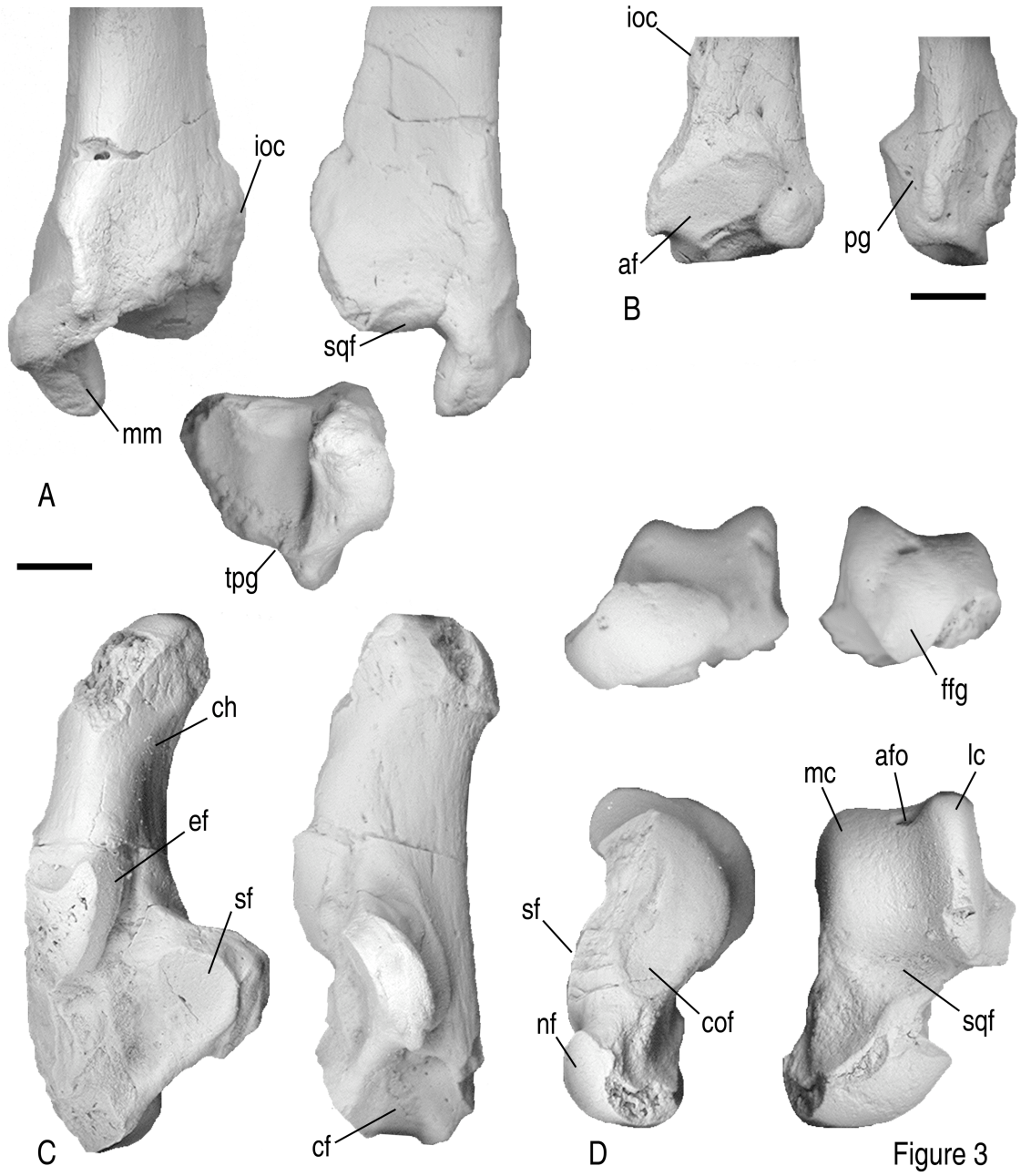

Figure 4.3. Hindlimb elements of CM 71139, *Zionodon satanus*. **A**, right distal tibia in posterior view (left), anterior view (right) and distal view (middle). **B**, right distal fibula in medial view (left) and posterior view (right). **C**, right calcaneus in dorsal view (left) and medial view (right). **D**, left astragalus in anterior view (top left), posterior view (top right), medial view (bottom left) and dorsal view (bottom right). **af**, astragalar facet; **afo**, superior astragalar foramen; **cf**, cuboid facet; **ch**, calcaneal heel; **cof**, cotylar fossa; **ef**, ectal facet; **ffg**, flexor fibularis groove; **ioc**, interosseus crest; **lc**, lateral condyle; **mc**, medial condyle; **mm**, medial malleolus; **nf**, navicular facet; **pg**, peroneal groove; **sf**, sustentacular facet; **sqf**, squatting facet; **tpg**, tibialis posterior groove. Scale bar = 2 mm.

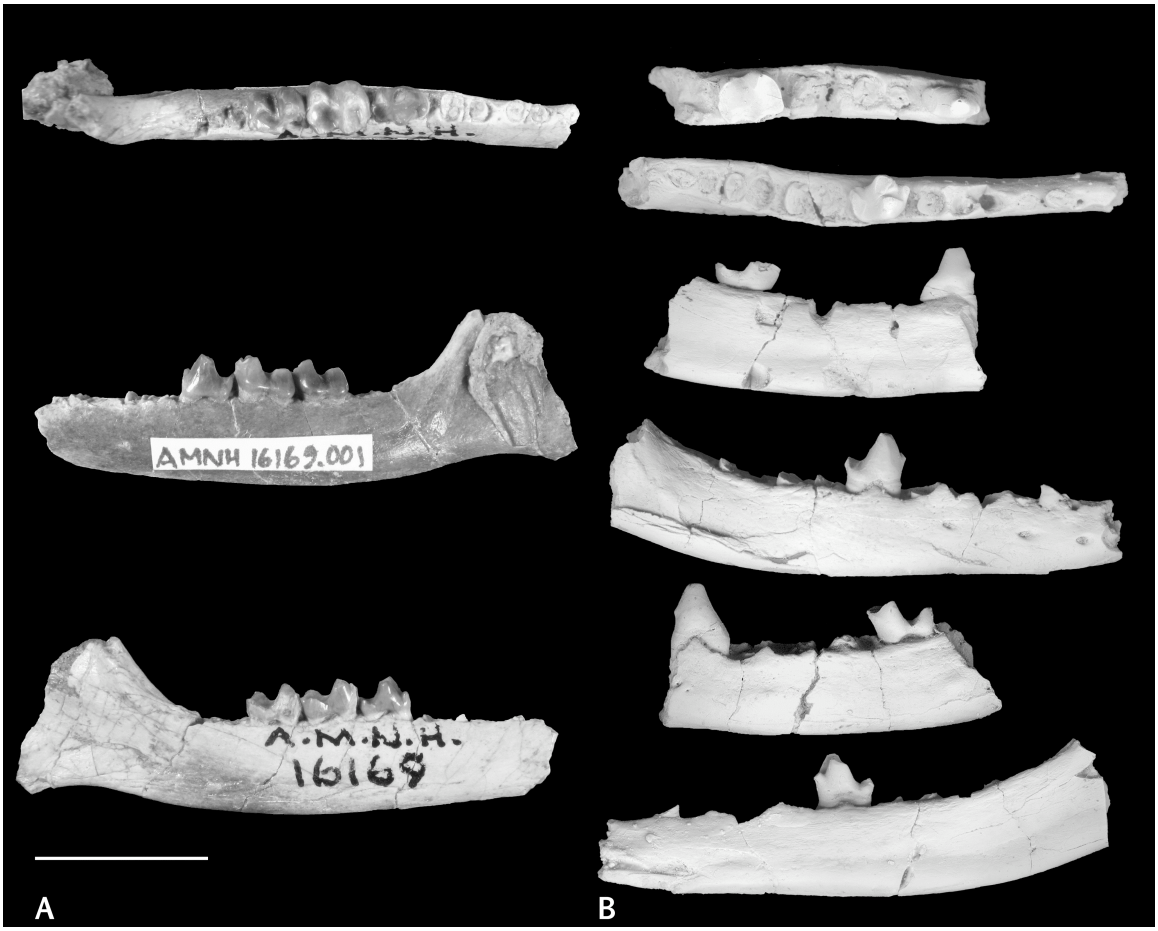

Figure 4.4. Jaws of *Zionodon satanus* compared to the holotype of *Creotarsus*. **A**, left dentary of *Creotarsus* (AMNH 16169) with P_4–M_2. **B**, Left and right dentaries of *Zionodon satanus* (CM 71139) with L P_3, M_2, R P_4; views as in figure 4.1 A. The two jaws are similar in size and in dental morphology. The teeth of *Creotarsus* are more bunodont than those of *Zionodon*, and the anterior teeth appear to have been more reduced. The general shape of the P_4 is similar in both taxa, being unreduced with a prominent paraconid. The molars are similar in having thin enamel that wears down quickly, and in their reduction in size such that $M_1 > M_2 > M_3$. Scale bar = 5 mm.

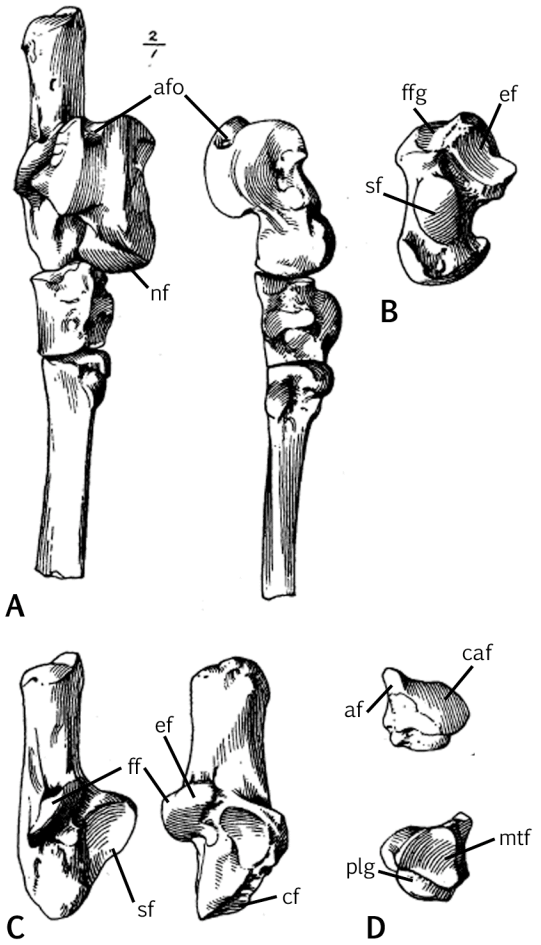

Figure 4.5. Tarsals of the holotype of *Creotarsus* (AMNH 16169). **A**, articulated right astragalus, calcaneus, cuboid and metatarsal IV in dorsal view (left) and medial view (right). **B**, right astragalus in plantar view. **C**, right calcaneus in dorsal view (left) and medial view (right). **D**, right cuboid in proximal view (top) and distal view (bottom). These bones have been lost, but the illustration shows that in general appearance they are similar to their homologues in *Zionodon*. In particular the shape of the astragalar head, shape of the sustentacular facet and deep flexor fibularis groove on the astragalus, the presence of a fibular facet and the oblique cuboid facet on the calcaneus, and the distinct, strongly concave astragalar facet on the cuboid are reminiscent of the condition in *Zionodon*. **af**, astragalar facet; **afo**, superior astragalar foramen; **cf**, cuboid facet; **caf**, calcaneal facet; **ef**, ectal facet; **ff**, fibular facet; **ffg**, flexor fibularis groove; **mtf**, metatarsals IV and V; **nf**, navicular facet; **pg**, peroneal groove; **sf**, sustentacular facet (modified from Matthew 1918).

CHAPTER FIVE

Skeletal remains of Uintan *Pantolestes*.

5.1 Introduction

Pantolestids are known from the early Tertiary of North America, Europe and Asia (and possibly Africa). They are characterized by a robust postcranial skeleton with short heavily muscled limbs and a generalized bunodont dentition (Boyer and Georgi, 2007; Rose and Koenigswald, 2005). Ecologically they were similar to river otters and beavers in being semi-aquatic and good diggers (Gunnell et al., 2008; Rose and Koenigswald, 2005). The phylogenetic placement of the group remains uncertain. They are generally referred to the superordinal group "Proteutheria" which is at best a paraphyletic assemblage of relatively large-bodied mammals compared to other early primitive mammals. Within Proteutheria, they are placed in their own order, Pantolesta, together with some enigmatic late Eocene taxa (Gunnell et al., 2008; Rose, 2006). There is some evidence that pantolestids have a close relationship with palaeanodonts and leptictids (Rose, 1999, 2006; Rose and Lucas, 2000). To confuse matters further, leptictids and palaeanodonts are often placed within widely different modern orders: leptictids in the order Lypotyphla together with modern Erinaceomorpha and Soricomorpha (Rose and Lucas, 2000); and palaeanodonts with either the Xenarthra (sloths, anteaters, and armadillos, Simpson, 1931) or Pholidota (pangolins, Rose, 2006, 2008; Rose and Emry, 1993). From a general evolutionary perspective, pantolestids are one of many groups of primitive mammals that radiated long ago and for which we do not know precise phylogenetic placement.

North American Pantolestidae achieves its highest diversity in the Paleocene with eight species placed in two subfamilies, the Pantolestinae and Pentacodontinae. Pentacodontines became extinct at the end of the Paleocene. Only one genus of pantolestid (*Palaeosinopa*) is present in the Wasatchian and it survived into the early Bridgerian where it overlapped temporally with the genus *Pantolestes*. There are currently five known species of *Pantolestes*, all of which occurred during the Bridgerian. Later pantolestids are known but rare. The latest surviving pantolestans are *Simidectes*, known from the late Uintan of the Uinta Formation and the late Uintan to Duchesnean of southern California (Gunnell et al., 2008; Rasmussen et al., 1999; Robinson et al., 2004; Walsh, 1996), and *Chadronia*, from the early Chadronian of Nebraska (Cook, 1954; Gunnell et al., 2008). Several accounts of pantolestids have been published of poor dental and isolated postcranial remains from several Uintan localities including the Uinta Formation in Utah and the Washakie Formation in Colorado, but none have been formally described or named due to the fragmentary nature of the remains. (Gunnell et al., 2008; Stucky et al., 1996; Thornton and Rasmussen, 2001). Despite the lack of attention, there may be as many as four species of pantolestid from the Uinta Formation in the Carnegie Museum collection housed at Washington University, at least one of which is new.

Postcrania are well known for the North American Bridgerian pantolestids *Palaeosinopa* and *Pantolestes natans*, and for the middle Eocene *Buxolestes* from Germany (Matthew, 1909; Rose and Koenigswald, 2005). Isolated postcranial remains of other North American Bridgerian pantolestids have also been reported (Matthew, 1909; Rose and Koenigswald, 2005). Based upon these specimens, it appears that pantolestids

were fairly conservative in morphology through time, space, and a large size range. The smallest pantolestids are represented by some early species of *Palaeosinopa* and by *Pantolestes elegans* which were comparable in size with modern minks. *Pantolestes natans* is the largest pantolestid, which was similar in body size to an extant river otter (Gunnell et al., 2008; Matthew, 1909; Rose and Koenigswald, 2005). However, because later specimens are fragmentary, it has not been possible to assess the nature of their postcranial morphology through time as well.

A long overlooked pantolestid specimen from the Uinta Formation (UF) in the Yale Peabody Museum collection represents the most complete Uintan pantolestid material known. The specimen consists of a complete postcanine lower dentition and partial postcranium found by John Clarke in during the Princeton University expedition to Utah in 1936. This specimen together with isolated pantolestid postcranial remains from the Uinta Formation housed at Washington University and the Washakie Formation (WF) in the Sand Wash Basin, Colorado (housed at the DMNH), allows an assessment of the functional adaptations of Uintan pantolestids. The new specimens also inform our picture of the taxonomic diversity of Uintan pantolestids compared to that of earlier time periods. Pantolestid specimens examined for this paper are listed in table 5.1.

In this chapter I will describe new postcranial remains of pantolestids from the UF and compare them with Uintan and Bridgerian postcrania in order to assess the probable locomotor behavior of the UF pantolestids.

5.2 Paleobiology of the Pantolestidae

Matthew (1909) was the first to suggest a semi-aquatic lifestyle for *Pantolestes*, even going so far as to suggest a potential relationship with walruses. He based his

interpretations upon a well-preserved skeleton of *P. natans* and on fragmentary remains from other species of pantolestids. Door upheld this interpretation based on morphology of the skull of *Palaeosinopa* and other pantolestids. The discovery of several complete skeletons of *Buxolestes*, a European pantolestid, from ancient lake deposits in Messel, Germany revealed that *Buxolestes piscator* closely resembled otters, beavers and known North American pantolestids in limb morphology. Furthermore, the long, robust tail, and morphology of the cervical and lumbar vertebrae corroborates the assertion that *Buxolestes piscator* was aquatic (Koenigswald, 1980; Pfretzschner, 1993). A smaller pantolestid species form Messel, *Buxolestes minor*, is interpreted as fossorial, lacking aquatic specializations (Pfretzschner, 1999). New skeletons of *Palaeosinopa* from late Wasatchian deposits in the Green River Formation in Wyoming further support an aquatic way of life for pantolestids, and also suggest some digging behavior (Rose and Koenigswald, 2005). Researchers have identified river otters and beavers as the closest living analogues for extant pantolestids (Dorr, 1977; Koenigswald, 1980; Pfretzschner, 1993; Rose and Koenigswald, 2005). Recent analysis of semi-circular canal morphology in a skull of *Pantolestes longicaudus* revealed differences in the proportions of posterior and lateral canals compared to terrestrial fossil mammals, perhaps indicating a semi-aquatic lifestyle for *P. longicaudus* (Boyer and Georgi, 2007). Fossilized remains of fish have been found in the stomach of both *Buxolestes* and *Palaeosinopa*, corroborating possible aquatic affinities (Koenigswald, 1980; Rose and Koenigswald, 2005).

5.3 Description

5.3.1 Forelimb

5.3.1.1 Scapula

Two scapular fragments consisting of the glenoid fossa and part of the blade are known (Figure 5.1). The glenoid of CM 71090 is broken cranially, but that of YPM-PU 14645 is complete. The costal (medial) border of the glenoid fossa is round whereas the lateral border is straight, giving it a somewhat "D"-shaped outline. The humeral articular surface is generally concave, but at the craniolateral margin of the glenoid it extends onto the lateral surface of the glenoid rim, perhaps for articulation with the greater tubercle of the humerus. The humeral articular surface also extends onto the lateral surface of the supraglenoid tubercle, which is large and medially inflected. YPM-PU 14645 preserves a pit on the caudal surface of the scapular neck for insertion of the triceps brachii. CM 71090 may have a smaller pit. No other pantolestid scapulae are known except for those preserved in slabs from Messel, Germany, and the Green River Formation, Wyoming (Koenigswald, 1980, 1986; Rose and Koenigswald, 2005), and none of these specimens has an exposed glenoid region.

5.3.1.2 Humerus

Three humeral fragments are known from the UF. YPM-PU 14645 includes a fairly complete distal humerus with humeral shaft including most of the deltopectoral crest but unfortunately missing the humeral head and tubercles (Figure 5.2). CM 71157 is a proximal humeral diaphysis including the proximal portion of the deltopectoral crest but missing the proximal humeral epiphysis. CM 80591 includes a complete humeral head, tubercles and proximal shaft as well as portions of the distal end. CM 71157 and

YPM-PU 14645 are of comparable size, whereas CM 80591 is significantly larger. The humerus of YPM-PU 14645 is sigmoid in shape in lateral view with well developed brachial and delto-pectoral crests. The humeral head of CM 80591 has the characteristic asymmetrical shape of pantolestid humeri, with the lateral portion of the head being lower than the medial portion. The appearance of this asymmetry is somewhat exaggerated by the high greater tubercle and the low, reduced lesser tubercle. The greater tubercle is much larger than the lesser tubercle and projects above the humeral head. The lesser tubercle is small and situated well below the humeral head.

The deltopectoral crest of YPM-PU 14645is a raised shelf-like feature distal to the greater tubercle consisting of the pectoralis crest on the medial edge and the deltoid crest on the lateral edge. On the proximo-lateral portion of the deltopectoral crest in CM 71157, there is a distinct ridge leading to a raised, rough tubercle for attachment of the deltoid that begins at the margin of the epiphyseal surface of the greater tubercle. This feature is somewhat distorted by crushing and is broken in CM 71157. The pectoralis crest on the medial margin of the deltopectoral crest in YPM-PU 14645 is rough and terminates in a rounded, medially projecting tubercle. The pectoralis crest is separated from the humeral shaft by a fossa, agreeing in morphology with that of CM 71157 and CM 80591. Dorsal to this fossa and located proximal to the termination of the pectoral crest is a small rough area for attachment of the teres major. The deltoid crest is not as pronounced as the pectoralis crest and terminates in a low, rounded ridge just opposite the termination of the pectoralis crest. The area on the ventral portion of the humerus circumscribed by the deltoid and pectoral crests (deltopectoral crest) is damaged, but it

was broad and shelf-like. Although the proximal portion of the humerus is missing, it is apparent that the deltopectoral crest terminated distal to midshaft.

The distal humerus is broad with a prominent medial epicondyle and a large entepicondylar foramen. The brachial crest is well-developed and directed dorsolaterally. The ventral surface of the crest is concave, and the dorsal surface is convex. The brachial crest originates just proximal to the termination of the deltopectoral crest and extends distally to the lateral epicondyle. The lateral margin of this crest is rugose and expands at the distal end. The brachial crest probably extended for almost half of the length of the humerus. The capitulum is round rather than cylindrical with a distinct capitular tail at the proximo-lateral end. The center of the trochlea merged gradually with the capitulum and was not separated from it by a ridge.

Humeri are known from *Pantolestes natans* (AMNH 12152), *P. phocipes* (AMNH 11547) and a Bridgerian pantolestid (USNM 521350). In general all humeri are similar, but the Bridgerian taxa are consistently more robust than the Uintan specimens with more extensive crests than can be determined in YPM-PU 14645 (although the difference in robustness may be due to the immature nature of the individual). The main differences in the morphology of the proximal humerus are the migration of the humeral head distally toward the lesser tubercle, and the reduction and distal displacement of the lesser tubercle of CM 80591 compared to the Bridgerian specimens. In the Bridgerian pantolestids, the lesser tubercle is more proximodistally extensive and placed more proximally than in CM 80591. In the latter specimen, the lesser tubercle is completely distal to the line of epiphesial fusion, whereas the tubercle rises above this point in the earlier specimens.

5.3.1.3 Ulna

There is one proximal ulna associated with YPM-PU 14645, and a slightly larger specimen (CM 80784) consisting of a distal ulnar shaft including the styloid process to just distal to the semilunar notch (Figure 5.3). The olecranon process is robust and long, though the length relative to the shaft cannot be determined due to the incomplete nature of the specimen. The proximal epiphysis is missing, but the proximal portion of the olecranon process is expanded and medially inflected. On the lateral surface of the ulna, distal to the olecranon is a shallow extensor fossa. There is a deeper but less distally extensive fossa on the medial aspect of CM 80784 just medial to the semilunar notch though the proximal extent cannot be assessed. The radial notch of both specimens is flat and separate from the humeral facet of the semilunar notch. Distal to the semilunar notch, a large pit is present for attachment of the brachialis m. that is deep and proximodistally long.

The body of the ulna in CM 80784 is mediolaterally compressed with a thicker posterior margin and a thin blade-like interosseus crest along the anterior edge. In lateral view the shaft is straight with its distal end reflected posteriorly. The styloid process is small and is not distinctly separate from the carpal articular surface of the distal ulna. The extensor fossa of CM 80784 is only weakly defined proximally and is not present distally. On the lateral aspect at mid-shaft is a short raised ridge. On the distal end of the lateral shaft there is a raised ridge delimiting the groove for the extensor carpi ulnaris posterior to it. Anterior to this ridge is another groove and a smaller, shorter ridge. The medial aspect of the shaft is smooth and unmarked distal to the semilunar notch except for a short sharp ridge situated along the anterior margin just medial to the interosseus

crest, perhaps marking the proximal insertion for the pronator quadratus m. The medial surface of the distal end is strongly concave, though this may be somewhat distorted by crushing.

The ulna of YPM-PU 14645 is similar in size to that of USNM 521305 (Rose and Koenigswald, 2005; plate 8 B) , but is slightly less robust. The radial notch in YPM-PU 14645 is narrower and the pit for insertion of the brachialis muscle is deeper. CM 80784 is straighter in lateral view than USNM 521305, which is more sinuous.

5.3.2 Hindlimb

5.3.2.1 Femur

A proximal femur lacking epiphyses is present with YPM-PU 14645 (Figure 5.4). All of the trochanters are broken at the base. The femoral head overhangs the anterior surface of the femur. The lesser trochanter appears to have been directed posteromedially rather than straight medially. The third trochanter appears to have been a distinct projection and was joined to the greater trochanter by a rounded ridge.

The femur of YPM-PU 14645 does not differ consistently in morphology from those of the earlier Bridgerian pantolestids. In size and general morphology it compares well with AMNH 11620, although the third trochanter may be positioned slightly more distally in the Uintan specimen. It appears that the third trochanter was more proximally placed than in *P. natans* or in USNM 521350 (Rose and Koenigswald, 2005 plate 8 C, E-G).

5.3.2.2 Tibia

YPM-PU includes a partial tibia, with the proximal end broken off and the distal end lacking the epiphysis (Figure 5.4). The tibial shaft is somewhat damaged in the

middle, but it appears to preserve the characteristic sinuous shaft and cnemial tubercle that are typical of pantolestids. The cnemial tubercle is located distal to the midshaft of the tibia. The tibia and fibula were not fused, but there is evidence of an extensive connection between the two elements on the lateral surface of the distal tibial shaft. It is possible that the tibia and fibula may have been fused in a fully adult individual as most of the epiphyses are not yet fused to the diaphyses in this specimen. Fusion of the tibia and fibula is somewhat variable in Bridgerian pantolestids ranging from full fusion in specimens such as AMNH 11620 to unilateral fusion in the holotype of *Pantolestes natans* (AMNH 12152). These elements are separate in *Palaeosinopa*. In general appearance, the tibia of YPM-PU 14645 resembles that of USNM 521350 (Rose and Koenigswald, 2005 plate 8 H), although the latter specimen is more robust.

5.3.2.3 Calcaneus

There are no complete pantolestid calcanei known from the UF, but there are five distal calcanei that belong to two different sizes, two larger specimens and three smaller ones. The smaller specimens are probably comparable in size to the specimen from YPM. There is also a larger distal calcaneus (DMNH 29877) known from the early Uintan of the Washakie Formation (WF) in Colorado.

All specimens are generally similar in morphology except for size (Figure 5.5). The ectal facet is transversely broader than proximodistally long and is generally flat. It is oriented at approximately 45˚ to the long axis of the calcaneus and points disto-dorsally. At the dorsal edge, the articular surface becomes convex as it extends onto the dorso-medial aspect of the ectal process. Lateral to the ectal facet, the fibular facet is flat to slightly convex except at the dorsal edge, where it is distinctly convex. In the small

specimens the fibular facet is more than half the width of the ectal facet, and in the larger calcanei approximately half the width of the ectal facet (Figures 5.5, 5.9).

There is some overlap between the ectal and sustentacular facets. The sustentacular facet of all calcanei in which it is preserved is positioned distally, extending from just proximal to the distal margin of the ectal facet to the distal margin of the calcaneus. The sustentaculum is narrow and elongate, and it is somewhat rectangular or rhomboidal in shape. The distal calcaneus is short. The peroneal tubercle is positioned distally, obliquely opposite the sustentaculum and approximating the sustentaculum in size and shape. The cuboid facet of the calcaneus is roughly triangular and is angled slightly to the long axis of the shaft so that the articular surface points slightly disto-medially. The calcaneal heel is not preserved in any of the specimens, but the plantar border of the calcaneus appears to be concave. This is in part due to a large plantar tubercle located at the distal margin of the calcaneus just below the cuboid facet. In the specimen from the WF, the plantar border of the calcaneus is flatter, and the plantar tubercle smaller, but still robust.

Two Bridgerian indeterminate pantolestid calcanei (YPM 17212 a and b) from the Yale Peabody collections resemble the Uintan specimens in general morphology. YPM 17212a approximates the larger specimens from the UF in size, but it is smaller than DMNH 28977. YPM 17212b is significantly smaller than any known Uintan postcranial specimens, but it resembles the specimens from the UF in morphology. The calcaneus of *Pantolestes natans* (AMNH 12152) is slightly larger than DMNH 28977 but differs from this specimen and the other Uintan calcanei in the morphology of the ectal process. The ectal facet and fibular facet in this taxon are subequal in width, which contrasts with the

distinctly narrower fibular facet in the Uintan calcanei. The fibular facet of *P. natans* is also flatter and less spool-shaped, and it does not wrap around the posterior aspect of ectal process like it does in the Uintan specimens. The plantar border of the calcaneus of *P. natans* is concave, like the specimens from the UF and unlike DMNH 28977.

5.3.2.4 Astragalus

There is one complete pantolestid astragalus known from the Uinta Formation (CM 71159) and one from the Washakie Formation (DMNH 2123). CM 71159 appears to be larger than would be expected based upon the size of elements such as the humerus from YPM-PU 14645, but not significantly so. The specimen from the WF is significantly larger than that from the UF and probably represents a different species (Figure 5.6).

The Uintan astragali are similar to each other morphologically. The body is broad and low with a moderately grooved trochlea and rounded condyles of approximately equal height. A medially oriented process is present at the plantar border of the medial condyle. The lateral trochlear wall is vertical and bears a crescent shaped facet for the lateral malleolus of the fibula. A small dorsal astragalar foramen is present, and in the specimen from the UF, there is also a small foramen located just plantar to the midline of the trochlea where the astragalar neck joins the body.

The neck is slightly shorter than the trochlea and broad in CM 71159, and is shorter but narrower in DMNH 2321. The astragalar head is wide transversely and dorsoventrally shallow. The lateral side of the head is roughly twice as deep as the medial side in the UF astragalus, whereas in the WF pantolestid the maximum depth of the head is in the midline, with the lateral side slightly shallower and the medial side much

shallower. The navicular facet extends medially onto the side of the neck until approximately the point at which the neck joins the body. The outline of the navicular facet is sinuous in distal (anterior) view rather than being a simple ellipse or ovoid facet. The astragalar head of the DMNH 2321 is somewhat rounder than that of CM 71159 and the navicular facet extends farther dorsally onto the neck.

On the plantar surface of the UF astragalus, the ectal facet is large, concave and triangular. There is a distinct notch in the lateral border of this facet for the talofibular ligament (Rose and Koenigswald, 2005). The ectal facet is separated by the sustentacular facet by a deep sulcus and possibly a plantar astragalar foramen. In the WF astragalus, the ectal facet is more rectangular than triangular due to an expansion of the distal border towards the sustentacular facet. The sulcus separating the two facets is deep but narrower than in the UF specimen. The sustentacular facet is about one third the size of the ectal facet in DMNH 2321 and about half the size of the ectal facet in CM 71159. It is pyriform and in CM 71159 there is a narrow extension projecting proximally toward the flexor fibularis groove trochlea. There is no proximal extension of the sustentaculum in DMNH 2321 (Rose and Koenigswald, 2005). The sustentacular facet is convex except for the small proximal extension, which is concave. The sustentacular facet is confluent with the navicular facet. There is a faint groove on the plantar surface of the trochlea for the tendon of the flexor fibularis muscle.

In general morphology the Uintan astragali resemble Bridgerian pantolestid astragali, with most of the variation being in size. The most pronounced differences are between the different size classes of astragali, such that the small Bridgerian and Uintan astragali resemble each other more than they do the larger astragali and vice versa. *P.*

natans is larger than both Uintan specimens, but closer in size to DMNH 2321. The astragalar neck of *P. natans* is shorter than in CM 71159 but similar in relative length to DMNH 2321. The head is rounder than in either specimen as well as in smaller specimens from the Bridgerian, and is less inflected medially. The navicular facet extends farther laterally in *P. natans* than in other pantolestids.

5.3.2.5 Navicular

One navicular from the UF is included with CM 71159. The plantar tubercle is broken, but is otherwise complete. DMNH includes a complete navicular (Figure 5.6). The astragalar facet is concave and has a shape that corresponds to the navicular facet on the astragalus, transversely broad and dorso-plantarly shallow, and is deeper laterally and shallower medially. The plantar tubercle of DMNH 2321 is robust at its base with a distinct forward projecting process at its distal end. The distal surface of the navicular preserves three facets for articulation with the cuneiforms. On the medial margin of CM 71159 is a small, flat ovoid facet that extends slightly onto the dorsal surface of the navicular. This facet may have articulated with a medial sesamoid, and it is not present in DMNH 2321. The facet for the entocuneiform is long transversely and dorso-plantarly shallow. It is convex in both directions, with a smaller dorso-plantar radius of curvature. The facet for the mesocuneiform is slightly convex and separated from the entocuneiform facet by a faint ridge. It is ovoid in shape and shallow in CM 71159 whereas in DMNH 2321 the facet is more trapezoidal and deeper. The facet for the ectocuneiform is flat and triangular and is separated from the mesocuneiform facet by a sharp ridge. It is approximately twice the size of the facet for the mesocunieform and faces disto-laterally.

There is a smaller, roughly triangular facet on the planto-lateral margin of the navicular, probably for contact with the cuboid.

The only other pantolestid navicular known is with AMNH 12152. It more closely resembles the navicular of DMNH 2321 in size and in the shape of the facet for the mesocuneiform.

5.3.2.6 Cuboid

An isolated cuboid (CM 71160) has been assigned to the Pantolestidae based on size, morphology and the presence of other pantolestid remains from the same locality. No other pantolestid cuboids have been reported. The allocation of this element to Pantolestidae should remain tentative until associated pantolestid remains can confirm its membership in this group. The cuboid is robust and not elongate. The calcaneal facet on the proximal surface of the cuboid is roughly triangular and gently convex. There is a robust peroneal tubercle, which is located more plantarly than laterally. A deep peroneal groove is present dorsal to the peroneal tubercle and plantar to the facet for metatarsals IV and V. On the medial surface of the cuboid is a large triangular facet with the apex oriented plantarly. The dorsal margin of the facet is divided into two separate, equal-sized portions by a wedge of non-articular bone. This may indicate that this facet articulated with a bone other than the navicular. The lack of a distinct cuboid facet on the astragalar head suggests that the cuboid did not articulate with the astragalus and may have instead articulated with the ectocuneiform. Alternately, the facet could have contacted the ectocuneiform and third metatarsal. There is a single, continuous facet for metatarsals IV and V. The majority of this facet is concave, but the lateral margin of it is sharply convex with the articular surface extending onto the planto-lateral aspect of the cuboid just dorsal

to the peroneal groove (Figure 5.6).

5.3.2.7 Cuneiforms

DMNH 2321 preserves a complete mesocuneiform and a partial proximal entocuneiform. The facet for the navicular on the entocuneiform is concave and cup like. The mesocuneiform is small and irregularly shaped. the facet for the navicular is slightly concave dorso-ventrally. There is a facet on the medial surface for the entocuneiform and a smaller facet laterally for the ectocuneiform. The distal facet for metatarsal II is irregular in shape, but this facet is probably broken dorsally. It appears from the unbroken proximal edge that there would have been a small dorsal projection to articulate with the dorsal facet on the second metatarsal (Figure 5.6).

The only other reported pantolestid entocuneiform is included in AMNH 12152. The entocuneiform is rectangular in outline with a deep and narrow, convex surface for articulation with the first metatarsal on the disto-medial surface. The navicular articular surface is concave as in DMNH 2321.

5.3.2.8 Metapodials and Phalanges

DMNH 2321 preserves metatarsals II, III and IV as well as two proximal phalanges, three intermediate phalanges and the distal tip of an ungual phalanx. The second and third metatarsals have broken proximal ends, but the fourth metatarsal is complete. Two specimens from the Uinta Formation (CM 71001 and CM 71090) include fragments of metapodials and phalanges that cannot be attributed to either the manus or pes with confidence. The metatarsals are robust with MT III being the longest and II and IV being shorter but approximately equal to each other in length. The metatarsal heads are cylindrical with a small medial keel on the plantar surface. The head of MT III is

broader than those of the other two metatarsals. On all three metatarsals, the dorsal surface of the head recessed compared to the shaft, creating the appearance of a bony ridge separating the articular surface from the rest of the bone. The shafts of MT II and IV are marked by a distinct ridge along the proximal portion of the dorsal shaft (Figure 5.6).

CM 71090 includes one metapodial head and a portion of the shaft. The distal articular surface is cylindrical and robust. The plantar portion is damaged, but the keel on the ventral portion of the head appears to have been weak. The head is not recessed as in DMNH 2321. The shaft just proximal to the head is generally round in cross section, but a sulcus is present on the dorso-lateral (or dorso-medial) surface of the shaft as is a corresponding bony ridge dorsal to it as in the DMNH specimen. The large size of the metapodial relative to the calcaneus preserved with this specimen may indicate that it is a metatarsal. CM 71001 includes the right and left bases of metatarsal III and a small metapodial head. The small size of the metapodial head may suggest that it is a metacarpal, but it could represent a reduced lateral metatarsal as well. The ventral keel is present but not large and the articular surface for the proximal phalanx does not extend onto the dorsal surface of the head, unlike the metatarsal head in CM 71090. The proximal articular surface at the base of MT III is deep dorso-plantarly and narrow transversely. The facet is wedge shaped and slightly convex dorsally and slightly concave at the plantar end. A small portion of the dorso-medial articular surface extends onto the medial aspect of the metatarsal base and faces medially for articulation with MT II. The articular surface extends onto the lateral surface both dorsally and ventrally. The ventral extension of the lateral articular surface is separated by the main articular surface by a

sharp ridge and points proximo-laterally rather than straight laterally, giving the ventral portion of the metapodial base a twisted appearance. The shaft of metatarsal III is sub-triangular in cross section near the base and becomes more circular distally. A shallow sulcus is present on the medio-lateral portion of the shaft just before the break, corresponding with a wide, indistinct ridge of bone on the lateral portion of the dorsal surface of the shaft.

The proximal and intermediate phalanges included in DMNH 2321 are broad and flat. The proximal phalanges are deeper proximally than distally. The proximal articular surface is concave and preserves a shallow ventral groove corresponding to the small ventral keel of the metatarsal heads. The distal articular surface is restricted primarily to the plantar and distal aspects of the bone. The intermediate phalanges are also deeper proximally than distally, but the distal surface does extend well onto the dorsal surface. The flexor tubercles on all phalanges are indistinct. The fragment of the ungual phalanx preserves the distal portion of the claw. From this portion it appears that the claw was not strongly curved and was broad and uncompressed (Figure 5.6).

There are six proximal phalangeal fragments associated with pantolestid material from the UF. One of these is very large and robust and is therefore probably from the pes, however the rest are ambiguous. The largest one (associated with CM 71001) is almost complete except for one half of the head. The proximal portion of the proximal phalanges resemble those of DMNH 2321. In the specimens from the UF there is a dorsal keel extending from the base of each phalanx distally such that the cross-section of the base of the phalanges is triangular. This is broader on the largest phalanx and more mediolaterally compressed on the phalanx associated with CM 71090, in which the

proximal portion of this ridge is tubercle-like and roughened. This ridge is not seen in the phalanges of DMNH 2321. The flexor tubercles on the plantar surface of the UF specimens are small and distally placed.

5.4 Functional Interpretations

5.4.1 Forelimb

The overall strength of the muscle markings on the humerus suggest a heavily-muscled forelimb, with well developed rotator cuff and shoulder muscles as well as supinators and flexors of the forearm. These muscles are better-developed in diggers than in aquatic forms, but are pronounced in the latter as well (Dunn and Rasmussen, 2007; Rose and Koenigswald, 2005; Simpson, 1945). The large greater tubercle and reduced lesser tubercle of the humerus are similar to other fossil pantolestids and palaeanodonts and also resemble the condition in extant *Castor*, *Lontra*, *Lutra* and *Enhydra* (Gunnell et al., 2008; Koenigswald, 1980; Rose and Koenigswald, 2005). The greater tubercle in *Enhydra* and *Lutra* projects mostly dorsally and laterally rather than proximally above the head. Thus the greater tubercle of more aquatic mammals tends to be lower than that of mammals that swim but also burrow such as *Castor*. The proximally projecting greater tubercle of pantolestids, including the Uintan pantolestid, suggests more emphasis on digging behavior than in otters. The reduction in size of the lesser tubercle seems to be loosely correlated with aquatic behavior, being larger in *Castor* and *Lutra*, both of which spend time in terrestrial environments, than in *Enhydra*, which rarely moves on land. The further reduction in the size of the lesser tubercle in the Uintan pantolestid in relation to Bridgerian species may suggest a greater reliance on aquatic environments in the Uintan

forms. The sinuous profile of the humerus of YPM-PU 14645 is also consistent with a semi-aquatic way of life.

The robust and medially inflected olecranon process in YPM-PU 14645 suggests that the Uintan pantolestid engaged in digging behavior. Aquatic mammals also have robust olecranon processes, but those of scratch-diggers are generally longer and more robust (Hildebrand, 1985; Rose and Koenigswald, 2005). The flat, narrow radial notch indicates that little supination took place between the proximal radius and ulna, which is characteristic of both swimmers and diggers (Rose and Chinnery, 2004; Rose and Koenigswald, 2005). The prominent extensor ridge on the distal ulna suggests well developed extensors of the wrist, which is also characteristic of digging mammals (Rose et al., 1992).

Overall the morphology of the forelimb of the Uintan pantolestids is consistent with a semi-aquatic and semi-fossorial lifestyle as has been suggested for other North American pantolestid species (Gunnell et al., 2008; Matthew, 1909; Rose and Koenigswald, 2005). The fragmentary nature of the Uintan remains makes a thorough analysis of the differences in locomotion between the younger and older specimens, but there does not appear to be a consistent signal for either more terrestriality, fossoriality or natatoriality. Some features, such as the greater reduction of the lesser tuberosity in CM 80591 may suggest more aquatic behavior than in earlier pantolestids, but the high, robust greater tuberosity and robust, medially-inflected olecranon process suggest that Uintan pantolestids as a whole probably engaged in digging as well.

5.4.2 Hindlimb

Unfortunately the proximal hindlimb of Uintan pantolestids is known only from the fragmentary proximal femur and tibial shaft of YPM-PU 14645, which offer little in the way of functional information. The morphology of these elements is consistent with those elements known from other pantolestids. The sigmoid shape of the tibia in lateral view is consistent with a semi-aquatic lifestyle, and the extensive articular surface for the fibula suggests that the distal tibio-fibular joint was largely immobile. This feature, together with the shape of the tibial shaft, suggests terrestrial or aquatic habits rather than arboreal ones (Rose and Koenigswald, 2005).

Whereas the tarsals of pantolestids are very distinctive in shape, little is known about the functional significance of these distinctive features. The shape of the astragalus of pantolestids most closely resembles that of beavers among extant mammals (Rose and Koenigswald, 2005). The short neck together with the short distal calcaneus suggests that pantolestids were not swift terrestrial runners, and the extensive fibular facet on the calcaneus suggests that the ankle was not flexible, and confined to motion in a parasagittal plane. Overall the tarsal elements are broad, suggesting a broad foot: the astragalar trochlea is wide and shallow, the astragalar head deviates medially, especially in CM 71159, the navicular is wide and shallow, and base of the entocuneiform is wide. This suggests an animal with a hind foot with a considerable surface area, such as that in a swimming mammal used for forward propulsion. The tarsal elements are also proximodistally short relative to their width, suggesting powerful rather than quick movements. The robust metatarsals also suggest a heavy foot. The extensor ridges on the distal ends of the metatarsals serve as a barrier to hyperextension of the proximal

phalanges. Such ridges are often seen on the metacarpals of digging animals, and are also present on the metatarsals of some armadillos but have not otherwise been identified in pantolestids (Rose et al., 1992; Simpson, 1941). The presence of these ridges suggest that the proximal phalanges were often forcefully extended on the metatarsals, which is consistent with bracing the body when digging or propelling the body forward through the water. The shape of the fragmentary phalanx, being flat and somewhat broad, is also consistent with a fossorial or semi-aquatic lifestyle (Hildebrand, 1985; Koenigswald, 1980; Rose and Koenigswald, 2005).

5.5 Diversity of Uintan Pantolestids

There are five species of *Pantolestes* known from the Bridgerian. The smallest species is *P. elegans* for which there are no described postcranial remains (Dorr, 1977; Marsh, 1872; Matthew, 1909). *Pantolestes longicaudus* is the most common Bridgerian taxon, and was named for a several caudal vertebrae found with the holotype and which indicated that the tail was long (Cope, 1872; Matthew, 1909). The first good postcranial remains, including those of *P. longicaudus*, were reported by Matthew (1909), at which time he named the remaining three species of *Pantolestes*: *P. phocipes*, *P. natans* and *P. intermedius*. The dentitions of the largest pantolestids, *P. natans* and *P. phocipes*, are approximately the same size, but the humerus of *P. natans* is significantly larger relative to the dentition than is that of *P. phocipes* (according to the measurements reported in Matthew, 1909). *P. intermedius* was named from postcranial elements alone on the basis that it was intermediate in size between *P. phocipes* and *P. longicaudus* and outside the range of variation of either species. However, the fact that pantolestids were known from only twelve specimens at the time calls into question whether an accurate idea of

interspecies variability was possible. No dental specimens have been assigned to *P. intermedius* to date.

Unfortunately, associated pantolestid dental and postcranial remains are still rare. The available sample of unassociated postcranial remains, especially astragali and calcanei, has increased since the time of Matthew. A plot of astragalar mid-trochlear width and total astragalar length in several Bridgerian specimens from the YPM, AMNH, and the USNM reveals three different sizes of astragali (Figure 5.7). The largest is that of *Pantoletes natans* (AMNH 12521; no astragali of *P. phocipes* are known). The wide separation of *P. natans* from the other pantolestids is due less to astragalar length and more to mid-trochlear width, indicating that the astragalus of *P. natans* is proportionately wider than that of other pantolestids, as is evident when just astragalar length is considered (Figure 5.8). The smallest astragali may represent either *P. elegans* or *P. longicaudus* and those intermediate in size may represent either *P. longicaudus* or *P. intermedius*. Based on the relative abundance of dental remains, it is most probable that the smallest are *P. elegans* and the larger are *P. longicaudus*. No dental specimens have yet been attributed to *P. intermedius*. The largest of these middle-sized pantolestids is 26.6% - 27.7% larger than the smallest in the sample, close to Matthew's (1909) threshold of 30%. This allows the possibility that "*P. intermedius*" may be a large individual of *P. longicaudus*. It is also possible that more than one species is represented in the sample of intermediately-sized pantolestids, but associated dental remains will be necessary to decide whether this is the case. When the astragali from the Uinta Formation (CM 71159) and the Washakie Formation (DMNH 2321) are included in the plot, CM 71159 falls close to the clump of intermediate Bridgerian pantolestids and DMNH 2321

falls between this group and *P. natans* (Figure 5.7). It is closer to *P. natans* in length than in width (Figure 5.8).

A similar pattern is present when the width of the ectal process on the calcaneus is plotted with the width of the calcaneal ectal facet, though there are fewer Bridgerian calcanei known than astragali (Figure 5.9). The Uintan calcaneal specimens occupy much the same position in the calcaneal plot. In this case it appears that the middle size category may be divided into two distinct groups, but more specimens are necessary to determine that this is not simply an artifact of the small sample. These postcranial remains do not reflect the full diversity of pantolestids during the Uintan, as dental remains suggest up to four different species in the Uinta Formation alone during the Uintan.

5.6 Discussion

The lack of complete limb bones of the Uintan pantolestids precludes a metric analysis of limb proportions in relation to possible locomotor behavior. Overall, the most obvious feature of the Uintan pantolestid skeletal elements is their resemblance to those of earlier pantolestids. Where there are differences in morphology, they are subtle, suggesting that the locomotor behavior of pantolestids living during the Uintan was much the same as those in the Bridgerian. As far as can be determined by the fragmentary postcranial remains, pantolestids in the Uintan are no less dependent on an aquatic lifestyle than those in the Bridgerian. Pantolestids have been found in mainly lacustrine sediments of the Green River Formation and Messel, Germany, but this does not suggest that they did not also rely on rivers. The remains are often found in the margins of these lake sediments rather than in the center, suggesting that they relied upon the shore for

food and shelter, which is not surprising (Dorr, 1977; Rose and Koenigswald, 2005). The presence of pantolestid material in the UF suggests that these animals relied on rivers as a source of water rather than lakes. The ancient lakes that were present in the region of northeastern Utah, southwestern Wyoming, and southeastern Colorado during the Bridgerian and early Uintan were virtually dry by the late Uintan, giving rise to a series of rivers and streams (Bradley, 1937; Buchheim et al., 2000; Gazin, 1958). It might be expected that most pantolestid remains come from the relatively wetter Uinta B member of the Uinta Formation than the drier Uinta C member, but this is not the case (Table 5.2). Not only is there no significant difference in the number of pantolestid specimens from the two members, but there is also no considerable difference in the number of localities producing pantolestid remains in the two members.

Based upon the preliminary estimate of four species in the Uinta Formation and at least one more in the Washakie Formation, it appears that there are approximately five species of pantolestid present in the Uintan of North America. This is equivalent to the number of species of *Pantolestes* present in the Bridgerian. Pantolestids are not considered abundant at any time period, and although they may have been just as diverse in the Uintan as the Bridgerian, they were less abundant. The fact that pantolestids are able to maintain diversity despite the change in general ecology from the Bridgerian to the Uintan may be due to several factors. One factor might be adaptive flexibility in pantolestids, but if this were the case we would expect to see significant changes in skeletal morphology. Another explanation is that the types of environments in which pantolestids lived persisted through the Bridgerian into the Uintan, though the decrease in

abundance of pantolestid remains suggests that these environments were perhaps rarer during the Uintan.

5.6.2 Implications for Primate Evolution

Localities from the early and late Uintan of the UF yield both primate and pantolestid remains, suggesting that these two creatures were part of a local faunal community. Reconstructing the behavior of other members of the primate faunal community can give us insight into the role that ancestral primates played in these communities, and enrich our understanding of the paleobiology of fossil primates. The presence of semi-aquatic pantolestids in the late Uintan of the UF suggests that there were major sources of water such as rivers that may have supported gallery forests that served as a last refuge for primates in the increasingly arid late Uintan (Dorr, 1977).

5.7 Summary

The purpose of this chapter was to describe new pantolestid remains from the UF and to attempt to reconstruct the paleobiology of Uintan pantolestids as compared to those from the Wasatchian and Bridgerian. The postcrania of Uintan pantolestids do not differ significantly from those from earlier time periods, suggesting that they were probably semi-aquatic, even into the late Uintan, and probably relied on rivers and streams. These major water sources would have supported gallery forests in which primates survived into the late Uintan.

Table 5.1. List of pantolestid specimens examined for this chapter.

Taxon	Specimen No.	Age	Description
Pantolestes sp.	YPM-PU 14645	Early Uintan	R dentary, P_3-M_3; L dentary M_1-M_3; isolated L P_3 and L P_4; R partial humerus; R scapular glenoid fossa; L prox ulna; L proximal femur; R distal tibia; Vertebrae: C1, 4 thoracics, 3 lumbars, 1 sacral, 3 proximal caudal
Pantolestid indet.	CM 71159	Late Uintan	R astragalus; L distal calcaneus; L navicular
Pantolestid indet.	CM 71160	Late Uintan	L cuboid
Pantolestid indet.	CM 71137	Late Uintan	R distal calcaneus
Pantolestid indet.	CM 71090	Late Uintan	L distal calcaneus; R scapular glenoid; and assoc. fragments
Pantolestid indet.	CM 71001	Early Uintan	R distal calcaneus; assoc phalanges and hindlimb fragments
Pantolestid indet.	CM 71157	Late Uintan	L proximal humeral diaphysis
Pantolestid indet.	CM 71110	Early Uintan	L distal calcaneus
Pantolestid indet.	CM 80591	Late Uintan	L proximal humerus and assoc. fragments
Pantolestid indet.	CM 80784	Late Uintan	L distal ulna and shaft
Pantolestid indet.	DMNH 2321	Early Uintan	R astragalus; R navicular; R entocuneiform; R mesocuneiform; R MT II–IV; and assoc phalanges
Pantolestid indet.	DMNH 29877	Early Uintan	R calcaneus
Pantolestes natans	AMNH 12152	Bridgerian	Skull and jaws; skeletal elements including humerus, femur, tibia, calcaneus, astragalus, navicular
Pantolestes phocipes	AMNH 11547	Bridgerian	R dentary with M_{2-3}, L dentary with P_4–M_3; humerus, carpals, MC II–III
Pantolestes intermedius	AMNH 11619	Bridgerian	R humerus
Pantolestes sp.	AMNH 11620	Bridgerian	L tibia
Pantolestes sp.	YPM 17212 a	Bridgerian	L calcaneus
Pantolestes sp.	YPM 17212 b	Bridgerian	R calcaneus

Table 5.1 cont.

Pantolestes sp.	YPM 43230	Bridgerian	R astragalus
Pantolestes sp.	YPM 43229	Bridgerian	L astragalus
Pantolestes sp	YPM 43236	Bridgerian	R astragalus
Pantolestes sp.	YPM 43238	Bridgerian	L astragalus
Pantolestes sp.	YPM 43239	Bridgerian	R astragalus
Pantolestes sp.	YPM 43234	Bridgerian	R astragalus
Pantolestes sp.	YPM 43241	Bridgerian	L astragalus
Pantolestes sp.	YPM 43242	Bridgerian	R astragalus
Pantolestes sp.	YPM 43244	Bridgerian	L astragalus
Pantolestes sp.	YPM 43243	Bridgerian	R astragalus

Table 5.2. Abundance of UF pantolestids by member and faunal assemblage zone (FAZ). All the localities within member B yielding pantolestid remains fall within the early Uintan, and all of those within member C fall within the late Uintan. FAZ 1 represents faunal communities living within the earliest and wettest period of the Uintan represented within the UF. FAZ 2 is slightly later and more arid, and FAZ 3 represents the late Uintan and the most arid period represented within the UF. Although Uintan pantolestids appear to have been aquatic, they are not more abundant in the earlier, wetter periods than they are in the later, arid periods.

Member	FAZ*	No. localities with pantolestid remains	No. specimens
B	1	1	3
	2	6	7
C	3	6	9

* from Townsend, 2004

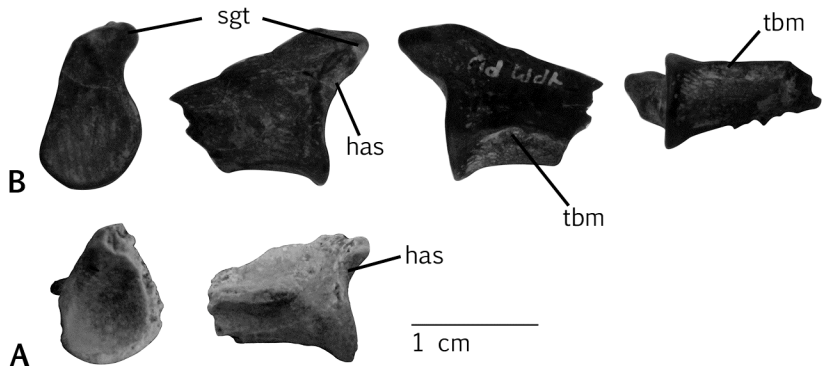

Figure 5.1. Glenoid fossa of two Uintan pantolestids: **A**, CM 71090; **B**, YPM-PU 14645. **has**, articular surface for the humerus; **sgt**, supraglenoid tubercle; **tbm**, pit for the triceps brachii. muscle.

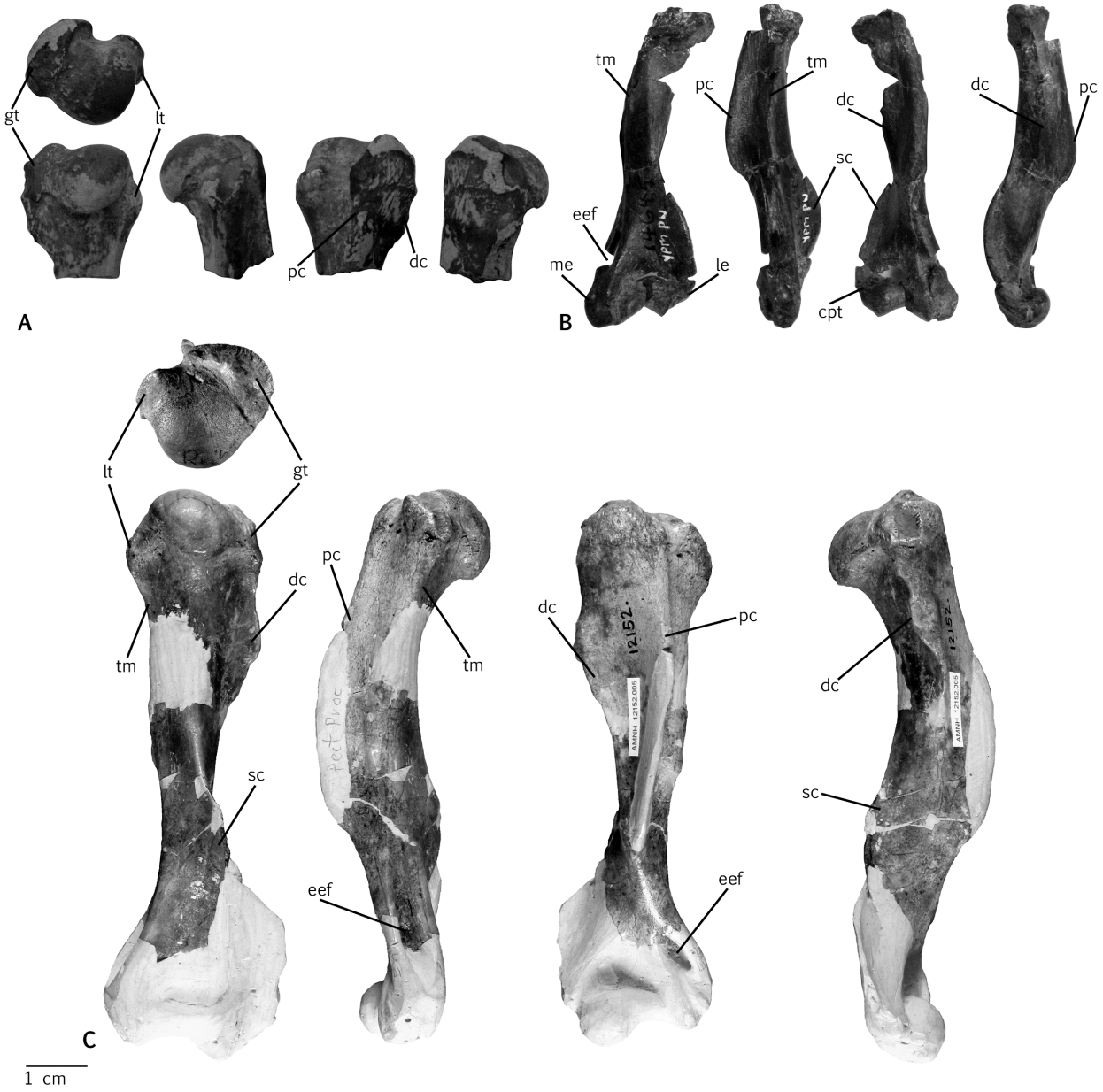
gt
lt
pc
dc
A
tm
eef
me
le
B
pc
tm
dc
sc
cpt
dc
pc
lt
gt
dc
tm
sc
C
pc
tm
eef
dc
pc
eef
dc
sc
1 cm

Figure 5.2. Humerus of Uintan and Bridgerian pantolestids. **A**, CM 80591 in proximal (top), dorsal, medial, ventral and lateral views (left to right). **B**, YPM-PU 14645 in dorsal, medial, ventral and lateral views (left to right). **C**, AMNH 12152 *Pantolestes natans* in proximal (top), dorsal, medial, ventral and lateral views (left to right). White areas are reconstructed. **cpt**, capitular tail; **dc**, deltoid crest; **eef**, entepicondylar foramen; **gt**, greater tuberosity; **le**, lateral epicondyle; **lt**, lesser tuberosity; **me**, medial epicondyle; **pc**, pectoral crest; **sc**, supinator crest; **tm**, teres major attachment site.

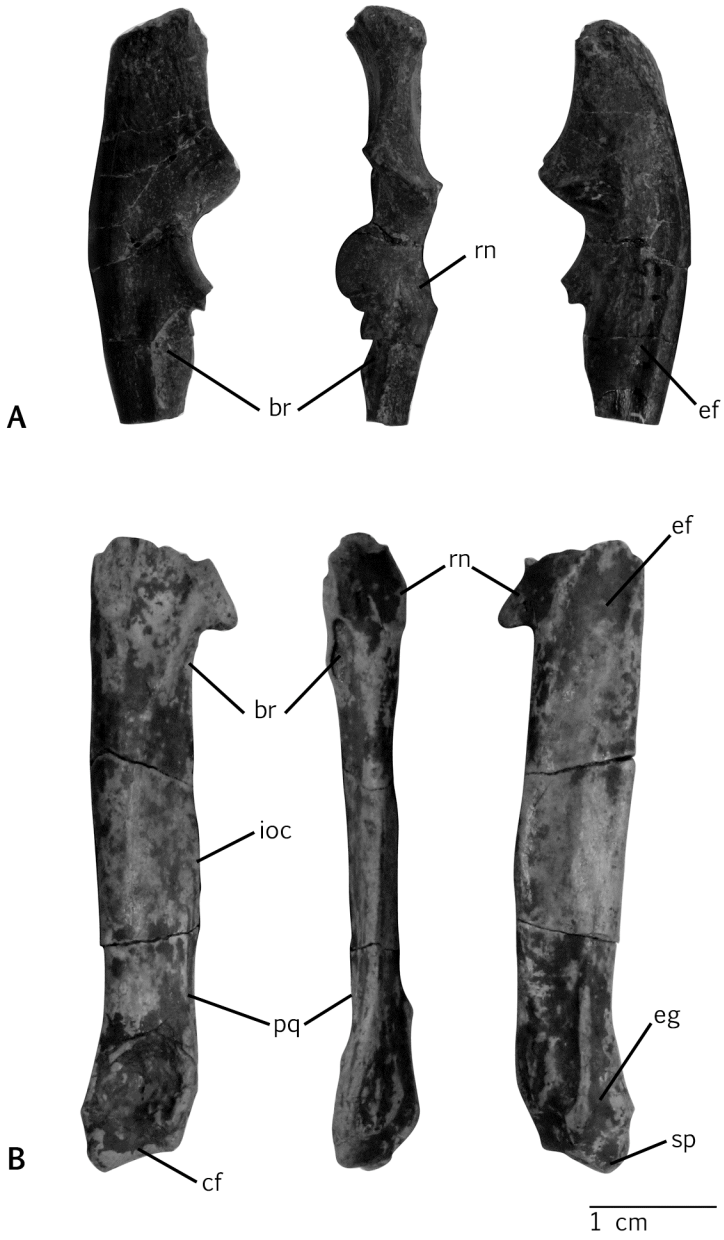

Figure 5.3. Ulna of Uintan pantolestids. **A**, YPM-PU 14645 in (right to left) medial, anterior and lateral views. **B**, CM 80784 in (right to left) medial, anterior and lateral views. **br**, pit for attachment of the brachialis muscle; **cf**, facet for articulation with the carpals; **ef**, extensor fossa; **eg**, groove for the tendon of the extensor carpi ulnaris muscle; **ioc**, interosseus crest; **pq**, pronator quadratus; **rn**, radial notch; **sp**, styloid process.

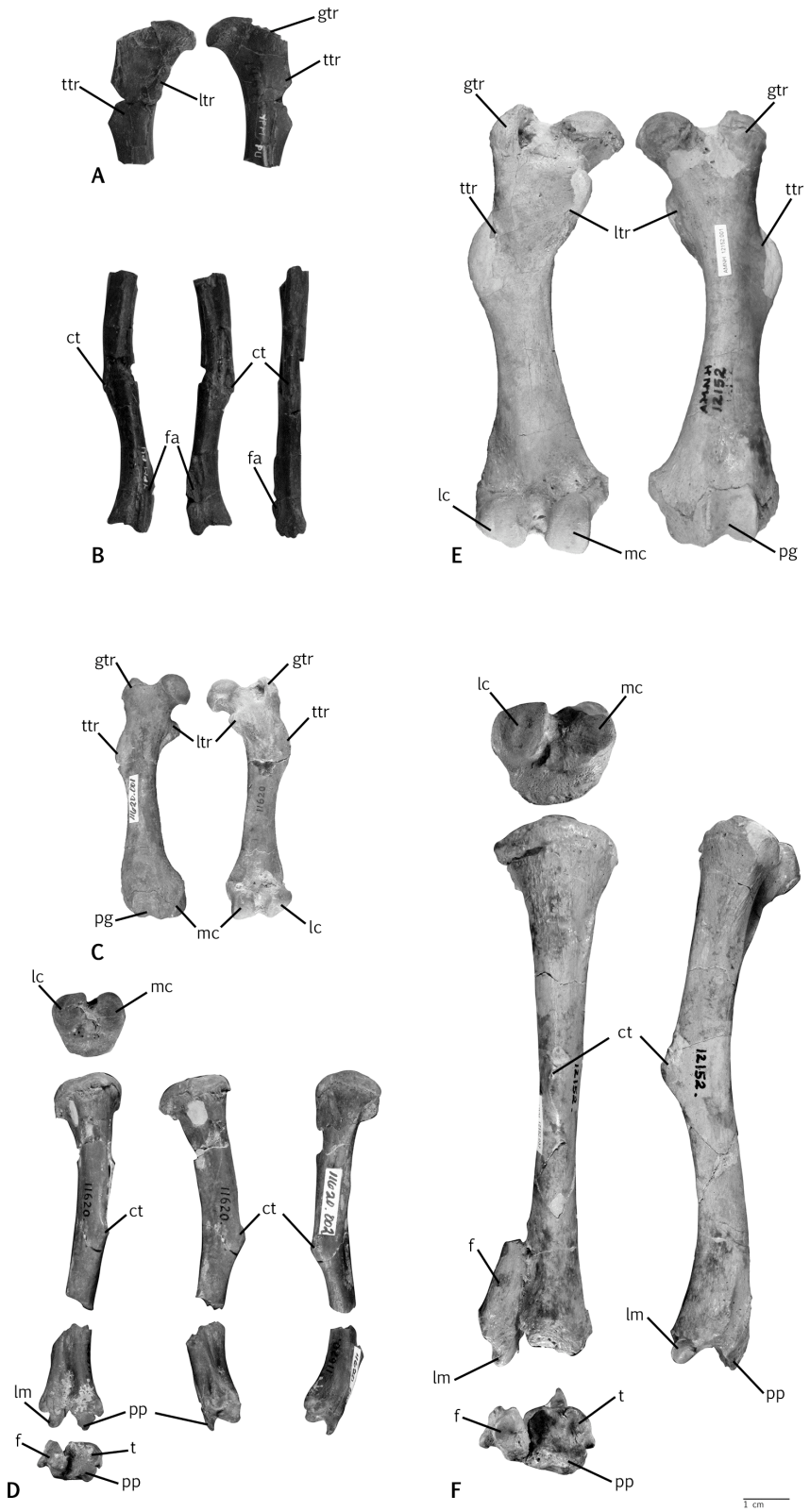
gtr
ttr
ttr
ltr
A
ct
ct
fa
fa
B
gtr
gtr
ttr
ttr
ltr
lc
mc
pg
E
gtr
gtr
ttr
ttr
ltr
pg
mc
lc
C
lc
mc
ct
ct
lm
pp
f
t
pp
D
lc
mc
ct
f
lm
lm
pp
f
t
pp
F
1 cm

Figure 5.4. Femur and tibia of Uintan and Bridgerian pantolestids. **A**, YPM-PU 14645 proximal femur in posterior (left) and anterior (right) views. **B**, YPM=PU 14645 tibia in (left to right) medial, lateral and anterior views. **C**, AMNH 11620 femur in anterior (left) and posterior (right) views. **D**, AMNH 11620 tibia in proximal (top left), anterior (middle left) and distal (bottom left), lateral (middle) and medial (right) views. **E**. AMNH 12152 *Pantolestes natans* femur in posterior (left) and anterior (right) views. **F**. AMNH 12152 *Pantolestes natans* tibia in proximal (top left), anterior (middle left) and distal (bottom left), and medial (right) views. **ct**, cnemial tuberosity; **f**, fibula; **fa**, site for articulation with the fibula; **gtr**, greater trochanter; **lc**, lateral condyle; **lm**, lateral malleolus; **ltr**, lesser trochanter; **mc**, medial condyle; **pg**, patellar groove; **pp**, posterior process of the tibia; **t**, tibia; **ttr**, third trochanter.

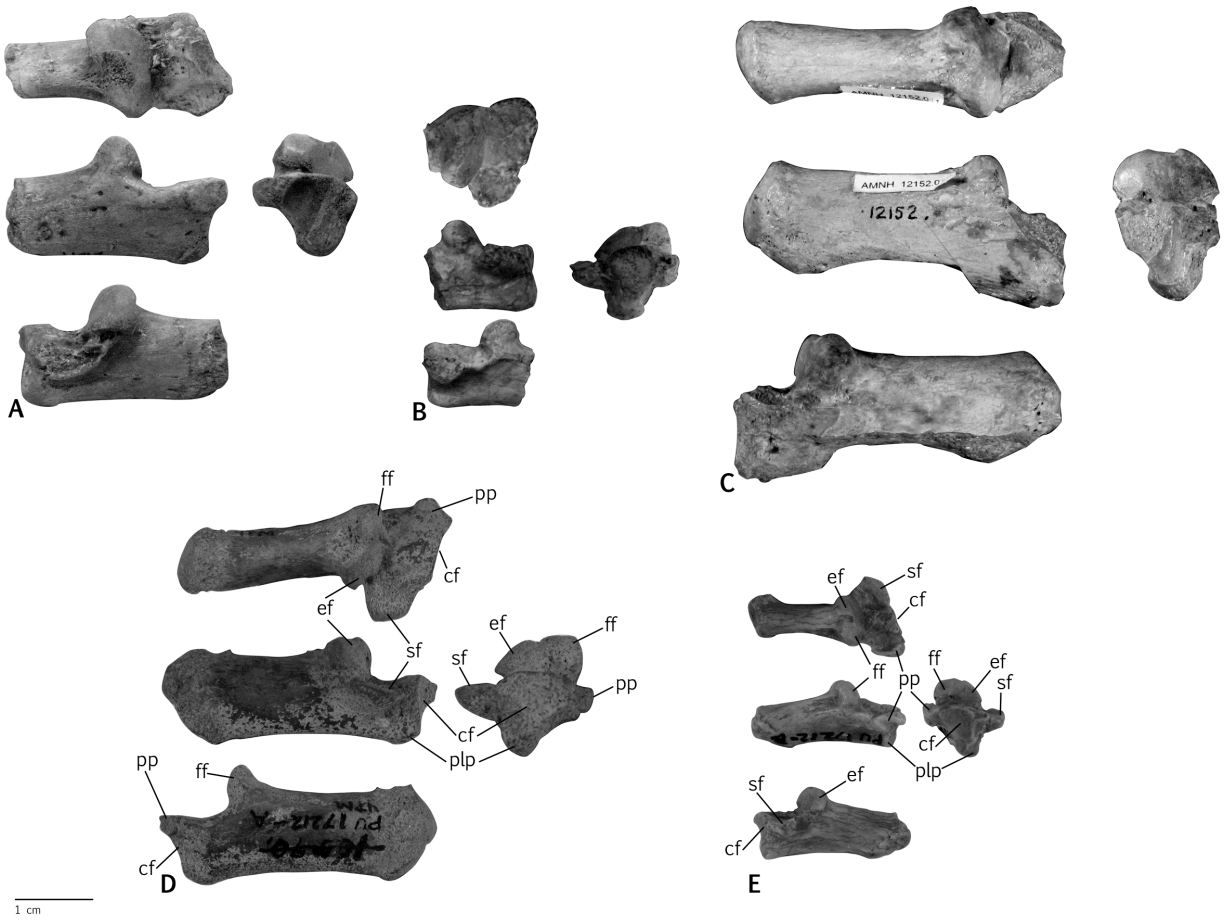

Figure 5.5. Calcanei of Uintan and Bridgerian pantolestids. **A**, DMNH 29877 R calcaneus in dorsal (top), lateral (middle), medial (bottom) and distal (right) views. **B**, CM 71159 L calcaneus in dorsal (top), medial (middle), lateral (bottom) and distal (right) views. **C**, AMNH 12152 *Pantolestes natans* R calcaneus in dorsal (top), lateral (middle), medial (bottom) and distal (right) views. **D**, YPM-PU 17212 a L calcaneus in dorsal (top), medial (middle), lateral (bottom) and distal (right) views. **E**, YPM-PU 17212 b R calcaneus in dorsal (top), lateral (middle), medial (bottom) and distal (right) views. **cf**, cuboid facet; **ef**, ectal facet; **ff**, fibular facet; **pp**, peroneal process; **plp**, plantar process; **sf**, sustentacular facet.

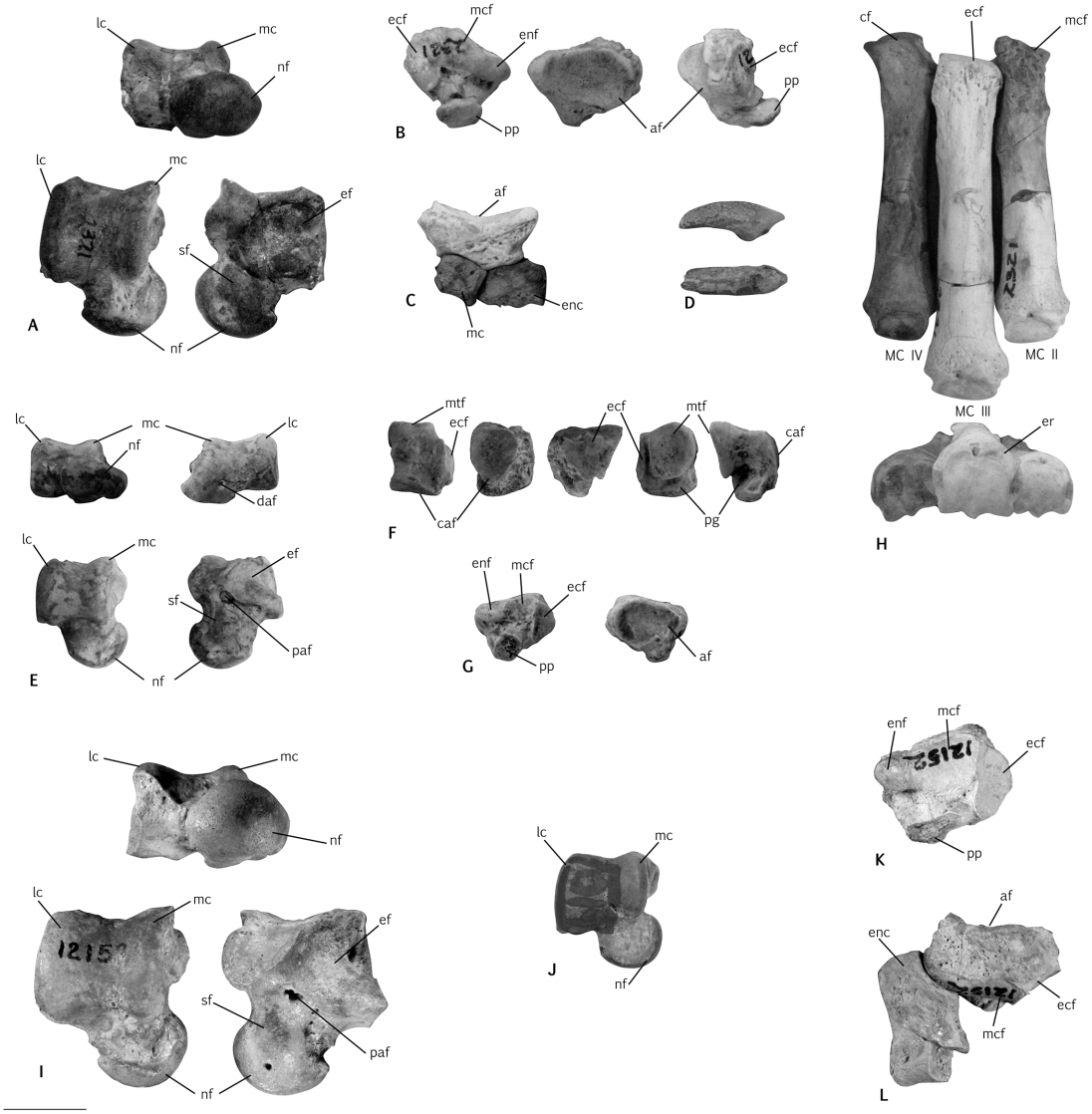
lc
mc
nf
A
sf
ef
paf
daf
B
ecf
mcf
enf
pp
af
C
enc
D
E
F
mtf
caf
pg
G
H
cf
MC IV
MC II
MC III
er
I
J
K
L

Figure 5.6. Tarsal, metatarsal and pedal elements of Uintan and Bridgerian pantolestids. **A**, DMNH 2321 R astragalus in distal (top), dorsal (bottom left) and plantar (bottom right) views. **B**, DMNH 2321 R navicular in distal (left), proximal (middle), and lateral (right) views. **C**, DMNH 2321 R navicular, mesocuneiform and entocuneiform fragment in dorsal view. **D**, DMNH 2321 ungual phalanx in lateral (top) and ventral (bottom) views. **E**, CM 71159 R astragalus in distal (top left), posterior (top right), dorsal (bottom left) and plantar (bottom right) views. **F**, CM 71160 L cuboid in (left to right) dorsal, proximal, medial, distal and lateral views. **G**, CM 71159 L navicular in distal (left) and proximal (right) views. **H**, DMNH 2321 R metatarsals II, III, and IV in dorsal view (top) and distal view (bottom). **I**, AMNH 12152 *Pantolestes natans* R astragalus in distal (top left), posterior (top right), dorsal (bottom left) and plantar (bottom right) views. **J**, YPM-PU 43230 pantolestid R astragalus in dorsal view. **K**, AMNH 12152 *Pantolestes natans* L navicular in distal view. **L**, AMNH 12152 *Pantolestes natans* L navicular and entocuneiform in dorsal view. **af**, astragalar facet; **cf**, cuboid facet; **caf**, calcaneal facet; **daf**, dorsal astragalar foramen; **ef**, ectal facet; **er**, extensor ridge; **ecf**, ectocuneiform facet; **enc**, entocuneiform; **enf**, entocuneiform facet; **lc**, lateral condyle; **mc**, medial condyle; **mcf**, mesocuneiform facet; **mtf**, metatarsal facet; **nf**, navicular facet; **pg**, peroneal groove; **pp**, plantar process; **paf**; plantar astragalar foramen; **sf**, sustentacular facet.

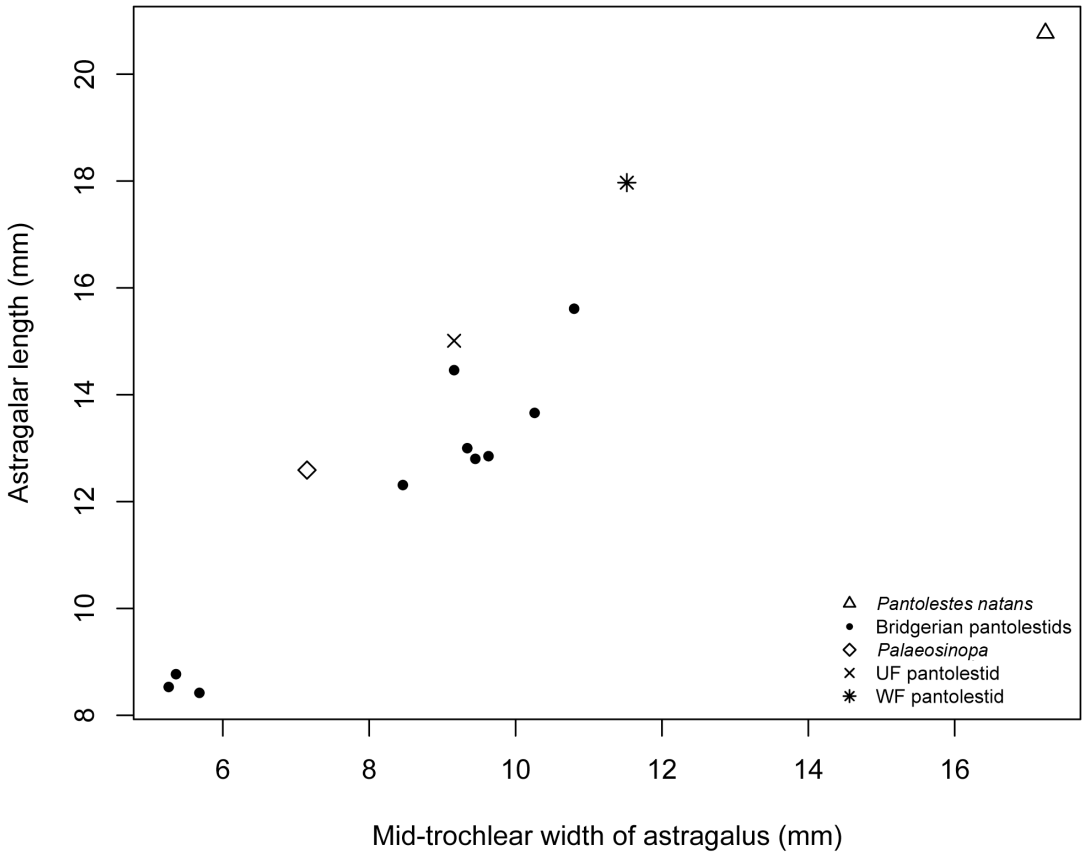

Figure 5.7. Plot of astragalar dimensions of Eocene pantolestids. Note the three size groups and the position of the UF and WF pantolestids compared to Bridgerian pantolestids and *Pantolestes natans*.

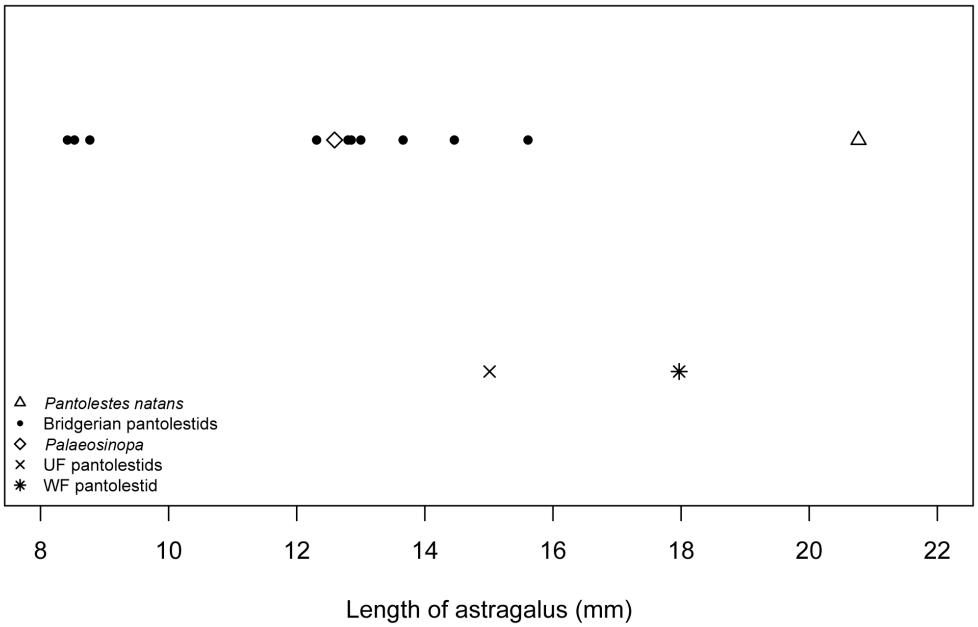

Figure 5.8. Plot of astragalar length of Eocene pantolestids. Note again the three size groups of Bridgerian pantolestids. The UF pantolestid falls towards the upper size range of the Bridgerian pantolestids and the WF pantolestid falls in between that group and the largest pantolestid, *Pantolestes natans*.

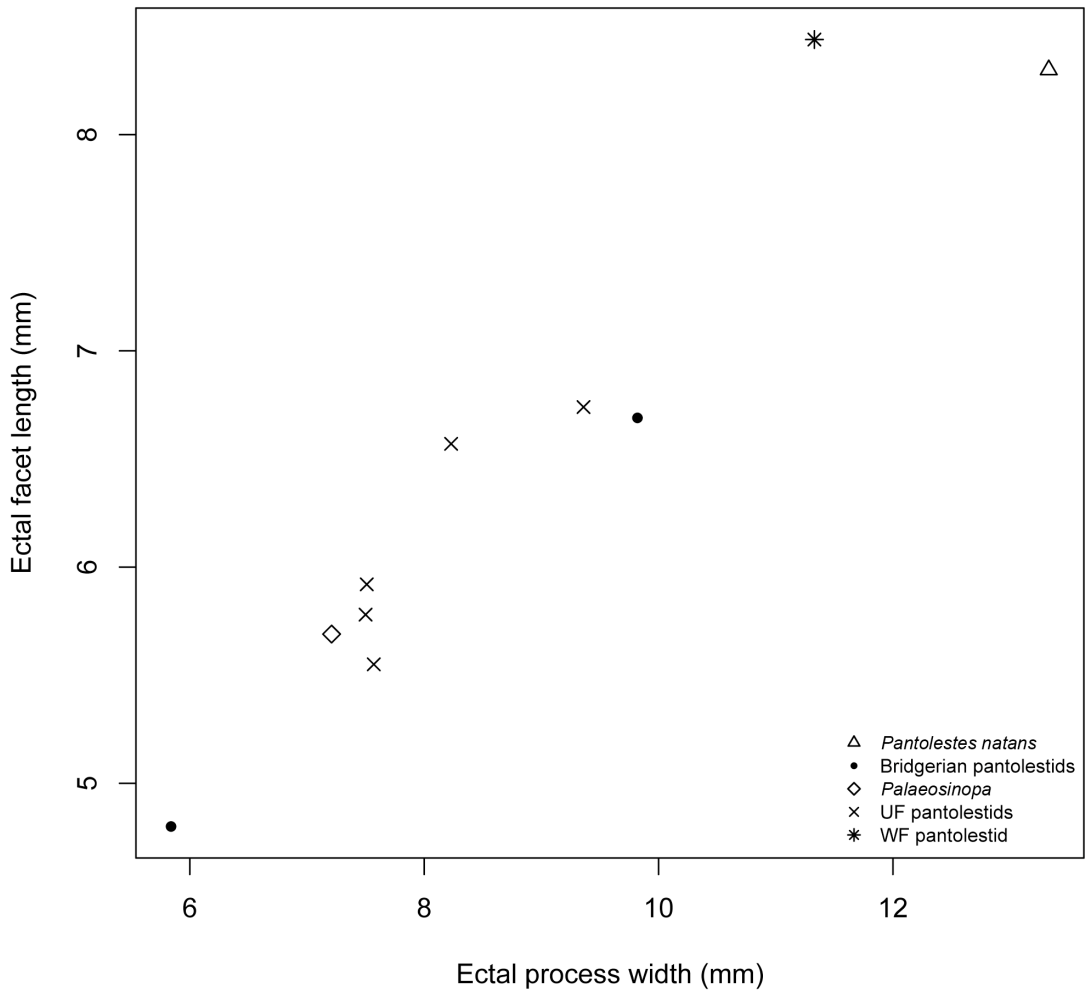

Figure 5.9. Plot of calcaneal dimensions of Eocene pantolestids. The pattern of size ranges is similar to that when the astragali are plotted. Note that the WF pantolestid is closer to *Pantolestes natans* in calcaneal morphology than in astragalar morphology.

CHAPTER SIX

Ecomorphology of Habitat Change in Extant Mammals

6.1 Introduction

Ecomorphology is based upon the assumption that morphology must be related to the local habitat if an organism is to effectively exploit its environment (Bock, 1990; Bock and Wahlert, 1965; DeGusta and Vrba, 2003; Losos and Miles, 1994; Van Valkenburgh, 1994; Wainright and Reilly, 1994). Paleontologists commonly use ecomorphological techniques in two major ways: to reconstruct past habitats and to trace morphological changes through time in an ecological context. By far the most common ecomorphological method employed in reconstructing Paleogene environments is ecological diversity analysis (EDA) in which the ecological profile of the community as a whole is used to infer habitat type (Gagnon, 1997; Gunnell et al., 1995; Reed, 1998; Townsend, 2004). This technique is useful for reconstructing habitat types because it takes into account the dietary and locomotor adaptations of as many members of the community as possible regardless of taxonomic affinity; these analyses are often called "taxon-free." Ecological diversity analysis is not useful for tracking changes in adaptations within evolutionary lineages, which is the goal of this project, because it depends on all members of the community (Van Valkenburgh, 1994).

An ecomorphological method that has been widely used in the reconstruction of Neogene, and particularly Plio-Pleistocene, habitats concerns the analysis of single elements that are numerous at a certain locality such as bovid astragali and phalanges, bovid femora, cercopithecoid distal femora, distal and proximal humeri, and proximal

ulnae and suid limb and ankle bones (Bishop, 1994; DeGusta and Vrba, 2003; Elton, 2001; Kappelman, 1988; Kappelman et al., 1997). In contrast to EDA, this element-specific method focuses on identifying morphological features that can be used to discriminate between different habitat categories that are utilized by members of ecologically diverse groups. Once these features are identified in extant animals, they can be applied to isolated fossil elements and used to estimate the habitat in which those animals most probably lived (DeGusta and Vrba, 2003, 2005a,b; Kappelman, 1988; Kappelman et al., 1997; Van Valkenburgh, 1994).

Similar techniques that combine elements of both EDA and the element-specific method are used to trace the evolution of "guilds" through time. (Kay et al., 1999; Van Valkenburgh, 1999; Wesley-Hunt, 2005). In some ways, this technique resembles stratophenetics (Bown and Rose, 1987; Gingerich, 1979). Stratophenetics has been used primarily in the construction of phylogenies, but Gingerich (1979: 42) recognized that phylogeny represents the evolutionary history of a lineage, which "… traces both genealogical relationships *and adaptations* through time [italics added]." Using this approach, researchers have shown that hypercarnivorous mammals (whose diets consist almost entirely of vertebrate flesh, and inferred from dental morphology) have been present in North America since the middle Eocene, but the taxonomic configuration of this ecological profile differs depending on the time period (Van Valkenburgh, 1999; Wesley-Hunt, 2005). In another example, the increasing hypsodonty, selenodonty and lophodonty of "ungulates" (including artiodactyls, perissodactyls and other archaic ungulate groups) have been shown to correlate with an increase in prevalence of grasslands (Jernvall et al., 1996, 2000; Jacobs et al., 1999; Kay et al., 1999). In the latter

example, it is important to note that the focus is on identifying trends that can be mapped through time. There is no single degree of hypsodonty that is characteristic of any one type of open habitat; one cannot determine the percent of grass cover based upon a specific hypsodonty index. However, there is a robust correlation of hypsodonty index with consumption of grass, such that one animal with a higher hypsodonty index probably consumed more grass and lived in a more open environment than one with a lower index.

Both habitat reconstruction and the tracing of ecological patterns through time rely on identifying features that correlate with habitat type, but how these features are interpreted differs. In this project, my ultimate goal is not to predict habitat type from postcranial morphology, but to evaluate whether or not changes in habitat are reflected in changes in the postcranial morphology of a faunal group through time, as described in the hypsodonty example above. For example: whereas studies focused on habitat prediction may hypothetically seek to be able to pick up an isolated element and diagnose the habitat in which its owner lived, the object of this study would be to be able to pick up two elements and evaluate if one came from an animal living in more open habitats than the other. The current study focuses on evolutionary divergences in morphology and cannot make any claims about habitat based on one element in isolation.

Previous ecomorphological studies using the element-specific method have mainly involved Plio-Pleistocene taxa, most of which can be placed reliably within modern taxonomic groups. Kappelman et al. (1997), for example could identify all postcranial remains at least to the level of an extant tribe within the family Bovidae. Because modern and fossil taxa in these analyses are closely related, the morphology of

the fossil taxa fits well within the morphological distribution of their extant relatives. This allows them to be reliably classified based on a knowledge of modern morphology (DeGusta and Vrba, 2003; Kappelman, 1988; Kappelman et al., 1997; Reed, 1998). The older the fossil sample, the more error is associated with uniformitarian assumptions (Gagnon, 1997; Townsend, 2004; Van Valkenburgh, 1994). Most Eocene artiodactyls, for example, belong to extinct families that are only distantly related to modern groups (Janis et al., 1998; Lander, 1998; Martinez and Sudre, 1995; Prothero, 1998a, b; Stucky, 1998). Eocene artiodactyls, as a whole, retain many primitive characteristics compared to modern ones and so, in a character-based analysis, they tend to group with more "primitive"-looking modern taxa (such as tragulids) or entirely outside of the distribution of modern taxa rather than with taxa that share a habitat preference (Martinez and Sudre, 1995; Rose, 1985). Ecomorphological analysis is compromised under such conditions.

One can circumvent the complications associated with clade-specific uniformitarianism by identifying features that correlate with habitat preference across a broad range of modern taxa and analyzing those features in the fossils. If certain features can be seen to differ in a consistent way in correlation with differences in habitat across a wide range of taxa, one can assume that these features responded similarly in the past. This assumption is strengthened if these features have a functional explanation (Van Valkenburgh, 1994). This is commonly done in traditionally descriptive paleontology when interpreting individual fossils, but it has not been applied to the ecomorphology of isolated postcranial elements.

In this chapter, I identify quantitative features of the astragalus and distal humerus that can be used to distinguish mammals that inhabit open habitats from those that inhabit

closed habitats across a wide range of orders. Once I identify these features, they allow interpretation of fossil mammals for which there are no living analogs or close relatives. In the next chapter I apply these metrics to a sample of fossil artiodactyls from the Uinta Formation in Utah to interpret potential morphological responses to habitat change that occurred there during the middle Eocene.

6.2 Data

6.2.1 Pairwise Comparisons

The difficulty in comparing traits across disparate mammalian taxa such as those that are included in my sample is that for any given trait, taxa that are more closely related will tend to resemble each other more than those that are more distantly related regardless of shared habitats or behaviors (Felsenstein, 1985; Maddison, 2000; Møller and Birkhead, 1992). In general, similarities between any two taxa will either be due to a close phylogenetic relationship or to convergent evolution and it is the job of the comparative method to differentiate between them. If two taxa share a more recent common ancestor to the exclusion of the rest of the taxa in a given sample, any similarities should be attributed to their common ancestry; any differences cannot be due to that shared ancestor and must be due to something else (Felsenstein, 1985; Møller and Birkhead, 1992). The method of pairwise comparisons involves examining pairs of closely related taxa for association between two uncorrelated variables and is frequently used in comparative biology (Ackerly, 2000; Maddison, 2000; Martins, 2000; Møller and Birkhead, 1992; Orzack and Sober, 2001). This method is particularly appropriate for identifying associations across a large number of higher level taxa or in taxa for which phylogeny is poorly known (Ackerly, 2000; Møller and Birkhead, 1992). Using this

method, a study concerning morphological correlates of swimming might compare a whale to a warthog, a seal to a wolf and a sea turtle to a tortoise (Figure 6.1). These comparisons are independent of phylogeny in that evolutionary changes related to the adoption of life in the water must have occurred between each pair independently (Burt, 1989; Maddison, 2000; Orzack and Sober, 2001). Using this method one might find that animals adapted for swimming consistently differ from terrestrial animals in having longer phalanges, or shorter limbs relative to body length.

The sample of extant taxa was specifically structured to answer the question "do features of the astragalus and distal humerus differ consistently between animals inhabiting open habitats and those inhabiting closed habitats?" Species were selected in pairs of sister taxa; one taxon of each pair inhabited open habitats and the other inhabited closed habitats. The phylogeny I used is a composite based upon several sources (cited in Figure 6.2). The determination of habitat preference for each taxon was based upon accounts in the literature as well as other ecomorphological studies and are cited in Table 6.1.

6.2.2 Selection of Taxa

Previous ecomorphological studies have noted that limb joint morphology of open-country taxa differs from that of closed-country taxa in being more stable, restricting movement to a parasagittal plane, whereas that of closed-country taxa is less restricted, allowing more medio-lateral mobility (Bishop, 1994; DeGusta and Vrba, 2003; Kappelman, 1988; Kappelman et al., 1997). This indicates that the differences between open and closed-country taxa are essentially similar to the differences between cursorial and ambulatory, and between terrestrial and arboreal mammals, but on a more

subtle scale (Andersson, 2004; Heinrich and Rose, 1997; Jenkins and Camazine, 1977; Kappelman, 1988; Van Valkenburgh, 1987).

Few mammalian groups contain the ideal pair configuration for my comparisons: taxa that employ the same form of locomotion with one occupying open and one occupying closed habitats. When possible, I constructed pairs based upon the above criteria. To expand my sample, I used pairs of terrestrial vs. arboreal taxa, or ambulatory vs. cursorial taxa with arboreal/ambulatory taxa representing the mobile joint configuration of closed-country taxa and terrestrial/cursorial taxa representing the more stable joint configuration of open-country taxa. This allowed me to include 25 pairs of taxa from eight orders in the analysis (Table 6.1, Figure 6.2): Hyracoidea, Scandentia, Lagomorpha, Xenarthra, Perissodactyla, Artiodactyla, Carnivora and Primates. Previous studies reveal that Artiodactyla, Carnivora and Primates show morphological differentiation in the postcrania in correlation with postural, behavioral or habitat differences (Andersson, 2004; Carrano, 1997; DeGusta and Vrba, 2003; Elton, 2001; Kappelman, 1988; Kappelman et al., 1997; Rose, 1993; Van Valkenburgh, 1987). I used many of the metrics and methods of these previous researchers. The other mammalian orders were included to investigate the possibility that the morphological patterns seen in primates, carnivores and artiodactyls may be more broadly applicable to other members of the class.

The assumption that the difference in morphology between open/closed-country taxa is equivalent to the difference in morphology between cursorial/ambulatory and terrestrial/arboreal taxa can potentially confound my results. Essentially, I am testing for more stable vs. more mobile joint shape, not necessarily open vs. closed-country. This is

a conservative assumption in that if I am incorrect in assuming parallel differences between these categories it will be detrimental to my analysis, rather than producing a spurious association.

At least one and up to nine pairs per order were included. Following the methods of Carrano (1997) one specimen from each species was measured to eliminate bias that may be caused by common species being more numerous in the analysis. The resulting data set consisted of 51 species, 26 representing open habitats and 25 representing closed. The number of taxa is unequal because in one case (Hominidae) I used separate comparative taxa for measurement of the astragalus (*Pan* vs. *Homo*) and humerus (*Pan* vs. *Gorilla*). Artiodactyls and carnivores are more diverse than the other orders included in the data set and thus form a majority of the pairs (9 artiodactyl pairs, 6 carnivore pairs). Trends within these two groups therefore could drive the analysis. However, because these two orders are distantly related, any shared trends would be helpful rather than harmful to my analysis. A qualitative assessment of phylogenic trends is presented at the end of the analysis.

6.2.3 Metrics

I used standard length and width measurements of the joint surfaces as well as measurements that have been shown to distinguish between habitat types, locomotor patterns and postural categories in previous studies (Figure 6.3 and 6.4; Table 6.2; Andersson, 2004; Bishop, 1994; Carrano, 1997; DeGusta and Vrba, 2003; Elissamburu and Vizcaíno, 2004; Rose, 1988; Van Valkenburgh, 1987, 1988). The measurements were taken with Mitutoyo digimatic digital calipers and from digital photographs using Adobe Photoshop CS3 Extended. I calculated ratios based on these previous studies and

on biomechanical principles (Table 6.2).

6.3 Methods

6.3.1 Standardization

I divided each measurement by the geometric mean (GM) of all measurements for each specimen to standardize them for body size. The GM is widely used in morphometric studies as a way to account for body size while preserving shape information often removed by residuals (Jungers et al., 1995; Richtsmeier et al., 2002). The use of residuals as a control for size is often recommended over the use of ratios on the grounds that ratios are often negatively correlated with the denominator, and so do not "correct for" size (Jungers et al., 1995). However, residuals have some unattractive properties. The regression line from which residuals are taken varies depending on the sample and is strongly affected by outliers. One consequence of this latter point is that the largest and smallest individuals in a sample appear to be more similar in shape than they actually are (Jungers et al., 1995). The notion that measurements should be uncorrelated with size to identify shape differences has been called into question by several researchers. Oxnard (1978: 233) notes that shape and size are intimately related and that correlation of some shapes with size does not necessarily mean that these shapes "*are* size." It is also noted that completely removing the effect of size also removes critical information about shape (Jungers et al., 1995).

Ratios using the GM (Mosimann and Malley, 1979) have been shown to identify isometric individuals in an experimental sample, whereas residuals did not. This suggests that the ratios do a better job of correctly translating shape into metrics than residuals, and are therefore more desirable for studying shape. Another attractive property of GM

is that it is a function of the individual specimen and is unaffected by other points in the analysis (Jungers et al., 1995).

6.3.2 Sign Test

I analyzed standardized measurements (the measurement divided by the geometric mean) and ratios made from raw measurements in pairs of open-country taxa (OCT) and closed country-taxa (CCT). The sign test is a nonparametric paired-comparisons test that is performed on the differences between two sets of data. This test does not take the magnitude of the difference into account, but instead counts the number of negative differences versus the number of positive differences. The null hypothesis is that there are equal numbers of negative and positive differences in the population, as would be expected if there were no actual or patterned difference between the two samples (Burt, 1989; Sokal and Rohlf, 1995). The sample should follow a binomial distribution with equal probability of getting either a positive or negative difference in any comparison.

The sign test is commonly used in pairwise-comparison methods to identify associations between two variables and has been shown to yield robust and conservative results (Ackerly, 2000; Burt, 1989; Maddison, 2000). Compared to methods such as phylogenetic independent contrasts (PIC), which incorporate data from internal as well as tip nodes, it has several advantages: it does not require knowledge of branch lengths or assumptions about models of evolution and requires less phylogenetic information. However, the necessity that the comparisons must be phylogenetically independent generally leads to small sample sizes and low power (Ackerly, 2000; Burt, 1989; Maddison, 2000; Orzack and Sober, 2001). The combination of the low power and

conservative nature of the sign test makes significant associations somewhat difficult to detect. Once an association is found to be significant with this method, it is can be interpreted as representing a true relationship with high confidence (Ackerly, 2000).

In this analysis, sample group 1 consists of OCT from each taxonomic group and group 2 consists of CCT. A positive difference (+) indicates that OCT have a higher value than CCT for a given measurement and a negative difference (−) indicates that CCT have a higher value than OCT for a given measurement. A set of hypotheses was tested within each analysis using various measurements. A total of 19 standardized measurements and ratios were used to test a priori hypotheses based upon biomechanical principles and previous studies. These were evaluated using a one-tailed p-value. To test for other associated measurements for which there was no a priori hypothesis, a variety of other ratios and standardized measurements were examined for a posteriori interpretation using a two-tailed p-value.

The null hypothesis for all tests is that there is no morphological difference between OCT and CCT. If this is the case, there should be an equal number of positive and negative differences, signifying that they are equally clustered around zero. If either positive or negative differences are significantly more abundant than the alternative, the null hypothesis is rejected in favor of the alternative hypothesis. The alternative hypothesis is dependent on the measurement in question. Summaries of the measurements, hypotheses and results of the sign tests are given in Tables 6.3 and 6.4. The measurements discussed here refer to those in Table 6.2.

6.3.3 Mann-Whitney U

Once significant relationships were identified with the sign test, I performed one-

tailed paired-sample Mann-Whitney U tests for differences in medians between OCT and CCT on the entire data set and unpaired tests on pooled artiodactyls. The alternative hypotheses for each set of tests was based upon the results of the sign test, such that if the sign test showed that open taxa have larger values for the variable in question, the alternative hypothesis for the Mann-Whitney test is that the difference in the medians is positive. Likewise if the sign test showed that open taxa have smaller values for the variable, the alternative hypothesis for the Mann-Whitney is that the difference in the medians is negative.

6.3.4 Hypotheses

Standardized measurements and ratios that are discussed by name in this chapter are listed in Table 6.3.

Astragalus.—OCT are larger in body mass than CCT.

If OCT are larger, then the geometric mean of all astragalar measurements (AGM) for OCT will be consistently larger than the AGM for CCT.

The ankle joints of OCT are more restricted to movement in a parasagittal plane than those of CCT, which are more mobile.

This hypothesis is based on the biomechanical assertion that the ankle joints of more cursorial taxa are restricted to parasagittal movements and minimize medio-lateral movements. If the ankles of OCT are more restricted, then the relative minimum trochlear diameter (A3/AGM) and the relative trochlear width (A13/GM) should be consistently smaller in OCT than in CCT; and the relative astragalar trochlear depth ([A14+A15]/AGM) and astragalar trochlear ratio ([A14+A15]/A13) should be

consistently larger in OCT than in CCT.

The navicular facets of OCT are dorso-plantarly deeper than those of CCT.

It has frequently been observed that the navicular facet of terrestrial taxa is deeper than that of arboreal taxa (Heinrich and Rose, 1997). This is due to an emphasis on parasagittal excursion of the navicular on the astragalar head in terrestrial taxa versus a more medio-lateral excursion in arboreal taxa. If this is the case, the relative navicular facet depth (A10/AGM) should be greater in OCT than in CCT.

The navicular facets of CCT are wider (medio-laterally) relative to the dorso-ventral height than those of OCT.

This is based on the observation that increased medio-lateral width is associated with greater transverse mobility of the ankle. If this is the case, the navicular facet ratio will be higher (A5/A10) in CCT than in OCT.

The medial length of the astragalus is shorter than the lateral length in open-country artiodactyls than in closed-country artiodactyls.

DeGusta and Vrba (2003) found this to be the case, but they did not give a functional explanation. If this is the case, the medial astragalar ratio (A1/A7) will be greater than one in OCT and approximately equal to one in CCT. This hypothesis is testable only in artiodactyls (N = 9).

The medial condyle is shorter (proximo-distally) relative to the length of the lateral

condyle in CCT, and the astragalar condyles are more equal in length (proximo-distally) in OCT.

This hypothesis is based on previous studies that found that the condyles were asymmetrical in extant plantigrade taxa (Carrano, 1997) and on observations from fossil taxa (Dunn and Rasmussen, 2009; Dunn et al., 2006; Heinrich and Rose, 1997). If this is true, the condylar ratio (A2/A4) will be approximately equal to one in OCT and less than one in CCT.

Humerus.—OCT are larger in body mass than CCT.

If OCT are larger, the geometric mean of all humeral measurements (HGM) for OCT will be consistently larger than the AGM for CCT.

The distal humeri of CCT are wider (medio-laterally) than those of OCT.

This hypothesis is based on the observation that the main flexor and extensor muscles originate on the epicondyles. In more cursorial mammals, the muscles (and epicondyles) are often smaller and the epicondyles are directed posteriorly to redirect the action of the flexors and extensors to produce a strictly parasagittal movement (Rose, 1993). On the other hand, in CCT a more complex substrate might require more medio-lateral control of the wrist giving rise to larger epicondyles that are medially or laterally directed. This results in a relatively broader distal humerus in CCT and a narrower one in OCT. If the distal humeri of CCT are broader, the relative epicondylar width (H1/HGM) and the epicondylar width ratio (H1/H2) will be consistently greater in CCT than in OCT.

The humeral trochleas of OCT are narrower (medio-laterally) than those of CCT.

A narrower trochlea suggests restriction of movement at the joint to a parasagittal direction as would be expected in OCT whereas a wider trochlea suggests greater medio-lateral or supinatory abilities as would be expected in CCT. If this is the case, the relative humeral trochlear width (H3/HGM) and the humeral trochlear ratio (H3/H2) will consistently be smaller in OCT than in CCT.

The distal articular surface of OCT is deeper (dorso-ventrally) than that of CCT.

This hypothesis is based upon two observations. The first is that an increased excursion at the elbow joint permits a longer stride in cursorial taxa and is facilitated by a more antero-posteriorly deep joint surface. The second is that arboreal and ambulatory taxa often bear a disproportionate amount of weight on their hindlimbs whereas more cursorial taxa carry their weight more equally between their fore and hindlimbs. An increase in the depth of the articular surface would more evenly distribute the weight of the animal. If this is the case, the relative articular surface depth (H6/HGM) and humeral articular surface ratio (H6/H7) will be larger in OCT than in CCT.

The olecranon fossa of OCT is narrower than that of CCT.

This is based on the idea that in cursorial taxa, the distal humerus acts more like a hinge joint, minimizing medio-lateral movements. A narrow olecranon fossa indicates a more hinge-like motion at the elbow. If this is the case, the relative olecranon fossa width (H7/HGM) will be smaller in OCT than CCT, and the olecranon fossa ratio (H2/H7) will be larger in OCT than in CCT.

6.4 Results

Raw measurements, standardized measurements and residuals are not normally distributed. Both the sign test and Mann-Whitney test are non-parametric and make no assumptions about the shape of the parent distribution (Sokal and Rohlf, 1995; Verzani, 2005), so I did not transform the data.

6.4.1 Sign Test

Eleven of the 18 one-tailed tests had significant results and seven did not. Five of the two-tailed tests had significant results. Because of the small samples, I used a threshold of $\alpha = 0.10$ and noted where significance was achieved at the more conventional level of $\alpha = 0.05$. The results are summarized in Tables 6.4 and 6.5 and are discussed in detail below. Box plots of all significant results are shown in Figures 6.6, 6.7 and 6.8.

Astragalus.—Ten of the tests on astragalar measurements had significant results (Figure 6.6 and 6.8). Of the one-tailed tests, the geometric mean of all measurements (AGM), relative minimum astragalar trochlear diameter, and navicular facet ratio were significant at $\alpha = 0.05$; and relative navicular facet depth, relative astragalar trochlear depth and the astragalar condylar ratio were significant at $\alpha = 0.10$. Of the two-tailed tests, relative medial condyle length (A2/AGM) was significant at $\alpha = 0.05$; relative medial length (A1/AGM), and relative medial condylar depth (A15/AGM) were significant at $\alpha = 0.10$. The astragalar condylar ratio showed significant results but with trends opposite of what my hypothesis predicted.

Humerus.—Six of the tests on humeral measurements had significant results (Figure 6.7 and 6.8): relative epicondylar width, and humeral articular surface ratio were

significant at α = 0.05; HGM relative humeral trochlear width, humeral trochlear ratio, and relative height of the articular surface (H5/HGM) were significant at α = 0.10.

6.4.2 Mann-Whitney U

Fourteen of the variables that showed significant trends using the sign test were found to have significantly different medians with the paired-sample Mann-Whitney tests: AGM, relative medial condyle length (A2/AGM), relative minimum astragalar trochlear diameter, relative astragalar trochlear depth, relative minimum astragalar trochlear diameter, medial condyle height relative to intermediate astragalar height (A9/A11), HGM, relative epicondylar width (H1/HGM), and relative humeral trochlear width (H3/HGM) were significant at α = 0.05; relative navicular facet depth, relative medial condylar depth (A15/AGM), navicular facet ratio, humeral trochlear ratio, and humeral articular surface ratio were significant α = 0.1.

Four of the variables were found to have significantly different means among pooled artiodactyls: relative minimum astragalar trochlear diameter, relative epicondylar width and humeral articular surface ratio were significant at α = 0.05; navicular facet ratio was significant at α = 0.1 (tables 6.4 and 6.5).

6.5 Discussion

6.5.1 Morphological Correlates of Habitat Change

Astragalus.—Several previous studies have shown that astragalar measurements can be useful in distinguishing between animals that inhabit different habitats, use different locomotor modes, or belong to different postural categories (Carrano, 1997; DeGusta and Vrba, 2003; Kappelman, 1988; Kappelman et al., 1997; Van Valkenburgh, 1987). Researchers using a discriminant function analysis to predict habitat type in a

sample of extant bovids based on astragalar measurements stressed that "ecomorphology" is really just the study of functional morphology in the context of ecology, although they made little attempt to interpret their results with regard to function (DeGusta and Vrba, 2003). They did not give an account of which measurements most affected the classification of bovids into habitat types, but gave a brief description of "morphotypes" based on three measurements (length, width and intermediate height) for each of their four habitat categories: open, light cover, heavy cover, and forest. They noted that astragali from open-country artiodactyls are shorter relative to their width than those from artiodactyls that inhabit other habitat types; forest taxa have thicker astragali (greater intermediate height) than the other taxa with open-country taxa having thicker astragali than heavy-cover taxa and light-cover taxa, but thinner astragali than forest taxa. Their graphical depiction of morphotypes also suggests that artiodactyls from open-country habitats have shorter medial lengths relative to lateral lengths, although they did not discuss this in the text.

Carrano (1997) used a discriminant function analysis as well as t-tests to classify mammals from several different groups into the postural categories "digitigrade" and "plantigrade" using measurements from the hindlimb in a wide selection of eutherian mammals excluding unguligrade taxa (artiodactyls and perissodactyls). He found many measurements of the hindlimb useful in distinguishing between the two postural categories. The two measurements that are directly relevant to the current study for which he had significant results are astragalar condylar symmetry and depth. He found that digitigrade taxa have deeper astragalar trochleas and more symmetrical condyles compared to plantigrade taxa. Although Carrano (1997) used postural differences rather

than locomotor differences, he suggested that these categories may be closely associated. Van Valkenburgh (1987) also hypothesized that the astragalar trochlea should be deeper in cursorial carnivores as opposed to more ambulatory ones, but she did not find a statistically significant result for this measurement.

The results of this study corroborate and expand upon the results of these previous studies as well as more qualitative observations that are commonly made in the literature. In agreement with Carrano (1997), I found that OCT in general have deeper trochleas than CCT. This is demonstrated by several measurements: A3/AGM, the relative minimum astragalar trochlear diameter, is larger in CCT than in OCT; (A14 + A15)/AGM, relative astragalar trochlear depth, is larger in OCT than in CCT; A15/AGM, the relative medial condylar depth, is larger in OCT than in CCT. In contrast to the study by Carrano (1997) I found that that CCT have higher astragalar condylar ratios (A2/A4) and longer relative medial condyle length (A2/AGM), suggesting that CCT have more symmetrical condyles than OCT. In agreement with DeGusta and Vrba (2003), I found that CCT have thicker astragali relative to medial condyle height (A9/A11). I did not find a strong relationship between medial (A1) or lateral length (A7) of the astragalus and habitat. The weak evidence I did find for a relationship between the length of the astragalus when measured medially and the size of the astragalus (A1/AGM) suggests that OCT have a longer medial length than CCT, which is the opposite of what they found. It is possible that this negative result is due to the small number of artiodactyl pairs in my sample. In addition to these findings, this study is the first to demonstrate quantitatively that across mammals, OCT have deeper navicular facets relative to astragalar size (A10/AGM), and narrower navicular facets relative to their height

(A5/A10). All of the results with the exception of the finding that CCT have thicker astragali (A9/A11), which is in agreement with previous results, and long medial condyles (A2/A4) are in accord with the biomechanical principles described above.

Humerus.—The morphology of the distal humerus has been regarded as informative for locomotor behavior in a variety of taxa including carnivores (Andersson, 2004), primates (Rose, 1988, 1993), and rodents (Elissamburu and Vizcaíno, 2004). Traditionally ratios have been constructed for the entire humerus (see Vizcaíno and Elisamburu, 2004). Studies involving the distal end specifically (such as Rose, 1988, 1993), have been more qualitative in nature.

I find that OCT have narrower distal humeri relative to the size of the humerus (H1/HGM) than OCT. This supports the traditional idea that a more mobile forearm (and by extension a wider distal humerus) in mammals that live in closed environments, or that move on complex substrates, allows these mammals to accommodate irregularities in the substrate during locomotion. I also find that OCT have narrower humeral trochleas relative to humeral size (H3/HGM) and relative to humeral articular surface width (H3/H2) and that OCT have deeper articular surfaces when measured laterally relative to humeral size (H5/HGM) and relative to the width of the olecranon fossa (H6/H7). All of the results are consistent with biomechanical principles described in section 6.3.3.

6.5.2 Phylogenetic Observations

The results discussed above deal with general trends across disparate mammalian taxa, but the way in which different taxonomic groups respond to each variable needs to be addressed, specifically artiodactyls. Artiodactyls as a whole follow the same trends as the other mammals in 101 out of 144 comparisons that were performed within that clade.

Artiodactyls followed the mammalian pattern in 72.2% of the comparisons for astragalar measurements and 66.7% for humeral measurements. For the astragalar measurements, the Giraffidae, Suidae and Cephalophini followed the mammalian trends in astragalar measurements the least, with each showing opposite trends in four out of 10 astragalar measurements (table 6.9); the Tayassuidae, Neotragini, and Tragelaphini each showed opposite trends in three features; Capriolinae and Reduncini showed opposite trends in only one variable, and the Cervinae agreed with the mammalian trends in all astragalar measurements. With regard to the six humeral variables, Cervinae had the highest incidence of exhibiting opposite trends for humeral measurements, agreeing with the general mammalian condition only in one measurement; Tragelaphini showed opposite relationships in three variables; Reduncini, Neotragini, Suidae and Tayassuidae did so in two instances; Capriolinae and Cephalophini showed only one opposite relationship, and the Giraffidae always followed the mammalian pattern. Importantly, the artiodactyls as a whole are not consistently different from the other mammals sampled in any one measurement. This suggests that artiodactyl astragalar and humeral morphology responds to the same adaptive pressures as other mammals, which is a fundamental assumption in the interpretation of fossil taxa.

There were only two groups of perissodactyls in this study (in contrast to the nine artiodactyl clades). Perissodactyla as a whole follows mammalian trends in 19 out of 30 (63.3%) comparisons performed within the group. With reference to the astragalar measurements, the Rhinoceratidae showed a trend opposite from the majority of mammals for four variables and the Equidae did so for one. This also supports the assumption that similar selective pressures are exerted on perissodactyl astragali and

those of other mammals. Rhinocerotids showed only one opposite relationship for the humeral measurements, but the Equidae showed an opposite relationship in every humeral variable except for one. This suggests that caution should be used in the interpretation of fossil equid humeri, as they might respond to ecological pressures in a unique way with respect to other mammals. The results of this study demonstrate that, despite their extreme postcranial specializations associated with unguligrady, ungulate postcrania can be successfully analyzed together with those of other mammal groups.

Overall, the primates behaved poorly, following the general mammalian trend only 56.7% of the time (58.3% of astragalar measurements and 55.6% of humeral measurements). The fact that primates do not follow the general mammalian pattern in humeral morphology is not surprising as all primates regardless of habitat retain supinatory ability at the elbow and engage in manual manipulation of objects. The Cercopithecidae is the group of primates that agrees with the mammalian pattern the most, following the general trend for 100% of humeral measurements and for 80% of all measurements; lemurids agreed with the general mammalian trend the least, following the general trend in only 33.3% of humeral and 44.4% of astragalar measurements. Xenarthrans did not follow the general mammalian trend in most of the comparisons, especially with regard to astragalar morphology, agreeing with the mammalian trend in only two out of nine measurements. The group that agreed with the general mammalian trends most frequently was the Hyracoidea, which differed in only one out of 15 measurements. Leporids agreed with the mammalian trend 53.3% of the time. Scandentians agreed 66.7% of the time, although this pertains only to the astragalar measurements as I was not able to measure a humerus of *Ptilocercus*. Carnivores agreed

with the mammalian trend 76.7% of the time; the Felidae differ only in one of the 15 measurements.

6.6 Summary

The primary goal of this chapter is to identify morphological responses to habitat change in the astragalus and distal humerus that hold across a broad selection of mammalian groups. My results show that 17 measurements including transformed linear measurements and ratios consistently differentiate mammals from open and closed environments. This is the first study to attempt to correlate differences in habitat with differences in postcranial morphology in such a broad range of orders, and it is also the first time that some of these measurements have been identified and quantified as ecologically informative. This result allows the interpretation of fossil taxa for which there are no close living relatives. In the next chapter I will apply these measurements to a sample of isolated artiodactyl astragali from the Uinta Formation to evaluate the morphological response of those taxa to habitat degradation occurring at that time.

Table 6.1. Extant taxa included in the analysis. Habitat classification based upon Nowak, 1994, Kappelman, 1988 and DeGusta and Vrba, 2003.

Taxon	Open	Closed
Hyracoidea		
Procaviidae	*Procavia capensis*	*Dendrohyrax arboreus*
Perissodactyla		
Equidae	*Equus grevyi*	*Equus asinus*
Rhinocerotidae	*Ceratotherium simum*	*Rhinoceros unicornis*
Artiodactyla		
Suidae	*Phacochoerus aethiopicus*	*Potamochoerus porcus*
Tayassuidae	*Catagonus wagneri*	*Tayassu pecari*
Cervidae		
Cervinae	*Axis axis*	*Muntiacus muntjac*
Capriolinae	*Rangifer tarandus*	*Pudu mephistopheles*
Giraffidae	*Giraffa camelopardalis*	*Okapia johnstoni*
Bovidae		
Tragelaphini	*Taurotragus oryx*	*Tragelaphus imberbis*
Reduncini	*Kobus kob*	*Kobus megaceros*
Neotragini	*Ourebia ourebi*	*Madoqua guentheri*
Cephalophini	*Sylvicapra grimmia*	*Cephalophus dorsalis*
Scandentia		
Tupaidae	*Tupaia glis*	
Ptilocercidae		*Ptilocercus loweii*
Primates		
Lemuridae	*Lemur catta*	*Varecia variegata*
Lorisidae	*Galago senegalensis*	*Loris tardigradus*
Cercopithecidae	*Erythrocebus patas*	*Allenopithecus nigrovindis*
Hominidae	*Homo sapiens* (A) *Gorilla gorilla* (H)	*Pan troglodytes*
Carnivora		
Felidae	*Leptailurus serval*	*Leopardus weidii*
Canidae	*Lycaon pictus*	*Urocyon cinereoargentius*
Ursidae	*Ursus arctos*	*Helarctos malayanus*
Viverridae	*Civettictis*	*Arctictis*
Procyonidae	*Bassariscus astutus*	*Potos flavus*
Mustellidae	*Gulo gulo*	*Martes americana*
Lagomorpha		
Leporidae	*Lepus californicus*	*Nesolagus timminsi*
Xenarthra		
Myrmecophagidae		*Tamandua tridactyla*
Dasypodidae	*Euphractus sexinctus*	

Table 6.2. Measurements included in the ecomorphological analyses. The numbers refer to the numbered measurements in Figures 6.3 and 6.4.

Element	Number	Description
Astragalus	A1	total length (taken medially)
	A2	medial condyle length
	A3	minimum length of trochlea
	A4	lateral condyle length
	A5	navicular facet width
	A6	total distal width (artiodactyls only)
	A7	total lateral length (artiodactyls only)
	A8	maximum trochlear width
	A9	medial condyle height
	A10	navicular facet height
	A11	intermediate height (artiodactyls only)
	A12	lateral condyle height
	A13	width between highest points of medial and lateral condyles
	A14	distance from lateral condylar crest to deepest part of the groove
	A15	distance from medial condylar crest to deepest part of the groove
Humerus	H1	maximum width of distal humerus across the epocondyles
	H2	maximum width of articular surface
	H3	maximum width of trochlea
	H4	maximum medial height of trochlea
	H5	maximum lateral height of articular surface
	H6	maximum dorsovenral depth of trochlea
	H7	width of olecranon fossa

Table 6.3. Standardized measurements and unstandardized ratios mentioned by name in the text. GM = the geometric mean of all measurements.

Element	Ratio	Name
Astragalus	A2 / AGM	Relative medial condylar length
	A3 / AGM	Relative minimum astragalar trochlear diameter
	A10 / AGM	Relative navicular facet depth
	A13 / AGM	Relative astragalar trochlear width
	A15 / AGM	Relative medial condylar depth
	(A14 + A15) / AGM	Relative astragalar trochlear depth
	A1 / A7	Medial astragalar ratio
	A2 / A4	Astragalar condylar ratio
	A5 / A10	Navicular facet ratio
	(A14 + A15) / A13	Astragalar trochlear ratio
Humerus	H1 / HGM	Relative epicondylar width
	H3 / HGM	Relative humeral trochlear width
	H6 / HGM	Relative articular surface depth
	H7 / HGM	Relative olecranon fossa width
	H1 / H2	Epicondylar width ratio
	H2 / H7	Olecranon fossa ratio
	H3 / H2	Humeral trochlear ratio
	H6 / H7	Humeral articular surface ratio

Table 6.4. Results of the one-tailed tests of a priori hypotheses. H_o: O = C. All of the measurements that had significant results showed the expected pattern except for A2/A4, the astragalar condylar ratio, suggesting that CCT have more symmetrical astragali than OCT.

Variable	N	H_a	No. +	No. -	Sign Test	Mann-Whitney U Paired	Mann-Whitney U Pooled Artiodactyls
Astragalus							
AGM	25	O > C	17	8	**	**	
A3 / AGM x 100	25	O < C	8	17	**	**	**
A10 / AGM x 100	25	O > C	16	9	*	*	
A13 / AGM x 100	25	O < C	14	11			
(A14 + A15) / AGM x 100	25	O > C	16	9	*	**	
A1 / A7	9	O < C	3	6			
A2 / A4	25	O > C	10	15	*	**	
A5 / A10	25	O < C	7	18	**	*	*
(A14 + A15) /A13	25	O > C	14	11			
Humerus							
HGM	24	O > C	15	9	*	**	
H1 / HGM x 100	24	O < C	8	16	**	**	**
H3 / HGM x 100	24	O < C	9	15	*	**	
H6 / HGM x 100	24	O > C	12	12			
H7 / HGM x 100	23	O < C	10	13			
H1 / H2	24	O < C	10	14			
H2 / H7	23	O > C	13	10			
H3 / H2	24	O < C	9	15	*	*	
H4 / H5	23	O > C	17	6	**	*	**

* = $p < 0.10$
** = $p < 0.05$

Table 6.5. Results of two-tailed tests for the remainder of the data. H_o: O = C; H_a: O ≠ C. Four additional astragalar variables and one additional humeral variable showed significant differences between OCT and CCT.

Variable	N	No. +	No. -	Sign Test	Mann-Whitney U Paired
Astragalus					
A1 / AGM	25	17	8	*	
A2 / AGM x 100	25	6	19	**	**
A4 / AGM x 100	25	11	12		
A5 / AGM x 100	25	13	12		
A6 / AGM x 100	9	3	6		
A7 / AGM x 100	9	6	3		
A8 / AGM x 100	25	11	14		
A9 / AGM x 100	25	14	11		
A11 / AGM x 100	9	6	3		
A12 / AGM x 100	25	10	15		
A14 / AGM x 100	25	15	10		
A15 / AGM x 100	25	17	8	*	*
A2 / A3	25	12	13		
A8 / A5	25	12	13		
A8 / A6	9	2	7		
A9 / A11	9	1	8	**	**
A9 / A12	25	11	14		
Humerus					
H2 / HGM x 100	24	10	14		
H4 / HGM x 100	24	14	10		
H5 / HGM x 100	24	16	8	*	
H2 / H6	24	10	14		
H4 / H5	24	14	10		

* = $p < 0.10$

** = $p < 0.05$

Table 6.6. Frequency with which taxonomic groups followed the trends exhibited across mammals for measurements with a significant relationship in the sign test. A = astragalar measurements; H = humeral measurements; T = total number of measurements. Ungulates (Artiodactyla and Perissodactyla) do not show consistent differences in pattern compared to the other mammal groups.

Taxon	Number of Comparisons			Number of tests that followed the overall trend			%		
	A	H	T	A	H	T	A	H	T
Perissodactyla	18	12	30	13	6	19	72.2	50.0	63.3
Rhinoceratidae	9	6	15	5	5	10	55.6	83.3	66.7
Equidae	9	6	15	8	1	9	88.9	16.7	60.0
Xenarthra	9	5	14	2	2	4	22.2	40.0	28.6
Leporidae	9	6	15	5	3	8	55.6	50.0	53.3
Artiodactyla	90	54	144	65	36	101	72.2	66.7	70.1
Giraffidae	10	6	16	6	6	12	60.0	100.0	75.0
Suidae	10	6	16	6	4	10	60.0	66.7	62.5
Tayassuidae	10	6	16	7	4	11	70.0	66.7	68.8
Cervinae	10	6	16	10	1	11	100.0	16.7	68.8
Capriolinae	10	6	16	8	5	13	80.0	83.3	81.3
Reduncini	10	6	16	8	4	12	80.0	66.7	75.0
Neotragini	10	6	16	7	4	11	70.0	66.7	68.8
Cephalophini	10	6	16	6	5	11	60.0	83.3	68.8
Tragelaphini	10	6	16	7	3	10	70.0	50.0	62.5
Hyracoidea	9	6	15	8	6	14	88.9	100.0	93.3
Primates	36	24	60	20	14	34	55.6	58.3	56.7
Lemuridae	9	6	15	4	2	6	44.4	33.3	40.0
Lorisidae	9	6	15	6	3	9	66.7	50.0	60.0
Cercopithecidae	9	6	15	6	6	12	66.7	100.0	80.0
Hominidae	9	6	15	4	3	7	44.4	50.0	46.7
Scandentia	9	-	9	6	-	6	66.7	-	66.7
Carnivora	54	36	90	41	28	69	75.9	77.8	76.7
Felidae	9	6	15	8	6	14	88.9	100.0	93.3
Canidae	9	6	15	6	3	9	66.7	50.0	60.0
Ursidae	9	6	15	6	6	12	66.7	100.0	80.0
Viverridae	9	6	15	5	5	10	55.6	83.3	66.7
Procyonidae	9	6	15	8	5	13	88.9	83.3	86.7
Mustellidae	9	6	15	8	3	11	88.9	50.0	73.3

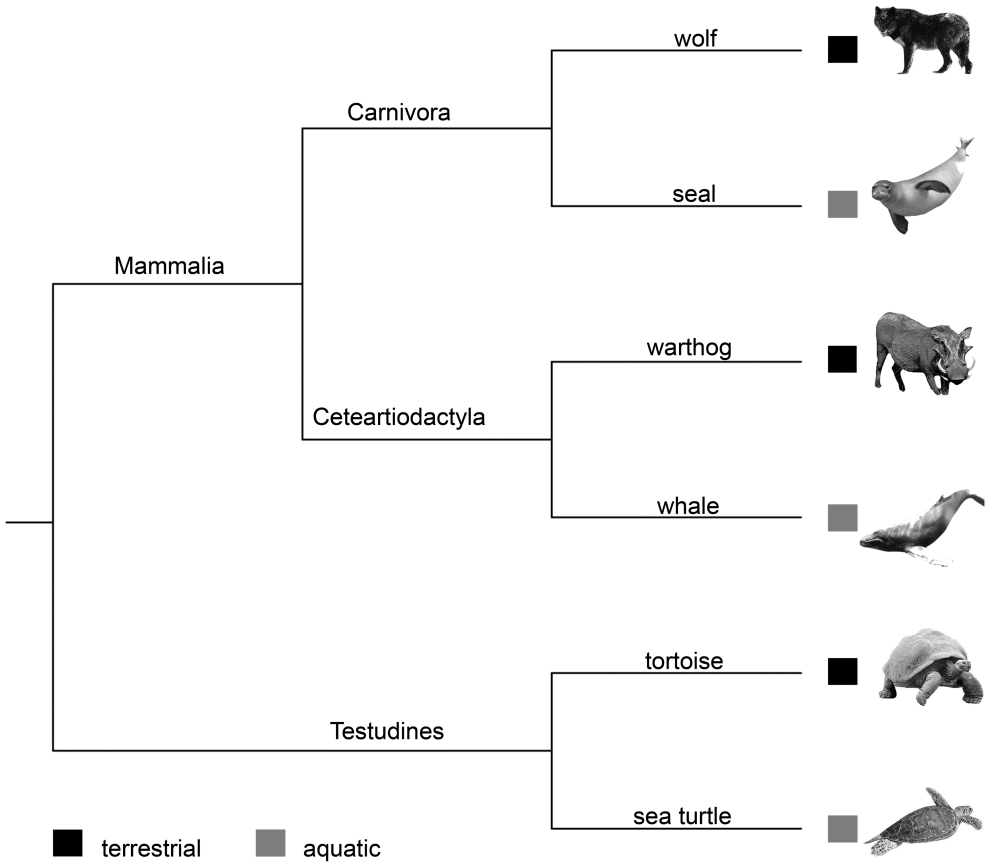

Figure 6.1. Illustration of the principle of using pairwise comparisons as a way to correct for phylogeny when examining behavioral character correlation in a broad range of taxa. In this simplified example, features shared by sea turtles, whales and seals such as a long phalanges, and presence of flippers are not seen in the terrestrial sister taxa and are thus correlated with an aquatic life style.

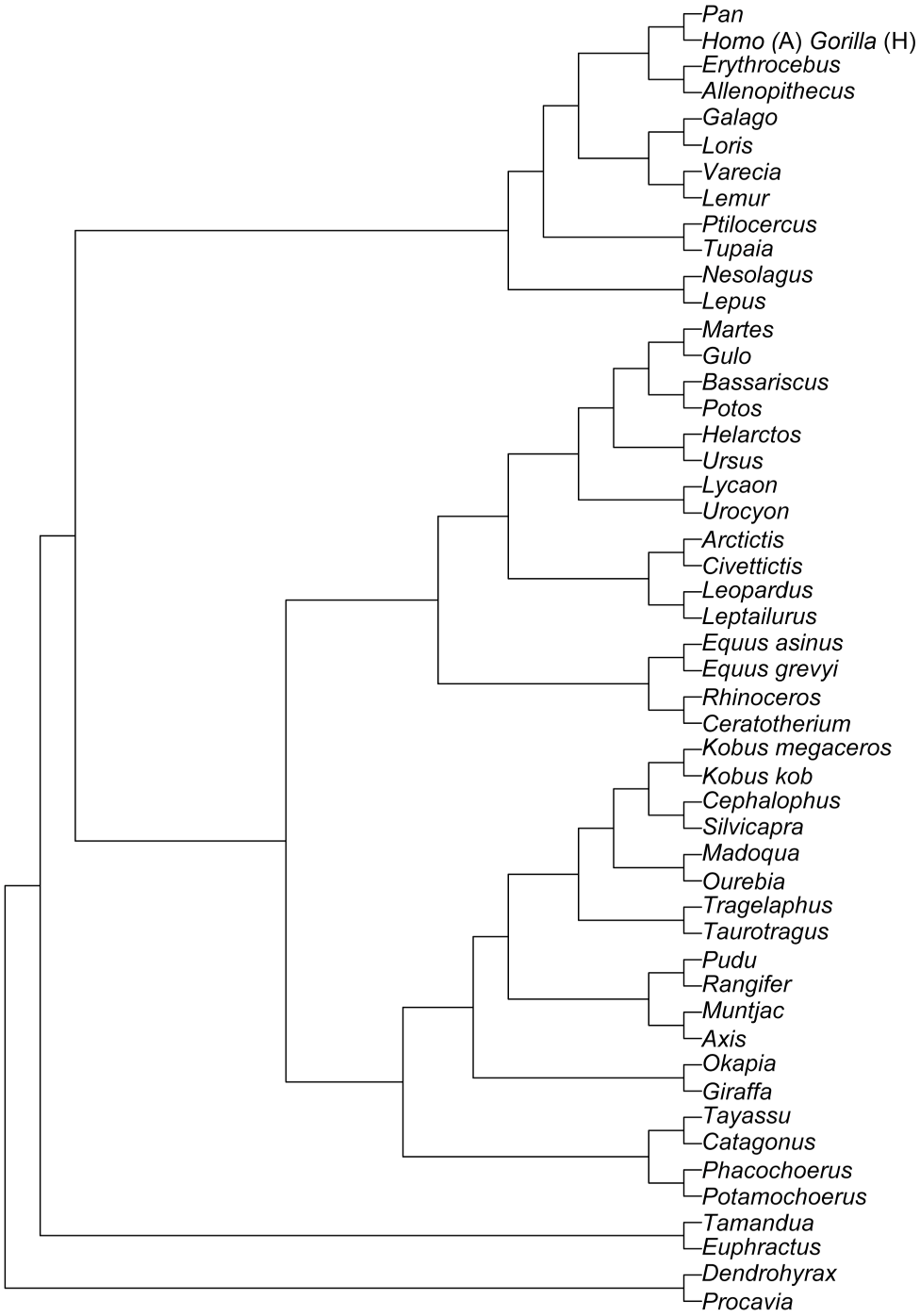

Figure 6.2. Dendrogram showing phylogenetic structure of the taxa used in this study. Primate phylogeny from Fleagle (1999); artiodactyl phylogeny from Matthee et al. (2001); carnivore phylogeny from Flynn et al. (2005), relationships among major mammal groups from Murphy et al. (2001).

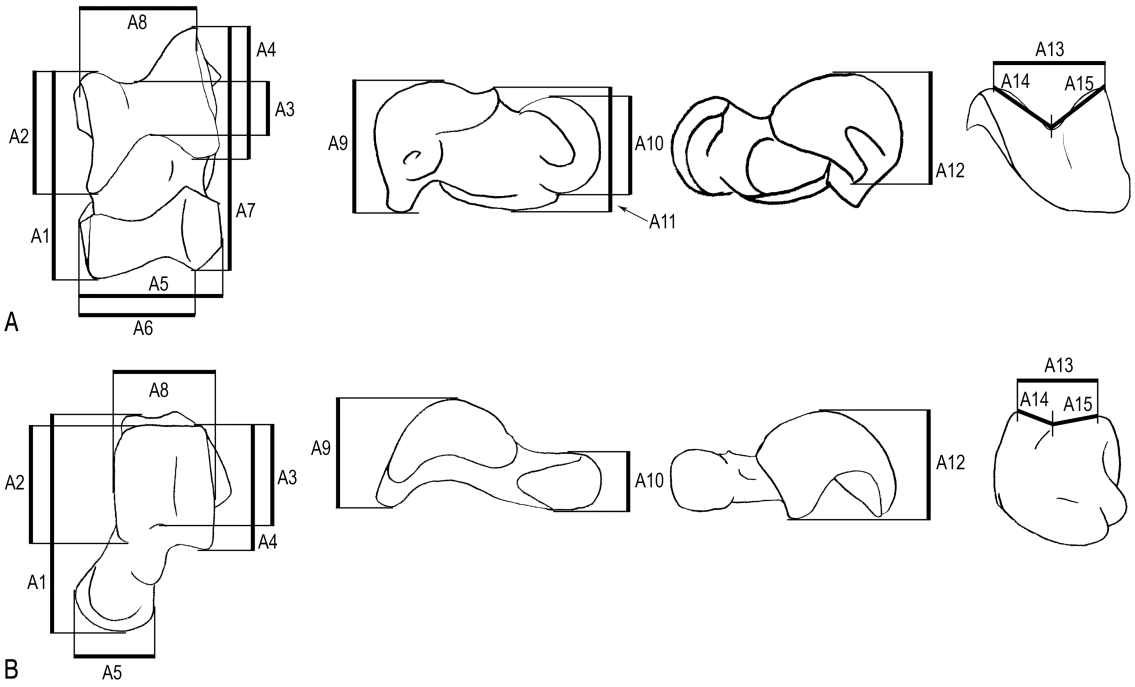

Figure 6.3. Astragalar measurements included in the ecomorphological analyses each row in dorsal, medial, lateral and posterior views (from left to right). **A**, artiodactyl; **B**, primate (representing generalized mammalian condition). Measurements are described in table 6.2.

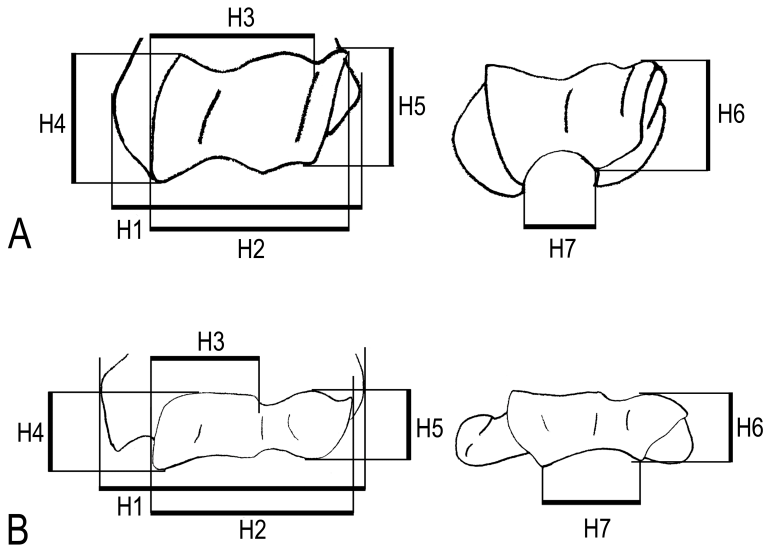

Figure 6.4. Distal humeral measurements included in the ecomorphological analyses each row in ventral and distal views (from left to right). **A**, artiodactyl; **B**, primate (representing generalized mammalian condition). Measurements are described in table 6.2.

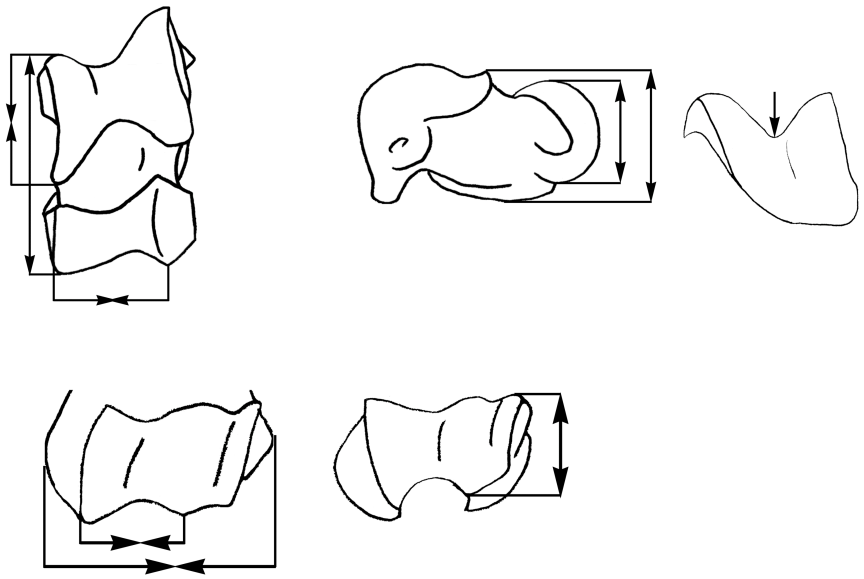

Figure 6.5. Diagram of **A**, artiodactyl astragalus in (left to right) dorsal, medial, and posterior views; and **B**, artiodactyl distal humerus in (left to right) ventral and distal views with arrows indicating the changes in dimensions in OCT relative to CCT. In general the astragali of OCT have longer medial lengths, shorter medial condyles, narrower navicular facets, thicker intermediate heights (artiodactyls only), deeper navicular facets and deeper trochleas. The distal humeri of OCT are narrower, have narrower trochlas, and deeper joint surfaces.

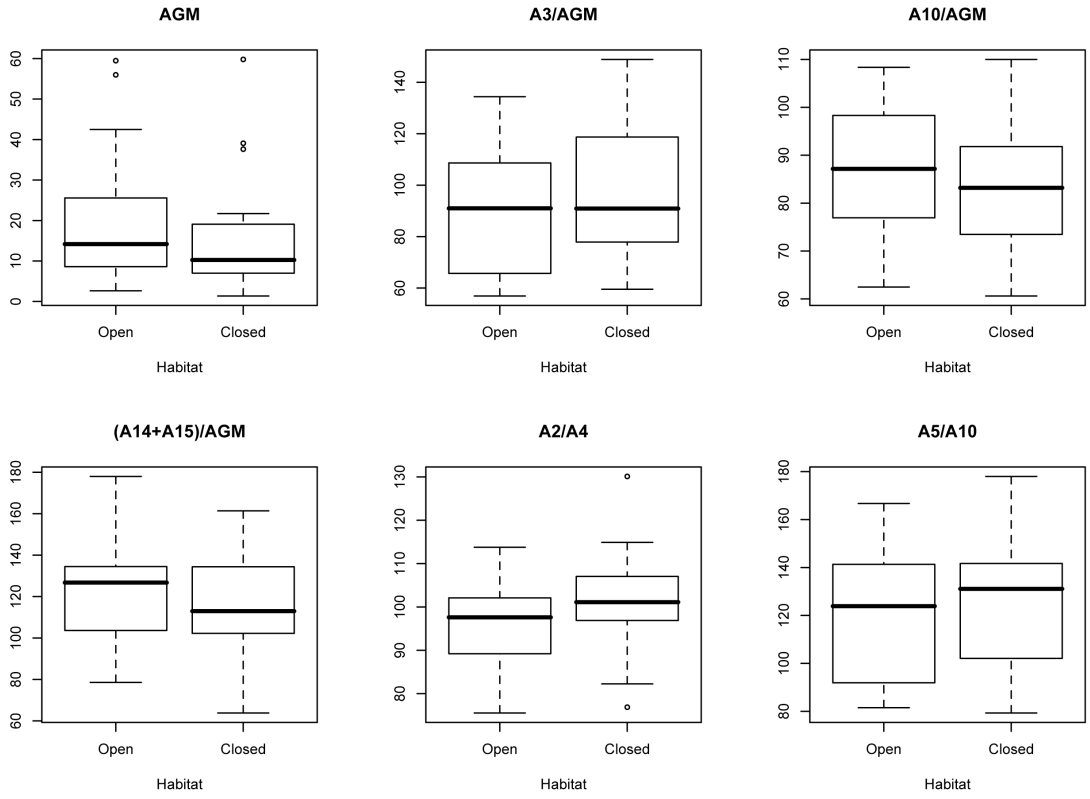

Figure 6.6. Box plots of astragalar variables with significant one-tailed tests. The dark bar represents the median and the box connects the upper and lower quartiles. Whiskers extend to the minimum and maximum points unless the values of those points lie more than 1.5 times the interquartile range from the upper or lower hinge, in which case they are marked separately as outliers. Group 1 is OCT and group 2 is CCT. In all cases there is significant overlap between the distributions as is expected. The relative position of the median of each distribution reflects the relationship between OCT and CCT indicated by the Sign and Mann-Whitney U tests (with the exception of A3/AGM). For example, the median AGM of OCT (group 1) is larger than that of CCT (group 2). Summary statistics for each variable divided by habitat category are given in Appendix 6A, Table 6A.3.

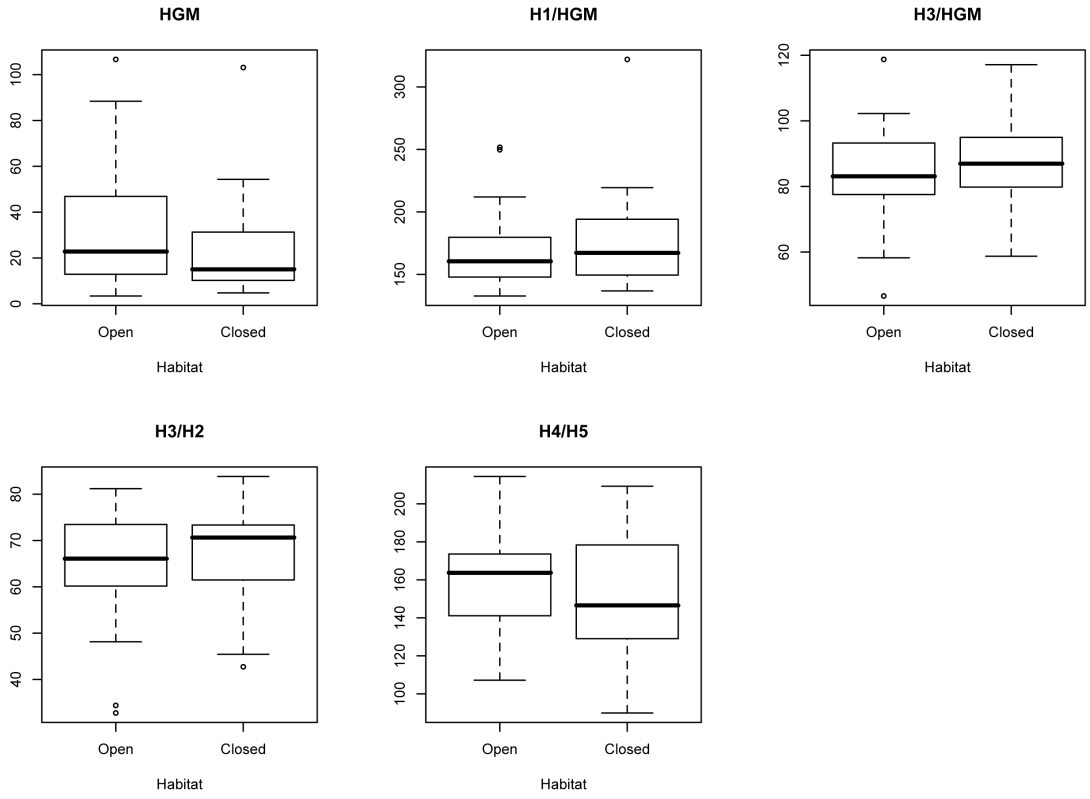

Figure 6.7. Box plots of distal humeral variables with significant one-tailed tests. See the explanation of boxplots in Figure 6.5. As in astragalar dimensions, there is significant overlap between the distributions in each group, but the median of each distribution reflects the relationship between OCT and CCT indicated by the Sign and Mann-Whitney U tests.

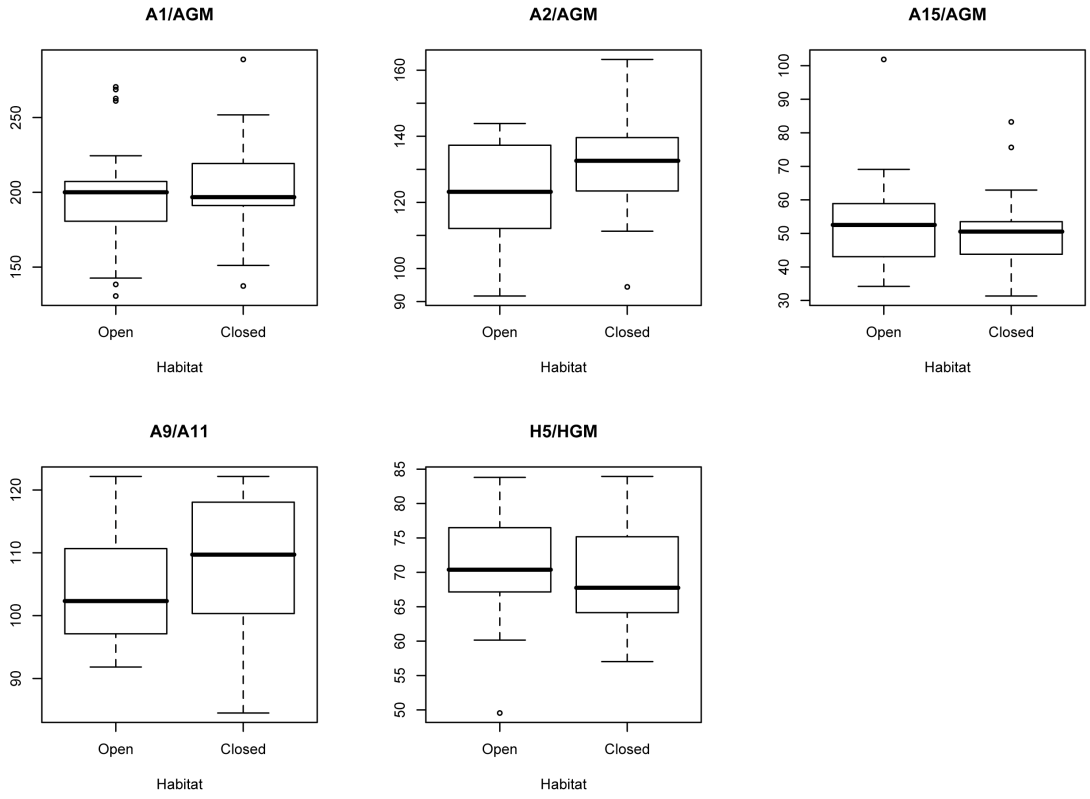

Figure 6.8. Box plots of variables with significant two-tailed tests. See the explanation of boxplots in Figure 6.5. Again, there is significant overlap between the distributions in each group, but the median of each distribution reflects the relationship between OCT and CCT indicated by the Sign and Mann-Whitney U tests.

CHAPTER SEVEN

A Quantitative Assessment of Ecomorphological Change Across the Uinta B-C Boundary

7.1 Introduction

One of the most striking differences between the mid continental faunas of the Bridgerian and Uintan North American Land Mammal Ages (NALMAs) is the low number of primates in the latter compared to their abundance in the former (Gazin, 1958; Rasmussen et al., 1999; Townsend, 2004; Townsend et al., 2006; Williams and Kirk, 2008). Primates are one of the most common components of early Eocene faunas from the Wasatchian and Bridgerian. Not only are they common, but they are incredibly diverse. In the Wasatchian NALMA, small-bodied largely insectivorous tarsiiform primates are extremely diverse with approximately ten genera (Gunnell and Rose, 2002; Rose, 2006), each including several species, existing throughout that period. The large-bodied frugivorous notharctine *Cantius*, occurs in the Wasatchian, where it is represented by several species; sometimes it is divided into two or more genera (Rose, 2007). Small-bodied tarsiiform primates remain small and diverse in sediments of Bridgerian age, and the notharctine primates, represented by *Notharctus*, become among the most common fossil mammals only to become extinct at the end of the Bridgerian NALMA (Gunnell, 1995; Rose, 2006). During the Uintan, the tarsiiform primates increase in size and develop more herbivorous dietary specializations to fill the niche vacated by the notharctines (Dunn et al., 2006; Rasmussen et al., 1999). Throughout the Bridgerian NALMA in the continental interior of North America, primates make up 11-15 percent of

the total fauna with a maximum of 11 species existing at one time. This is in stark contrast to the five species making up four to five percent of the total fauna in the Uintan (Gunnell and Bartels, 1999; Gunnell et al., 1995; Maas et al., 2988; Townsend, 2004; Williams and Kirk, 2008). This decrease in primate species richness is thought to be due to a loss of tree cover as the tropical rainforests that had covered most of the globe in the early Eocene began to retreat towards the tropics away from the poles (Clyde, 1998; Hutchison, 1992; Janis, 1993; Novacek, 1999; Prothero, 1985; Prothero, 1994; Retallack et al., 2004; Rose, 2006; Stucky, 1992; Wilf, 2000; Wing et al., 1995; Wing and Harrington, 2001; Wolfe, 1992). The fact that Southern California and Texas retain a relatively high percentage of primates during the Uintan supports this hypothesis as these places were located farther south and retained tropical conditions into even the late Eocene (Walsh, 1996; Williams and Kirk, 2008).

In contrast to the sharp decline in the richness and abundance of primates found in the Uintan of the continental interior of North America, there is a dramatic increase in the number of artiodactyls, especially selenodont artiodactyls (Gunnell and Bartels, 1999; Williams and Kirk, 2008). Primitive artiodactyls appear in North America in the early Wasatchian and maintain a presence throughout the Bridgerian (Janis et al., 1998; Rose, 2006; Stucky, 1998). These primitive artiodactyls are mostly small in body size and maintain a generalized bunodont dentition; they were probably mixed browsers and frugivores (Gazin, 1956). The first sign of specialized folivory in artiodactyls occurs in the Uintan NALMA with the appearance of several groups with selenodont molars, the most common of which is the Agriochoeridae (Gazin, 1956; Janis et al., 1998; Lander, 1998; Rose, 2006; Theodor, 1996, 1999). The radiation of selenodont artiodactyls during

this time is also thought to be due to a decrease in tree cover, allowing them to spread into new open terrestrial niches (Gazin, 1958; Gunnell and Bartels, 1999; Rasmussen et al., 1999). The situation that ultimately drove the primates to extinction in North America is the very thing that allowed the initial radiation of artiodactyls.

Several assumptions are implicit in the hypothesis that both the extinction of primates and radiation of artiodactyls are linked to loss of tree cover. One assumption is that primates did not adapt to a terrestrial way of life and remained dependent on trees. This can be tested directly by looking at locomotor adaptations of primates from the Uinta Formation as I did in chapter two. My analysis suggested that primates did retain an arboreal lifestyle into the late Uintan of the Uinta Formation (UF). Another assumption is that at least some artiodactyls became better adapted for more open habitats, which allowed them to radiate into new ecological niches. This assumption can also be tested directly by looking at how the locomotor adaptations of artiodactyls evolved throughout the Uintan.

Townsend (2004) divided the localities from the Uinta Formation into three time-averaged Uintan faunal assemblage zones (UFAZ). The fauna within each FAZ represents a community that was typical of early (UFAZ 1), middle (UFAZ 2) or late (UFAZ 3) periods within the Uintan in the Uinta Formation. The construction of FAZ allows taxa from different localities to be combined and treated as communities for comparison with extant communities. Her analysis of community structure in the Uinta Formation showed that UFAZ 1 was characterized by the most tree cover and UFAZ 3 the least with UFAZ 2 being intermediate between the two. She suggested that the base of UFAZ 3 represented the most significant shift towards open habitat in the Uinta

Formation, but that the presence of primates high in the UF indicated that there were some forested patches remaining (Townsend, 2004). She also found that the shift in community structure coincided stratigraphically with changes in lithology and taxonomy and interpreted these changes as evidence of habitat change.

If artiodactyls are radiating into new open habitat environments, then artiodactyl astragali should show progressively more open habitat features throughout the Uintan. Not only is the type of morphological change important but also the timing of those changes. If the major amount of habitat change occurred between UFAZ 2 and UFAZ 3, the morphological changes of artiodactyl astragali should coincide with or follow this boundary. If the transition occurred more gradually, as is suggested by the transitional nature of UFAZ 2, the morphological changes should not cluster around any one FAZ boundary (Townsend, 2004; Townsend et al., 2006).

The Washington University localities in the Uinta Formation span 366 vertical meters. Isolated postcranial elements, such as artiodactyl astragali are commonly found in the Uinta Formation. Most of the localities at which the fossils in the Washington University collection are found can be linked to a specific meter level in the stratigraphic sequence. Although specific rates of evolution cannot be addressed in this case without knowledge of rates of deposition throughout the section, meter level allows the localities to be ranked from earliest (lower) to latest (higher) and can be used as a rough proxy for time (Bown and Rose, 1987; Gingerich, 1979). The high preservation rate of artiodactyl astragali in the Uinta Formation together with the detailed stratigraphic section make it possible to investigate evolution of ankle morphology and locomotor behavior in Uintan artiodactyls.

In this chapter I address the question of whether fossil artiodactyls from the Uinta Formation adapted to open-country habitats by applying the measurements that were identified in chapter six as correlating with habitat change for extant mammals to a sample of artiodactyl astragali from the Uinta Formation in Utah.

7.2 Data

The fossil sample consists of artiodactyl astragali from the Uinta Formation in Utah collected by Washington University crews for the Carnegie Museum of Natural History and housed at Washington University. I had hoped to include distal humeri in this analysis, but there were not enough well-preserved specimens in the collection. Some of the astragali are associated with other skeletal or dental material, allowing them to be identified to family, and some were identified to family on the basis of similarity to elements of known taxonomic affiliation. It was not possible to classify many of the isolated astragali into more refined groups of artiodactyls as there are no established criteria for doing so. The largest subset of identified astragali in my sample belong to agriochoerids, although other astragali in the sample may also be attributable to this group. For this reason, results of analyses treating identified agriochoerid astragali alone should be viewed with caution. I used only specimens that appeared to be undistorted by the fossilization process.

7.3 Methods

Each of the tests described below was performed only with variables that were identified as correlating well with habitat type in the previous chapter: the geometric mean of all measurements (AGM), relative minimum astragalar trochlear diameter (A3/AGM), and navicular facet ratio (A5/A10), relative navicular facet depth

(A10/AGM), relative astragalar trochlear depth ([A14+A15]/AGM) and the astragalar condylar ratio (A2/A4), relative medial condyle length (A2/AGM) , relative medial length (A1/AGM), and relative medial condylar depth (A15/AGM) and ratio of medial condyle to intermediate height (A9/A11).

7.3.1 Standardization

Fossil astragali are rarely complete, so all measurements are not available for all individual elements. This is problematic when trying to decide how many measurements to include in the geometric mean (AGM) while maintaining a sufficiently large sample of fossil astragali. There were originally 86 artiodactyl astragali in my sample. Using the geometric mean of the three measurements A1, A5 and A6 reduced the sample to 71 specimens. The addition of one more measurement to the geometric mean would reduce the number of specimens to 66 and remove three specimens from UFAZ 1, which has the smallest number of specimens to begin with. I used the geometric mean of A1, A5 and A6 to standardize the measurements in the fossil sample. I calculated the geometric mean of these three measurements for the extant sample and found that it correlates strongly with the geometric mean of all measurements ($r = 0.995$, $p < 0.001$), which suggests that it is a comparable representation of body size.

7.3.2 Correlation with Stratigraphic Level

I plotted each variable as a function of the stratigraphic level of the locality from which it was collected to identify potential changes in the values of the variables through time. I examined agriochoerids for trends as well as artiodactyls as a whole. I also correlated each variable with stratigraphic level to test for potential trends.

7.3.3 Central Tendency

I first examined summary statistics and boxplots of the different variables from each FAZ. I then conducted one-tailed Mann Whitney tests of the differences between FAZs based upon the apparent trends in the summary statistics. Because the FAZs were constructed as representative communities, differences between the median values of variables among FAZs can be interpreted as representing adaptive changes in the artiodactyl community.

A shift in the median value of a variable in this kind of analysis does not necessarily indicate the loss or gain of new morphologies; it could also represent a shift in distribution of already existing forms. Hypothetically, if there are two morphological types of astragali, A and B, with A being more common than B in the older FAZ, the median value for a variable in the older FAZ will be closer to that of A than that of B. If in the next FAZ B becomes the most common type, the change in median value should shift towards the value for B. Alternatively, the introduction of a new type, C, with morphology more similar to B than A will have a similar effect on the Mann-Whitney test. As long as types A, B and C reflect the habitat, both scenarios indicate that the adaptations of the artiodactyl community have changed, which is all that is necessary for the purpose of this study.

7.3.4 Magnitude of Differences

The sign test is designed to identify differences, but does not provide information on magnitudes of differences (Ackerly, 2000). To get a sense of how differences between mean values within a FAZ compare to the differences between extant taxa from open-country and closed-country, I used a non-parametric Monte Carlo sampling method based

on my extant data to generate a null distribution against which to judge the magnitude of the changes in median between FAZs. To test for changes in median between two FAZs, *X* and *Y*, I sampled n_X and n_Y from the same variable in my extant data set with replacement regardless of habitat type. I then took the mean of each and calculated the absolute value of the difference between the means: $|\mu(n_X) - \mu(n_Y)|$ and divided that by the mean of the means: $((\mu(n_X) + \mu(n_Y))/2)$. The resulting quantity represents the difference of the means as a proportion of the average mean and has a minimum value of zero: $|\mu(n_X) - \mu(n_Y)| / ((\mu(n_X) + \mu(n_Y))/2)$. I used the proportion rather than an absolute measure of the difference in means to try to compensate for the smaller range of values in the fossil sample. I generated this value for 1,000 replications to generate a distribution of magnitudes of differences. I used the value at the upper 0.05 of the distribution as a threshold for statistical significance such that if the observed proportional difference in means between FAZ *X* and FAZ *Y* is at or above these values the difference in the means is considered to be greater than would be expected by chance alone (Table 7.1). I performed this sampling procedure on the entire range of extant taxa and on artiodactyls only.

This is a conservative test because the range of values in the extant sample is much greater, even when only the artiodactyls are considered, than that in the fossil sample, which yields greater proportional differences. This produces a distribution with a broader range of differences and makes it more difficult to achieve significance. The conservative nature of the distribution means that the achievement of significance indicates that the difference is probably true; however, failing to achieve significance should be interpreted as a lack of strong evidence for a difference rather than a lack of

difference.

7.3.5 Morphological Disparity

Morphological disparity is a measure of the amount of difference between distinct morphologies that exists at a point in time or in a location. It can be viewed as the amount of morphospace spanned by a set of morphologies. Any quantification of the cumulative difference among morphological variables can be used as a measure of morphological disparity. Using the variance of a morphological feature to represent disparity is a common practice, especially for fossils, because the variance is not particularly sensitive to sampling biases or the inherent incompleteness of the fossil record, which can introduce error (Ciampaglio et al., 2001; Foote, 1997). Disparity can be measured in a number of ways and applied to any group of organisms, be it ecological or phylogenetic in nature.

Morphological disparity has been found in numerous studies to be independent of taxonomic diversity suggesting that it reflects ecological rather than phylogenetic trends (Foote, 1993, 1996, 1997; Jernvall et al., 1996; Wesley-Hunt, 2005). Increases in morphological diversity have been interpreted as representing adaptive radiation into new environments and often happen before increases in taxonomic diversity (Jernvall et al., 1996, 2000).

Examining artiodactyls from the Uinta Formation for changes in variance among FAZs can reveal evolutionary trends. A change in the median value between two FAZ without an accompanying increase in variance would suggest that new morphologies are evolving and old ones are being lost, as would occur if artiodactyls were abandoning a primitive niche and moving into an entirely new one. An increase in variance between

two FAZ regardless of a change in the median value would suggest radiation of some artiodactyls into new ecological niches while some maintain residence in previous ones.

To test for changes in variance between FAZs, I conducted a nonparametric Monte Carlo sampling method to generate a null distribution against which to judge the magnitude of changes in variance between FAZ. The procedure was similar to the one described above for means except that instead of calculating a proportional difference in means, I calculated the absolute value of differences between the variances: $| \sigma^2(n_X) - \sigma^2(n_Y) |$ and divided that by the mean of the variances: $((\sigma^2(n_X) + \sigma^2(n_Y)) / 2)$. This represents the difference of the variances as a proportion of the mean of the two variances with a minimum value of 0: $| \sigma^2(n_X) - \sigma^2(n_Y) | / ((\sigma^2(n_X) + \sigma^2(n_Y)) / 2)$. I used the proportion rather than an absolute measure of the difference in total variance to account for differences in the variance of the fossil and extant samples. Again, I used the values from the upper 0.05 of the distribution as threshold values for statistical significance (Table 7.2). I performed this sampling procedure on the entire range of extant taxa and on artiodactyls.

7.4 Results

Out of the ten variables that were found to be significantly correlated with habitat change in the extant sample, eight showed some statistical significance in the sample of the fossil artiodactyl astragali: AGM, relative medial length (A1/AGM), relative medial condyle length (A2/AGM), relative minimum astragalar trochlear diameter (A3/AGM), relative navicular facet depth (A10/AGM), relative astragalar trochlear depth ([A14+A15]/AGM), navicular facet ratio (A5/A10) and ratio of medial condyle to intermediate height (A9/A11).

7.4.1 Correlation

Three of the plots revealed potential changes in proportions throughout the stratigraphic section (Figure 7.1): AGM appears to increase as meter level increases, and the ratio of medial condyle to intermediate height appears to decrease as the meter level increases. Of these, the ratio of medial condyle to intermediate height exhibited a significant negative correlation with meter level; AGM and meter level did not correlate significantly. When only the identified agriochoerids are examined, there is a strong positive correlation between AGM and meter level and between navicular facet ratio and meter level (meaning that the navicular facet of agriochoerids appears to get wider over time); and no correlation between the ratio of medial condyle to intermediate height and meter level.

7.4.2 Central Tendency

Four variables showed statistically significant differences in the median value between UFAZ 1 and UFAZ 2 (Table 7.3, Figure 7.2). The median of AGM and navicular facet ratio increased between UFAZ 1 and UFAZ 2, and that of relative medial length and relative minimum astragalar trochlear diameter decreased. Two variables showed a statistically significant difference between UFAZ 2 and UFAZ 3: the median ratio of medial condyle to intermediate height decreased and that of relative navicular facet depth increased. Two variables show statistically different medians between UFAZ 1 and UFAZ 3: the median of AGM increased and the median ratio of medial condyle to intermediate height decreased.

AGM increased between UFAZ 1 and UFAZ 2 and also between UFAZ 1 and UFAZ 3, suggesting that the overall size of artiodactyls increased between the first two

FAZs and overall throughout the Uintan of the Uinta Formation. I reported in the last chapter that open-country taxa (OCT) were generally larger than closed-country taxa (CCT). The relative medial length of the astragalus decreased between UFAZ 1 and UFAZ 2 suggesting that artiodactyls in UFAZ 2 resembled CCT more than OCT in this feature. I used the minimum length of the trochlea as one of several measures of astragalar depth. The reduction in relative minimum depth of the trochlea in UFAZ 2 compared to UFAZ 1 suggests that artiodactyls in UFAZ 2 had narrower trochleas and more resembled OCT in this feature. I found that the navicular facet ratio is greater in UFAZ 2 than in UFAZ 1, suggesting that the navicular facet is wider in UFAZ 2. This feature also showed a positive correlation with meter level when only agriochoerids were considered, suggesting that the navicular facet of agriochoerids became relatively wider through time. CCT were found to have wider navicular facets than OCT.

From UFAZ 2 to UFAZ 3 the relative navicular facet width (A10/AGM) decreased, which suggests that the artiodactyls in UFAZ 3 resemble OCT more than those in UFAZ 2 when this feature is considered. The ratio of medial condyle to intermediate height increased from UFAZ 2 to UFAZ 3 and from UFAZ 1 to UFAZ 3. In addition, this ratio had a significant negative correlation with meter level also suggesting that it decreased through time. OCT were found to have a smaller value of this ratio than CCT.

A hypothetical typical artiodactyl astragalus from UFAZ 2 would be larger, with shorter medial length, a deeper trochlea and wider navicular facet than one from UFAZ 1 (Figure 7.3). This differs from the condition in UFAZ 1 in ways resembling both OCT and CCT. A hypothetical astragalus from UFAZ 3 in general had a narrower navicular

facet relative to size and a thicker body relative to the medial condyle than one from UFAZ 2, differences that are more characteristic of OCT than of CCT. Finally, a hypothetical typical astragalus from UFAZ 3 would be larger with a thicker body relative to the medial condyle height than one from UFAZ 1. These trends are also more consistent with a shift towards the morphology of an OCT and away from that of a CCT.

7.4.3 Magnitude of Differences

Of the variables that showed a significant difference in medians with the Mann-Whitney test only the comparison of the ratio of medial condyle to intermediate height between UFAZ 1 and UFAZ 3 showed a significant proportional difference when compared to the distribution of extant artiodactyls. Three comparisons approached significance: the difference in medians for relative navicular facet depth and the ratio of medial condyle to intermediate height between UFAZ 2 and UFAZ 3, and those for relative medial length, relative minimum trochlear diameter and navicular facet ratio between UFAZ 1 and UFAZ 2 were within 0.05 mm from the cutoff for the artiodactyl sample. Neither of the differences in AGM approached significance when compared to the null distribution, but the difference in AGM between UFAZ 1 and UFAZ 2 was greater than that between UFAZ 1 and UFAZ 3. None of the measurements was significant when compared to the distribution for all mammals. As discussed in section 7.3.3, this lack of statistical significance when compared to the null distribution created from the extant sample, does not necessarily suggest that there is no biologically meaningful difference between the FAZ.

7.4.4 Morphological Disparity

When the non-parametric re-sampling method was used to test for significant

differences in the variance, three variables had significant results and all were increases in variance. Relative minimum diameter of the astragalar trochlea exhibited an increase in variance between UFAZ 1 and UFAZ 3 when compared to the distribution from only the artiodactyls in the extant sample but not when compared to the distribution generated from all taxa. Relative depth of the astragalar trochlea exhibited an increase in variance between UFAZ 1 and UFAZ 3 when compared to both distributions. Navicular facet ratio exhibited increases in variance between UFAZ 2 and UFAZ 3 and between UFAZ 1 and UFAZ 3 when compared to both distributions.

Three of the four increases in variance were located between UFAZ 1 and UFAZ 3 and one is between UFAZ 2 and UFAZ 3. This suggests that the evolution of morphological disparity occurred gradually throughout the Uintan rather than occurring between any two FAZ. An increase in variance can be interpreted as an increase in morphological disparity, which is often associated with adaptive radiation. An increase in morphological disparity rather than a loss of some morphologies and development of new ones suggests that some artiodactyls were moving into new habitats while others remained in old ones.

7.5 Discussion

Most previous assessments of habitat change in the Uintan suggested that the early Uintan (UFAZ 1 and UFAZ 2) was similar in the degree of tree cover and moisture to the late Bridgerian in being closed, subtropical forests. The late Uintan (UFAZ 3) was traditionally viewed as the beginning of more open habitats and seasonal climates (Bradley, 1937; Gazin, 1955, 1958; Gunnell and Bartels, 1999; Townsend, 2004). The more recent of these assessments have been made through ecological diversity analysis

(EDA), which does not take into account the evolution of individual lineages. This is the first study to look at the evolution of postcranial morphology in a single taxon throughout the Uintan and its implications for habitat change. This study corroborates the conclusions of previous studies that habitats became more open through the Uintan, but it does not support the assertion that this occurred primarily between the early and late Uintan. Instead, this study suggests that the morphology of artiodactyl astragali evolved to resemble open-country taxa in several characteristics gradually and this, in turn, supports the hypothesis of gradual habitat change.

7.5.1 Implications for Uintan Habitat Change

The majority of the differences I found were between UFAZ 1 and UFAZ 2. Four variables had significant differences in the medians between UFAZ 1 and UFAZ 2, two had significant differences between UFAZ 2 and UFAZ 3 and two between UFAZ 1 and UFAZ 3. This suggests that artiodactyls acquired morphological characteristics in a mosaic fashion gradually throughout the Uintan, rather than all at once between the early and late Uintan. This is consistent with the observation by Townsend (2004) that the UFAZ 2 appeared to be transitional in faunal composition between UFAZ 1 and UFAZ 3, but it is inconsistent with her final conclusion that UFAZ 3 is the most unlike the other two, which are more similar to each other in habitat.

Most differences in morphology suggest that where younger artiodactyl astragali differ in morphology from those of the older artiodactyls, it is similar to the way in which OCT differ from CCT. The two exceptions occur between UFAZ 2 and UFAZ 1. It is possible that this reflects sampling bias and could indicate that artiodactyls in UFAZ 1 and UFAZ 2 are more similar to each other in morphology than to those in UFAZ 3. A

larger sample size and a greater degree of taxonomic control are needed to determine if this is the case.

That the increases in variance occur largely between UFAZ 1 and UFAZ 3 rather than between adjacent FAZs suggests a gradual transition to more open habitats rather than a single abrupt change between UFAZ 2 and UFAZ 3.

All significant differences between UFAZ 3 and earlier FAZ suggest that the artiodactyls inhabiting UFAZ 3 were more adapted to open habitats than were those in the preceding FAZ. This supports the hypothesis that habitats within the Uinta Formation were becoming more open. The increase in morphological disparity between FAZ suggests that forested areas were still present during the late Uintan in the Uinta Formation, which explains the rare primate remains from these levels.

The disparity between rate of habitat change suggested by EDA and the current study might be explained by the nature of the habitat change that is occurring. The presence of primates and pantolestids in the late Uintan of the UF indicates that there was probably at least some tree cover, and probably enough water to support small gallery forests. It is likely that the habitat chance in the UF did not occur in a uniform fashion, but instead fragmented into a mosaic habitat with patches of open grasslands and remnant woodlands. The presence of arboreal forest taxa will bias EDA results in the direction of forest habitats (Townsend, 2004) whereas this analysis highlights any differences in postcranial morphology between FAZs, irrespective of whether they correlate with open or closed habitats. If the habitat of the UF changed from more closed in UFAZ 1 to a more fragmented mosaic habitat in UFAZ 3, the results of this study and EDA would not be mutually exclusive and would in fact, complement each other.

7.5.2 Implications for Primate Evolution

Many researchers have noted the inverse relationship between primate and artiodactyl diversity during the Uintan of North America and have related both to the loss of subtropical forests and the beginning of more open temperate habitats (Gazin, 1955, 1958; Gunnell and Bartels, 1999; Williams and Kirk, 2008). This relationship implies that artiodactyls radiated into open habitats and that primates retained arboreal adaptations. However, until now no one has attempted to trace the evolution of artiodactyl locomotor adaptations through the Uintan specifically to address this question.

Had artiodactyls not shown any significant changes in morphology, it would have called into question the assumption that the change in habitats was so drastic as to drive primates extinct. If other members of the faunal community did not have to adapt to changing conditions, why did the primates? However, the results of this study do consistently suggest that artiodactyls did evolve more cursorial ankles throughout the Uintan in the Uinta Formation, suggesting that there is a relationship between open habitats and artiodactyl radiation. This supports the suggestion that arboreal environments are indeed becoming more scarce and the magnitude of the change impacts mammalian evolution. Because primates from the Uinta Formation maintain arboreal adaptations throughout the Uintan (see Chapter Two), this reinforces the validity of a link between dwindling primate populations and a reduction in tree cover.

7.5.3 Considerations and Limitations

Taphonomy is an important consideration when trying to identify size and shape trends in a fossil assemblage. It is possible that fossil accumulations at different stratigraphic levels represent different depositional environments with different size

biases (Behrensmeyer, 1979; Clyde et al., 2005). For example, paleochannel deposits tend to preserve mostly large taxa whereas overbank deposits preserve small to medium mammals. The UF contains both paleochannel and overbank deposits, with the paleochannel deposits (represented by coarser sandstones) being more common in the Uinta B than in the Uinta C (Peterson in Osborn, 1895; Thornton and Rasmussen, 2001). The artiodactyl taxa that are present in the Uinta Formation are all small to medium sized mammals, such as would be found in overbank deposits. The largest artiodactyl in the UF is *Achaenodon*, a semi-aquatic pig-like animal. This taxon is found in channel sandstones and is extremely rare in the WU collection, represented only by one jaw, one isolated tooth and an astragalus. I did not include this astragalus in my sample due to its large size in relation to the rest of the fossil astragali. Given the larger number of paleochannels lower in the section, one might expect there to be larger animals represented in FAZ 1 and 2 when compared to FAZ 3. However, the opposite is true, larger astragali are found higher in the section than are found lower (Figure 7.1, AGM). This figure also demonstrates that small artiodactyl astragali are present throughout the section, although the smallest astragali do occur lower in FAZ 1. This suggests that there is not a significant taphonomic size bias in the sample.

Of the ten astragalar variables identified as correlating with habitat in Chapter 6, six of them had some significant result in the fossil taxa. Three of the variables that did not show significant changes in the fossil sample were strongly correlated with habitat change in the previous chapter. I especially expected the relative depth of the astragalar trochlea to become greater throughout the Uintan, but it remained very stable between FAZs, with the only significant change being an increase in variance between UFAZ 1

and UFAZ 3. I was surprised that the ratio of medial condyle to intermediate height showed several highly significant trends in the fossil taxa since there is no obvious functional significance for this ratio and it was found to be significantly associated with habitat change in Chapter 6 only in the a posteriori tests. Although a functional explanation for ecomorpholgical variables strengthens their utility in such analyses, the lack of this information does not entirely negate their utility (DeGusta and Vrba, 2003; Van Valkenburgh, 1994). Further investigation into this ratio is warranted.

It is not entirely surprising that only a subset of the variables showed significant results. In the analysis of extant taxa, there was no strong evidence of a functionally diagnostic "package" of characters related to the shift between closed and open habitats. That is, there was no suite of characters that always changed in unison. The additive acquisition of these characters in the fossil sample may be interpreted as evidence of mosaic evolution, with certain traits being more responsive to changes in habitat or substrate, and others responding later.

It is also possible that chance is responsible for the fact that only a few variables showed significant trends. Overall, the differences between FAZs are small and could be due to or exaggerated by sampling bias or measurement error. Moreover, the samples from each FAZ are small and as such are more susceptible to such biases. A more robust answer can come only with an increase in the fossil sample and with either more associated artiodactyl postcranial material or better ways of identifying isolated artiodactyl postcrania to more specific taxonomic units. This would allow a more critical examination of what is driving the trends that I have observed in this analysis: are there certain artiodactyl groups that are evolving, whereas others are not, or is there differential

preservation of certain taxa in parts of the UF skewing the results?

In an ideal analysis, each fossil would be identified to the family level or below which would allow the identification of different evolutionary trends within each group. However, for reasons discussed above, this is not currently possible. This is a concern in that evolutionary trends that occur only in some groups can influence the results, but it is more likely that differential evolution in distinct artiodactyl groups would obscure any trends, making it more difficult to find significant results. For example, if two lineages of artiodactyls are evolving in opposite directions for a certain feature and these lineages were grouped as a single evolving population, there would be no significant correlation with meter level. This pattern was observed in two of my variables (Figure 7.1 AGM and A5/A10) which showed no correlation with meter level for the whole group but significant correlation in the Agriochoeridae. Because this ambiguity works against finding significant results, when such results are found, they can be considered robust.

7.6 Summary

The primary goal of this chapter was to examine a sample of artiodactyl astragali from the Uinta Formation for changes in morphology from which to infer changes in habitat. My results show that eight of the ten variables tested have a significant result, some from several different tests. Most of the morphological changes occurring throughout the Uintan were consistent with adaptation to a more open environment. The pattern of increasing variance and accumulation of morphological differences suggests that habitat became more open gradually rather than concentrated at a single point in time. This study supports the hypothesis that artiodactyls did adapt to increasingly open habitats during the Uintan and that a reduction in tree cover occurred during this time.

This implies that primates, which retained arboreal adaptations throughout the Uintan, became more scarce as the number of trees declined.

Table 7.1 Simulated proportional difference thresholds generated from the extant data set using all taxa (AT) and artiodactyls only (AO). The threshold value is a nonparametric statistic marking the upper 5% of the null distribution ($\alpha = 0.05$) with which to compare proportional differences in the fossil sample. Measurements are in mm.

	1:2		**2:3**		**1:3**	
	AT	**AO**	**AT**	**AO**	**AT**	**AO**
AGM	0.59	0.42	0.49	0.35	0.52	0.36
A1/AGM x 100	0.12	0.05	0.11	0.04	0.11	0.04
A2/AGM x 100	0.08	0.07	0.06	0.06	0.08	0.06
A3/AGM x 100	0.18	0.12	0.15	0.09	0.17	0.11
A10/AGM x 100	0.12	0.06	0.10	0.05	0.10	0.05
A15/AGM x 100	0.18	0.17	0.16	0.14	0.17	0.15
(A14+A15)/AGM x 100	0.16	0.11	0.13	0.09	0.15	0.11
A2/A4	0.10	0.05	0.08	0.05	0.09	0.05
A5/A10	0.16	0.06	0.15	0.05	0.14	0.06
A9/A11*		0.09		0.07		0.08

*A9/A11 can be calculated for artiodactyls only

Table 7.2. Simulated proportional variance difference thresholds generated from the extant data set using all taxa (AT) and artiodactyls only (AO). The threshold value is a nonparametric statistic marking the upper 5% of the null distribution ($\alpha = 0.05$) with which to compare proportional differences in variance from the fossil sample. Measurements are in mm.

	1:2		**2:3**		**1:3**	
	AT	**AO**	**AT**	**AO**	**AT**	**AO**
AGM	1.41	1.43	1.29	1.17	1.37	1.31
A1/AGM x 100	1.09	1.13	1.00	1.01	0.96	1.02
A2/AGM x 100	0.99	0.74	0.85	0.59	0.96	0.68
A3/AGM x 100	0.88	0.70	0.72	0.54	0.77	0.59
A10/AGM x 100	0.88	0.91	0.68	0.76	0.75	0.82
A15/AGM x 100	1.38	1.50	1.22	1.29	1.25	1.40
(A14+A15)/AGM x 100	1.15	1.28	0.91	1.03	1.14	1.11
A2/A4	1.27	1.24	1.09	0.91	1.23	1.20
A5/A10	0.76	0.87	0.61	0.64	0.67	0.70
A9/A11*		1.04		0.79		1.05

*A9/A11 can be calculated for artiodactyls only

Table 7.3 One-tailed Mann-Whitney U tests for differences of the median between FAZs. 1:2 indicates a test between UFAZ 1 and UFAZ 2 and so on. Note that the significant differences occur between all FAZs and are not clustered around a single faunal zone transition.

	1:2 Relationship		**2:3 Relationship**		**1:3 Relationship**	
AGM	1 < 2	**	2 > 3		1 < 3	*
A1/AGM x 100	1 > 2	*	2 < 3		1 > 3	
A2/AGM x 100	1 < 2		2 < 3		1 < 3	
A3/AGM x 100	1 > 2	*	2 < 3		1 > 3	
A10/AGM x 100	1 < 2		2 < 3	*	1 < 3	
A15/AGM x 100	1 < 2		2 > 3		1 < 3	
(A14+A15)/AGM x 100	1 < 2		2 < 3		1 < 3	
A2/A4	1 > 2		2 < 3		1 < 3	
A5/A10	1 < 2	*	2 > 3		1 > 3	
A9/A11	1 > 2		2 > 3	**	1 > 3	*

* $p < 0.05$
** $p < 0.01$

Table 7.4 Absolute differences (D) and proportional differences (P) between medians of fossil artiodactyl astragalar dimensions between each FAZ. A negative difference denotes that the median of the following FAZ was greater than that in the preceding FAZ and thus an increase. A positive differences denotes a decrease. None of the differences was significant when compared to the distribution for all taxa. Of the three that were significant compared to the artiodactyl distribution, all occurred either between UFAZ 2 and UFAZ 3 or UFAZ 1 and UFAZ 3. Measurements are in mm.

	1:2		**2:3**		**1:3**	
	D	**P**	**D**	**P**	**D**	**P**
AGM	3.0	0.30	2.5	0.25	-0.5	0.06
A1/AGM x 100	3.9	0.02	-2.7	0.02	1.2	0.01
A2/AGM x 100	-1.2	0.01	-0.9	0.01	-2.1	0.02
A3/AGM x 100	5.4	0.09	-2.6	0.04	2.8	0.05
A10/AGM x 100	-0.5	0.01	-3.0	0.04	-3.5	0.05*
A15/AGM x 100	-2.6	0.08	1.4	0.04	-1.2	0.04
(A14+A15)/AGM x 100	-3.0	0.04	-1.0	0.01	-4.0	0.05
A2/A4	1.0	0.01	-1.9	0.02	-0.9	0.01
A5/A10	-4.4	0.05	7.9	0.09*	3.5	0.04
A9/A11	3.6	0.03	5.1	0.05	8.7	0.08*

*indicates a significant difference compared to the distribution of artiodactyls ($p < 0.05$)

Table 7.5. Differences in variance (D) and proportional differences (P) in variance for fossil astragali. A negative difference denotes that the variance of the following FAZ was greater than that in the preceding FAZ and thus an increase. A positive differences denotes a decrease. Measurements are in mm.

	1:2		2:3		1:3	
	D	**P**	**D**	**P**	**D**	**P**
AGM	1.17	0.22	-11.07	1.07	-9.90	0.90
A1/AGM x 100	0.76	0.02	-58.94	0.60	-58.18	0.59
A2/AGM x 100	9.45	0.16	8.91	0.18	18.36	0.34
A3/AGM x 100	-8.72	0.45	-5.19	0.20	-13.91	0.64[§]
A10/AGM x 100	23.26	0.68	-21.64	0.65	1.62	0.04
A15/AGM x 100	-11.35	0.75	7.83	0.47	-3.51	0.31
(A14+A15)/AGM x 100	-29.91	1.10	-2.98	0.07	-32.80	1.15*
A2/A4	-2.88	0.07	-15.70	0.31	-18.58	0.38
A5/A10	6.87	0.09	-203.04	1.14*	-196.17	1.08*
A9/A11	22.05	0.43	12.67	0.38	34.72	0.78

*indicates a significant difference compared to the distribution of all taxa ($p < 0.05$)
[§]indicates a significant difference compared to the distribution of artiodactyls ($p < 0.05$)

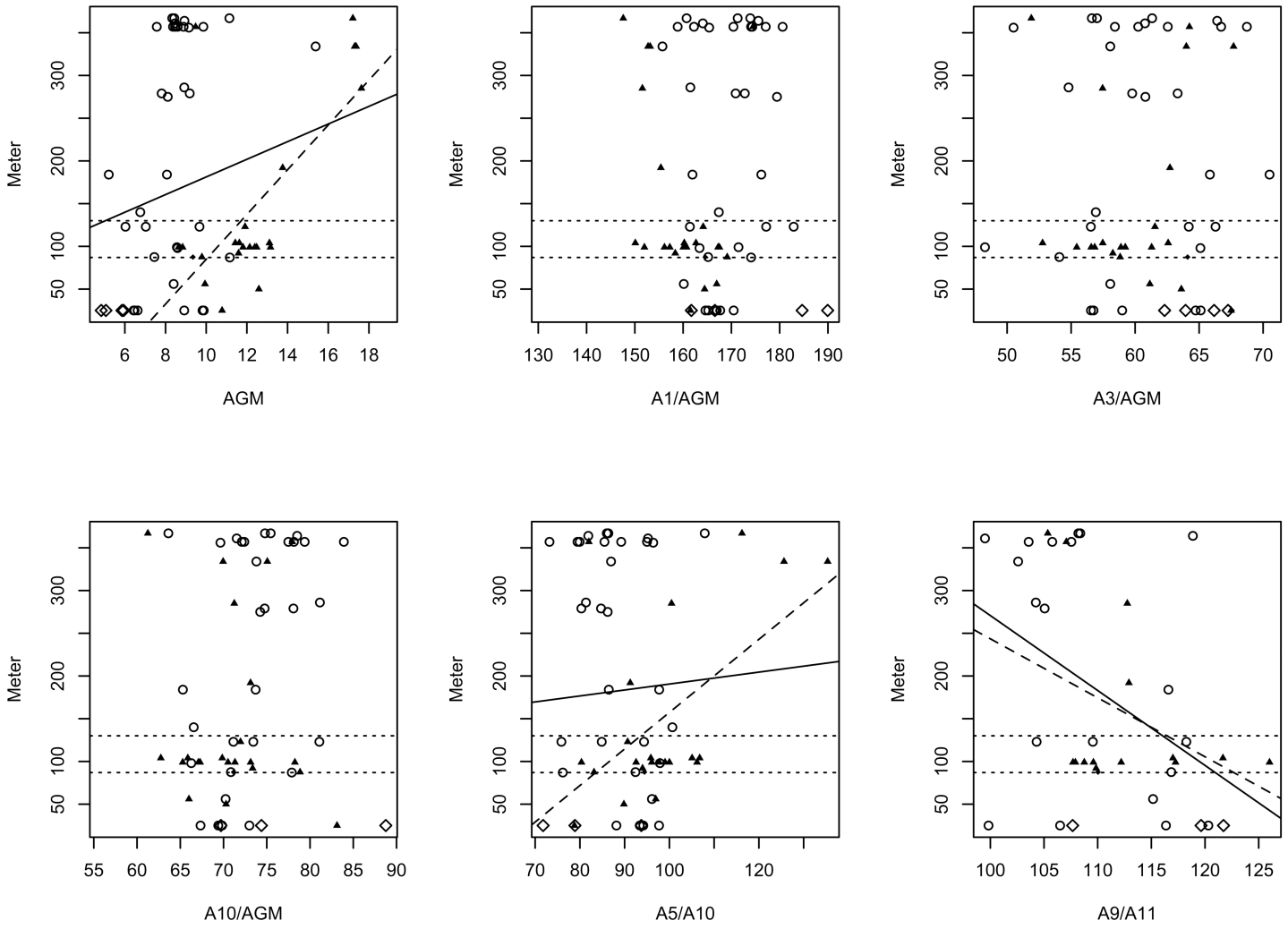
Meter
50
100
200
300
6
8
10
12
14
16
18
AGM
130
140
150
160
170
180
190
A1/AGM
50
55
60
65
70
A3/AGM
55
60
65
70
75
80
85
90
A10/AGM
70
80
90
100
120
A5/A10
100
105
110
115
120
125
A9/A11

Figure 7.1. Plots of variables by meter level showing the change in distribution of variables from oldest (bottom) to youngest (top) in the Uinta Formation. Dotted lines signify the divisions between FAZs. Variables with statistically significant correlations have regression lines plotted: solid lines represent all artiodactyls and dashed lines represent agriochoerids only. AGM, navicular ratio (A5/A10) and ratio of medial condyle to intermediate height (A9/11) all showed statistically significant correlations with meter level for agriochoerids only. Only A9/11 showed statistical significance for all artiodactyls. The rest of the variables seem to remain stable throughout the section and do not show a strong directional signal. ○ = unidentified artiodactyls; ▲ = agriochoerids; ◆ = homacodonts; ◇ = protoceratids.

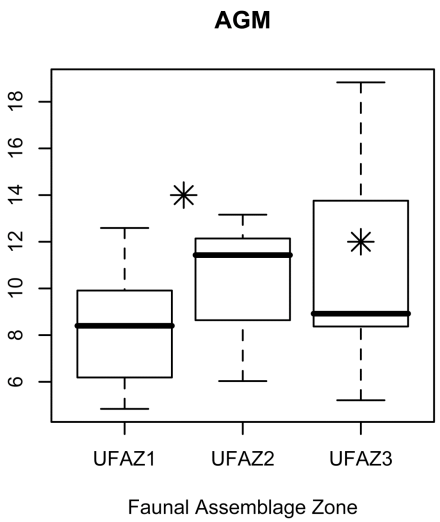
AGM
6
8
10
12
14
16
18
UFAZ1
UFAZ2
UFAZ3
Faunal Assemblage Zone

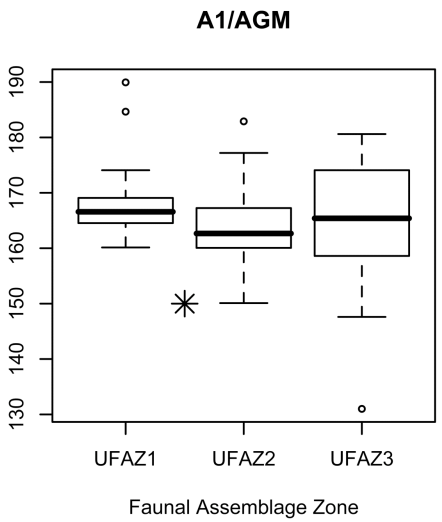
A1/AGM
130
140
150
160
170
180
190
UFAZ1
UFAZ2
UFAZ3
Faunal Assemblage Zone

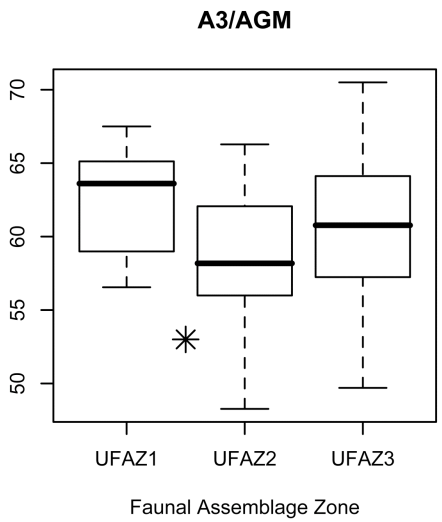
A3/AGM
50
55
60
65
70
UFAZ1
UFAZ2
UFAZ3
Faunal Assemblage Zone

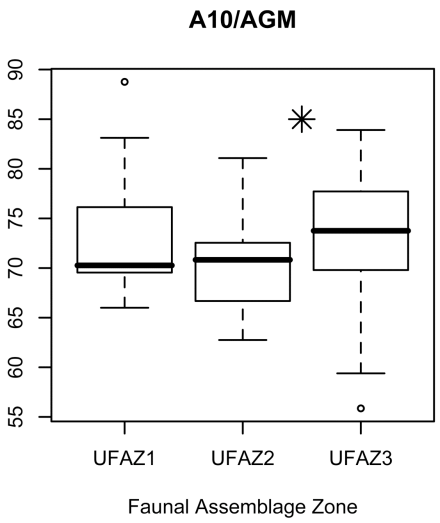
A10/AGM
55
60
65
70
75
80
85
90
UFAZ1
UFAZ2
UFAZ3
Faunal Assemblage Zone

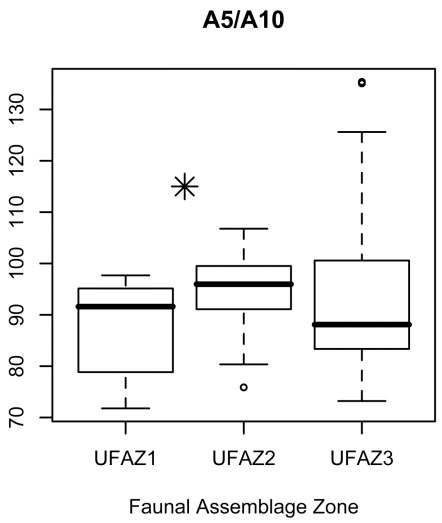
A5/A10
70
80
90
100
110
120
130
UFAZ1
UFAZ2
UFAZ3
Faunal Assemblage Zone

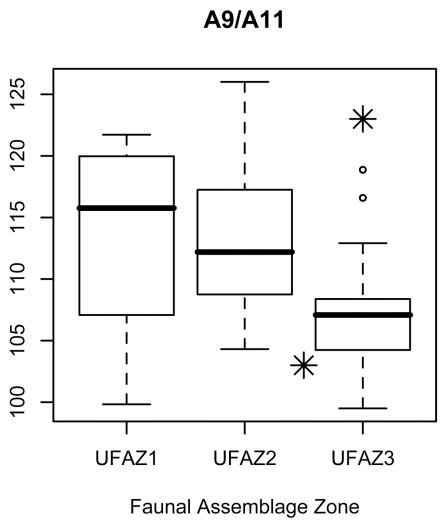
A9/A11
100
105
110
115
120
125
UFAZ1
UFAZ2
UFAZ3
Faunal Assemblage Zone

Figure 7.2. Box pots of all variables with significant results for the fossil sample separated by FAZ. The dark bar represents the median and the box connects the upper and lower quartiles. Whiskers extend to the minimum and maximum points unless the values of those points lie more than 1.5 times the interquartile range from the upper or lower hinge, in which case they are marked separately as outliers. Asterisks between FAZ indicate a significant difference; asterisks marking UFAZ 3 indicate a difference between UFAZ 1 and UFAZ 3.

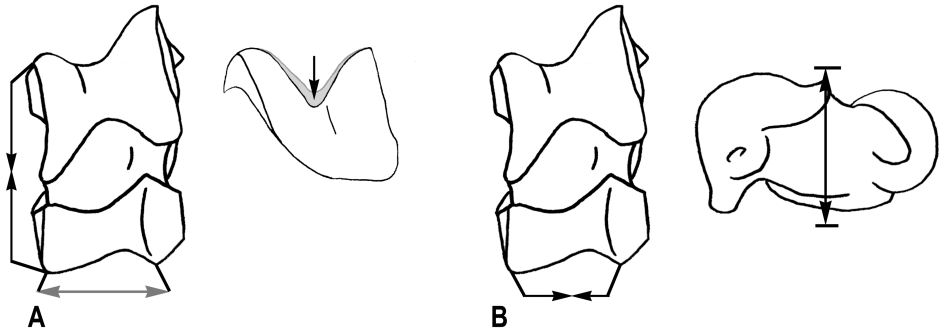

Figure 7.3. Diagram of artiodactyl astragali **A**, in dorsal (left) and posterior (right) views representing the dimensions for which artiodactyl astragali from UFAZ 2 differ from those from UFAZ 1; **B**, in dorsal (left) and medial (right) views representing the dimensions for which artiodactyl astragali from UFAZ 3 differ from those from UFAZ 1 and UFAZ 2. Gray arrows indicate that the difference is consistent with a shift from an open-country to a closed-country morphology, black arrows indicate that the difference is consistent with a shift from a closed-country to an open-country morphology. Note that most morphological differences are consistent with a shift from a more mobile closed-country morphology to a more stable open-country morphology; the one exception occurs between UFAZ 1 and UFAZ 2 (the navicular facet of UFAZ 2 artiodactyls is wider than those of UFAZ 1 artiodactyls).

CHAPTER EIGHT

Summary and Conclusions

8.1 Introduction

The primary goal of this dissertation is to examine how functional adaptations of several mammalian taxa evolved as a response to habitat change that was occurring during the Uintan as represented by the Uinta Formation, and to discuss the implications of these results for the dwindling primate populations there. I reached this objective through a series of steps. First, I described new skeletal material from primates and other mammals to reconstruct members of the Uintan faunal community (Chapters Two, Three, Four and Five). This step provided an in-depth look into the paleobiology of primates and other members of the primate community. Second, I identified metrics that discriminate the shape of the astragali and distal humeri in open-country from closed-country mammals in a broad range of mammalian taxa (Chapter Six). This analysis provided a necessary framework within which to evaluate morphological evolution in Uintan artiodactyls. Finally, I used these metrics to analyze changes in morphology of Uintan artiodactyl astragali stratigraphically in an ecomorphological context (Chapter Seven). This project is the first to document ecomorphological trends across such a wide range of extant mammal taxa and the first to trace morphological evolution of artiodactyl astragali using precise stratigraphic data.

Previous studies concerning the lithology and ecological diversity of fossil communities throughout the Uinta Formation have documented changing environments

from woodlands to more open habitats and have suggested that the decline of primates is linked to the loss of trees (Bradley 1937; Gazin 1958; Townsend 2004). However, relatively few attempts have been made to examine adaptations in primates and other groups of mammals for evidence of a response to climate change. In Chapter One I developed four predictions based upon the hypothesis that mammals from the Uinta Formation were evolving to live in an open habitat. In this chapter I summarize the main conclusions of my dissertation in reference to those listed in Chapter One and discuss the significance of these results for primate evolution.

8.2 Postcranial Morphology of Uintan Mammals

In Chapter One, I predicted that mammal skeletons from late Uintan deposits in the Uinta Formation would show more terrestrial and cursorial adaptations compared to their relatives from early Uintan localities in the UF. I have shown that this is true for some taxa and not others. The two groups of mammals (primates and pantolestids) that do not become more terrestrial in the late Uintan become extremely rare or extinct at the end of this period; the group that upholds my prediction (rodents) continues to radiate in later time periods. The results are discussed below for primates, rodents, insectivores and pantolestids. Artiodactyls are discussed in a later section of the chapter.

8.2.1 Primates

In Chapter Two I report on new primate hindlimb elements from two early Uintan genera, *Ourayia* and *Chipetaia*, and one late Uintan genus *Mytonius*. The new postcranial elements of *Ourayia* and *Chipetaia* suggest that these taxa were arboreal leapers that probably also engaged in vertical clinging and support previous interpretations of locomotor behavior (Dunn et al. 2006). Although the new elements of *Mytonius* are

fragmentary, they suggest that this genus was also arboreal, and may have relied less on leaping and more on climbing. Primates did not uphold my prediction and retained arboreal adaptations in the late Uintan.

8.2.2 Rodents

In Chapter Three I described new postcranial elements from *Uintaparamys leptodus* from the early Uintan and a complete skeleton of *Pseudotomus eugenei* from the late Uintan. In contrast to previous analyses, I suggested that *U. leptodus* was arboreal based upon features of the shoulder, elbow and pes (Wood 1962). The skeleton of *P. eugenei* indicates that this taxon was terrestrial and probably semi-fossorial. Rodents did exhibit a trend consistent with my prediction.

8.2.3 Insectivores

In Chapter Four, I described postcranial elements of *Zionodon*, a hedgehog-like insectivore. This genus is found only in the early Uintan, and thus I could not compare the morphology with a later-occurring relative. I reconstructed this genus as terrestrial, but not cursorial, perhaps habitually traveling over uneven substrates such as a forest floor. In order to test my prediction, I would need to identify a relative of *Zionodon* from the late Uintan.

8.2.4 Pantolestidae

In Chapter Five, I described postcranial elements of pantolestids, otter-like primitive mammals, from the early Uintan Washakie Formation and Uinta Formation and those from the late Uintan of the UF. Based upon these elements, I suggested that pantolestids remained committed to rivers throughout the Uintan much like their

ancestors in the Bridgerian. Pantolestids did not become more terrestrial, and did not uphold my prediction.

8.3 Ecomorphology in Extant Mammals

I predicted that the distal humeri and astragali of closed-country taxa would be distinguishable from those of open-country taxa in a diverse sample of mammals based on biomechanical principles and previous research (Andersson 2004; Carrano 1997; DeGusta and Vrba 2003; Rose 1988; Rose 1993; Van Valkenburgh 1987). In Chapter Six, I was able to identify five measurements of the distal humerus and nine measurements of the astragalus that differ consistently between closed-country and open-country mammals using a pairwise sign test and Mann-Whitney paired-comparisons tests.

8.4 Ecomorphology of Uintan Artiodactyls

In Chapter One I predicted that the shape of the astragalus of artiodactyls from late Uintan of the Uinta Formation would differ from that of artiodactyls from the early Uintan in the same way as open-country taxa differ from closed-country taxa, thus suggesting that artiodactyls from the late Uintan are more adapted for movement in open-country habitats. I specifically predicted that the two early Uintan FAZs (UFAZ1 and UFAZ2) would be more similar to each other than either was to UFAZ3, signifying that the major change in habitat occurred between UFAZ2 and UFAZ3. In Chapter Seven, I reported that artiodactyl astragali accumulate morphological changes that are consistent with a shift from a closed-country to an open-country morphology. This was broadly consistent with my predictions. However, I did not find that these changes occurred mainly between UFAZ2 and UFAZ3, but that they were distributed evenly between FAZs. This suggests that artiodactyl morphology evolved gradually throughout the

Uintan, perhaps reflecting a more gradual shift in habitat than has been suggested previously (Townsend 2004).

8.5 Significance for Uintan Primate Diversity

The sharp decline in primate diversity and abundance between Bridgerian and Uintan NALMAs and throughout the Uintan NALMA in the continental interior of North America has long been noted. This decline has been attributed to the loss of forested habitats in this region based upon taxonomic radiation and dental specialization of artiodactyls, lithological changes and changes in mammal community structure, and the higher diversity of primates in southern localities that likely retained a more tropical habitat until later. (Bradley 1937; Gazin, 1958; Peterson (in Osborn) 1985; Rasmussen et al. 1999; Gunell and Rose 2002; Townsend 2004; Townsend et al. 2006; Williams and Kirk 2008). In this dissertation I have added another perspective to the issue of Uintan primate decline. I have found that the mammalian lineages that continue to radiate after the Uintan (rodents and artiodactyls) show more terrestrial adaptations in the late Uintan than in the early Uintan, whereas those that become more scarce or go extinct after the Uintan (primates and pantolestids) retain the same adaptations in the late Uintan as their ancestors from the early Uintan. What this suggests is that those groups that were able to adapt to the more open environment of the late Uintan were the ones to survive, whereas those that did not or could not adapt to the increasingly arid conditions became extinct. While this may seem like common sense, these patterns have not been documented previously within specific groups of mammals. My results strengthen the link between primate decline and deforestation in the middle Eocene.

APPENDIX A. RAW MEASUREMENTS FOR PRIMATES (IN MM).

Table A.1. Measurements of extant primates.

			Femur				Tibia	
Taxon	**Specimen No.**	**Family**	**Length from head**	**Length from greater**	**Depth of condyles**	**Width of condyles**	**Length**	**Distal width**
Cheirogaleus major	USNM 85653	Cheirogaleidae	54.38	54.78	7.74	8.08	56.38	6.01
Microcebus murinus	USNM 83655	Cheirogaleidae	25.21	25.25	3.68	3.72	30.91	2.59
Daubentonia madagascariensis	USNM 305066	Daubentoniidae	127.17	127.19	14.86	16.87	125.66	9.21
Daubentonia madagascariensis	USNM 199694	Daubentoniidae	–	–	–	–	–	–
Varecia variegata	USNM 538407	Lemuridae	144.19	145.85	19.69	20.77	133.65	15.25
Eulemur mongoz	USNM 337946	Lemuridae	104.90	106.27	13.24	13.85	103.07	8.13
Eulemur fulvus	USNM 589434	Lemuridae	132.70	135.39	17.53	18.71	134.15	12.77
Lemur catta	USNM 589559	Lemuridae	140.80	144.08	18.75	19.37	131.64	11.46
Hapalemur griseus	USNM 83668	Lemuridae	99.42	101.36	12.92	12.65	96.84	7.67
Propithecus diadema	USNM 06350	Indriidae	–	–	27.19	26.55	194.00	16.46
Avahi laniger	USNM 83651	Indriidae	137.36	138.74	17.51	15.74	118.47	9.67
Lepilemur mustelinus	USNM 49668	Megaladapidae	107.82	110.75	15.24	14.19	98.49	10.33
Perodicticus potto	USNM 49547	Lorisidae	80.08	79.21	9.77	14.32	81.08	9.43
Loris tardigradus	USNM 265737	Lorisidae	70.13	69.53	5.77	8.06	69.19	5.07
Nycticebus coucang	USNM 395654	Lorisidae	91.55	89.04	11.47	13.88	85.90	10.22
Arctocebus calabarensis	USNM 511930	Lorisidae	62.69	62.57	6.98	8.51	56.53	6.09
Galago alleni	USNM 49548	Galagidae	67.65	67.18	8.29	7.80	61.77	5.76

			Femur				Tibia	
Taxon	**Specimen No.**	**Family**	**Length from head**	**Length from greater**	**Depth of condyles**	**Width of condyles**	**Length**	**Distal width**
Galago crassicaudatus	USNM 397662	Galagidae	92.96	92.63	12.12	12.02	88.30	9.90
Galago senegalensis	USNM 397967	Galagidae	59.78	59.83	8.18	7.02	57.45	5.94
Tarsius bancanus	USNM 578570	Tarsiidae	68.47	68.18	7.72	6.25	67.35	7.03
Tarsius spectrum	USNM 49404	Tarsiidae	61.00	60.68	7.56	6.27	59.96	6.20
Tarsius syrichta	USNM 282761	Tarsiidae	55.92	56.57	7.21	5.77	56.88	6.95
Aotus trivirgatus	USNM 267589	Aotidae	87.08	86.08	10.03	12.37	89.16	7.94
Chiropotes satanas	USNM 339661	Pithecidae	135.66	134.79	14.41	19.53	125.23	12.78
Cebus apella	USNM 397258	Cebidae	121.38	121.94	12.91	17.63	114.23	11.40
Saimiri oerstedii	USNM 582701	Cebidae	91.29	90.74	10.19	12.43	91.03	7.41
Callimico goeldii	USNM 464991	Callitrichidae	72.41	72.00	9.15	11.10	72.12	7.06
Leontopithecus rosalia	USNM 58111	Callitrichidae	73.03	73.13	8.64	10.86	76.33	5.41
Callithrix jacchus	USNM 503889	Callitrichidae	54.97	54.89	7.17	8.53	54.43	5.07
Saguinas oedipus	USNM 501097	Callitrichidae	65.00	64.97	8.28	10.24	67.07	5.67
Cebuella pygmaea	USNM 336325	Callitrichidae	36.92	36.96	4.49	5.67	38.01	3.37

	Tibia		Astragalus				
Taxon	Distal depth	Proximal width	Total width	Total length	Trochlear width	Head width	Head depth
Cheirogaleus major	5.51	8.85	5.57	9.76	4.04	3.19	2.48
Microcebus murinus	2.33	3.88	2.56	4.58	1.72	1.66	1.37
Daubentonia madagascariensis	10.21	16.47	–	–	–	–	–
Daubentonia madagascariensis	–	–	10.73	17.80	6.77	8.05	5.76
Varecia variegata	11.81	21.40	12.90	21.12	8.34	8.76	6.42
Eulemur mongoz	7.65	14.15	8.73	14.06	5.95	5.29	4.17
Eulemur fulvus	10.21	17.85	11.16	16.89	7.82	6.94	5.20
Lemur catta	10.99	19.26	11.72	17.03	8.09	7.88	5.59
Hapalemur griseus	7.43	12.50	8.60	13.18	5.56	5.46	3.95
Propithecus diadema	15.68	27.19	16.29	24.75	12.87	12.55	8.82
Avahi laniger	8.59	16.16	9.35	16.46	6.06	6.27	5.16
Lepilemur mustelinus	8.86	14.02	9.41	14.77	6.14	5.80	4.41
Perodicticus potto	9.13	13.15	8.94	11.04	4.84	6.14	3.55
Loris tardigradus	5.21	7.85	–	–	–	–	–
Nycticebus coucang	7.98	14.47	9.30	11.78	4.73	7.04	3.65
Arctocebus calabarensis	5.40	8.42	–	–	–	–	–
Galago alleni	4.51	7.86	5.23	8.99	3.49	3.25	2.77
Galago crassicaudatus	7.89	12.23	8.83	13.69	5.90	5.49	4.33
Galago senegalensis	4.79	7.48	5.39	7.91	3.76	3.27	2.65
Tarsius bancanus	3.63	6.85	4.60	6.66	3.37	2.97	2.59

	Tibia		Astragalus				
Taxon	**Distal depth**	**Proximal width**	**Total width**	**Total length**	**Trochlear width**	**Head width**	**Head depth**
Tarsius spectrum	3.37	6.14	4.08	5.54	3.08	2.57	2.09
Tarsius syrichta	3.62	6.21	4.23	6.73	3.46	2.94	2.55
Aotus trivirgatus	7.07	12.58	7.61	12.73	5.50	5.01	3.86
Chiropotes satanas	9.23	18.08	12.29	17.05	9.32	7.95	6.62
Cebus apella	8.68	16.79	10.58	15.94	7.89	7.25	5.58
Saimiri oerstedii	6.81	11.74	7.83	11.16	5.40	5.16	4.03
Callimico goeldii	5.25	10.42	6.23	10.12	4.67	4.53	2.94
Leontopithecus rosalia	6.69	10.19	6.07	8.73	4.58	4.29	3.12
Callithrix jacchus	3.92	8.30	4.69	7.14	3.64	3.14	2.58
Saguinas oedipus	4.45	9.40	5.72	8.83	3.81	3.46	2.96
Cebuella pygmaea	3.14	5.28	3.11	4.80	2.17	2.24	1.75

Taxon	Medial condyle length	Lateral condyle length	Trochlear length	Medial depth	Lateral depth	Navicular Length	Proximal width
Cheirogaleus major	4.65	4.70	4.60	4.54	4.04	6.57	3.96
Microcebus murinus	2.06	2.15	2.09	1.92	1.79	6.07	2.06
Daubentonia madagascariensis	–	–	–	–	–	–	–
Daubentonia madagascariensis	9.99	8.63	9.50	8.51	7.52	7.05	9.74
Varecia variegata	10.09	9.84	11.02	10.91	9.63	10.42	12.75
Eulemur mongoz	6.32	6.24	6.56	6.77	6.14	10.01	6.56
Eulemur fulvus	7.52	8.66	9.18	8.63	7.47	11.94	8.68
Lemur catta	7.64	8.50	8.47	8.28	7.11	12.19	8.99
Hapalemur griseus	5.57	6.49	6.55	6.39	5.78	9.91	6.63
Propithecus diadema	13.28	11.99	12.26	13.58	10.31	10.61	16.11
Avahi laniger	8.20	8.17	8.48	7.65	5.82	7.93	8.74
Lepilemur mustelinus	6.35	7.50	7.60	6.50	6.16	11.60	7.15
Perodicticus potto	6.96	6.35	8.00	4.81	4.90	5.12	9.69
Loris tardigradus	–	–	–	–	–	–	–
Nycticebus coucang	8.07	5.60	7.98	5.82	5.67	4.45	10.34
Arctocebus calabarensis	–	–	–	–	–	3.72	6.45
Galago alleni	4.86	4.78	4.67	4.16	3.54	20.10	5.25
Galago crassicaudatus	7.03	7.39	7.38	6.06	5.94	27.10	9.41
Galago senegalensis	4.26	4.27	4.43	3.83	3.28	22.42	4.25
Tarsius bancanus	4.15	3.69	3.77	3.53	2.32	22.44	3.66

Taxon	Medial condyle length	Lateral condyle length	Trochlear length	Medial depth	Lateral depth	Navicular Length	Proximal width
Tarsius spectrum	3.47	3.48	3.39	3.13	2.03	20.71	3.31
Tarsius syrichta	3.95	3.48	3.51	3.51	2.23	20.72	4.77
Aotus trivirgatus	6.60	6.43	6.47	6.36	5.17	6.02	6.63
Chiropotes satanas	10.31	10.87	10.82	9.76	7.57	10.04	10.60
Cebus apella	9.71	9.20	9.36	8.08	7.41	8.28	9.88
Saimiri oerstedii	7.06	7.14	7.21	6.58	5.33	6.30	7.20
Callimico goeldii	5.28	4.94	5.16	5.13	4.25	4.09	6.73
Leontopithecus rosalia	5.30	5.46	4.93	4.49	3.89	4.02	6.17
Callithrix jacchus	4.58	4.08	4.51	3.62	3.22	3.51	5.27
Saguinas oedipus	5.49	5.15	4.74	4.56	3.63	4.11	5.92
Cebuella pygmaea	3.21	2.63	2.68	2.18	2.18	2.34	3.32

	Calcaneus						
Taxon	**Distal width**	**Length**	**Proximal length**	**Ectal facet length**	**Cuboid facet height**	**Cuboid facet width**	**Distal length**
Cheirogaleus major	5.45	14.26	7.37	3.63	2.65	3.07	6.89
Microcebus murinus	3.07	8.36	3.29	1.68	1.35	1.61	5.07
Daubentonia madagascariensis	–	–	–	–	–	–	–
Daubentonia madagascariensis	–	23.37	13.40	7.54	7.03	5.01	9.97
Varecia variegata	–	28.20	17.37	9.78	6.47	8.38	10.83
Eulemur mongoz	9.21	20.56	10.65	5.42	3.94	5.86	9.91
Eulemur fulvus	11.27	27.26	14.39	8.27	5.69	6.46	12.87
Lemur catta	12.10	25.83	14.79	7.11	5.43	6.81	11.04
Hapalemur griseus	8.82	18.51	9.32	5.26	4.00	4.99	9.19
Propithecus diadema	–	31.69	18.75	10.42	9.71	8.38	12.94
Avahi laniger	–	21.35	12.36	8.27	5.29	6.11	8.99
Lepilemur mustelinus	9.46	24.05	12.78	5.14	4.37	5.67	11.27
Perodicticus potto		12.81	8.16	4.03	5.68	4.22	4.65
Loris tardigradus	–	–	–	–	–	–	–
Nycticebus coucang	–	18.17	9.80	4.47	5.41	4.18	8.37
Arctocebus calabarensis	–	9.23	5.33	2.39	3.11	2.84	3.90
Galago alleni	4.73	25.58	7.46	2.80	2.83	2.20	18.12
Galago crassicaudatus	7.86	34.97	11.85	5.09	4.89	4.35	23.12
Galago senegalensis	5.46	28.20	7.46	2.97	2.63	2.76	20.74
Tarsius bancanus	4.57	28.67	6.27	3.18	2.57	2.31	22.40

	Calcaneus						
Taxon	**Distal width**	**Length**	**Proximal length**	**Ectal facet length**	**Cuboid facet height**	**Cuboid facet width**	**Distal length**
Tarsius spectrum	4.02	26.27	6.02	3.04	1.99	2.28	20.25
Tarsius syrichta	3.57	26.35	6.23	2.75	2.89	2.27	20.12
Aotus trivirgatus	–	18.96	10.24	5.71	3.89	5.43	8.72
Chiropotes satanas	–	26.75	15.87	8.62	5.52	8.50	10.88
Cebus apella	–	24.70	12.83	5.88	4.95	7.35	11.87
Saimiri oerstedii	–	18.02	9.76	5.32	3.60	5.21	8.26
Callimico goeldii	–	14.85	8.24	4.26	3.13	4.72	6.61
Leontopithecus rosalia	–	14.62	8.18	4.09	2.94	4.35	6.44
Callithrix jacchus	–	11.62	6.15	3.04	2.71	3.49	5.47
Saguinas oedipus	–	13.76	7.69	4.29	3.09	4.21	6.07
Cebuella pygmaea	–	7.57	4.12	1.99	1.64	2.28	3.45

Taxon	Cuboid Length	Calcaneal facet depth	Calcaneal facet width	Metatarsal facet depth	Metatarsal facet width
Cheirogaleus major	6.04	2.65	3.42	2.58	3.12
Microcebus murinus	3.51	1.33	1.62	1.36	1.39
Daubentonia madagascariensis	–	–	–	–	–
Daubentonia madagascariensis	10.60	4.26	7.49	5.05	6.78
Varecia variegata	13.73	6.05	8.83	6.13	7.77
Eulemur mongoz	8.83	4.15	5.78	3.73	5.70
Eulemur fulvus	10.63	4.72	7.41	5.04	6.67
Lemur catta	11.85	5.42	7.98	5.17	7.35
Hapalemur griseus	9.00	3.52	5.51	4.05	4.42
Propithecus diadema	16.02	7.66	10.24	8.26	8.88
Avahi laniger	9.42	5.04	6.43	4.60	6.43
Lepilemur mustelinus	9.42	4.40	5.73	4.18	5.25
Perodicticus potto	6.23	3.88	5.53	3.97	3.73
Loris tardigradus	–	–	–	–	–
Nycticebus coucang	7.88	6.26	3.70	4.10	5.25
Arctocebus calabarensis	3.53	3.51	3.02	2.55	2.78
Galago alleni	7.56	2.55	2.51	2.33	2.64
Galago crassicaudatus	12.05	3.64	5.47	4.28	4.22
Galago senegalensis	6.69	2.48	2.61	2.15	2.53
Tarsius bancanus	3.86	2.08	2.79	2.52	1.75

Taxon	Cuboid Length	Calcaneal facet depth	Calcaneal facet width	Metatarsal facet depth	Metatarsal facet width
Tarsius spectrum	3.63	1.82	2.29	2.23	1.65
Tarsius syrichta	3.75	1.89	2.54	1.72	2.37
Aotus trivirgatus	7.01	3.21	6.45	3.64	4.08
Chiropotes satanas	9.65	5.18	8.67	5.16	7.06
Cebus apella	8.52	4.31	6.92	4.86	5.98
Saimiri oerstedii	6.59	3.29	5.72	3.59	4.36
Callimico goeldii	5.23	2.93	4.59	3.17	3.70
Leontopithecus rosalia	4.86	2.94	4.70	3.23	3.82
Callithrix jacchus	3.94	2.26	3.68	2.73	2.91
Saguinas oedipus	4.47	2.75	4.72	3.05	3.67
Cebuella pygmaea	3.49	1.52	2.48	1.69	1.99

Table A.2. Measurements of fossil primates (in mm).

			Femur		Astragalus		
Taxon	**Specimen No.**	**Family**	**Depth of condyles**	**Width of condyles**	**Total width**	**Total length**	**Trochlear width**
Smilodectes gracilis	AMNH 131762	Notharctidae	–	–	10.29	17.50	6.84
Notharctus tenebrosus	AMNH 131935	Notharctidae	–	–	10.33	18.51	7.03
Notharctus tenebrosus	AMNH 131772	Notharctidae	–	–	–	–	–
Notharctus sp.	YPM 12159	Omomyidae	17.77	17.41	–	–	–
Notharctus sp.	YPM 12159	Omomyidae	18.60	17.03	–	–	–
Notharctus sp.	YPM 12156	Notharctidae	17.50	17.59	11.83	19.09	7.82
Notharctus tenebrosus	YPM 12906	Notharctidae	–	–	–	–	–
Notharctus tenebrosus	YPM 12959	Notharctidae	17.59	17.95	–	–	–
Notharctus tenebrosus	YPM 12959	Notharctidae	17.25	17.44	–	–	–
Notharctus sp.	YPM 39817	Notharctidae	–	–	–	–	–
Notharctus sp.	YPM 39816	Notharctidae	–	–	14.63	22.82	9.13
Notharctus sp.	YPM 44468	Notharctidae	–	–	–	–	–
Notharctus sp.	YPM 44458	Notharctidae	–	–	–	–	–
Cantius trigonodus/abditus	USGS 5900	Notharctidae	16.14	15.33	–	–	–
Cantius sp.	USGS 4724	Notharctidae	15.58	15.01	–	–	–
Cantius cf. *mckennai*	USGS 25029	Notharctidae	–	–	–	–	–
Hemiacodon gracilis	YPM 24461	Omomyidae	–	–	4.75	8.44	3.56
Hemiacodon gracilis	YPM 24458	Omomyidae	–	–	4.72	8.33	3.69
Hemiacodon gracilis	YPM 24456	Omomyidae	–	–	4.90	8.79	3.55
Hemiacodon gracilis	YPM 24455	Omomyidae	–	–	4.51	7.98	3.49
Hemiacodon gracilis	YPM 24474	Omomyidae	–	–	–	–	–
Hemiacodon gracilis	YPM 24475	Omomyidae	–	–	–	–	–
Hemiacodon gracilis	YPM 24462	Omomyidae	–	–	4.86	8.51	3.61

Taxon	Specimen No.	Family	Femur		Astragalus		
			Depth of condyles	Width of condyles	Total width	Total length	Trochlear width
Hemiacodon gracilis	YPM 24463	Omomyidae	–	–	4.72	8.16	3.57
Hemiacodon gracilis	YPM 24464	Omomyidae	–	–	5.10	8.35	3.40
Hemiacodon gracilis	YPM 24473	Omomyidae	–	–	4.37	7.68	3.26
Hemiacodon gracilis	YPM 24457	Omomyidae	–	–	–	–	–
Hemiacodon gracilis	YPM 24466	Omomyidae	–	–	4.74	8.45	3.75
Hemiacodon gracilis	YPM 24467	Omomyidae	–	–	4.91	8.56	3.49
Hemiacodon gracilis	YPM 24472	Omomyidae	–	–	–	–	–
Hemiacodon gracilis	YPM 24711	Omomyidae	–	–	–	–	–
Hemiacodon gracilis	YPM 30461	Omomyidae	–	–	4.86	8.43	3.52
Hemiacodon gracilis	YPM 44511	Omomyidae	–	–	–	–	–
Hemiacodon gracilis	YPM 44526	Omomyidae	–	–	–	–	–
Hemiacodon gracilis	YPM 44526	Omomyidae	–	–	–	–	–
Hemiacodon gracilis	YPM 44520	Omomyidae	–	–	–	–	–
Hemiacodon gracilis	YPM 44520	Omomyidae	–	–	–	–	–
Hemiacodon gracilis	YPM 13600	Omomyidae	–	–	–	–	–
Hemiacodon gracilis	YPM 44515	Omomyidae	9.25	9.04	–	–	–
Chipetaia lamporea	CM 71178	Omomyidae	–	–	4.53	8.99	3.64
Chipetaia lamporea	CM 70904	Omomyidae	–	–	–	–	–
Chipetaia lamporea	CM 70914	Omomyidae	–	–	–	–	4.26
Chipetaia lamporea	CM 80208	Omomyidae	–	–	–	–	3.94
Chipetaia lamporea	CM 80235	Omomyidae	–	–	–	–	4.30
Chipetaia lamporea	CM 80253	Omomyidae	–	–	–	–	3.90
Chipetaia lamporea	CM 71168	Omomyidae	–	–	–	–	–
Ourayia uintensis	AMNH 2019	Omomyidae	–	–	–	–	–
Ourayia uintensis	CM 71130	Omomyidae	15.19	12.94	–	–	–

Taxon	Specimen No.	Family	Femur		Astragalus		
			Depth of condyles	Width of condyles	Total width	Total length	Trochlear width
Ourayia uintensis	CM 70902	Omomyidae	–	–	–	–	6.28
Ourayia uintensis	CM 80247	Omomyidae	–	–	–	–	6.41
Ourayia uintensis	CM 70905	Omomyidae	–	–	–	–	6.19
Ourayia uintensis	CM 80587	Omomyidae	–	–	–	–	–
Ourayia uintensis	CM 70918	Omomyidae	–	–	–	–	–
Ourayia uintensis	CM 70917	Omomyidae	–	–	–	–	–
Ourayia uintensis	CM 70920	Omomyidae	–	–	–	–	–
Ourayia sp.	SDNM 4020	Omomyidae	–	–	–	–	–
Mytonius hopsoni	CM 80586	Omomyidae	–	–	–	–	5.71
Mytonius hopsoni	CM 71174	Omomyidae	–	–	–	–	–
cf. omomyidae	CM 71158	Omomyidae	–	–	–	–	–

Taxon	Astragalus Neck length	Head width	Head depth	Medial condyle	Lateral condyle	Ectal facet length	Ectal facet width	Trochlear length
Smilodectes gracilis	6.55	6.81	5.22	8.45	8.22	7.86	4.43	–
Notharctus tenebrosus	7.11	7.70	5.89	9.89	9.18	–	–	–
Notharctus tenebrosus	–	–	–	–	–	–	–	–
Notharctus sp.	–	–	–	–	–	–	–	–
Notharctus sp.	–	–	–	–	–	–	–	–
Notharctus sp.	8.41	7.41	5.57	9.73	8.23	7.14	4.33	9.55
Notharctus tenebrosus	–	–	–	–	–	–	–	–
Notharctus tenebrosus	–	–	–	–	–	–	–	–
Notharctus tenebrosus	–	–	–	–	–	–	–	–
Notharctus sp.	–	–	–	–	–	–	–	–
Notharctus sp.	9.38	9.30	7.74	10.33	11.46	9.51	5.28	11.20
Notharctus sp.	–	–	–	–	–	–	–	–
Notharctus sp.	–	–	–	–	–	–	–	–
Cantius trigonodus/abditus	–	–	–	–	–	–	–	–
Cantius sp.	–	–	–	–	–	–	–	–
Cantius cf. *mckennai*	–	–	–	–	–	–	–	–
Hemiacodon gracilis	4.19	3.25	2.80	4.18	4.25	3.49	2.17	4.23
Hemiacodon gracilis	3.90	3.09	2.77	4.40	4.98	3.66	1.96	4.75
Hemiacodon gracilis	4.52	3.46	2.73	4.17	4.17	3.46	2.20	4.19
Hemiacodon gracilis	4.26	2.97	2.37	4.04	4.36	3.18	1.79	4.28
Hemiacodon gracilis	–	–	–	–	–	–	–	–
Hemiacodon gracilis	–	–	–	–	–	–	–	–
Hemiacodon gracilis	4.32	3.15	2.62	4.43	4.62	3.28	2.16	4.71
Hemiacodon gracilis	3.55	3.16	2.45	4.49	4.46	3.58	2.12	4.53

Taxon	Astragalus Neck length	Head width	Head depth	Medial condyle	Lateral condyle	Ectal facet length	Ectal facet width	Trochlear length
Hemiacodon gracilis	3.66	2.90	2.73	4.40	4.62	3.56	1.95	4.79
Hemiacodon gracilis	3.94	2.87	2.64	3.83	4.16	3.05	1.69	4.17
Hemiacodon gracilis	–	–	–	–	–	–	–	–
Hemiacodon gracilis	3.61	3.39	2.71	4.29	4.54	3.68	2.16	4.81
Hemiacodon gracilis	3.86	3.26	2.73	4.12	4.20	3.05	2.23	4.39
Hemiacodon gracilis	–	–	–	–	–	–	–	–
Hemiacodon gracilis	–	–	–	–	–	–	–	–
Hemiacodon gracilis	3.99	3.23	2.77	4.14	4.65	3.65	2.23	4.80
Hemiacodon gracilis	–	–	–	–	–	–	–	–
Hemiacodon gracilis	–	–	–	–	–	–	–	–
Hemiacodon gracilis	–	–	–	–	–	–	–	–
Hemiacodon gracilis	–	–	–	–	–	–	–	–
Hemiacodon gracilis	–	–	–	–	–	–	–	–
Hemiacodon gracilis	–	–	–	–	–	–	–	–
Hemiacodon gracilis	–	–	–	–	–	–	–	–
Chipetaia lamporea	4.31	3.07	2.60	4.18	4.59	–	–	4.86
Chipetaia lamporea	–	–	–	–	–	–	–	–
Chipetaia lamporea	–	–	–	4.85	5.40	–	–	5.61
Chipetaia lamporea	–	–	–	4.92	5.34	–	–	5.32
Chipetaia lamporea	–	3.38	2.66	5.07	5.33	–	–	5.38
Chipetaia lamporea	–	–	–	–	–	–	–	–
Chipetaia lamporea	–	–	–	–	–	–	–	–
Ourayia uintensis calcaneus	–	–	–	–	–	–	–	–
Ourayia uintensis	–	–	–	–	–	–	–	–

Taxon	Astragalus Neck length	Head width	Head depth	Medial condyle	Lateral condyle	Ectal facet length	Ectal facet width	Trochlear length
Ourayia uintensis	–	–	–	6.26	7.90	–	–	7.77
Ourayia uintensis	–	–	–	7.19	8.29	–	–	8.40
Ourayia uintensis	–	–	–	7.16	8.64	–	–	8.52
Ourayia uintensis	–	5.47	3.89	–	–	–	–	–
Ourayia uintensis	–	–	–	–	–	–	–	–
Ourayia uintensis	–	–	–	–	–	–	–	–
Ourayia uintensis	–	–	–	–	–	–	–	–
Ourayia sp.	–	–	–	–	–	–	–	–
Mytonius hopsoni	–	–	–	7.33	7.68	–	–	7.75
Mytonius hopsoni	–	–	–	–	–	–	–	–
cf. omomyidae	–	–	–	–	–	–	–	–

	Navicular					Calcaneus			
Taxon	Medial height	Lateral height	Length	Proximal width	Distal width	Length	Proximal length	Ectal facet width	Ectal facet length
Smilodectes gracilis	8.71	8.06	–	–	–	–	–	–	–
Notharctus tenebrosus	9.41	8.01	–	–	–	–	–	–	–
Notharctus tenebrosus	–	–	–	–	–	–	–	–	–
Notharctus sp.	–	–	–	–	–	–	–	–	–
Notharctus sp.	–	–	–	–	–	–	–	–	–
Notharctus sp.	9.55	8.53	–	–	–	24.49	14.03	7.35	3.62
Notharctus tenebrosus	–	–	–	–	–	26.24	15.08	8.72	3.81
Notharctus tenebrosus	–	–	8.91	8.08	9.19	24.69	14.18	7.94	3.64
Notharctus tenebrosus	–	–	–	–	–	24.49	13.82	7.84	3.30
Notharctus sp.	–	–	–	–	–	25.06	14.74	7.11	3.62
Notharctus sp.	11.79	10.16	–	–	–	–	–	–	–
Notharctus sp.	–	–	–	–	–	–	–	–	–
Notharctus sp.	–	–	–	–	–	–	–	–	–
Cantius trigonodus/abditus	–	–	–	–	–	–	–	–	–
Cantius sp.	–	–	–	–	–	–	–	–	–
Cantius cf. *mckennai*	–	–	8.11	6.29	6.83	–	–	–	–
Hemiacodon gracilis	4.14	3.79	–	–	–	–	–	–	–
Hemiacodon gracilis	4.47	3.94	9.04	4.77	3.82	–	–	–	–
Hemiacodon gracilis	4.42	3.87	–	–	–	–	–	–	–
Hemiacodon gracilis	–	–	–	–	–	–	–	–	–
Hemiacodon gracilis	–	–	–	–	–	13.92	6.17	2.49	1.79
Hemiacodon gracilis	–	–	–	–	–	15.63	7.58	2.97	1.84
Hemiacodon gracilis	4.40	3.65	–	–	–	–	–	–	–
Hemiacodon gracilis	4.11	3.49	–	–	–	–	–	–	–

	Navicular					Calcaneus			
Taxon	Medial height	Lateral height	Length	Proximal width	Distal width	Length	Proximal length	Ectal facet width	Ectal facet length
Hemiacodon gracilis	4.32	3.68	–	–	–	–	–	–	–
Hemiacodon gracilis	4.02	3.10	–	–	–	–	–	–	–
Hemiacodon gracilis	–	–	–	–	–	15.77	7.69	3.44	1.77
Hemiacodon gracilis	4.55	3.87	–	–	–	–	–	–	–
Hemiacodon gracilis	4.37	3.67	–	–	–	–	–	–	–
Hemiacodon gracilis	–	–	–	–	–	14.98	7.32	2.85	2.00
Hemiacodon gracilis	–	–	–	–	–	16.33	7.99	3.30	2.38
Hemiacodon gracilis	4.72	3.63	–	–	–	–	–	–	–
Hemiacodon gracilis	–	–	6.94	3.94	3.81	–	–	–	–
Hemiacodon gracilis	–	–	–	–	–	–	–	–	–
Hemiacodon gracilis	–	–	–	–	–	–	–	–	–
Hemiacodon gracilis	–	–	–	–	–	–	–	–	–
Hemiacodon gracilis	–	–	–	–	–	–	–	–	–
Hemiacodon gracilis	–	–	–	–	–	15.44	7.40	3.03	1.91
Hemiacodon gracilis	–	–	–	–	–	–	–	–	–
Chipetaia lamporea	4.26	3.18	–	–	–	–	–	–	–
Chipetaia lamporea	–	–	11.08	4.91	6.17	–	–	–	–
Chipetaia lamporea	4.82	3.76	–	–	–	–	–	–	–
Chipetaia lamporea	4.02	3.88	–	–	–	–	–	–	–
Chipetaia lamporea	–	–	–	–	–	–	–	–	–
Chipetaia lamporea	–	–	–	–	–	–	9.28	3.73	2.51
Chipetaia lamporea	–	–	–	–	–	–	8.26	3.44	2.05
Ourayia uintensis calcaneus	–	–	–	–	–	–	–	5.40	3.67
Ourayia uintensis	–	–	–	–	–	–	–	–	–

	Navicular					Calcaneus			
Taxon	**Medial height**	**Lateral height**	**Length**	**Proximal width**	**Distal width**	**Length**	**Proximal length**	**Ectal facet width**	**Ectal facet length**
Ourayia uintensis	6.48	5.84	–	–	–	–	–	–	–
Ourayia uintensis	6.36	6.37	–	–	–	–	–	–	–
Ourayia uintensis	7.23	6.77	–	–	–	–	–	–	–
Ourayia uintensis	–	–	–	–	–	–	–	–	–
Ourayia uintensis	–	–	–	–	–	–	–	–	–
Ourayia uintensis	–	–	12.92	6.82	7.55	–	–	–	–
Ourayia uintensis	–	–	12.86	7.09	7.80	–	–	–	–
Ourayia sp.	–	–	–	–	–	22.34	11.22	5.90	3.14
Mytonius hopsoni	5.91	5.83	–	–	–	–	–	–	–
Mytonius hopsoni	–	–	–	–	–	–	9.45	4.98	3.05
cf. omomyidae	–	–	–	–	–	–	5.88	2.26	1.61

Taxon	Sustentacular facet length	Sustentacular facet width	Cuboid facet depth	Cuboid facet width	Distal length	Cuboid Length	Calcaneal facet length
Smilodectes gracilis	–	–	–	–	–	–	–
Notharctus tenebrosus	–	–	–	–	–	–	–
Notharctus tenebrosus	–	–	–	–	–	10.37	5.37
Notharctus sp.	–	–	–	–	–	–	–
Notharctus sp.	–	–	–	–	–	–	–
Notharctus sp.		4.58	5.63		10.46	–	–
Notharctus tenebrosus	10.95	4.80	6.14	8.78	11.16	–	–
Notharctus tenebrosus	–	3.61	5.65	–	10.51	–	–
Notharctus tenebrosus	10.46	4.34	5.58	7.08	10.67	–	–
Notharctus sp.	10.25	4.11	5.33	7.79	10.32	–	–
Notharctus sp.	–	–	–	–	–	–	–
Notharctus sp.	–	–	–	–	–	11.82	4.89
Notharctus sp.	–	–	–	–	–	11.17	5.07
Cantius trigonodus/abditus	–	–	–	–	–	–	–
Cantius sp.	–	–	–	–	–	–	–
Cantius cf. *mckennai*	–	–	–	–	–	8.93	3.52
Hemiacodon gracilis	–	–	–	–	–	–	–
Hemiacodon gracilis	–	–	–	–	–	–	–
Hemiacodon gracilis	–	–	–	–	–	–	–
Hemiacodon gracilis	–	–	–	–	–	–	–
Hemiacodon gracilis	–	–	2.68	3.35	7.75	–	–
Hemiacodon gracilis	–	–	2.78	3.55	8.05	–	–
Hemiacodon gracilis	–	–	–	–	–	–	–
Hemiacodon gracilis	–	–	–	–	–	–	–

Taxon	Sustentacular facet length	Sustentacular facet width	Cuboid facet depth	Cuboid facet width	Distal length	Cuboid Length	Calcaneal facet length
Hemiacodon gracilis	–	–	–	–	–	–	–
Hemiacodon gracilis	–	–	–	–	–	–	–
Hemiacodon gracilis	6.68	1.76	2.63	3.56	8.08	–	–
Hemiacodon gracilis	–	–	–	–	–	–	–
Hemiacodon gracilis	–	–	–	–	–	–	–
Hemiacodon gracilis	7.20	1.79	–	–	7.66	–	–
Hemiacodon gracilis	–	2.31	–	–	8.34	–	–
Hemiacodon gracilis	–	–	–	–	–	–	–
Hemiacodon gracilis	–	–	–	–	–	–	–
Hemiacodon gracilis	–	–	–	–	–	7.95	3.11
Hemiacodon gracilis	–	–	–	–	–	7.19	2.71
Hemiacodon gracilis	–	–	–	–	–	–	–
Hemiacodon gracilis	–	–	–	–	–	–	–
Hemiacodon gracilis	6.97	1.53	2.78	3.43	8.04	–	–
Hemiacodon gracilis	–	–	–	–	–	–	–
Chipetaia lamporea	–	–	–	–	–	–	–
Chipetaia lamporea	–	–	–	–	–	–	–
Chipetaia lamporea	–	–	–	–	–	–	–
Chipetaia lamporea	–	–	–	–	–	–	–
Chipetaia lamporea	–	–	2.96	4.17	–	–	–
Chipetaia lamporea	–	–	–	–	–	–	–
Chipetaia lamporea	–	–	–	–	–	–	–
Ourayia uintensis calcaneus	11.42	3.21	4.53	5.53	14.28	–	–
Ourayia uintensis	–	–	–	–	–	–	–

Taxon	Sustentacular facet length	Sustentacular facet width	Cuboid facet depth	Cuboid facet width	Distal length	Cuboid Length	Calcaneal facet length
Ourayia uintensis	–	–	–	–	–	–	–
Ourayia uintensis	–	–	–	–	–	–	–
Ourayia uintensis	–	–	–	–	–	–	–
Ourayia uintensis	–	–	–	–	–	11.30	4.78
Ourayia uintensis	–	–	–	–	–	11.77	4.47
Ourayia uintensis	–	–	–	–	–	–	–
Ourayia uintensis	–	–	–	–	–	–	–
Ourayia sp.	9.50	–	3.90	5.59	11.12	–	–
Mytonius hopsoni	–	–	–	–	–	–	–
Mytonius hopsoni	–	–	–	–	–	–	–
cf. omomyidae	–	–	–	–	–	–	–

Taxon	Calcaneal facet width	MT facet depth	MT facet width
Smilodectes gracilis	–	–	–
Notharctus tenebrosus	–	–	–
Notharctus tenebrosus	7.26	4.28	5.93
Notharctus sp.	–	–	–
Notharctus sp.	–	–	–
Notharctus sp.	–	–	–
Notharctus tenebrosus	–	–	–
Notharctus tenebrosus	–	–	–
Notharctus tenebrosus	–	–	–
Notharctus sp.	–	–	–
Notharctus sp.	–	–	–
Notharctus sp.	7.37	5.12	5.28
Notharctus sp.	7.33	4.97	5.96
Cantius trigonodus/abditus	–	–	–
Cantius sp.	–	–	–
Cantius cf. *mckennai*	5.61	3.39	–
Hemiacodon gracilis	–	–	–
Hemiacodon gracilis	–	–	–
Hemiacodon gracilis	–	–	–
Hemiacodon gracilis	–	–	–
Hemiacodon gracilis	–	–	–
Hemiacodon gracilis	–	–	–
Hemiacodon gracilis	–	–	–
Hemiacodon gracilis	–	–	–

Taxon	Calcaneal facet width	MT facet depth	MT facet width
Hemiacodon gracilis	–	–	–
Hemiacodon gracilis	–	–	–
Hemiacodon gracilis	–	–	–
Hemiacodon gracilis	–	–	–
Hemiacodon gracilis	–	–	–
Hemiacodon gracilis	–	–	–
Hemiacodon gracilis	–	–	–
Hemiacodon gracilis	–	–	–
Hemiacodon gracilis	–	–	–
Hemiacodon gracilis	4.36	2.63	2.87
Hemiacodon gracilis	4.39	2.26	2.67
Hemiacodon gracilis	–	–	–
Hemiacodon gracilis	–	–	–
Hemiacodon gracilis	–	–	–
Hemiacodon gracilis	–	–	–
Chipetaia lamporea	–	–	–
Chipetaia lamporea	–	–	–
Chipetaia lamporea	–	–	–
Chipetaia lamporea	–	–	–
Chipetaia lamporea	–	–	–
Chipetaia lamporea	–	–	–
Chipetaia lamporea	–	–	–
Ourayia uintensis calcaneus	–	–	–
Ourayia uintensis	–	–	–

Taxon	Calcaneal facet width	MT facet depth	MT facet width
Ourayia uintensis	–	–	–
Ourayia uintensis	–	–	–
Ourayia uintensis	–	–	–
Ourayia uintensis	6.61	4.00	4.44
Ourayia uintensis	5.66	–	–
Ourayia uintensis	–	–	–
Ourayia uintensis	–	–	–
Ourayia sp.	–	–	–
Mytonius hopsoni	–	–	–
Mytonius hopsoni	–	–	–
cf. omomyidae	–	–	–

APPENDIX B. RAW MEASUREMENTS FOR RODENTS (IN MM).

				Glenoid		Humerus			
Taxon	**Specimen No.**	**Family**	**Behavior**	**Width**	**Length**	**Length**	**Distal width**	**Distal articular surface width**	**Trochlear depth**
Manitsha tanka	AMNH 3908	Ischyromyidae	–	–	–	120.4	33.3	21.2	14.1
Pseudotomus eugenei	CM 71105	Ischyromyidae	–	–	–	95.7	33.6	21.4	12.4
Pseudotomus petersoni	AMNH 2018	Ischyromyidae	–	–	–	–	–	–	–
Pseudotomus robustus	AMNH 13091	Ischyromyidae	–	–	–	–	25.1	15.7	9.5
Anomalurus pelii	FMNH 62223	Anomaluridae	Arboreal	6.65	9.49	95.15	13.57	10.33	6.43
Coendu mexicanus	FMNH 15611	Erethizontidae	Arboreal	7.35	9.72	67.52	17.26	11.73	9.2
Erethizon dorsatum	FMNH 47173	Erethizontidae	Arboreal	11.54	17.23	103.68	25.89	18.99	15.12
Phloeomys sp.	FMNH 101751	Muridae	Arboreal	6.13	10.75	58.37	17.61	9.87	6.99
Aeromys thomasi	FMNH 90437	Sciuridae	Arboreal	6.38	10.07	94.94	12.66	8.88	5.76
Petaurista magnifica	FMNH 114365	Sciuridae	Arboreal	6.25	9.09	84.55	12.54	9.11	6.07
Ratufa bicolor	FMNH 46649	Sciuridae	Arboreal	6.11	10.9	72.31	17.86	11.74	7.06
Sciurus carolinensis	FMNH 156885	Sciuridae	Arboreal	4.35	7.16	45.45	11.76	6.84	4.59
Aplodontia rufa	FMNH 41388	Aplodontidae	Fossorial	5.49	9.21	49	16.16	8.83	5.98
Castor canadensis	FMNH 44871	Castoridae	Fossorial	12.55	18.39	86.29	34.5	19.85	9.98
Ondatra zibethicus	FMNH 34897	Cricetidae	Fossorial	4.62	6.56	40.28	14.08	7.41	4.47
Myocastor coypus	FMNH 49892	Myocastoridae	Fossorial	9.23	16.6	76.36	22.79	14.15	10.37
Cynomys ludovicianus	FMNH 60483	Sciuridae	Fossorial	4.88	8.26	44.48	12.79	7.98	5.53
Marmota monax	FMNH 41087	Sciuridae	Terrestrial	8.83	15.02	78.04	23.16	13.9	10.01
Cuniculus paca	FMNH 152058	Agoutidae	Terrestrial	10.05	12.87	83.05	20.08	14.84	11.02
Capromys piloroides	FMNH 47770	Capromyidae	Terrestrial	8.03	14.01	72.9	19.41	14.33	8.51
Cavia porcellus	FMNH 122239	Caviidae	Terrestrial	4.31	5.9	38.78	7.69	5.34	4.22
Dasyprocta leporina	FMNH 46207	Dasyproctidae	Terrestrial	8.86	10.82	87.89	14.6	10.9	9.06
Dinomys branickii	FMNH 166523	Dinomyidae	Terrestrial	12.23	19.16	117.48	31.03	21.37	15.49
Hydrochoerus hydrochoerus	FMNH 60735	Hydrochoeridae	Terrestrial	20.86	25.7	180.5	39.45	25.41	23.52
Hystrix africaeaustralis	FMNH 47389	Hystricidae	Terrestrial	16.18	19.61	103.77	31.4	19.81	16.23
Trichys fasciculate	FMNH 68750	Hystricidae	Terrestrial	6.46	8.21	54.15	12.3	8.86	6.12
Cricetomys gambianus	FMNH 177861	Nesomyidae	Terrestrial	4.98	7.89	47.69	13.25	7.97	5.14
Thryonomys gergorianus	FMNH 108212	Thryonomyidae	Terrestrial	6.77	9.14	60.61	12.52	9.82	7.91

	Humerus			Radius				
Taxon	Trochlear width	Head length	Head width	Length	Maximum head width	Minimum head width	Minimum distal width	Maximum distal width
Manitsha tanka	14.7	–	–	98.6	14.5	10.2	–	–
Pseudotomus eugenei	14.9	–	–	82.8	12.3	9.1	–	–
Pseudotomus petersoni	–	–	–	–	–	–	–	–
Pseudotomus robustus	10.7	–	–	–	–	–	–	–
Anomalurus pelii	6.89	10.72	9.32	85.42	5.93	5.14	4.26	5.01
Coendu mexicanus	7.38	11.23	8.85	61.97	8.32	6.02	4.3	6.89
Erethizon dorsatum	12.72	20.01	17.03	106.86	12.95	10.47	8.74	13.02
Phloeomys sp.	7.29	11.31	9.27	51.55	6.77	4.97	3.47	6.03
Aeromys thomasi	6.09	9.59	9.17	94.38	7.34	5.62	3.98	5.56
Petaurista magnifica	7	10.05	8.23	84.14	7.79	6.03	4.26	5.92
Ratufa bicolor	6.97	11.06	9.5	58.67	8.09	6.73	5.35	7.42
Sciurus carolinensis	4.25	6.98	6.1	43.83	5.01	4.2	2.62	4.22
Aplodontia rufa	5.17	8.96	6.77	45.58	6.31	4.33	3.55	7.12
Castor canadensis	11.76	16.73	16.49	92.73	12.69	8.46	6.61	8.22
Ondatra zibethicus	5.29	7.39	5.95	40.07	5.18	2.93	2.21	3.97
Myocastor coypus	12.86	14.56	10.66	84.99	10.48	7.18	5.3	9.27
Cynomys ludovicianus	5.5	7.05	6.99	42.27	5.6	3.96	2.48	5.27
Marmota monax	9.15	15.24	13.4	67.24	10.33	7.14	5.25	8.09
Cuniculus paca	9.87	14.87	13.96	66.24	11.14	6.52	6.14	7.79
Capromys piloroides	9.5	15.56	11.26	66.6	9.85	6	4.32	8.34
Cavia porcellus	4.34	6.61	6.37	33.95	4.93	2.96	2.2	4.65
Dasyprocta leporina	7.74	12.83	11.46	83.03	9.17	6.33	5.21	6.69
Dinomys branickii	14.59	22.25	17.78	105.92	14.17	9.35	7.85	12.14
Hydrochoerus hydrochoerus	18.58	28.84	31.76	127.01	23.75	12.37	–	–
Hystrix africaeaustralis	13.97	20.56	20.95	86.17	14.62	9.44	8.86	14.46
Trichys fasciculate	5.76	8.77	8.8	40.63	5.97	3.5	4	4.37
Cricetomys gambianus	5.58	8.88	7.22	46.04	5.14	3.64	3.64	4.67
Thryonomys gergorianus	7.56	10.6	9.69	48.81	7.36	4.38	3.61	6.71

	Ulna					Metacarpal length				
Taxon	Length	Olecranon process length	Shaft length	Radial notch breadth	Trochlear notch breadth	MC I	MC II	MC III	MC IV	MC V
Manitsha tanka	126.3	25.2	101.1	7.9	8.5	–	23.6	31.9	–	23.7
Pseudotomus eugenei	106.9	22.7	84.2	6.2	8.5	–	24.7	30.1	27.5	21.7
Pseudotomus petersoni	–	–	–	–	–	–	–	–	–	–
Pseudotomus robustus	–	–	–	–	–	6.8	20.7	25.1	24.6	19.5
Anomalurus pelii	99.86	13.06	86.8	4.64	3.41	4.25	12.46	14.01	13.78	13.42
Coendu mexicanus	73.91	9.46	64.45	5.69	4.2	4.92	13.8	15.62	14.43	12.34
Erethizon dorsatum	131.03	19.64	111.39	10.46	7.73	6.01	18.58	21.02	20.67	16.92
Phloeomys sp.	64.75	11.23	53.52	5.08	3.74	–	13.58	15.11	14.03	9.75
Aeromys thomasi	104.46	6.72	97.74	3.78	3.19	–	–	–	–	–
Petaurista magnifica	95.49	8.28	87.21	3.87	2.85	2.73	10.29	13.26	15.12	13.21
Ratufa bicolor	70.02	11.15	58.87	5.5	4.13	2.82	–	17.13	18.1	12.36
Sciurus carolinensis	53.07	7.78	45.29	2.28	2.54	1.91	10.54	13.71	14.18	10.68
Aplodontia rufa	59.85	12.94	46.91	4.49	4.03	4.1	10.32	13.26	11.64	9.74
Castor canadensis	122.12	28.55	93.57	12.51	6.34	5.22	14.47	20.79	18.44	12.63
Ondatra zibethicus	52.55	9.92	42.63	4.93	2.09	2.24	7.16	10.23	8.47	5.35
Myocastor coypus	107.06	20.09	86.97	9.18	5.46	5.88	15.92	21.58	17.68	13.4
Cynomys ludovicianus	52.62	9.72	42.9	4.59	3.32	2.9	9.23	13.33	9.64	6.78
Marmota monax	86.12	17.47	68.65	8.11	5.87	3.66	20.16	22.82	20.23	16.5
Cuniculus paca	88.29	18.61	69.68	8.94	4.01	6.28	20.54	25.26	23.24	17.44
Capromys piloroides	85.32	16.33	68.99	7.17	5.69	4.87	15.42	20.46	19.3	15.12
Cavia porcellus	44.06	9.87	34.19	4.43	1.37	–	8.87	11.11	9.24	7.27
Dasyprocta leporina	98.9	15.25	83.65	6.44	2.96	5.75	28.04	30.74	26.07	16.32
Dinomys branickii	136.36	27.3	109.06	11.38	7.7	5.2	22.54	22.96	25.13	19.64
Hydrochoerus hydrochoerus	167.5	43.85	123.65	18.26	9.08	–	52.48	62.26	49.45	30.64
Hystrix africaeaustralis	116.04	27.46	88.58	12.91	7.49	4.77	24.82	28.04	26.95	23.03
Trichys fasciculate	52.52	10.95	41.57	4.5	3.36	4.42	13.46	15.82	13.93	10.09
Cricetomys gambianus	56.52	9.53	46.99	3.87	2.86	2.88	10.1	12.28	11.02	8
Thryonomys gergorianus	66.5	15.57	50.93	6.18	2.37	6.96	13.28	16.08	13.02	9.08

Taxon	Manual phalanges Length of proximal	Depth of ungual III	Length of ungual III	Femur Length from head	Length from greater trochanter	Head depth	Head width	Depth of condyles	Width of condyles
Manitsha tanka	21.1	–	17.4	–	–	–	–	–	–
Pseudotomus eugenei	13.1	8.0	16.7	–	134.7	–	–	30	34.6
Pseudotomus petersoni	–	–	–	–	–	–	–	24.1	22.4
Pseudotomus robustus	15.3	–	10.6	115.4	119.3	–	–	22.1	27.1
Anomalurus pelii	13.19	6.93	10.85	109.75	109.9	10.24	10	11.73	12.9
Coendu mexicanus	10.45	5.59	15.52	77.95	77.25	11.46	11.27	13.41	16.42
Erethizon dorsatum	12.12	7.97	20.79	116.7	116.57	17.93	17.84	24.01	26.09
Phloeomys sp.	10.92	5.3	9.52	70.12	71.03	10.2	10.26	13.62	15.04
Aeromys thomasi	–	–	–	112.29	113.81	8.18	8.09	11.58	12.25
Petaurista magnifica	13.56	5.94	–	107.06	107.96	8.43	8.45	11.94	12.53
Ratufa bicolor	14.62	6.85	8.57	86.6	86.11	10.4	10.36	13.12	15.51
Sciurus carolinensis	10.59	3.8	–	58.79	59.18	5.95	6.09	8.72	10.11
Aplodontia rufa	7.4	4.08	10.75	56.9	57.57	7.27	7.31	10.55	13.24
Castor canadensis	11.51	5.6	14.32	108.75	112.08	16.89	16.92	25.29	29.53
Ondatra zibethicus	6.96	3.14	7.14	48.52	49.09	7.17	7.1	11.74	11.39
Myocastor coypus	12.3	5.51	11.35	89.8	92.47	12.29	12.1	21.34	22.61
Cynomys ludovicianus	6.69	–	–	51.75	52.73	6.16	6.38	9.06	10.94
Marmota monax	13.04	5.01	12	87.11	87.63	10.9	10.95	16.5	19.63
Cuniculus paca	8.69	3.86	9.41	100.77	107.25	11.6	11.63	27.21	23.05
Capromys piloroides	10.48	5.14	8.93	87.14	89.13	11.92	11.95	18.62	20.02
Cavia porcellus	5.11	2.03	–	44.07	45.21	4.98	4.92	9.3	8.15
Dasyprocta leporina	9.51	4	9.17	101.99	107.75	11.15	10.96	25.18	20.96
Dinomys branickii	13.06	–	–	130.21	137.37	15.63	15.43	25.94	26.36
Hydrochoerus hydrochoerus	22.22	–	–	195.5	204.5	22.23	23.38	51	40.42
Hystrix africaeaustralis	13.6	8.24	16.11	114.35	122.53	16.73	16.53	24.85	29.66
Trichys fasciculate	7.73	–	–	60.38	64.5	7.45	7.25	12.38	12.56
Cricetomys gambianus	6.34	2.21	4.25	60.73	62.38	6.61	6.64	12.64	12.04
Thryonomys gergorianus	6.2	3.29	9.98	87.91	90.45	9.63	9.63	19.36	17.66

Taxon	Patellar groove width	Tibia Length	Distal width	Distal depth	Proximal depth	Proximal width	Medial condyle depth	Medial condyle width
Manitsha tanka	–	–	–	–	–	–	–	–
Pseudotomus eugenei	13.1	137	16.3	19.2	27.7	32.5	19.9	13.3
Pseudotomus petersoni	8.1	–	–	–	–	–	14.4	8.3
Pseudotomus robustus	10.2	124.9	12.7	14	20.3	25.8	15.4	10.1
Anomalurus pelii	7.21	114.11	7.42	7.34	11.3	13.52	8.68	5.72
Coendu mexicanus	7.42	73.34	8.74	7.65	14.64	18.59	11.18	7.06
Erethizon dorsatum	10.23	114.29	14.58	12.95	22.92	26.11	18.69	11.61
Phloeomys sp.	5.34	68.28	8.81	7.29	12.67	15.94	10.94	5.86
Aeromys thomasi	7.18	115.3	6.76	7.15	8.37	12.03	7.98	4.85
Petaurista magnifica	7.36	113.01	6.61	7.68	9.2	13.02	8.97	5.08
Ratufa bicolor	7.83	85.59	9.1	6.11	11.51	14.95	10.9	5.8
Sciurus carolinensis	4.38	67.16	5.67	5.16	6.97	10.08	3.93	6.68
Aplodontia rufa	4.96	58.17	7.08	5.96	9.61	12.68	8.06	4.89
Castor canadensis	14.03	134.4	17.3	15.61	25.9	29.81	19.93	13.61
Ondatra zibethicus	4.54	64.47	6.5	6.37	10.37	12.57	7.23	4.47
Myocastor coypus	7.84	111.69	11.11	8.81	16.61	22.1	14.04	8.36
Cynomys ludovicianus	4.4	53.2	5.41	5.59	8.16	10	6.71	4.22
Marmota monax	8.97	84.53	8.01	8.43	12.63	17.82	12.76	6.84
Cuniculus paca	8.18	99.05	11.82	11.3	18.07	23.08	14.66	8.38
Capromys piloroides	8.19	91.95	10.97	10.68	16.91	20.77	15.16	9.32
Cavia porcellus	3.1	50.66	5.23	4.21	7.24	8.45	6.54	3.32
Dasyprocta leporina	7.72	121.1	9.32	11.64	19.66	21.64	14.55	7.65
Dinomys branickii	15.19	131.33	15.72	14.07	22.72	29.09	20.53	11.95
Hydrochoerus hydrochoerus	16.97	196.5	22.38	18.73	36.98	41.64	29.67	17.89
Hystrix africaeaustralis	13.52	110.86	18.82	12.43	22.42	28.62	17.85	12.88
Trichys fasciculate	4.76	61.75	7.53	6.12	9.91	12.59	8.22	4.83
Cricetomys gambianus	3.57	68.71	6.8	5.47	10	11.96	8.15	4.99
Thryonomys gergorianus	5.53	78.99	9.29	8.02	15.17	16.84	13.13	7.37

Taxon	Lateral condyle depth	Lateral condyle width	Astragalus Width	Length	Condyle width	Neck length	Head width	Head depth
Manitsha tanka	–	–	–	–	–	–	–	–
Pseudotomus eugenei	18.9	14.1	21.2	24.6	14.4	10.4	15.1	8.9
Pseudotomus petersoni	15.3	10.9	–	–	–	7.5	11.4	5.6
Pseudotomus robustus	15.8	11.8	–	–	–	–	–	–
Anomalurus pelii	10.17	6.55	7.12	14.77	6.28	7.11	5.72	4.36
Coendu mexicanus	10.64	8.62	9.6	11.31	8.06	5.61	6.37	4.82
Erethizon dorsatum	16.13	11.62	15.28	17.25	12.35	7.83	8.85	6.77
Phloeomys sp.	11.23	7.14	9.51	10.48	8.27	6.37	6.36	4.81
Aeromys thomasi	8.28	6.43	–	–	–	–	–	–
Petaurista magnifica	9.38	6.33	8.07	13.49	5.96	5.82	6.67	5.08
Ratufa bicolor	11.38	7.55	8.8	13.16	7.87	6.55	7.44	4.79
Sciurus carolinensis	6.38	5.32	5.36	8.97	4.1	4.02	4.47	3.28
Aplodontia rufa	7.97	6.27	6.62	8.64	4.93	3.59	4.67	2.76
Castor canadensis	18.07	13.07	20.44	23.43	15.95	9.29	12.18	7.04
Ondatra zibethicus	8.57	5.2	7.93	9.34	4.67	4.75	5.11	3.17
Myocastor coypus	13.03	10.5	13.28	16.28	7.89	5.84	8.58	5.3
Cynomys ludovicianus	7.26	5.38	5.84	8.43	4.56	3.7	3.98	2.91
Marmota monax	11.62	8.64	10.8	12.55	7.51	4.53	7.17	5.3
Cuniculus paca	12.72	10.98	13.35	18.01	9.21	7.21	8.78	6.44
Capromys piloroides	14.41	9.87	12.76	14.39	7.76	5.11	8.84	6.68
Cavia porcellus	5.32	4.01	6.39	5.01	3.55	2.51	3.22	2.64
Dasyprocta leporina	14.92	10.22	11.08	17.65	6.7	7.84	9.01	5.31
Dinomys branickii	20.12	14.14	17.68	22.88	12.41	10.31	11.71	8.53
Hydrochoerus hydrochoerus	32.08	21.21	26.53	29.11	17.02	13.31	21.03	12.4
Hystrix africaeaustralis	18.38	13.22	18.3	18.94	13.13	6.55	10.53	8.86
Trichys fasciculate	7.46	6.19	8.08	9.9	5.77	4.15	4.56	3.77
Cricetomys gambianus	7.92	5.38	7.37	10.41	5.87	5.02	4.46	3.27
Thryonomys gergorianus	12.16	8.92	9.97	12.52	7.25	5.79	6.29	4.84

Taxon	Medial condyle length	Lateral condyle length	Ectal facet length	Ectal facet width	Sustentacular facet length	Sustentacular facet width	Calcaneus Length	Tuberosity length
Manitsha tanka	–	–	–	–	–	–	–	–
Pseudotomus eugenei	13.9	16.6	–	–	–	–	41	16.5
Pseudotomus petersoni	–	–	–	–	–	–	32.5	14.6
Pseudotomus robustus	–	–	–	–	–	–	–	–
Anomalurus pelii	5.31	7.33	6.32	4.19	5.31	3.52	20.44	4.83
Coendu mexicanus	6.94	8.13	6.88	3.81	5.6	4.14	15.97	6.11
Erethizon dorsatum	10.48	12.44	11.35	7.77	10.55	5.82	28.95	14
Phloeomys sp.	5.73	7.54	6.48	6.08	4.15	3.4	20.6	9.04
Aeromys thomasi	–	–	–	–	–	–	–	–
Petaurista magnifica	6.15	7.76	7.22	4.41	5.64	3.66	20.59	7.33
Ratufa bicolor	5.19	7.88	7.31	4.96	6.54	4.61	21.25	8.28
Sciurus carolinensis	4.02	5.58	4.71	2.95	4.39	2.4	13.82	5.22
Aplodontia rufa	5.01	5.26	4.87	3.63	4.28	2.75	14.61	5.19
Castor canadensis	14.6	15.11	12.55	11.56	17.28	6.45	49.93	28.98
Ondatra zibethicus	4.99	5.61	4.7	3.79	5.37	2.2	14.44	6.56
Myocastor coypus	11.01	9.44	9.36	8.27	11.12	5.37	31.97	14.07
Cynomys ludovicianus	4.3	5.66	4.83	3.31	5.25	2.47	12.81	4.58
Marmota monax	6.84	8.91	8	5.56	6.45	4.7	22.08	8.92
Cuniculus paca	10.69	10.5	7.77	7.21	10.96	4.68	33.73	14.25
Capromys piloroides	10.06	10.67	8.48	7.79	8.31	4.66	29.7	12.4
Cavia porcellus	4.79	4.13	3.32	3.41	3.82	1.61	13	5.58
Dasyprocta leporina	11.23	11.59	8.16	7.76	11.15	3.88	35.44	14.36
Dinomys branickii	14.96	13.93	11.46	11.14	15.02	7.26	42.67	17.56
Hydrochoerus hydrochoerus	21.85	19.85	18.3	13.34	15.44	10.33	69.89	33.92
Hystrix africaeaustralis	13.9	15.54	13.54	7.11	10.38	8.01	32.8	13.62
Trichys fasciculate	6.48	6.65	6.58	3.04	5.41	3.23	18.95	8.62
Cricetomys gambianus	4.52	6.06	5.76	4.44	3.24	2.51	17.05	7.16
Thryonomys gergorianus	7.88	8.58	7.86	6.11	7.72	3.65	28	10.52

Taxon	Tuberosity width	Tuberosity height	Ectal facet length	Ectal faced width	Sustentacular faced length	Sustentacular facet width	Cuboid facet length	Metatarsal length MT I	Metatarsal length MT II
Manitsha tanka	–	–	–	–	–	–	–	–	–
Pseudotomus eugenei	9.6	12.5	–	–	–	–	–	24.2	40.4
Pseudotomus petersoni	–	10.8	–	–	–	–	–	–	–
Pseudotomus robustus	–	–	–	–	–	–	–	25.8	39.7
Anomalurus pelii	2.76	5.78	6.48	2.77	3.88	3.48	5.26	17.86	23.07
Coendu mexicanus	4.01	7.22	6.41	4.65	4.66	3.8	4.86	9.75	16.31
Erethizon dorsatum	8.38	12.76	10.5	7.46	8.64	6.34	7.72	13.7	21.42
Phloeomys sp.	7	4.19	5.65	4.39	3.82	3.66	5.01	11.8	19.1
Aeromys thomasi	–	–	–	–	–	–	–	–	–
Petaurista magnifica	3.29	6.89	6.84	3.13	4.08	3.96	4.74	17.22	24.85
Ratufa bicolor	3.25	6.91	7.66	3.82	4.5	4.71	5.62	19.33	27.66
Sciurus carolinensis	2.15	5.3	4.33	2.22	2.5	2.75	3.05	17.85	23.27
Aplodontia rufa	3.02	4.72	5.07	2.76	3.05	2.67	3.91	9.98	16.61
Castor canadensis	17.33	14.11	9.99	10.42	17.04	5.75	13.16	29.3	40.44
Ondatra zibethicus	4.95	4.97	5.09	4.41	3.31	2.99	3.85	15.4	23.86
Myocastor coypus	11.89	7.52	9.08	6.37	6.28	4.29	6.83	23.24	35.81
Cynomys ludovicianus	3.13	4.73	4.23	2.66	3.17	2.87	3.2	10.43	17.08
Marmota monax	4.53	8.31	7.68	3.77	4.27	4.81	5.48	16.38	26.7
Cuniculus paca	6.47	10.15	8.62	5.17	5.14	5.03	5.68	–	29.53
Capromys piloroides	8.27	8.16	7.83	5.82	6.45	5.9	6.8	15.37	25.78
Cavia porcellus	3.01	3.81	3.43	2.57	2.54	2.1	3.18	–	15.41
Dasyprocta leporina	5.74	10.26	6.45	6.3	5.39	5.18	8.02	–	48.16
Dinomys branickii	15.89	12.89	9.69	8.69	12.88	5.7	8.74	11.88	31.95
Hydrochoerus hydrochoerus	11.62	21.99	18.01	10.93	11.09	11.7	12.42	–	57.41
Hystrix africaeaustralis	9.67	14.88	13.37	6.88	9.5	8.72	8.82	13.11	24.7
Trichys fasciculate	3.85	5.78	6.33	2.83	4.27	2.89	4.71	11.42	17.61
Cricetomys gambianus	3.64	4.77	4.87	3.22	2.67	2.79	4.18	15.04	23.23
Thryonomys gergorianus	6.48	6.44	7.6	5.09	4.94	3.99	6.45	5.69	19.7

Taxon	MT III	MT IV	MT V	Pedal phalanges Proximal phalanx III	Depth of ungual III	Length of ungual III
Manitsha tanka	–	–	–	–	–	–
Pseudotomus eugenei	47.8	45.3	31.8	19.7	10.4	–
Pseudotomus petersoni	–	–	–	–	–	–
Pseudotomus robustus	45.7	43.9	32.5	20.3	–	14.4
Anomalurus pelii	24.11	26.38	25.63	12.34	–	–
Coendu mexicanus	16.79	17.01	16.35	11.09	5.95	15.68
Erethizon dorsatum	22.88	25.05	24.85	12.8	8.79	20.34
Phloeomys sp.	20.72	20.99	15.79	13.04	6.9	12.92
Aeromys thomasi	–	–	–	–	–	–
Petaurista magnifica	25.43	26.78	24.76	12.63	5.83	–
Ratufa bicolor	29.4	31.7	26.6	14.37	6.9	9.42
Sciurus carolinensis	23.75	25.34	21.86	11.31	3.94	–
Aplodontia rufa	16.29	16.78	14.59	7.4	3.65	7.31
Castor canadensis	47.25	54.06	35.38	28.86	7.32	18.39
Ondatra zibethicus	23.11	26.8	21.27	13.29	4.55	8.73
Myocastor coypus	44.68	40.95	27.82	26.14	6.43	13.71
Cynomys ludovicianus	17.79	16.91	12.52	7.63	–	–
Marmota monax	27.62	27.51	21.37	13.96	5.17	10.42
Cuniculus paca	32.67	32.53	15.3	11	5.17	13.07
Capromys piloroides	26.52	28.11	21.58	11.31	6.49	13.27
Cavia porcellus	15.93	13.63	–	6.36	3.29	6.8
Dasyprocta leporina	50.23	45.39	–	18.46	5.4	15.02
Dinomys branickii	37.29	38.9	–	14.93	–	–
Hydrochoerus hydrochoerus	62.05	55.38	13.97	30.47	–	–
Hystrix africaeaustralis	28.18	28.54	24.69	13.21	7.3	12.83
Trichys fasciculate	20.14	20.08	15.19	9.04	–	–
Cricetomys gambianus	22.93	23.44	18.2	7.67	2.97	6.38
Thryonomys gergorianus	21.97	19.78	12.09	10.59	5.76	–

APPENDIX C. RAW MEASUREMENTS FOR PANTOLESTID TARSALS (IN MM)

		Astragalus						
Taxon	**Spec. No.**	**Width**	**Length**	**Trochlear width**	**Head width**	**Head depth**	**Medial condyle length**	**Lateral condyle length**
Pantolestes natans	AMNH 12152	23.53	20.77	17.24	11.08	7.36	13.07	12.78
Pantolestes	YPM 43229	7.27	8.42	5.68	4.89	3.41	5.51	5.73
Pantolestes	YPM 43230	11.45	12.80	9.45	7.78	5.18	7.80	9.94
Pantolestes	YPM 43236	11.23	13.00	9.34	7.66	5.22	7.90	8.25
Pantolestes	YPM 43238	10.49	12.31	8.46	7.22	4.77	7.07	7.89
Pantolestes	YPM 43234	7.30	8.77	5.36	5.13	3.54	5.55	5.30
Pantolestes	YPM 43239	7.06	8.53	5.26	5.00	2.99	5.07	5.10
Pantolestes	YPM 43241	12.97	15.61	10.80	8.82	5.53	9.12	9.77
Pantolestes	YPM 43242	–	14.46	9.16	8.02	5.78	8.74	8.68
Pantolestes	YPM 43244	11.04	12.85	9.63	7.19	5.73	6.67	8.18
Pantolestes	YPM 43243	12.34	13.66	10.26	7.41	5.03	8.17	9.43
Palaeosinopa ?incerta	USNM 493930	10.20	12.59	7.15	6.33	4.27	6.99	8.23
Pantolestidae	CM 71159	12.17	15.01	9.16	8.50	4.97	9.16	8.53
Pantolestidae	CM 71001	–	–	–	6.94	4.44	–	–
Pantolestidae	CM 71090	–	–	–	–	–	–	–
Pantolestidae	CM 71110	–	–	–	–	–	–	–
Pantolestidae	CM 71137	–	–	–	–	–	–	–
Pantolestidae	CM 71160	–	–	–	–	–	–	–
Pantolestidae	00-171	–	–	–	–	–	–	–
Pantolestidae	DMNH 29877	–	–	–	–	–	–	–
Pantolestidae	DMNH 2321	14.07	17.97	11.52	10.08	6.57	11.98	12.50
Pantolestes sp.	YPM-PU 17272a	–	–	–	–	–	–	–
Pantolestes sp.	YPM-PU 17272b	–	–	–	–	–	–	–

	Astragalus							Calcaneus
Taxon	Ectal facet length	Ectal facet width	Sustentacular facet length	Sustentacular facet width	Trochlear length	Medial condyle height	Lateral condyle height	Length
Pantolestes natans	10.73	12.28	9.61	5.28	–	–	–	41.45
Pantolestes	4.46	4.59	4.52	2.66	5.67	4.85	3.60	–
Pantolestes	7.37	6.14	–	–	9.11	7.27	6.21	–
Pantolestes	0.89	6.34	6.88	3.80	8.49	7.14	6.24	–
Pantolestes	6.80	7.21	7.14	3.34	7.88	6.94	5.84	–
Pantolestes	5.26	4.00	4.25	2.74	5.30	4.63	3.84	–
Pantolestes	4.25	4.10	4.88	2.80	4.87	4.44	3.68	–
Pantolestes	7.78	7.53	7.34	3.76	10.07	8.48	7.48	–
Pantolestes	7.00	7.59	6.75	3.63	9.10	8.39	6.32	–
Pantolestes	6.95	6.75	8.26	3.08	8.78	7.10	6.44	–
Pantolestes	7.53	7.74	8.01	3.02	9.14	8.06	6.64	–
Palaeosinopa ?incerta	6.48	6.59	4.71	3.98	7.13	6.37	5.66	23.50
Pantolestidae	7.34	8.73	8.61	4.25	8.42	7.82	6.88	
Pantolestidae	–	–	–	–	–	–	–	–
Pantolestidae	–	–	–	–	–	–	–	–
Pantolestidae	–	–	–	–	–	–	–	–
Pantolestidae	–	–	–	–	–	–	–	–
Pantolestidae	–	–	–	–	–	–	–	–
Pantolestidae	–	–	–	–	–	–	–	–
Pantolestidae	–	–	–	–	–	–	–	–
Pantolestidae	8.90	9.28	7.46	4.58	12.24	10.33	9.32	
Pantolestes sp.	–	–	–	–	–	–	–	32.63
Pantolestes sp.	–	–	–	–	–	–	–	18.44

	Calcaneus							
Taxon	**Tuberosity length**	**Tuberosity width**	**Ectal facet length**	**Ectal facet width**	**Fibular facet width**	**Ectal process width**	**Proximal length**	**Cuboid facet height**
Pantolestes natans	28.26	8.51	9.19	8.30	6.42	13.33	–	–
Pantolestes	–	–	–	–	–	–	–	–
Pantolestes	–	–	–	–	–	–	–	–
Pantolestes	–	–	–	–	–	–	–	–
Pantolestes	–	–	–	–	–	–	–	–
Pantolestes	–	–	–	–	–	–	–	–
Pantolestes	–	–	–	–	–	–	–	–
Pantolestes	–	–	–	–	–	–	–	–
Pantolestes	–	–	–	–	–	–	–	–
Pantolestes	–	–	–	–	–	–	–	–
Pantolestes	–	–	–	–	–	–	–	–
Palaeosinopa ?incerta	–	–	4.10	5.69	2.33	7.21	17.05	4.17
Pantolestidae	–	–	5.67	6.74	2.80	9.36	–	6.42
Pantolestidae	–	–	4.35	5.78	2.36	7.50	–	–
Pantolestidae	–	–	5.45	6.57	2.84	8.23	–	6.06
Pantolestidae	–	–	4.83	5.92	2.81	7.51	–	–
Pantolestidae	–	–	5.11	5.55	3.26	7.57	–	–
Pantolestidae	–	–	–	–	–	–	–	–
Pantolestidae	–	–	–	–	–	–	–	–
Pantolestidae	–	–	8.09	8.44	4.05	11.33	–	8.15
Pantolestidae	–	–	–	–	–	–	–	–
Pantolestes sp.	–	–	6.06	6.69	4.81	9.82	24.48	6.97
Pantolestes sp.	–	–	4.54	4.80	2.12	5.84	13.48	3.89

	Calcaneus	Cuboid						Navicular	
Taxon	Cuboid facet width	Length	Width	Calcaneal facet height	Calcaneal facet width	Metatarsal facet height	Metatarsal facet width	Width	Height
Pantolestes natans	–	–	–	–	–	–	6.42	–	–
Pantolestes	–	–	–	–	–	–	–	–	–
Pantolestes	–	–	–	–	–	–	–	–	–
Pantolestes	–	–	–	–	–	–	–	–	–
Pantolestes	–	–	–	–	–	–	–	–	–
Pantolestes	–	–	–	–	–	–	–	–	–
Pantolestes	–	–	–	–	–	–	–	–	–
Pantolestes	–	–	–	–	–	–	–	–	–
Pantolestes	–	–	–	–	–	–	–	–	–
Pantolestes	–	–	–	–	–	–	–	–	–
Pantolestes	–	–	–	–	–	–	–	–	–
Palaeosinopa ?incerta	6.47	–	–	–	–	–	–	–	–
Pantolestidae	5.97	–	–	–	–	–	–	10.19	7.73
Pantolestidae	–	–	–	–	–	–	–	–	–
Pantolestidae	5.91	–	–	–	–	–	–	–	–
Pantolestidae	–	–	–	–	–	–	–	–	–
Pantolestidae	–	–	–	–	–	–	–	–	–
Pantolestidae	–	6.73	7.33	6.09	5.42	6.45	4.91	–	–
Pantolestidae	–	–	–	–	–	–	–	–	–
Pantolestidae	8.03	–	–	–	–	–	–	–	–
Pantolestidae	–	–	–	–	–	–	–	13.04	9.33
Pantolestes sp.	7.96	–	–	–	–	–	–	–	–
Pantolestes sp.	4.04	–	–	–	–	–	–	–	–

APPENDIX D. MEASUREMENTS OF ALL EXTANT MAMMALS USED IN THE ECOMORPHOLOGICAL ANALYSIS (IN MM).

Species	Spec. No.	Group	Habitat	A1*	A2	A3	A4	A5	A6	A7
Ceratotherium simum	AMNH 54456	Perissodactyla: Rhinoceratidae	Open	77.73	66.30	54.12	71.48	70.39	–	–
Rhinoceros unicornis	AMNH 54456	Perissodactyla: Rhinoceratidae	Closed	82.13	73.21	46.57	71.70	64.28	–	–
Equus grevyi	FMNH 127865	Perissodactyla: Equidae	Open	59.67	60.18	33.93	52.89	48.90	–	–
Equus asinus somalicus	FMNH 18851	Perissodactyla: Equidae	Closed	56.85	58.77	34.20	52.48	43.87	–	–
Euphractus sexcinctus	AMNH 133288	Xenarthra	Open	15.56	9.08	7.32	10.72	7.67	–	–
Tamandua tridactyla mexicana	AMNH 172986	Xenarthra	Closed	14.26	7.98	6.26	10.38	8.84	–	–
Lepus californicus melanotis	AMNH 131874	Lagomorpha: Leporidae	Open	11.10	4.74	3.62	5.54	3.72	–	–
Nesolagus timminsi	AMNH 276142	Lagomorpha: Leporidae	Closed	10.61	5.42	4.09	6.59	4.38	–	–
Giraffa camelopardalis	AMNH 82001	Artiodactyla: Giraffidae	Open	94.05	70.59	32.78	72.32	54.70	76.73	104.63
Okapia johnstoni	AMNH 51215	Artiodactyla: Giraffidae	Closed	64.40	46.12	25.84	44.65	35.12	49.40	74.83
Phacochoerus aethiopicus alleni	AMNH 82078	Artiodactyla: Suidae	Open	37.08	24.27	15.51	23.33	13.48	23.52	40.64
Potamochoerus porcus daemonensis	AMNH 90006	Artiodactyla: Suidae	Closed	37.92	25.58	16.94	25.30	16.71	26.14	42.31
Catagonus wagneri	FMNH 157396	Artiodactyla: Tayassuidae	Open	29.34	18.71	12.86	18.85	12.08	18.51	34.08
Tayassu pecari albirostris	AMNH 215158	Artiodactyla: Tayassuidae	Closed	28.59	20.90	12.18	21.11	12.94	17.99	31.72
Axis axis	AMNH 54488	Artiodactyla: Cervinae	Open	31.51	18.12	9.11	20.31	13.14	22.92	34.83
Muntiacus munjac	AMNH 54562	Artiodactyla: Cervinae	Closed	25.09	15.50	10.31	16.00	12.13	17.03	26.94
Rangifer tarandus carabou	FMNH 10933	Artiodactyla: Capriolinae	Open	51.46	29.97	15.54	30.69	24.07	37.51	54.49
Pudu mephistopheles	FMNH 86846	Artiodactyla: Capriolinae	Closed	17.36	9.96	6.38	11.00	7.95	11.25	18.24
Kobus kob alurae	AMNH 53387	Artiodactyla: Reduncini	Open	43.67	29.84	13.85	26.43	20.07	27.52	45.86
Kobus megaceros	AMNH 82135	Artiodactyla: Reduncini	Closed	40.90	28.78	14.42	27.68	18.38	26.08	42.79
Ourebia ourebi ourebi	AMNH 216388	Artiodactyla: Neotragini	Open	24.32	16.60	6.88	16.33	11.47	14.64	25.68
Madoqua guentheri	AMNH 27835	Artiodactyla: Neotragini	Closed	15.46	10.26	5.97	9.24	6.86	9.07	16.17

Species	Spec. No.	Group	Habitat	A1*	A2	A3	A4	A5	A6	A7
Silvicapra grimmea roosevelti	AMNH 53088	Artiodactyla: Cephalophini	Open	21.39	14.52	6.78	13.71	8.54	13.37	22.47
Cephalophus dorsalis	MNH 52924	Artiodactyla: Cephalophini	Closed	23.27	16.57	8.45	15.53	9.95	15.74	25.06
Taurotragus oryx patersonianus	FMNH 35114	Artiodactyla: Tragelaphini	Open	76.00	44.39	26.07	48.10	35.46	53.19	80.96
Tragelaphus imberbis australis	FMNH 105028	Artiodactyla: Tragelaphini	Closed	42.69	24.67	12.93	25.02	17.70	27.97	45.33
Procavia capensis syrica	AMNH 184992	Hyracoidea	Open	9.82	6.17	6.26	7.84	7.37	–	–
Dendrohyrax	AMNH 187789	Hyracoidea	Closed	9.19	6.56	5.95	7.42	6.55	–	–
Lemur catta	AMNH 170740	Primates: Lemuridae	Open	17.26	7.86	7.64	8.79	6.66	–	–
Varecia variegatta	AMNH 100512	Primates: Lemuridae	Closed	20.60	10.32	9.25	10.74	8.77	–	–
Galago senegalensis	AMNH 187359	Primates: Galagidae	Open	8.33	3.52	3.59	4.66	3.24	–	–
Loris tardigradus	AMNH 150038	Primates: Galagidae	Closed	7.85	4.92	4.49	4.95	4.59	–	–
Erythrocebus patas patas	USNM 257013	Primates: Cercopithecidae	Open	21.96	14.92	11.55	13.36	11.25	–	–
Allenopithecus nigrovindis	USNM 395131	Primates: Cercopithecidae	Closed	15.45	10.17	8.57	9.66	7.19	–	–
Gorilla gorilla beringii	USNM 176225	Primates: Hominidae	Open	63.05	38.36	34.98	40.54	39.64	–	–
Homo sapiens	**	Primates: Hominidae	Open	51.63	23.45	34.38	28.87	31.39	–	–
Pan troglodytes	USNM 176227	Primates: Hominidae	Closed	38.51	25.94	23.29	22.76	21.65	–	–
Tupaia glis	USNM 121855	Scandentia	Open	6.91	3.67	2.83	3.53	3.05	–	–
Ptilocercus loweii	USNM 121855	Scandentia	Closed	3.90	1.79	2.01	1.92	1.78	–	–
Leptailurus serval liptosticta	FMNH 18956	Carnivora: Felidae	Open	23.28	14.54	12.92	16.30	12.02	–	–
Leopardus weidii pirrensis	FMNH 70568	Carnivora: Felidae	Closed	21.53	13.99	12.38	13.97	9.95	–	–
Lycaon pictus	FMNH 194128 (zoo)	Carnivora: Canidae	Open	30.88	20.02	13.72	20.26	16.62	–	–
Urocyon cinereoargenteus	FMNH 175292	Carnivora: Canidae	Closed	16.67	10.61	7.81	10.74	8.79	–	–
Ursus arctos gyas	FMNH 63803	Carnivora: Ursidae	Open	46.18	37.82	34.23	41.04	37.84	–	–
Helarctos malayanus	FMNH 54201 (zoo)	Carnivora: Ursidae	Closed	3.49	24.64	16.64	23.02	18.21	–	–

Species	Spec. No.	Group	Habitat	A1*	A2	A3	A4	A5	A6	A7
Civettictis civetta schwarzi	FMNH 108174	Carnivora: Viverridae	Open	21.89	13.46	12.31	14.49	10.53	–	–
Arctictis binturong albifrons	FMNH 98270	Carnivora: Viverridae	Closed	27.48	18.10	14.32	16.42	11.80	–	–
Bassriscus astutus flavus	FMNH 129302	Carnivora: Procyonidae	Open	11.09	6.81	5.79	6.67	5.30	–	–
Potos flavus megalotus	FMNH 69630	Carnivora: Procyonidae	Closed	16.55	11.15	8.25	8.57	7.17	–	–
Gulo gulo luscus	FMNH 151027	Carnivora: Mustellidae	Open	27.97	18.96	16.25	18.88	14.97	–	–
Martes americana actuosa	FMNH 129322	Carnivora: Mustellidae	Closed	11.61	7.25	6.24	6.31	5.50	–	–

** specimen 133 from the osteological teaching collection at Washington University

Species	A8	A9	A10	A11	A12	A13	A14	A15	H1	H2	H3	H4	H5	H6	H7
Ceratotherium simum	83.23	53.08	54.08	–	30.10	86.92	55.33	40.43	170.36	119.91	97.36	111.50	65.77	100.84	73.00
Rhinoceros unicornis	89.28	61.04	54.75	–	41.76	78.29	47.98	34.55	171.75	113.52	95.14	97.67	72.34	91.64	69.48
Equus grevyi	48.66	49.62	34.66	–	37.56	41.61	28.81	24.20	81.67	77.49	55.78	49.15	43.06	43.41	24.68
Equus asinus somalicus	43.34	46.63	30.96	–	35.16	31.23	23.78	18.71	67.83	67.14	46.82	39.99	41.09	39.24	20.33
Euphractus sexcinctus	12.66	7.79	5.38	–	8.04	11.72	7.75	5.07	31.03	20.53	14.64	6.54	6.11	9.42	13.07
Tamandua tridactyla mexicana	13.31	6.36	7.03	–	6.65	12.72	8.85	4.52	43.63	17.18	12.69	7.38	8.64	10.21	–
Lepus californicus melanotis	4.56	5.41	4.06	–	3.50	3.92	2.25	2.02	8.45	6.27	4.40	6.32	3.89	5.92	3.59
Nesolagus timminsi	5.13	4.22	4.03	–	3.86	4.35	2.50	2.05	9.06	7.50	4.86	5.95	3.46	6.25	3.69
Giraffa camelopardalis	72.67	64.90	57.58	63.05	52.81	57.00	40.22	33.45	140.25	118.05	90.35	74.49	62.66	68.26	43.17
Okapia johnstoni	48.58	39.72	35.03	36.20	31.05	50.59	30.54	32.53	91.15	75.84	63.58	47.13	32.16	38.43	30.45
Phacochoerus aethiopicus alleni	18.97	23.32	16.54	19.09	15.78	17.20	10.87	9.72	46.89	35.83	27.15	29.27	24.40	31.75	18.15
Potamochoerus porcus daemonensis	21.91	24.31	15.74	19.90	17.44	19.61	13.26	8.52	47.58	31.88	23.21	28.88	22.59	30.85	18.08
Catagonus wagneri	15.78	16.37	12.94	14.58	14.69	18.16	12.18	8.87	34.26	28.06	18.47	22.80	19.92	22.34	13.30
Tayassu pecari albirostris	16.49	17.19	12.67	14.56	14.46	14.87	9.45	7.47	31.89	25.69	18.31	21.05	18.75	22.97	11.13
Axis axis	20.40	17.79	16.01	18.32	14.59	17.91	11.47	9.65	36.77	31.84	23.57	25.66	14.91	21.96	12.75
Muntiacus munjac	13.56	14.94	11.88	12.25	11.85	11.63	7.38	6.34	26.03	23.68	16.76	16.85	11.47	15.82	8.50
Rangifer tarandus carabou	31.38	31.01	28.96	33.77	23.42	31.39	19.63	18.47	62.17	55.50	35.31	41.48	34.20	38.53	17.97
Pudu mephistopheles	9.79	10.98	8.51	10.98	8.49	10.68	6.29	5.28	19.88	16.56	10.90	12.05	9.78	14.16	7.40
Kobus kob alurae	25.20	25.30	22.63	22.86	20.50	29.45	20.98	12.04	48.27	40.34	31.71	27.47	20.03	28.57	17.07
Kobus megaceros	23.28	24.47	20.49	21.07	19.64	22.55	15.28	13.46	50.35	42.40	33.38	32.01	21.33	25.60	17.47
Ourebia ourebi ourebi	13.70	13.60	11.38	13.29	11.32	13.09	8.82	6.75	21.26	20.08	14.64	15.56	11.65	14.93	8.92
Madoqua guentheri	8.58	7.20	7.70	8.52	5.60	6.56	4.09	3.24	13.65	13.27	8.99	10.23	6.67	8.88	5.64

Species	A8	A9	A10	A11	A12	A13	A14	A15	H1	H2	H3	H4	H5	H6	H7
Silvicapra grimmea roosevelti	12.29	10.84	10.38	10.86	8.91	10.99	7.20	6.10	20.65	17.89	14.19	13.67	10.98	12.41	7.58
Cephalophus dorsalis	14.70	12.26	10.98	11.62	10.29	13.16	9.16	6.35	24.01	20.39	16.34	14.33	10.02	13.82	9.68
Taurotragus oryx patersonianus	46.33	42.52	38.58	43.98	34.08	63.48	32.33	43.28	109.05	84.35	54.86	61.16	45.16	53.64	36.93
Tragelaphus imberbis australis	25.06	23.46	22.32	23.38	17.43	27.53	17.66	16.43	45.76	40.15	28.80	29.70	27.06	28.84	14.03
Procavia capensis syrica	7.38	5.17	5.95	–	6.50	6.67	4.66	2.05	15.07	10.43	7.39	8.19	7.58	9.28	7.87
Dendrohyrax	6.24	4.30	4.73	–	5.65	5.94	4.15	1.88	14.97	9.31	6.78	6.40	5.99	7.34	6.79
Lemur catta	6.89	8.00	5.84	–	7.79	4.84	2.29	2.72	17.55	13.30	6.40	5.67	5.79	6.59	5.84
Varecia variegatta	8.32	9.69	6.69	–	8.97	7.22	3.22	4.30	23.82	18.91	8.59	8.17	7.78	8.58	9.54
Galago senegalensis	3.47	3.71	2.78	–	3.46	2.76	1.47	1.40	8.49	5.76	1.98	2.52	2.34	2.69	2.51
Loris tardigradus	3.71	3.23	2.63	–	3.86	3.23	2.06	1.37	8.96	6.61	3.66	3.69	3.68	3.85	4.27
Erythrocebus patas patas	10.99	11.55	8.27	–	13.21	10.50	6.19	4.63	24.57	19.09	6.25	11.42	10.99	15.91	10.58
Allenopithecus	7.19	7.65	5.28	–	7.61	7.19	3.61	3.77	19.36	13.11	5.60	8.74	6.63	9.14	6.55
Gorilla gorilla beringii	35.16	37.04	29.71	–	34.37	33.32	23.84	9.81	102.64	70.50	38.97	41.80	33.40	41.63	36.78
Homo sapiens	30.44	31.41	19.06	–	28.92	25.92	17.4	8.749	–	–	–	–	–	–	–
Pan troglodytes	21.43	20.01	15.93	–	20.93	19.69	9.39	10.42	57.24	42.06	23.15	21.17	19.19	28.28	19.33
Tupaia glis	3.18	2.44	2.07	–	2.48	2.44	1.52	0.97	6.26	4.56	3.02	2.61	2.54	2.63	2.63
Ptilocercus loweii	1.59	1.67	1.14	–	1.62	8.50	4.38	4.23	–	–	–	–	–	–	–
Leptailurus serval liptosticta	11.09	13.51	9.13	–	10.74	11.97	8.29	4.34	27.57	21.23	13.18	14.82	11.40	16.99	9.60
Leopardus weidii pirrensis	10.22	11.11	7.12	–	10.69	10.34	6.80	4.27	24.74	17.22	12.96	12.10	9.44	13.09	8.45
Lycaon pictus	15.67	16.97	10.06	–	12.46	16.04	10.89	7.77	35.19	25.55	15.22	21.17	18.59	25.60	12.17
Urocyon cinereoargenteus	8.51	9.37	5.90	–	6.72	7.96	5.72	3.29	18.79	13.49	7.65	10.10	9.45	12.18	5.82
Ursus arctos gyas	41.85	33.86	27.27	–	25.72	43.00	27.37	17.49	101.60	72.65	44.12	36.02	37.38	56.85	26.56
Helarctos malayanus	24.74	20.63	11.57	–	15.58	24.79	16.23	10.52	69.71	48.60	30.96	21.78	24.83	38.71	23.58

Species	A8	A9	A10	A11	A12	A13	A14	A15	H1	H2	H3	H4	H5	H6	H7
Civettictis civetta schwarzi	11.76	11.61	7.45	–	10.14	14.18	8.59	6.42	26.25	20.10	13.33	13.34	11.15	14.53	9.89
Arctictis binturong albifrons	15.59	12.03	8.79	–	13.12	20.24	14.52	6.65	40.35	28.91	20.38	13.35	11.46	15.46	15.32
Bassriscus astutus flavus	4.99	5.10	3.64	–	4.60	4.97	2.93	2.19	12.92	10.36	5.96	6.24	4.67	6.75	5.13
Potos flavus megalotus	7.80	7.19	4.33	–	6.31	6.57	3.68	2.99	22.97	15.73	11.45	6.74	5.97	7.91	8.13
Gulo gulo luscus	14.49	15.02	8.98	–	14.11	15.99	10.60	5.78	40.39	30.76	19.39	16.17	17.24	21.55	14.95
Martes americana	5.01	5.03	3.09	–	4.64	4.81	3.25	1.67	12.28	9.60	5.69	5.67	4.62	6.89	5.17

APPENDIX E. MEASUREMENTS OF UINTAN ARTIODACTYL ASTRAGALI (IN MM)

CM No.	Taxon	Locality	Meter	UFAZ	A1	A2	A3	A4	A5	A6	A7	A8	A9
80787	?PROTOCERATID	WU-018	25	1	11.04	7.76	3.82	6.37	4.17	5.90	11.63	5.43	6.28
80787	HOMACODONT	WU-018	25	1	8.93	5.41	3.20	5.12	2.84	4.46	9.31	4.54	4.51
80787	HOMACODONT	WU-018	25	1	9.63	6.08	3.41	–	3.23	4.19	–	4.81	4.49
80787	HOMACODONT	WU-018	25	1	9.76	6.11	3.65	5.62	3.94	5.23	9.92	4.85	5.03
80787	?PROTOCERATID	WU-018	25	1	10.91	6.92	4.29	–	4.36	6.12	–	–	5.88
80787	?PROTOCERATID	WU-018	25	1	10.71	6.57	4.19	–	4.23	5.88	–	–	5.69
80788	AGRIOCHOERID	WU-177	108	2	9.69	13.54	8.23	11.57	7.94	10.49	21.19	10.31	11.65
80789	AGRIOCHOERID	WU-185	334	3	26.42	17.01	11.07	16.86	16.38	11.96	29.76	15.16	–
80789	AGRIOCHOERID	WU-185	334	3	26.61	–	11.76	17.04	16.38	12.03	29.27	–	–
80790	ARTIODACTYLA	WU-187	367	3	14.66	–	5.17	8.39	5.47	7.47	15.19	7.23	7.73
80791	AGRIOCHOERID	WU-110	99	2	20.34	13.25	–	–	8.32	10.58	–	–	11.68
80792	ARTIODACTYLA	WU-185	334	3	23.95	16.95	8.93	–	9.87	15.39	–	14.56	13.49
80793	AGRIOCHOERID	WU-173	367	3	25.40	16.63	8.93	16.39	12.25	16.38	28.87	15.64	15.16
80794	ARTIODACTYLA	WU-192	367	3	17.91	11.90	6.31	11.63	7.65	10.10	19.79	9.44	10.35
80794	ARTIODACTYLA	WU-192	367	3	14.27	8.73	4.75	7.90	5.38	7.53	15.60	7.21	7.65
80795	ARTIODACTYLA	WU-198	356	3	15.13	–	4.62	8.83	6.14	8.24	15.74	7.42	–
80796	HOMACODONT	WU-210	357	3	8.45	5.39	2.78	4.87	–	–	–	4.78	4.37
80796	AGRIOCHOERID	WU-210	357	3	16.54	10.14	6.09	10.83	6.06	8.50	17.72	8.61	9.38
80797	ARTIODACTYLA	WU-215	275	3	14.55	8.81	4.93	8.11	5.19	7.06	15.06	6.85	7.93
80798	ARTIODACTYLA	WU-210	357	3	14.75	9.03	4.95	8.19	5.26	7.84	15.69	7.04	–
80798	ARTIODACTYLA	WU-210	357	3	15.05	10.34	5.84	8.53	5.22	7.81	15.87	7.27	–
80798	ARTIODACTYLA	WU-210	357	3	15.50	9.54	–	–	5.89	7.70	–	–	–
80798	ARTIODACTYLA	WU-210	357	3	13.66	8.48	–	–	5.89	7.90	–	–	7.26
80798	ARTIODACTYLA	WU-210	357	3	16.81	10.97	6.17	–	6.26	9.12	–	–	9.16
80799	ARTIODACTYLA	WU-223	357	3	12.28	7.91	5.05	–	4.89	7.22	–	–	6.98
80801	AGRIOCHOERID	WU-002	104	2	21.33	13.36	6.92	–	8.78	12.04	–	–	11.68
80802	AGRIOCHOERID	WU-008	56	1	16.60	10.83	6.08	–	6.36	9.31	–	9.20	–
80803	AGRIOCHOERID	WU-002	104	2	18.64	12.51	7.28	11.16	7.67	11.01	20.15	10.21	10.94
80804	AGRIOCHOERID	WU-018	25	1	17.42	–	7.28	11.19	7.06	10.20	19.02	8.72	–
80805	AGRIOCHOERID	WU-001	104	2	17.16	10.36	6.57	–	8.04	10.83	–	9.26	–
80806	ARTIODACTYLA	WU-015	56	1	13.46	9.31	4.88	8.57	5.67	7.78	14.80	7.40	8.05

CM No.	Taxon	Locality	Meter	UFAZ	A1	A2	A3	A4	A5	A6	A7	A8	A9
80807	AGRIOCHOERID	WU-045	285	3	26.72	18.23	10.13	18.07	12.62	16.25	30.13	14.24	15.38
80808	ARTIODACTYLA	WU-049	364	3	15.68	10.05	5.93	8.46	5.74	7.91	16.10	7.20	8.63
80809	ARTIODACTYLA	WU-050	361	3	13.88	9.02	5.14	8.41	5.76	7.57	15.31	6.82	7.94
80810	ARTIODACTYLA	WU-018	25	1	14.95	9.24	–	8.95	5.78	8.20	15.86	7.44	7.54
80810	ARTIODACTYLA	WU-018	25	1	16.39	–	5.57	9.15	6.32	9.13	17.05	8.17	–
80811	ARTIODACTYLA	WU-058	98	2	14.03	9.32	5.59	8.66	5.57	8.10	15.34	7.42	–
80812	HOMACODONT	WU-018	25	1	9.61	5.58	3.80	5.33	3.88	5.63	9.99	5.28	5.10
80813	AGRIOCHOERID	WU-091	192	3	21.38	15.83	8.63	13.70	9.18	13.27	25.13	12.12	12.68
80814	ARTIODACTYLA	WU-090	184	3	13.07	7.97	5.69	7.65	5.15	7.81	14.73	6.44	7.31
80815	ARTIODACTYLA	WU-022	87	1	19.42	11.43	–	–	6.62	10.80	–	–	–
80816	AGRIOCHOERID	WU-104	–	3	24.67	17.21	9.36	15.94	14.21	19.05	27.46	15.72	15.30
80817	ARTIODACTYLA	WU-105	286	3	14.41	9.04	4.89	9.33	5.89	8.37	15.72	7.85	8.85
80818	AGRIOCHOERID	WU-110	99	2	20.00	12.82	7.48	12.37	9.19	12.40	21.57	10.90	11.76
80819	AGRIOCHOERID	WU-110	99	2	14.79	9.52	5.42	9.53	5.56	8.41	16.11	7.77	8.58
80819	AGRIOCHOERID	WU-110	99	2	18.91	12.48	6.55	–	7.95	10.97	–	10.11	10.77
80819	AGRIOCHOERID	WU-110	99	2	13.59	9.07	5.09	9.16	5.85	8.12	14.49	7.05	7.55
80819	AGRIOCHOERID	WU-110	99	2	19.35	12.56	7.01	–	8.59	11.45	–	–	12.11
80820	ARTIODACTYLA	WU-114	–	2	15.59	9.77	5.05	9.10	6.15	8.77	16.97	8.19	8.58
80821	AGRIOCHOERID	WU-112	–	3	27.00	18.11	10.22	–	11.57	15.79	–	14.84	14.61
80822	ARTIODACTYLA	WU-117	123	2	15.61	10.11	6.41	9.68	6.49	8.93	17.35	8.53	9.26
80822	ARTIODACTYLA	WU-117	123	2	11.03	7.41	3.41	6.07	3.71	5.36	11.38	5.23	5.85
80823	ARTIODACTYLA	WU-122	279	3	13.35	8.59	4.67	7.43	4.90	7.29	14.61	6.20	–
80823	ARTIODACTYLA	WU-122	279	3	15.88	9.16	5.82	–	5.82	8.40	–	–	8.10
80824	AGRIOCHOERID	WU-131	50	1	20.71	14.30	8.01	13.47	7.95	12.13	22.84	10.86	–
80825	ARTIODACTYLA	WU-110	99	2	14.67	9.01	4.13	8.73	5.29	8.07	15.78	7.53	–
80826	ARTIODACTYLA	WU-136	140	3	11.32	6.93	3.85	–	4.53	6.03	–	–	–
80827	AGRIOCHOERID	WU-110	99	2	20.05	13.33	7.39	12.63	8.18	11.84	22.80	11.15	12.10
80828	ARTIODACTYLA	WU-090	184	3	9.18	5.25	3.43	4.66	3.32	4.64	9.38	4.57	–
80829	AGRIOCHOERID	WU-117	123	2	19.55	13.92	7.33	12.31	7.77	11.12	21.91	10.33	–
80830	ARTIODACTYLA	WU-117	123	2	12.45	8.03	4.51	7.15	4.38	6.36	13.37	6.69	6.29
80831	ARTIODACTYLA	WU-018	25	1	16.33	9.62	5.59	8.34	6.40	9.24	17.02	7.98	–

CM No.	A10	A11	A12	A13	A14	A15
80787	4.73	5.22	–	4.58	3.13	2.25
80787	3.60	3.77	4.52	3.68	2.28	1.90
80787	4.50	4.17	–	3.71	2.45	1.67
80787	–	–	–	4.07	2.60	2.00
80787	4.63	5.89	–	–	–	2.28
80787	4.33	4.89	–	–	–	2.60
80788	9.04	10.28	9.95	7.16	5.21	3.27
80789	12.10	14.22	14.60	12.33	8.27	6.51
80789	13.04	–	15.24	–	8.38	–
80790	6.36	–	–	4.99	3.72	2.63
80791	8.66	10.74	–	–	–	3.42
80792	11.35	13.15	–	–	–	5.60
80793	10.54	14.39	12.42	12.50	7.86	6.66
80794	7.09	9.55	9.24	7.06	5.39	3.24
80794	6.23	7.07	6.74	5.97	4.34	2.77
80795	6.37	–	–	–	4.52	–
80796	–	–	4.13	3.90	2.52	1.98
80796	7.39	8.76	8.76	6.85	5.18	3.52
80797	6.02	–	7.33	6.00	4.55	3.19
80798	6.62	7.51	–	5.76	4.41	2.81
80798	7.13	8.01	–	6.34	4.19	3.44
80798	6.89	8.03	–	–	–	3.15
80798	6.20	7.01	–	–	–	3.72
80798	7.83	8.66	–	–	–	3.45
80799	5.48	6.49	–	–	–	2.55
80801	9.16	9.60	–	–	–	5.29
80802	6.56	7.82	–	6.74	4.69	3.05
80803	7.30	9.35	9.34	7.85	5.52	4.20
80804	8.96	9.64	8.94	–	2.90	–
80805	7.53	8.95	–	7.42	5.39	3.37
80806	5.90	6.99	7.33	6.04	4.46	2.74

CM No.	A10	A11	A12	A13	A14	A15
80807	12.56	13.64	13.17	13.25	8.64	6.92
80808	7.01	7.26	7.59	5.54	4.06	2.74
80809	6.05	7.98	7.62	5.91	4.76	2.68
80810	6.19	7.08	7.79	5.75	4.22	2.80
80810	–	–	8.81	–	5.04	–
80811	5.69	7.94	–	5.54	3.97	2.98
80812	4.14	4.19	4.68	3.96	2.68	1.89
80813	10.06	11.23	11.14	9.14	5.87	5.33
80814	5.27	6.27	6.64	5.81	3.88	2.79
80815	8.69	–	–	–	–	3.55
80816	10.52	15.05	13.24	11.11	7.74	5.80
80817	7.24	8.49	5.78	5.93	3.99	3.07
80818	9.28	10.73	–	8.68	6.56	4.13
80819	6.92	7.95	7.44	6.34	4.22	3.50
80819	7.95	9.60	–	8.56	6.06	4.47
80819	6.32	7.01	7.30	5.86	4.38	2.97
80819	8.09	9.61	–	–	–	4.83
80820	6.72	7.58	7.60	7.36	5.34	3.73
80821	10.11	13.51	–	13.03	9.12	6.83
80822	6.88	7.83	6.57	6.82	5.03	2.73
80822	4.89	5.34	–	3.94	2.67	2.14
80823	6.10	6.88	5.58	–	4.01	–
80823	6.87	7.71	–	–	–	3.11
80824	8.85	10.96	9.36	–	6.36	–
80825	–	7.19	–	5.68	4.06	2.31
80826	4.50	5.93	–	–	–	2.23
80827	8.37	10.32	9.38	9.19	6.50	5.08
80828	3.84	3.96	3.61	4.06	2.82	1.72
80829	8.57	10.03	9.50	9.48	6.66	4.30
80830	5.16	6.03	4.88	5.30	3.74	2.58
80831	–	–	–	7.18	4.71	3.53

LITERATURE CITED

Ackerly, D.D., 2000. Taxon sampling, correlated evolution and independent contrasts. Evolution 54, 1480-1492.

Anderson, D., 2008. Ischyromyidae. In: Janis, C.M., Gunnell, G.F., Uhen, M.D. (Eds.), Evolution of Tertiary Mammals of North America Volume 2: Small Mammals, Xenarthrans and Marine Mammals. Cambridge University Press, Cambridge, UK, pp. 311-335.

Andersson, K., 2004. Elbow-joint morphology as a guide to forearm function and foraging behaviour in mammalian carnivores. Zoological Journal of the Linnaean Society 142, 91-104.

Anemone, R.L., 1993. The functional anatomy of the hip and thigh in primates. In: Gebo, D.L. (Ed.) Postcranial Adaptation in Nonhuman Primates. Northern Illinois University Press, De Kalb, IL, pp. 150-174.

Anemone, R.L., Covert, H.H., 2000. New skeletal remains of *Omomys* (Primates, Omomyidae): functional morphology of the hindlimb and locomotor behavior of a Middle Eocene primate. Journal of Human Evolution 38, 607-633.

Ankel, F., 1972. Vertebral morphoogy of fossil and extant primates. In: Tuttle, R. (Ed.) The Functional and Evolutionary Biology of Primates. Aldine, Chicago, Illinois, pp. 223-240.

Argot, C., 2001. Functional-adaptive anatomy of the forelimb in the Didelphidae, and the paleobiology of the Paleocene marsupials *Mayulestes ferox* and *Pucadelphys andinus*. Journal of Morphology 247, 51-79.

Argot, C., 2002. Functional-adaptive analysis of the hindlimb anatomy of extant marsupials and the paleobiology of the Paleocene marsupials *Mayulestes ferox* and *Pucadelphys andinus*. Journal of Morphology 253, 76-108.

Baba, H., 1975. On the squatting facets of primates. In: Kondo, S., Kawai, M., Ehara, A. (Eds.), Contemporary Primatology. Karger, Basel, pp. 25-29.

Barnett, C.H., Napier, J.R., 1953. The rotary mobility of the fibula in eutherian mammals. Journal of Anatomy 87, 11-21.

Beard, K.C., Dawson, M.R., 1999. Intercontinental dispersal of Holarctic land mammals near the Paleocene/Eocene boundary: paleogeographic, paleoclimatic and biostratigraphic implications. Bulletin de la Societe geologique de France 170, 697-706.

Beard, K.C., Krishtalka, L., Stucky, R.K., 1992. Revision of the Wind River faunas, early Eocene of central Wyoming. Part 12. New species of omomyid primates (Mammalia: Primates: Omomyidae) and omomyid taxonomic composition across the early-middle Eocene boundary. Annals of the Carnegie Museum 61, 39-62.

Behrensmeyer, A.K., Western, D., Dechant Boaz, D.E., 1979. New perspectives in vertebrate paleoecology from a recent bone assemblage. Paleobiology 5, 12-21.

Berggren, W.A., Kent, D.V., Obradovich, J.D., Swisher, C.C., III, 1992. Toward a Revised Paleogene geochronology. In: Prothero, D.R., Berggren, W.A. (Eds.), Eocene-Oligocene Climatic and Biotic Evolution. Princeton University Press, New Jersey, pp. 29-45.

Best, T.L., 1996. *Lepus californicus*. Mammalian Species 530, 1-10.

Bishop, L. 1994. Pigs and the Ancestors: Hominids, Suids and Environments During the

Plio-Pleistocene of East Africa. Ph. D., Yale University.

Black, C.C., Dawson, M.R., 1966. A review of Late Eocene mammalian faunas from North America. American Journal of Science 264, 321-349.

Bloch, J.I., Boyer, D.M., 2002. Grasping primate origins. Science 298, 1606-1610.

Bloch, J.I., Silcox, M.T., Boyer, D.M., Sargis, E.J., 2007. New Paleocene skeletons and the relationship of plesiadapiforms to crown-clade primates. Proceedings of the National Academy of Science of the United States of America 104, 1159-1164.

Blondel, C., 1998. Le squelette appendiculaire de sept ruminants Oligocènes d'Europe; implications palèoècologiques. Comptes Rendus de l'Académie des Sciences Paris, Science de la Terre et des Planètes 326, 527-532.

Blondel, C., 2001. The Eocene-Oligocene ungulates from Western Europe and their environment. Palaeogeography, Palaeoclimatology, Palaeoecology 168, 125-139.

Bock, W.J., 1990. From biologische anatomie to ecomorphology. Netherlands Journal of Zoology 40, 254-277.

Bock, W.J., von Wahlert, G., 1965. Adaptation and the form-function complex. Evolution 19, 269-299.

Bowen, G.J., Clyde, W.C., Koch, P.L., Ting, S., Alroy, J., Tsubamoto, T., Wang, Y., 2002. Mammalian dispersal at the Paleocene/Eocene boundary. Science 295, 2062-2065.

Bown, T.M., Rose, K.D., 1987. Patterns of dental evolution in Early Eocene anaptomorphine primates (Omomyidae) from the Bighorn Basin, Wyoming. Journal of Paleontology 61, 1-162.

Boyer, D.M., Georgi, J.A., 2007. Cranial morphology of a pantolestid eutherian mammal

from the Eocene Bridger Formation, Wyoming, USA: Implications for relationships and habitat. Journal of Mammalian Evolution 14, 239-280.

Bradley, W.H., 1937. The biography of an ancient American lake. Annual Report of the Smithsonian Institution, 279-289.

Buchheim, H.P., Brand, L.R., Goodwin, H.T., 2000. Lacustrine to fluvial floodplain deposition in the Eocene Bridger Formation. Palaeogeography, Palaeoclimatology, Palaeoecology 162, 191-209.

Burke, J.J., 1935. Fossil rodents from the Uinta Eocene series. Annals of the Carnegie Museum 25, 5-12.

Burt, A., 1989. Comparative methods using phylogenetically independent contrasts. Oxford Surveys in Evolutionary Biology 6, 33-55.

Carrano, M.T., 1997. Morphological indicators of foot posture in mammals: a statistical and biomechanical analysis. Zoological Journal of the Linnaean Society 121, 77-104.

Carraway, L.N., Verts, B.J., 1993. *Aplodontia rufa*. Mammalian Species 431, 1-10.

Cashion, W.B., 1986. Geologic map of the Bonanza Quadrangle, Uintah County, Utah. United States Geological Survey Miscellaneous Field Studies Map MF-1865,

Ciampaglio, C.N., Kemp, M., McSchea, D.W., 2001. Detecting changes in morphospace occupation patterns in the fossil record: characterization and analysis of measures of disparity. Paleobiology 27, 695-715.

Clyde, W.C., 1998. Mammalian community response to the latest Paleocene thermal maximum: An isotaphonomic study in the northern Bighorn Basin, Wyoming. Geology 26, 1011-1014.

Clyde, W.C., 2001. Mammalian biostratigraphy of the McCullough Peaks Area in the Northern Bighorn Basin. In: Gingerich, P.D. (Ed.) Paleocene-Eocene Stratigraphy and Biotic Change in the Bighorn and Clarks Fork Basins, Wyoming, pp. 109-126.

Clyde, W.C., Finarelli, J.A., Christensen, K.E., 2005. Evaluating the relationship between pedofaces and faunal composition: implications for faunal turnover at the Paleocene-Eocene boundary. PALAIOS 20, 390-399.

Conroy, G.C., 1987. Problems of body mass estimation in fossil primates. International Journal of Primatology 8, 115-137.

Cook, H.J., 1954. A remarkable new mammal from the lower Chadron of Nebraska. American Midland Naturalist 52, 388-391.

Cope, E.D., 1872. Second account of new Vertebrata from the Bridger Eocene. Proceedings of the American Philosophical Society 12, 466-468.

Covert, H.H., Williams, B.A., 1993. Recently recovered specimens of North American Eocene omomyids and adapids and their bearing on debates about anthropoid origins. In: Fleagle, J.G., Kay, R.F. (Eds.), Anthropoid Origins. Plenum Press, New York, pp. 29-54.

Currano, E.D., Wilf, P., Wing, S.L., Labandeira, C.C., Lovelock, E.C., Royer, D.L., 2008. Sharply increased insect herbivory during the Paleocene-Eocene Thermal Maximum. Proceedings of the American Philosophical Society 105, 1960-1964.

Dagosto, M., 1983. Postcranium of *Adapis parisiensis* and *Leptadapis magnus* (Adapiformes, Primates). Folia Primatologica 41, 49-101.

Dagosto, M., 1985. The distal tibia of primates with special reference to the Omomyidae.

International Journal of Primatology 6, 45-75.

Dagosto, M., 1988. Implications of postcranial evidence for the origin of euprimates. Journal of Human Evolution 17, 35-56.

Dagosto, M., 1993. Postcranial anatomy and locomotor behavior in Eocene primates. In: Gebo, D.L. (Ed.) Postcranial Adaptation in Nonhuman Primates. Northern Illinois University Press, DeKalb, IL, pp. 199-219.

Dagosto, M., Gebo, D.L., 1994. Postcranial anatomy and the origin of the Anthropoidea. In: Fleagle, J.G., Kay, R.F. (Eds.), Anthropoid Origins. Plenum Press, New York, NY, pp. 567-593.

Dagosto, M., Gebo, D.L., Beard, K.C., 1999. Revision of the Wind River faunas, Early Eocene of central Wyoming. Part 14. Postcranium of *Shoshonius cooperi* (Mammalia: Primates). Annals of the Carnegie Museum 68, 175-211.

Davis, D.D., 1964. The giant panda: A morphological study of evolutionary mechanisms. Fieldiana Zoology Memoir 3, 1-339.

Decker, R.L., Szalay, F.S., 1974. Origins and function of the pes in the Eocene Adapidae (Lemuriformes, Primates). In: Jenkins, F.A., Jr. (Ed.) Primate Locomotion. Academic Press, New York, NY, pp. 261-292.

DeGusta, D., Vrba, E., 2003. A method for inferring paleohabitats from the functional morphology of bovid astragali. Journal of Archaeological Science 30, 1009-1022.

DeGusta, D., Vrba, E., 2005a. Methods for inferring paleohabitats from discrete traits of the bovid postcranial skeleton. Journal of Archaeological Science 32, 1115-1123.

DeGusta, D., Vrba, E., 2005b. Methods for inferring paleohabitats from the functional morphology of bovid phalanges. Journal of Archaeological Science 32, 1099-

1113.

Dorr, J.A., Jr., 1977. Partial skull of *Paleosinopa simpsoni* (Mammalia, Insectivora), latest Paleocene Hobac Formation, central western Wyoming, with some general remarks on the family Pantolestidae. Contributions from the Museum of Paleontology, University of Michigan 24, 281-307.

Douglass, E., 1914. Geology of the Uinta Formation. Bulletin of the Geological Society of America 25, 417-420.

Dunn, R.H., 2007. New tarsals of *Ourayia* and *Chipetaia*, omomyine primates from the Uinta Formation, Utah. American Journal of Physical Anthropology 132, 103.

Dunn, R.H., Rasmussen, D.T., 2007. Skeletal morphology and locomotor behavior of *Pseudotomus eugenei* (Rodentia, Paramyinae) from the Uinta Formation, Utah. Journal of Vertebrate Paleontology 27, 987-1006.

Dunn, R.H., Rasmussen, D.T., 2009. Skeletal Morphology of a new genus of Eocene insectivore (Mammalia, Erinaceomorpha) from Utah. Journal of Mammalogy 90, 321-331.

Dunn, R.H., Sybalsky, J.M., Conroy, G.C., Rasmussen, D.T., 2006. Hindlimb adaptations in *Ourayia* and *Chipetaia*, relatively large-bodied omomyine primates from the Middle Eocene of Utah. American Journal of Physical Anthropology 131, 303-310.

Eisenberg, J.F., 1989. Mammals of the Neotropics. University of Chicago Press, Chicago Illinois.

Eisenberg, J.F., Gould, E., 1970. The Tenrecs: A Study in Mammalian Behavior and Evolution. Smithsonian Institution Press, Washington D. C.

Elissamburu, A., Vizcaíno, S.F., 2004. Limb proportions and adaptations in caviomorph rodents (Rodentia: Caviomorpha). Zoological Journal of the Linnaean Society 262, 145-159.

Elton, S., 2001. Locomotor and habitat classifications of cercopithecoid postcranial material from sterkfontein Member 4, Bolt's Farm and Swartkrans Members 1 and 2, South Africa. Palaeontologia Africana 37, 115-126.

Emmons, L.H., 1997. Neotropical Rainforest Mammals: A Field Guide, 2 edn. University of Chicago Press, Chicago, Illinois.

Emry, R.J., Korth, W.W., 2001. *Douglassciurus*, new name for *Douglassia* Emry and Korth, 1996, not *Douglassia* Bartsch, 1934. Journal of Vertebrate Paleontology 21, 400.

Emry, R.J., Thorington, R.W., 1982. Descriptive and comparative osteology of the oldest fossil squirrel, *Protosciurus* (Rodentia; Sciuridae). Smithsonian Contributions to Paleobiology 47, 1-35.

Evanoff, E., Prothero, D.R., Lander, R., H, 1992. Eocene-Oligocene Climatic Change in North America: The White River Formation near Douglas, East-Central Wyoming. In: Prothero, D.R., Berggren, W.A. (Eds.), Eocene-Oligocene Climatic and Biotic Evolution. Princeton University Press, Princeton, New Jersey, pp. 116-130.

Evans, S.E., 2003. At the feet of the dinosaurs: the early history and radiation of lizards. Biological Review 78, 513-551.

Fagan, S.R., 1960. Osteology of *Mylagaulus laevis*, a fossorial rodent from the upper Miocene of Colorado. University of Kansas Paleontological Contributions 9, 1-

32.

Fairon-Demaret, M., Smith, T., 2002. Fruits and seeds from the Tienen Formation at Dormaal, Paleocene-Eocene transition in eastern Belgium. Review of Paleobotany and Palynology 122, 47-62.

Felsenstein, J., 1985. Phylogenetics and the comparative method. American Naturalist 125, 1-15.

Fleagle, J.G., Simons, E.L., 1982. The humerus of *Aegyptopithecus zeuxis*: a primitive anthropoid. American Journal of Physical Anthropology 59, 175-193.

Fleagle, J.G., Simons, E.L., 1983. The tibio-fibular articulation in *Apidium phiomense*, an Oligocene anthropoid. Nature 301, 238-239.

Fleagle, J.G., Simons, E.L., 1995. Limb skeleton and locomotor adaptations of *Apidium phiomense*, an Oligocene anthropoid from Egypt. American Journal of Physical Anthropology 97, 235-289

Foote, M., 1993. Discordance and concordance between morphological and taxonomic diversity. Paleobiology 19, 185-204.

Foote, M., 1996. Perspective: evolutionary patterns in the fossil record. Evolution 50, 1-11.

Foote, M., 1997. The evolution of morphological diversity. Annual Review of Ecology and Systematics 28, 129-152.

Ford, S.M., 1988. Postcranial adaptations of the earliest platyrrhine. Journal of Human Evolution 17, 155-192.

Gagnon, M., 1997. Ecological diversity and community ecology in the Fayum sequence (Egypt). Journal of Human Evolution 32, 133-160.

Gazin, C.L., 1955. A review of the upper Eocene Artiodactyla of North America. Smithsonian Miscellaneous Collections 128, 1-96.

Gazin, C.L., 1956. The geology and vertebrate paleontology of upper Eocene strata in the northeastern part of the Wind River Basin, Wyoming Pt. 2. The mammalian fauna of the Badwater Area. Smithsonian Miscellaneous Collections 131, 35.

Gazin, C.L., 1958. A review of the middle and upper Eocene primates of North America. Smithsonian Miscellaneous Collections 136, 1-112.

Gebo, D.L., 1987. Locomotor diversity in prosimian primates. American Journal of Primatology 13, 271-281.

Gebo, D.L., 1988. Foot Morphology and locomotor adaptation in Eocene primates. Folia Primatologica 50, 3-41.

Gebo, D.L., 1993. Functional Morphology of the Foot in Primates. In: Gebo, D.L. (Ed.) Postcranial Adaptation in Nonhuman Primates. Northern Illinois University Press, DeKalb; IL, pp. 175-196.

Gebo, D.L., Dagosto, M., Beard, K.C., Wang, J., 1999. A first metatarsal of *Hoanghonius stehlini* from the late Middle Eocene of Shanxi Province, China. Journal of Human Evolution 37, 801-806.

Gebo, D.L., Rose, K.D., 1993. Skeletal morphology and locomotor adaptation in *Prolimnocyon atavus*, an early Eocene hyaenodontid creodont. Journal of Vertebrate Paleontology 13, 125-144.

Gidley, J.W., 1907. A new horned rodent from the Miocene of Kansas. Proceedings of the United States National Museum 32, 627-636.

Gingerich, P.D., 1976. Cranial anatomy and evolution of Early Tertiary Plesiadapidae

(Mammalia, Primates). University of Michigan Papers in Paleontology 15, 1-140.

Gingerich, P.D., 1979. The stratophenetic approach to phylogeny reconstruction in vertebrate paleontology. In: Cracraft, J., Eldredge, N. (Eds.), Phylogenetic Analysis and Paleontology. Columbia University Press, New York, pp. 41-77.

Gingerich, P.D., 2003. Land-to-sea transition in early whales: evolution of Eocene Archaeoceti (Cetacea) in relation to skeletal proportions and locomotion in living semiaquatic mammals. Paleobiology 29, 429-454.

Godinot, M., Dagosto, M., 1983. The Astragalus of *Necrolemur* (Primates, Microchoerinae). Journal of Paleontology 57, 1321-1324.

Godinot, M., Smith, T., Smith, R., 1996. Mode de vie et affinities de *Paschatherium* (Condylarthra, Hyopsodontidae) d'apres ses os du tarse. Palaeovertebrata 25, 225-242.

Gould, E., 1978. The behavior of the Moonrat *Echinosorex gymnurus* (Erinaceidae) and the Pentail Shrew (Tupaiidae) with comments on the behavior of other Insectivora. Zeitschrift für Tierpsychologie 48, 1-27.

Gregory, W.K., 1920. On the structure and relations of *Notharctus* an American Eocene primate. Memoirs of the American Museum of Natural History 3, 49-243.

Gunnell, G.F., 1995. Omomyid primates (Tarsiiformes) from the Bridger Formation, middle Eocene, southern Green River Basin, Wyoming. Journal of Human Evolution 28, 147-187.

Gunnell, G.F., 1997. Wasatchian-Bridgerian (Eocene) paleoecology of the western interior of North America: changing paleoenvironments and taxonomic composition of omomyid (Tarsiiformes) primates. Journal of Human Evolution

32, 105-132.

Gunnell, G.F., Bartels, W.S., 1999. Middle Eocene vertebrates from the Uinta Basin, Utah, and their relationship with faunas from the southern Green River Basin, Wyoming. Utah Geological Survey Miscellaneous Publication 99-1, 429-442.

Gunnell, G.F., Bown, T.M., Bloch, J.I., Boyer, D.M., 2008. "Proteutheria". In: Janis, C.M., Gunnell, G.F., Uhen, M.D. (Eds.), Evolution of Tertiary Mammals of North America Volume2: Small Mammals, Xenarthrans and Marine Mammals. Cambridge University Press, Cambridge, UK, pp. 63-81.

Gunnell, G.F., Morgan, M.E., Maas, M.C., Gingerich, P.D., 1995. Comparative paleoecology of Paleogene and Neogene mammalian faunas: Trophic structure and composition. Palaeogeography, Palaeoclimatology, Palaeoecology 115, 256-286.

Gunnell, G.F., Rose, K.D., 2002. Tarsiiformes: Evolutionary history and adaptation. In: Hartwig, W.C. (Ed.) The Primate Fossil Record. Cambridge University Press, Cambridge, UK, pp. 45-82.

Heinrich, R.E., Rose, K.D., 1997. Postcranial morphology and locomotor behaviour of two early Eocene miacoid carnivorans, *Vulpavus* and *Didymictis*. Palaeontology 40, 279-305.

Hildebrand, M., 1985. Digging of quadrupeds. In: Hildebrand, M., Bramble, D.M., Liem, K.F., Wake, D.B. (Eds.), Vertebrate Functional Morphology. Belknap Press, Cambridge, MA, pp. 89-109.

Hintze, L.F., 1988. Geologic History of Utah, Provo, Utah.

Hoogland, J.L., 1996. *Cynomys ludovicianus*. Mammalian Species 535, 1-10.

Hooker, J.J., 1992. British mammalian paleocommunities across the Eocene-Oligocene transition and their environmental implications. In: Prothero, D.R., Berggren, W.A. (Eds.), Eocene-Oligocene Climatic and Biotic Evolution. Princeton University Press, New Jersey, pp. 494-515.

Hooker, J.J., 2001. Tarsals of the extinct insectivoran family Nyctitheriidae (Mammalia): evidence for archontan relationships. Zoological Journal of the Linnaean Society 132, 501-529.

Hooker, J.J., Collinson, M.E., Sille, N.P., 2004. Eocene-Oligocene mammalian faunal turnover in the Hampshire Basin, UK: calibration of the global time scale and the major cooling event. Journal of the Geological Society, London 161, 161-172.

Hooker, J.J., Collinson, M.E., Van Bergen, P.F., Singer, R.L., De Leeuw, J.W., Jones, T.P., 1995. Reconstruction of land and freshwater palaeoenvironments near the Eocene-Oligocene boundary, southern England. Journal of the Geological Society, London 152, 449-468.

Hutchison, J.H., 1992. Western North American reptile and amphibian record across the Eocene/Oligocene boundary and its climatic implications. In: Prothero, D.R., Berggren, W.A. (Eds.), Eocene-Oligocene Climatic and Biotic Evolution. Princeton University Press, New Jersey, pp. 451-463.

Ivany, L.C., P., P.W., Lohmann, K.C., 2000. Cooler winters as a possible cause of mass extinctions at the Eocene/Oligocene boundary. Nature 407, 887-890.

Jacobs, B.F., Kingston, J.D., Jacobs, L.L., 1999. The origin of grass-dominated ecosystems. Annals of the Missouri Botanical Gardens 86, 590-643.

Janis, C.M., 1993. Tertiary mammal evolution in the context of changing climates,

vegetation and tectonic events. Annual Review of Ecology and Systematics 24, 467-500.

Janis, C.M., Effinger, J.A., Harrison, J.A., Honey, J.G., Kron, D.G., Lander, B., Manning, E., Prothero, D.R., Stevens, M.S., Stucky, R.K., Webb, D., Wright, D.B., 1998. Artiodactyla. In: Janis, C.M., Scott, K.M., Jacobs, L.L. (Eds.), Evolution of Tertiary Mammals of North America Volume 1: Terrestrial Carnivores, Ungulates, and Ungulate-like Mammals. Cambridge University Press, Cambridge, UK, pp. 337-357.

Jenkins, F.A., Jr., 1973. The functional anatomy and evolution of the mammalian humeroulnar articulation. American Journal of Anatomy 137, 281-298.

Jenkins, F.A., Jr., Camazine, S.M., 1977. Hip structure and locomotion in ambulatory and cursorial carnivores. Journal of Zoology, London 181, 351-370.

Jenkins, S.H., Busher, P.E., 1979. *Castor canadensis*. Mammalian Species 120, 1-8.

Jernvall, J., Hunter, J.P., Fortelius, M., 1996. Molar tooth diversity, disparity, and ecology in Cenozoic ungulate radiations. Science 274, 1489-1492.

Jernvall, J., Hunter, J.P., Fortelius, M., 2000. Trends in the evolution of molar crown types in ungulate mammals: evidence from the northern hemisphere. In: Teaford, M.F., Smith, M.M., Ferguson, M.W.J. (Eds.), Development, Function and Evolution of Teeth. Cambridge University Press, Cambridge, pp. 269-281.

Jungers, W.L., Falsetti, A.B., Wall, C.E., 1995. Shape, Relative Size, and Size-Adjustments in Morphometrics. Yearbook of Physical Anthropology 38, 137-161.

Kappelman, J., 1988. Morphology and locomotor adaptations of the bovid femur in relation to habitat. Journal of Morphology 198, 119-130.

Kappelman, J., Plummer, T., Bishop, L., Duncan, A., Appleton, S., 1997. Bovids as indicators of Plio-Pleistocene paleoenvironments in East Africa. Journal of Human Evolution 32, 229-256.

Kay, R.F., Madden, R.H., Vucetich, M.G., Carlini, A.A., Mazzoni, M.M., Re, G.H., Heizler, M., Sandeman, H., 1999. Revised geochronology of the Casamayoran South American Land Mammal Age: climatic and biotic implications. Proceedings of the National Academy of Science of the United States of America 96, 13235-13240.

Kingdon, J., 1974. East African Mammals: an atlas of evolution in Africa. Academic Press, London.

Kirk, E.C., 2007. New specimens of *Mytonius* (Primates, Omomyoidea) from the Devil's Graveyard Formation, Texas. Journal of Vertebrate Paleontology 27S, 99A.

Koenigswald, W.v., 1980. Das Skelett eines Pantolestiden (Proteutheria, Mamm.) aus dem mittleren Eozän von Messel bei Darmstadt. Palaeontologische Zeitschrift 54, 267-287.

Koenigswald, W.v., 1986. Ein zweites Skelett von *Buxolestes* (Pantolestidae, Proteutheria, Mammalia) aus dem Mitteleozän von Messel bei Darmstadt. Carolinea 45, 36-42.

Koenigswald, W.v., Rose, K.D., Grande, L., Martin, R.D., 2005. First apatemyid skeleton from the lower Eocene Fossil Butte Member, Wyoming (USA), Compared to the European apatemyid from Messel, Germany. Palaeontographica Abteilung A 272, 149-169.

Köhler, M., Moyà-Solà, S., 1999. A finding of Oligocene primates on the European

continent. Proceedings of the National Academy of Science of the United States of America 96, 14664-14667.

Koprowski, J.L., 1994. *Sciurus carolinensis*. Mammalian Species 480, 1-9.

Korth, W.W., 1984. Earliest Tertiary evolution and radiation of rodents in North America. Bulletin of the Carnegie Museum of Natural History 24, 1-71.

Korth, W.W., 1994. Tertiary Record of Rodents in North America. Plenum Publishing Corporation, New York, New York.

Krishtalka, L., 1976. Adapisoricidae and Erinaceidae (Mammalia, Insectivora) of North America. Bulletin of the Carnegie Museum of Natural History 1, 1-40.

Krishtalka, L., 1978. The Paleontology and Geology of the Badwater Creek Area, Central Wyoming. Part 15: Review of the late Eocene Primates from Wyoming and Utah, and the Plesitarsiiformes. Annals of the Carnegie Museum 47, 335-360.

Krishtalka, L., Stucky, R.K., 1984. Middle Eocene marsupials (Mammalia) from northeastern Utah and the mammalian fauna from Powder Wash. Annals of the Carnegie Museum 53, 31-45.

Kwiecinski, G.G., 1998. *Marmota monax*. Mammalian Species 591, 1-8.

Lander, B., 1998. Oreodontoidea. In: Janis, C.M., Scott, K.M., Jacobs, L.L. (Eds.), Evolution of Tertiary Mammals of North America Volume 1: Terrestrial Carnivores, Ungulates, and Ungulate-like Mammals. Cambridge University Press, Cambridge, UK, pp. 402-425.

Legendre, S., Hartenberger, J.-L., 1992. Evolution of mammalian faunas in Europe during the Eocene and Oligocene. In: Prothero, D.R., Berggren, W.A. (Eds.), Eocene-Oligocene Climatic and Biotic Evolution. Princeton University Press,

New Jersey, pp. 516-528.

Lillegraven, J.A., 1980. Primates from later Eocene rocks of southern California. Journal of Mammalogy 61, 181-204.

Lillegraven, J.A., McKenna, M.C., Krishtalka, L., 1981. Evolutionary relationships of middle Eocene and younger species of *Centetodon* (Mammalia, Insectivora, Geolabididae) with a description of the dentition of *Ankylodon* (Adapisoricidae). University of Wyoming Publications 45, 1-115.

Losos, J.B., Miles, D.B., 1994. Adaptation, constraint and the comparative method: phylogenetic issues and methods. In: Wainright, P.C., Reilly, S.M. (Eds.), Ecological Morphology. University of Chicago Press, Chicago, pp. 60-98.

Maas, M.C., Anthony, M.R.L., Gingerich, P.D., Gunnell, G.F., Krause, D.W., 1995. Mammalian generic diversity and turnover in the Late Paleocene and Early Eocene of the Bighorn and Crazy Mountain Basins, Wyoming and Montana (USA). Palaeogeography, Palaeoclimatology, Palaeoecology 115, 181-207.

Maas, M.C., Krause, D.W., Strait, S.G., 1988. The decline and extinction of Plesiadapiformes (Mammalia: ?Primates) in North America: displacement or replacement. Paleobiology 14, 410-431.

MacLeod, N., Rose, K.D., 1993. Inferring locomotor behavior in paleogene mammals via eigenshape analysis. American Journal of Science 293, 300-355.

Maddison, W.P., 2000. Testing character correlation using pairwise comparisons on a phylogeny. Journal of Theoretical Biology 202, 195-204.

Magioncalda, R., Dupuis, C., Smith, T., Steurbaut, E., Gingerich, P.D., 2004. Paleocene-Eocene carbon isotope excursion in organic carbon and pedogenic carbonate:

Direct comparison in a continental stratigraphic section. Geology 32, 553-556.

Marsh, O.C., 1872. Preliminary description of new Tertiary mammals. American Journal of Science 4, 202-224.

Marsh, O.C., 1875a. Ancient lake basins of the Rocky Mountain Region. American Journal of Science 9, 49-52.

Marsh, O.C., 1875b. Notice of new Tertiary mammals IV. American Journal of Science 9, 239-250.

Martinez, J.-N., Sudre, J., 1995. The astragalus of Paleogene artiodactyls: comparative morphology, variability and prediction of body mass. Lethaia 28, 197-209.

Martins, E.P., 2000. Adaptation and the comparative method. Trends in Ecology and Evolution 15, 296-299.

Matthew, W.D., 1909. The Carnivora and Insectivora of the Bridger Basin, middle Eocene. Memoirs of the American Museum of Natural History 9, 291-576.

Matthew, W.D., 1910. On the osteology and relationships of *Paramys* and the affinities of the Ischyromyidae. Bulletin of the American Museum of Natural History 28, 43-72.

Matthew, W.D., 1918. A revision of the lower Eocene Wasatch and Wind River faunas. Bulletin of the American Museum of Natural History 34, 429-483.

McCarrol, S.M., Flynn, J.J., Turnbull, W.D., 1996. Biostratigraphy and magnetostratgraphy of the Bridgerian-Uintan Washakie Formation, Washakie Basin, Wyoming. In: Prothero, D.R., Emry, R.J. (Eds.), The Terrestrial Eocene-Oligocene Transition in North America. Cambridge University Press, Cambridge, England, pp. 25-39.

McKenna, M.C., Bell, S.K., 1997. Classification of Mammals Above the Species Level. Columbia University Press, New York.

Miller, K.G., 1992. Middle Eocene to Oligocene stable isotopes, climate and deep-water history: the Terminal Eocene event? In: Prothero, D.R., Berggren, W.A. (Eds.), Eocene-Oligocene Climatic and Biotic Evolution. Princeton University Press, New Jersey, pp. 160-177.

Møller, A.P., Birkhead, T.R., 1992. A pairwise comparative method as illustrated by copulation frequency in birds. American Naturalist 139, 644-656.

Mones, A., Ojasti, J., 1986. *Hydrochaeris hydrochaeris*. Mammalian Species 264, 1-7.

Mosimann, J.E., Malley, J.D., 1979. Size and shape variables. In: Orloci, L., Rao, C.R., Stiteler, W.M. (Eds.), Multivariate Methods in Ecological Work. International Cooperative, Fairland, Maryland, pp. 175-189.

Novacek, M.J., 1976. Insectivora and Proteutheria of the later Eocene (Uintan) of San Diego County, California. Natural History Museum of Los Angeles County Contributions in Science 283, 1-52.

Novacek, M.J., 1985. The Sespedectinae, a new subfamily of hedgehog-like insectivores. American Museum Novitates 2822, 1-24.

Novacek, M.J., 1999. 100 Million years of land vertebrate evolution: the Cretaceous-Early Tertiary transition. Annals of the Missouri Botanical Gardens 86, 230-258.

Novacek, M.J., Bown, T.M., Shankler, D., 1985. On the classification of Early Tertiary Erinaceomorpha (Insectivora, Mammalia). American Museum Novitates 2813, 1-22.

Nowak, R.M., 1991. Walker's Mammals of the World, 5 edn. The Johns Hopkins

University Press, Baltimore, MD.

O'Leary, M.A., Rose, K.D., 1995. Postcranial skeleton of the early Eocene mesonychid *Pachyaena* (Mammalia: Mesonychia). Journal of Vertebrate Paleontology 15, 401-430.

Off, E.C., Gebo, D.L., 2005. Galago Locomotion in Kibale National Park, Uganda. American Journal of Primatology 66, 189-195.

Orzack, S.H., Sober, E., 2001. Adaptation, Phylogenetic Inertia, and the Method of Controlled Comparisons. In: Orzack, S.H., Sober, E. (Eds.), Adaptationism and Optimality. Cambridge University Press

Osborn, H.F., 1895. Fossil mammals of the Uinta Basin. Expedition of 1894. Bulletin of the American Museum of Natural History 7, 71-105.

Osborn, H.F., 1929. The titanotheres of ancient Wyoming, Dakota and Nabraska. United States Geological Survey Monograph 55, 1-953.

Osborn, H.F., Matthew, W.D., 1909. Cenozoic mammal horizons of western North America. United States Geological Survey Bulletin 361, 1-138.

Oxnard, C., 1978. One biologist's view of morphometrics. Annual Review of Ecology and Systematics 9, 219-241.

Pérez, E.M., 1992. *Agouti paca*. Mammalian Species 404, 1-7.

Peterson, O.A., 1919. Report upon the material discovered in the Upper Eocene of the Uinta Basin by Earl Douglass in the years 1908-1909, and by O. A. Peterson in 1912. Annals of the Carnegie Museum 12, 40-141.

Pfretzschner, H.-U., 1993. Muscle reconstruction and aquatic locomotion in the middle Eocene *Buxolestes piscator* from Messel near Darmstadt. Kaupia 3, 75-87.

Pfretzschner, H.-U., 1999. *Buxolestes minor* n. sp. - ein neuer Pantolestide (Mammalia, Proteutheria) aus der Eozänen Messel-Formation. Courier Forschungsinstitut Senckenberg 216, 19-29.

Prothero, D.R., 1985. North American mammalian diversity and Eocene-Oligocene extinctions. Paleobiology 11, 389-405.

Prothero, D.R., 1994. The Eocene-Oligocene Transition: Paradise Lost. Columbia University Press, New York.

Prothero, D.R., 1996. Magnetic stratigraphy and biostratigraphy of the middle Eocene Uinta Formation, Uinta Basin, Utah. In: Prothero, D.R., Emry, R.J. (Eds.), The Terrestrial Eocene-Oligocene transition in North America. Cambridge University Press, Cambridge, England, pp. 3-24.

Prothero, D.R., 1998. Oromerycidae. In: Janis, C.M., Scott, K.M., Jacobs, L.L. (Eds.), Evolution of Tertiary Mammals of North America Volume 1: Terrestrial Carnivores, Ungulates, and Ungulate-like Mammals. Cambridge University Press, Cambridge, pp. 426-430.

Prothero, D.R., 1998. Protoceratidae. In: Janis, C.M., Scott, K.M., Jacobs, L.L. (Eds.), Evolution of Tertiary Mammals of North America Volume 1: Terrestrial Carnivores, Ungulates, and Ungulate-like Mammals. Cambridge University Press, Cambridge, pp. 431-438.

Prothero, D.R., Swisher, C.C.I., 1992. Magnetostratigraphy and Geochronology of the Terrestrial Eocene-Oligocene Transition in North America. In: Prothero, D.R., Berggren, W.A. (Eds.), Eocene-Oligocene Climatic and Biotic Evolution. Princeton University Press, Princeton, New Jersey, pp. 46-73.

Rasmussen, D.T., 1996. A new Middle Eocene omomyine primate from the Uinta Basin, Utah. Journal of Human Evolution 31, 75-87.

Rasmussen, D.T., Conroy, G.C., Friscia, A.R., Townsend, E.K., Kinkel, M.D., 1999. Mammals of the Middle Eocene Uinta Formation. Utah Geological Survey Miscellaneous Publication 99-1, 401-420.

Rasmussen, D.T., Conroy, G.C., Simons, E.L., 1998. Tarsier-like locomotor specializations in the Oligocene primate *Afrotarsius*. Proceedings of the National Academy of Science of the United States of America 95, 14848-14850.

Reed, K.E., 1998. Using large mammal communities to examine ecological and taxonomic structure and predict vegetation in extant and extinct assemblages. Paleobiology 24, 384-408.

Reeve, N., 1994. Hedgehogs. Cambridge University Press, Cambridge, UK.

Retallack, G.J., 2007. Cenozoic Paleoclimate on Land in North America. Journal of Geology 115, 271-294.

Retallack, G.J., Orr, W.N., Prothero, D.R., Duncan, A., Kester, P.R., Ambers, C.P., 2004. Eocene-Oligocene extinction and paleoclimatic change near Eugene Oregon. Geological Society of America Bulletin 116, 817-839.

Richtsmeier, J.T., Deleon, V.B., Lele, S.R., 2002. The Promise of Geometric Morphometrics. Yearbook of Physical Anthropology 45, 63-91.

Riggs, E.S., 1912. New or little known titanotheres from the lower Uintah Formation. Field Museum of Natural History Geological Series 159, 17-41.

Robinson, P., 1968. The Paleontology and Geology of the Badwater Creek Area, Central Wyoming. Part 4: Late Eocene Primates from Badwater Wyoming, with a

discussion of material from Utah. Annals of the Carnegie Museum 39, 307-326.

Robinson, P., Gunnell, G.F., Walsh, S.L., Clyde, W.C., Storer, J.E., Stucky, R.K., Froehlich, D.J., Ferrusquia-Villafranca, I., McKenna, M.C., 2004. Wasatchian Through Duchesnean Biochronology. In: Woodburne, M.O. (Ed.) Late Cretaceous and Cenozoic Mammals of North America: Biostratigraphy and Geochronology. Columbia University Press, New York, pp. 106-155.

Rose, K.D., 1981. The Clarkforkina Land-Mammal Age and Mammalian Faunal Composition Across the Paleocene-Eocene Boundary. University of Michigan Papers in Paleontology 26, 1-197.

Rose, K.D., 1985. Comparative osteology of North American dichobunid artiodactyls. Journal of Paleontology 59, 1203.

Rose, K.D., 1987. Climbing adaptations in the early Eocene mammal *Chriacus* and the origin of Artiodactyla. Science 236, 314-316.

Rose, K.D., 1990. Postcranial skeletal remains and adaptations in early Eocene mammals from the Willwood Formation, Bighorn Basin, Wyoming. In: Rose, K.D., Bown, T.M. (Eds.), Dawn of the Age of Mammals in the northern part of the Rocky Mountain Interior, North America. Geological Society of America, Boulder, Colorado, pp. 107-133.

Rose, K.D., 1994. The Earliest Primates. Evolutionary Anthropology 3, 159-173.

Rose, K.D., 1999. Postcranial skeleton of Eocene Leptictidae (Mammalia), and its implications for behavior and relationships. Journal of Vertebrate Paleontology 19, 355-372.

Rose, K.D., 2006. The Beginning of the Age of Mammals. Johns Hopkins University

Press, Baltimore, MD.

Rose, K.D., 2007. The postcranial skeleton of early Oligocene *Leptictis* (Mammalia: Leptictida), with a preliminary comparison to *Leptictidium* from the middle Eocene of Messel. Palaeontographica Abteilung A 278, 37-56.

Rose, K.D., 2008. Palaeanodonta and Pholidota. In: Janis, C.M., Gunnell, G.F., Uhen, M.D. (Eds.), Evolution of Tertiary Mammals of North America Volume2: Small Mammals, Xenarthrans and Marine Mammals. Cambridge University Press, Cambridge, UK, pp. 135-146.

Rose, K.D., Chinnery, B.J., 2004. Postcranial skeleton of early Eocene rodents. Bulletin of the Carnegie Museum of Natural History 36, 211-244.

Rose, K.D., Emry, R.J., 1993. Relationships of Xenarthra, Pholidota, and Fossil "Edentates": The Morphological Evidence. In: Szalay, F.S., Novacek, M.J., McKenna, M.C. (Eds.), Mammal Phylogeny: Placentals. Springer-Verlag, New York, pp. 81-102.

Rose, K.D., Emry, R.J., Gingerich, P.D., 1992. Skeleton of *Alcodontulum atopum* an early Eocene epoicotheriid (mammalia, palaeanodonta) from the Bighorn Basin, Wyoming. Contributions from the Museum of Paleontology, University of Michigan 28, 221-245.

Rose, K.D., Koenigswald, W.v., 2005. An exceptionally complete skeleton of *Palaeosinopa* (Mammalia, Cimolesta, Pantolestidae) from the Green River Formation, and other postcranial elements of the Pantolestidae from the Eocene of Wyoming (USA). Palaeontographica Abteilung A 273, 55-96.

Rose, K.D., Lucas, S.G., 2000. An early Paleocene palaeanodont (Mammalia, ?Pholidota)

from New Mexico, and the origin of Palaeanodonta. Journal of Vertebrate Paleontology 20, 139-156.

Rose, K.D., O'Leary, M.A., 1995. The manus of *Pachyaena gigantea* (Mammalia: Mesonychia). Journal of Vertebrate Paleontology 15, 855-859.

Rose, K.D., Walker, A., 1985. The skeleton of early Eocene *Cantius*, oldest lemuriform primate. American Journal of Physical Anthropology 66, 73-89.

Rose, M.D., 1988. Another look at the anthropoid elbow. Journal of Human Evolution 17, 193-224.

Rose, M.D., 1993. Functional Morphology of the Elbow and Forearm in Primates. In: Gebo, D.L. (Ed.) Postcranial Adaptation in Nonhuman Primates. Northern Illinois University Press, DeKalb, IL, pp. 70-95.

Sargis, E.J., 2002. Functional morphology of the hindlimb of tupaiids (Mammalia, Scandentia) and its phylogenetic implications. Journal of Morphology 254, 149-185.

Sarmiento, E.E., 1983. The significance of the heel process in anthropoids. International Journal of Primatology 4, 127-152.

Savage, D.E., Waters, B.T., 1978. A new omomyid primate from the Wasatch Formation of southern Wyoming. Folia Primatologica 30, 1-29.

Schaal, S., Ziegler, W. (Eds.), 1992. Messel: An insight into the history of life and of the Earth. Oxford University Press, Oxford.

Scott, W.B., Osborn, H.F., 1887. Preliminary report on the vertebrate fossils of the Uinta Formation, collected by the Princeton Expedition of 1886. Proceedings of the American Philosophical Society 24, 255-264.

Scott, W.B., Osborn, H.F., 1890. The Mammalia of the Uinta Formation. Transactions of the American Philosophical Society 16, 461-572.

Shapiro, L.J., 1993. Functional morphology of the vertebral column in primates. In: Gebo, D.L. (Ed.) Postcranial Adaptation in Nonhuman Primates. Northern Illinois University Press, DeKalb, Illinois, pp. 121-149.

Simons, E.L., 1961. The dentition of *Ourayia*:--It's bearing on relationships of omomyid prosimians. Postilla 54, 1-20.

Simpson, G.G., 1931. *Metachiromys* and the Edentata. Bulletin of the American Museum of Natural History 54, 295-381.

Simpson, G.G., 1940. Studies on the earliest primates. Bulletin of the American Museum of Natural History 77, 185-212.

Simpson, G.G., 1941. A giant rodent from the Oligocene of South Dakota. American Museum Novitates 1149, 1-16.

Simpson, G.G., 1945. The Principles of Classification and a Classification of Mammals. Bulletin of the American Museum of Natural History 85, 1-350.

Smith, T., Bloch, J.I., Strait, S.G., Gingerich, P.D., 2002. New species of *Macrocranion* (Mammalia, Lipotyphla) from the earliest Eocene of North America and its biogeographic implications. Contributions from the Museum of Paleontology, University of Michigan 30, 373-384.

Sokal, R.R., Rohlf, F.J., 1995. Biometry, 3 edn. W. H. Freeman and Company, New York.

Storch, G., 1993. Morphologie und Paläobiologie von *Macrocranion tenerum*, einem Erinaceomorphen aus dem Mittel-Eozän von Messel bei Darmstadt (Mammalia,

Lipotyphla). Senckenbergiana Lethaea 73, 61-81.

Storch, G., 1996. Paleobiology of Messel erinaceomorphs. Palaeovertebrata 25, 215-224.

Storch, G., Richter, G., 1994. Zur Paläobiologie Messeler Igel. Natur und Museum 124, 81-90.

Stucky, R.K., 1992. Mammalian faunas in North America of Bridgerian to early Arikareean "Ages" (Eocene and Oligocene). In: Prothero, D.R., Berggren, W.A. (Eds.), Eocene-Oligocene Climatic and Biotic Evolution. Princeton University Press, New Jersey, pp. 464-493.

Stucky, R.K., 1998. Eocene bunodont and bunoselenodont Artiodactyla ("dichobunids"). In: Janis, C.M., Scott, K.M., Jacobs, L.L. (Eds.), Evolution of Tertiary Mammals of North America Volume 1: Terrestrial Carnivores, Ungulates, and Ungulate-like Mammals. Cambridge University Press, Cambridge, UK, pp. 358-374.

Stucky, R.K., Prothero, D.R., Lohr, W.G., Snyder, J.R., 1996. Magnetic stratigraphy, sedimentology, and mammalian faunas of the early Uintan Washakie Formation, Sand Wash Basin, Northwestern Colorado. In: Prothero, D.R., Emry, R.J. (Eds.), The Terrestrial Eocene-Oligocene Transition in North America. Cambridge University Press, Cambridge, England, pp. 40-51.

Szalay, F.S., 1976. Systematics of the Omomyidae (Tarsiiformes, Primates) taxonomy, phylogeny and adaptations. Bulletin of the American Museum of Natural History 156, 157-450.

Szalay, F.S., 1977. Phylogenetic relationships and classification of the eutherian Mammalia. In: Hecht, M.K., Goody, P.C., Hecht, B.M. (Eds.), Major patterns in vertebrate evolution. Plenum Publishing, New York, New York

Szalay, F.S., 1985. Rodent and lagomorph morphotype adaptations, origins, and relationships: some postcranial attributes analyzed. In: Luckett, W.P., Hartenberger, J.-L. (Eds.), Evolutionary Relationships among Rodents A Multidisciplinary Analysis. Plenum Press, New York, New York, pp. 83-132.

Szalay, F.S., Dagosto, M., 1988. Evolution of hallucial grasping in the primates. Journal of Human Evolution 17, 1-33.

Szalay, F.S., Decker, R.L., 1973. Phylogeny of lemurs, galagos and lorises. Folia Primatologica 19, 88-103.

Szalay, F.S., Decker, R.L., 1974. Origins, evolution and function of the tarsus in late Cretaceous Eutheria and Paleocene primates. In: Jenkins, F.A., Jr. (Ed.) Primate Locomotion. Academic Press, New York, NY, pp. 223-260.

Tang, C., Pantel, J.H., 2005. Combining morphometric and paleoecological analyses: examining small-scale dynamics in species-level and community-level evolution. Palaeontologica Electronica 8, 1-10.

Terry, D.O.J., 2001. Paleopedology of the Chadron Formation of Northwestern Nebraska: implications for paleoclimatic change in the North American midcontinent across the Eocene-Oligocene boundary. Palaeogeography, Palaeoclimatology, Palaeoecology 168, 1-38.

Theodor, J.M. 1996. Phylogeny, locomotor evolution and diversity patterns in Eocene Artiodactyla. Ph. D., University of California at Berkeley.

Theodor, J.M., 1999. *Protoreodon walshi*, a new species of Agriochoerid (Oreodonta, Artiodactyla, Mammalia) from the late Uintan of San Diego County, California. Journal of Paleontology 73, 1179-1190.

Thomson, A., 1889. The influence of posture on the form of the articular surfaces of the tibia and astragalus in the different races. Journal of Anatomy and Physiology, London 23, 616-639.

Thorington, R.W., Darrow, K., 2000. Anatomy of the squirrel wrist: bones, ligaments, and muscles. Journal of Morphology 246, 85-102.

Thorington, R.W., Darrow, K., Betts, A.D.K., 1998. Comparative myology of the forelimb of squirrels (Sciuridae). Journal of Morphology 234, 155-182.

Thornton, M.L., Rasmussen, D.T., 2001. Taphonomic interpretatin of Gnat-Out-Of-Hell, an early Uintan small mammal locality in the Uinta Formation, Utah. In: Gunnell, G.F. (Ed.) Eocene Biodiversity: Unusual Occurrences and Poorly Sampled Habitats. Kluwer Academic/Plenum Publishers, New York, NY, pp. 299-316.

Tornow, M.A. 2005. Phylogenetic systematics of the Eocene primate superfamily Omomyoidea: an investigation using dental and postcranial data. Ph. D., Southern Illinois University Carbondale.

Townsend, K.E. 2004. Stratigraphy, Paleoecology, and Habitat Change in the Middle Eocene of North America. Ph. D., Washington University.

Townsend, K.E., Friscia, A.R., Rasmussen, D.T., 2006. Stratigraphic distribution of upper middle Eocene fossil vertebrate localities in the eastern Uinta Basin, Utah, with comments on Uintan biostratigraphy. The Mountain Geologist 43, 115-134.

Townsend, K.E., Rasmussen, D.T., 1995. Skeletal remains of the small artiodactyl, *Mesomeryx grangeri*, from the Uinta Formation, Uinta Basin, Utah. Journal of Vertebrate Paleontology 15, 57A.

Trinkaus, E., 1975. Squatting among the Neanderthals: A Problem in the Behavioral

Interpretation of Skeletal Morphology. Journal of Archaeological Science 2, 327-351.

Van Valen, L., 1967. New Paleocene insectivores and insectivore classification. Bulletin of the American Museum of Natural History 135, 221-284.

Van Valkenburgh, B., 1987. Skeletal indicators of locomotor behavior in living and extinct carnivores. Journal of Vertebrate Paleontology 7, 162-182.

Van Valkenburgh, B., 1988. Trophic diversity in past and present guilds of large predatory mammals. Paleobiology 14, 155-173.

Van Valkenburgh, B., 1994. Ecomorphological analysis of fossil vertebrates and their paleocommunities. In: Wainright, P.C., Reilly, S.M. (Eds.), Ecological Morphology. University of Chicago Press, Chicago, IL, pp. 140-168.

Van Valkenburgh, B., 1995. Tracking ecology over geological time: evolution within guilds of vertebrates. Trends in Ecology and Evolution 10, 71-75.

Van Valkenburgh, B., 1999. Major patterns in the history of carnivorous mammals. Annual Review of Earth and Planetary Sciences 27, 463-493.

Vaughan, T.A., Ryan, J.M., Czaplewski, N.J., 2000. Mammalogy, 4 edn. Saunders College Publishing, Orlando, FL.

Verzani, J., 2005. Using R for Introductory Statistics. Chapman and Hall/CRC, New York, NY.

Wainright, P.C., Reilly, S.M., 1994. Introduction. In: Wainright, P.C., Reilly, S.M. (Eds.), Ecological Morphology. University of Chicago Press, Chicago, IL, pp. 1-12.

Walsh, S.L., 1996. Middle Eocene mammalian faunas of San Diego County, California.

In: Prothero, D.R., Emry, R.J. (Eds.), The Terrestrial Eocene-Oligocene Transition in North America. Cambridge University Press, Cambridge, pp. 75-119.

Walsh, S.L., 1998. Notes on the anterior dentition and skull of *Proteroxoides* (Mammalia: Insectivora: Dormaliidae), and a new dormaliid genus from the early Uintan (Middle Eocene) of southern California. Proceedings of the San Diego Society of Natural History 34, 1-26.

Walsh, S.L., 1998. Fossil datum and paleobiological event terms, paleontostratigraphy, chronostratigraphy, and the definition of Land Mammal "Age" Boundaries. Journal of Vertebrate Paleontology 18, 150-179.

Walsh, S.L., 2000. Eubiostratigraphic units, quasibiostratigraphic units, and "assemblage zones". Journal of Vertebrate Paleontology 20, 761-775.

Wang, X., 1993. Transformation from plantigrady to digitigrady: Functional morphology of locomotion in *Hesperocyon* (Canidae: Carnivora). American Museum Novitates 3069, 1-23.

Wesley-Hunt, G.D., 2005. The morphological diversification of carnivores in North America. Paleobiology 31, 35-55.

White, T.G., Alberico, A.S., 1992. *Dinomys branickii*. Mammalian Species 410, 1-5.

Wilf, P., 2000. Late Paleocene - early Eocene climate changes in southwestern Wyoming: Paleobotanical analysis. Geological Society of America Bulletin 112, 292-307.

Williams, B.A., Kirk, E.C., 2008. New Uintan primates from Texas and their implications for North American patterns of species richness during the Eocene. Journal of Human Evolution doi:10.1016/j.hevol.2008.07.007,

Willner, G.R., Feldhamer, G.A., Sucker, E.E., Chapman, J.A., 1980. *Ondatra zibethicus*. Mammalian Species 141, 1-8.

Wilson, R.W., 1940. Californian paramyid rodents. Carnegie Institute of Washington Publication 514, 59-83.

Wilson, R.W., 1949. Additional Eocene rodent material from Southern California. Carnegie Institute of Washington Publication 584, 1-25.

Wing, S.L., 1987. Eocene and Oligocene floras and vegetation of the Rocky Mountains. Annals of the Missouri Botanical Gardens 274, 748-784.

Wing, S.L., Alroy, J., Hickey, L.J., 1995. Plant and mammal diversity in the Paleocene to Early Eocene of the Bighorn Basin. Palaeogeography, Palaeoclimatology, Palaeoecology 115, 117-155.

Wing, S.L., Harrington, G.J., 2001. Floral response to rapid warming in the earliest Eocene and implications for concurrent faunal change. Paleobiology 27, 539-563.

Wolfe, J.A., 1992. Climatic, floristic, and vegetational changes near the Eocene/Oligocene boundary in North America. In: Prothero, D.R., Berggren, W.A. (Eds.), Eocene-Oligocene Climatic and Biotic Evolution. Princeton University Press, New Jersey, pp. 421-436.

Wood, A.E., 1962. The Early Tertiary Rodents of the Family Paramyidae. Transactions of the American Philosophical Society 52, 1-261.

Wood, A.E., 1974. Early Tertiary vertebrate faunas, Vieja Group Trans-Pecos Texas: Rodentia. Bulletin of the Texas Memorial Museum 21, 1-112.

Wood, H.E., 1934. Revision of the Hyrachidae. Bulletin of the American Museum of Natural History 67, 181-295.

Wood, H.E., Chaney, R.W., Clark, J., Colbert, E.H., Jepsen, G.L., Reeside, J.B.J., Stock, C., 1941. Nomenclature and correlation of the North American continental Tertiary. Bulletin of the Geological Society of America 52, 1-48.

Woods, C.A., 1973. *Erethizon dorsatum*. Mammalian Species 29, 1-6.

Woods, C.A., Contreras, L., Willner-Chapman, G., Whidden, H.P., 1992. *Myocastor coypus*. Mammalian Species 398,

Wunderlich, R.E., Simons, E.L., Jungers, W.L., 1996. New pedal remains of *Megaladapis* and their functional significance. American Journal of Physical Anthropology 100, 115-139.

Yalden, D.W., 1971. The functional morphology of the carpus in ungulate mammals. Acta anatomica 78, 461-487.